Fall 12-2012

Polymer Surface Engineering Via Thiol-Mediated Reactions

Ryan Matthew Hensarling
University of Southern Mississippi

The University of Southern Mississippi

POLYMER SURFACE ENGINEERING VIA THIOL-MEDIATED REACTIONS

by

Ryan Matthew Hensarling

Abstract of a Dissertation
Submitted to the Graduate School
of The University of Southern Mississippi
in Partial Fulfillment of the Requirements
for the Degree of Doctor of Philosophy

December 2012

ABSTRACT

POLYMER SURFACE ENGINEERING VIA THIOL-MEDIATED REACTIONS

by Ryan Matthew Hensarling

December 2012

Synthesis of polymer brushes to decorate a surface with desired functionality typically involves surface-initiated polymerization (SIP) of functional, but non-reactive monomers. This approach suffers major drawbacks associated with synthesizing sufficiently thick polymer brushes containing surface-attached polymer chains of high molecular weight at high grafting density (i.e. cost, synthetic effort and functional group intolerance during polymerization). The research herein seeks to circumvent these limitations by the decoration of surfaces with polymer chains bearing specific pendent functional groups amenable to post-polymerization modification (PPM). In particular, this dissertation leverages PPM via a specific class of click reactions – thiol-click – that 1) enables the rapid generation of a diverse library of functional surfaces from a single substrates precursor, 2) utilizes a structurally diverse range of commercially available or easily attainable reagents, 3) proceeds rapidly to quantitative conversions under mild conditions and 4) opens the door to orthogonal and site-selective functionalization.

In the first two studies, radical-mediated thiol-yne and base-catalyzed thiol-isocyanate reactions are demonstrated as modular platforms for the rapid and practical fabrication of highly functional, multicomponent surfaces under ambient conditions. Brush surfaces expressing a three-dimensional configuration of alkyne or isocyanate functionalities were modified with high efficiency and short reaction times using a library

of commercially available thiols.

In the third study, two routes to multifunctional brush surfaces were demonstrated utilizing orthogonal thiol-click reactions. In the first approach, alkyne-functionalized homopolymer brushes were modified with multiple thiols via a statistical, radical-mediated thiol-yne co-click reaction; and in the second approach, statistical copolymer brushes carrying two distinctly-addressable reactive moieties were sequentially modified via orthogonal base-catalyzed thiol-X (where X represents an isocyanate, epoxy, or α-bromoester) and radical-mediated thiol-yne reactions.

In the fourth study thiol-click PPMs are investigated in depth to determine how surface constraints affect the modification process by probing the penetration depth of functional thiol modifiers into pendent isocyanate-containing polymer brushes via neutron reflectivity studies. Also, the synthesis of tapered block copolymer brush surfaces was demonstrated by exploiting the inherent mass transport limitations of post-polymerization modification processes on reactive brush surfaces.

In the fifth study a post-polymerization surface modification approach providing pendent thiol functionality along the polymer brush backbone using the photolabile protection chemistry of both *o*-nitrobenzyl and *p*-methoxyphenacyl thioethers was developed. Addressing the protecting groups with light not only affords spatial control of reactive thiol functionality but enables a plethora of thiol-mediated transformations with isocyanates and maleimides providing a modular route to create functional polymer surfaces.

The University of Southern Mississippi

POLYMER SURFACE ENGINEERING VIA THIOL-MEDIATED REACTIONS

by

Ryan Matthew Hensarling

A Dissertation
Submitted to the Graduate School
of The University of Southern Mississippi
in Partial Fulfillment of the Requirements
for the Degree of Doctor of Philosophy

Approved:

_Derek L. Patton_____
Director

_Sarah E. Morgan_____

_Marek W. Urban_____

_Charles L. McCormick_____

_James W. Rawlins_____

_Sarah A. Siltanen_____
Dean of the Graduate School

December 2012

DEDICATION

This dissertation is dedicated to my wonderful family for their love and support throughout the years.

To my parents, David and Sheilda, for their guidance, wisdom, and encouragement.

To my brother and nephew, Brad and Landon, for their inspiration.

To my fiancée, Diana, for her patience in all circumstances, selflessness, and immeasurable love.

To all my family, thank you for being there during life's ups and downs, its twists and turns.

ACKNOWLEDGMENTS

First and foremost, I would like to thank my friends, family and colleagues for their continuous guidance, knowledge and support throughout my graduate career. I would like to especially thank my advisor, Dr. Derek L. Patton, for his enthusiasm, scientific wisdom and friendship along the way. It has been an honor to work alongside him in the lab from the very beginning. Thanks for being a great mentor and always challenging me to do my best and think independently. I would also like to acknowledge my committee members – Drs. Sarah E. Morgan, Charles L. McCormick, Marek W. Urban and James W. Rawlins – for constant support and insightful suggestions from time to time. I would like to acknowledge the late Dr. Charles E. Hoyle for his pioneering work involving thiol-click chemistry and passion for science he instilled on me the brief time I knew him on a personal level. I would like to thank all the secretarial staff within the School of Polymers and High Performance Materials, in particularly, Mrs. Jody, Mrs. Beverly and Mrs. Candy for their assistance no matter what the circumstances.

I would also like to thank past and present members of the Patton Research Group – Santosh, Brad, Austin, Matt, Jananee, Wei, Emily, Li, Yidan, Stephen, Arthur, Ethan, Jared and Laken – for always keeping it interesting in the lab. Thanks for all the encouragement, laughter and helpful discussions. I would like to especially thank everyone I have had the privilege to collaborate with – Santosh Rahane, Arthur Leblanc, Brad Sparks, Wei Guo, Emily Hoff, Dr. Chris Stafford, Evan White, Dr. Jason Locklin, Vanessa Doughty and Dr. Justin Chan. It has been a pleasure to work with everyone throughout my graduate career. Special thanks to all the summer undergraduate students

– Vanessa, Wendy, Jake, Will and Eric – that I have had the privilege to mentor. Through the years, they have taught me more about myself than I taught them about polymer chemistry.

To all my friends and family, you know who you are, thank you for always being there for support in the difficult and challenging times. I am grateful to be able to pursue a life-long dream only a few minutes away from home. I thank my parents, grandparents, brother and nephew for always believing in me, even when I did not believe in myself.

Last but not least, I give my utmost appreciation for Diana, my fiancée and best friend. I thank you for your constant encouragement and understanding through all the long days and late nights in the lab. She has inspired me to do my best in all aspects of life and I look forward to the next chapter we will embark upon.

TABLE OF CONTENTS

LIST OF TABLES

Table

LIST OF ILLUSTRATIONS

Figure

LIST OF SCHEMES

Scheme

LIST OF ABBREVIATIONS

Å	angstroms
ACC	azide-alkyne cycloaddition
AFM	atomic force microscope
AgOTf	silver triflate
AIBN	azobisisobutyronitrile
Allyloxy-HPP	2-hydroxy-4’-(2-allyloxyethoxy)-2-methyl-propiophenone
AMA	allyl methacrylate
ATR-FTIR	attenuated total reflection – fourier transform infrared spectroscopy
b	block
BHT	butylated hydroxyl toluene
BrMA	2-(2-bromopropanoyloxy) ethyl methacrylate
$CDCl_3$	deutrated chloroform
CH_2Cl_2	dichloromethane
CO_2	carbon dioxide
COOH	carboxylic acid
C≡N	nitrile
CRP	controlled radical polymerization
Cu	copper
CuACC	copper-catalyzed azide-alkyne cycloaddition
Cu(I)Br	copper (I) bromide
CVD	chemical vapor deposition
DBU	1,8-diazabicyclo[5.4.0]undec-7-ene

DCM	dichloromethane
DDT	1-dodecanethiol
d_{25}-DDT	deutrated dodecanethiol
DI	deionized
DIPC	N,N'-diisopropyl carbodiimide
DMAEMA	dimethylaminoethyl methacrylate
DMAP	4-dimethylaminopyridine
DMAPS	N,N'-dimethyl-(methylmethacryloyl ethyl) ammonium propanesulfonate
DMF	dimethylformamide
DMPA	2,2-dimethoxy-2-phenyl acetophenone
DMPP	dimethylphenylphosphine
DNA	deoxyribonucleic acid
d_7-PPT	deutrated propanethiol
d-thiol	deutrated thiol
DTT	1,4 dithiothreitol
ESI-MS	electrospray ionization mass spectrometry
Et_3N	triethylamine
Et_2O	diethylether
EtOAc	ethyl acetate
FTIR	fourier transform infrared spectroscopy
GATR-FTIR	grazing-angle attenuated total reflection - fourier transform infrared spectroscopy
GMA	glycidyl methacrylate

grad	gradient
h	hour
H_2O	Water
HCl	hydrochloric acid
HDT	1,6-hexanedithiol
HEMA	hydroxyethyl methacrylate
HPP	2-hydroxy-4’-2-methylpropiophenone
HPP-$SiCl_3$	2-hydroxy-4’-(2-hydroxyethoxy)-2-methylpropiophenone trichlorosilane
HS-ssDNA	thiolated single-strand deoxyribonucleic acid
I	initiator
IR	infrared
K_2CO_3	potassium carbonate
KI	potassium Iodide
KOH	potassium hydroxide
LR	liquids reflectometer
MEG	maleimide-ethylene glycol disulfide
MeOH	methanol
$MgSO_4$	magnesium sulfate
min	minutes
MPA	3-mercaptopropionic acid
MPPMs	microporous polypropylene membranes
MPS	3-mercapto-1-propanesulfonic acid

MW	molecular weight
mW	milliwatts
N_2	nitrogen
NaCl	sodium chloride
NaOH	sodium hydroxide
n-BuLi	n-Butyl lithium
N	normal
NCO	isocyanate
NCOMA	2-isocyanatoethyl methacrylate
NH_2	amine
nm	nanometer
NMP	N-methylpyrrolidone
NMR	nuclear magnetic resonance
NO_2	nitrogen dioxide
NPC	p-nitrophenyl chloroformate
NR	neutron reflectivity
OCH_3	methoxy
OH	hydroxy
o-NB	ortho-nitrobenzyl
PAMA	poly(allyl methacrylate)
p(BrMA)	poly(2-(2-bromopropanoyloxy)ethyl methacrylate)
pDMAEMA	poly(dimethylaminoethyl methacrylate)
PDMS	polydimethylsiloxane

PEG-NH_2	amine functionalized poly(ethylene glycol)
p(GMA)	poly(glycidyl methacrylate)
PgMA-TMS	(3-trimethylsilylpropargyl) methacrylate
PgOH-TMS	3-trimethylsilyl-2-propyn-1-ol
pH	potential hydrogen
pHEMA	poly(hydroxyethyl methacrylate)
p-MP	para-methoxyphenacyl
pNCO	poly(isocyanatoethyl methacrylate)
pNCO-d_{25}-DDT	poly(isocyanatoethyl methacrylate) modified with deutrated dodecanethiol
pNCO-d_7-PPT	poly(isocyanatoethyl methacrylate) modified with deutrated propanethiol
POSS	mercaptopropylisobutyl Polyhedral Oligomeric Silsesquioxane
p(PgMA)	poly(propargyl methacrylate)
p(PgMA-TMS)	poly((3-trimethylsilylpropargyl) methacrylate)
PPGs	photolabile protecting groups
ppm	parts per million
PPM	post-polymerization modification
PPMA	poly(propargyl methacrylate)
Pt	platinum
PVDF	poly(vinylidene fluoride)
Q	wave vector transfer
r.t.	room temperature
SAMs	self-assembled monolayers

SEM	scanning electron microscopy
Si	silicon
SI-ATRP	surface-initiated atom transfer radical polymerization
SIP	surface-initiated polymerization
SN_2	bimolecular nucleophilic substitution
SiO_2	silicon dioxide
SIP	surface-initiated polymerization
SH	thiol
SLD	scattering length density
stat	statistical
REO	robust, efficient, orthogonal
TEA	triethylamine
TEM	transmission electron microscope
THF	tetrahydrofuran
TMS	trimethylsilane
TMSCl	trimethylchlorosilane
UV	ultraviolet
v	volume
W	watts
WCA	water contact angle
X	thiol or amine (Ch. IV) or isocyanate, epoxy, α-bromoester (Ch. V)
XPS	x-ray photoelectron spectroscopy
yne	alkyne

β-CD	beta-cyclodextrin
μCP	microcontact printing
2D	two-dimensional
3D	three-dimensional

CHAPTER I

BACKGROUND

Surface Engineering

Surface engineering collectively describes a set of processes – both physical and chemical – for the design and modification of surfaces, or the near-surface regions of a material enabling the surface to perform functions that are distinct from those functions demanded from the bulk of the material.[1] Independent control of the surface structure and chemical properties correlates to unique structure – property relationships with significant scientific interest and technological importance. As surfaces are ubiquitous in nature, surface engineering has played an important role in enabling technologies for everyday applications such as corrosion inhibition, wear resistance, antifouling, biomedical implants, and drug delivery systems among many others. Demand for these applications is increasing the necessity to fabricate soft material surfaces with precise control over architecture, domain size, functionality, polarity, and reactivity. Within the last decade, numerous strategies highlight the facile introduction of functional moieties onto the periphery (two-dimensional "2D") or throughout (three-dimensional "3D") planar and dimensionally complex surfaces. This background chapter will discuss several surface modification techniques with emphasis on the combination of surface-initiated polymerization and post-polymerization modification to control the interfacial chemistry of materials.

Self-Assembled Monolayers (SAMs)

Self-assembled monolayers (SAMs) are an organized layer of amphiphilic molecules in which one end of the molecule, the "head group", shows a preferential

affinity for a substrate, while the terminal end or "tail group" exhibits specific functionality in order to vary the wetting and interfacial properties of the surface. Selecting the type of head group depends on the application of the SAM and the specific identity of the substrate (i.e. oxides, noble metals, etc.). Luckily, the formation of a monolayer on the surface is not governed by the substrate used. Substrates can be planar surfaces, such as silicon and metals, or curved surfaces, such as nanoparticles enabling a broad range of technologies/applications to be targeted. The most widely studied systems of SAMs are gold-alkylthiolate, alkoxysilane and/or alkylphosphonic acid monolayers (Scheme 1). Several reviews have highlighted the utility of these systems.[2-4] Allara and Nuzzo produced the first gold-alkylthiolate monolayer in 1983 where they realized the utility of combining a relatively inert gold surface with a bifunctional organic molecule in a well-ordered, regularly oriented array.[5] Alkanethiols are molecules with an alkyl chain as the tail group and a thiol (SH) head group. Thiol molecules are used on noble metal substrates because of the strong affinity of sulfur for these metals. Alkanethiol and phosphonic acid SAMs produced by adsorption from solution are prepared by immersing a substrate – either a noble metal or metal oxide surface, respectively – into a dilute solution of either functional alkanethiol or phosphonic acid in ethanol for an extended period of time (e.g. 12 to 72 h) at room temperature followed by drying.[6] SAMs can also be adsorbed from the vapor phase. Alkoxysilane SAMs are often created in a reaction chamber under reduced pressure by silanization in which silane vapor flows over the substrate to form the monolayer.[7] Using this self-assembled approach, long chain aliphatic tail molecules have the ability to fully extend maximizing packing density and van der Waals interactions.[7] Also, a nice feature inherent to these systems is the

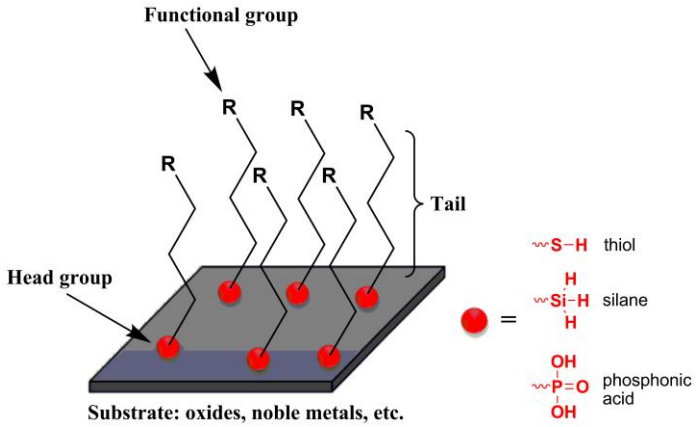

Scheme 1. Self-assembled Monolayers (SAMs) utilizing thiol, silane, and phosphonic acid "head groups" to facilitate chemisorption to oxide or noble metal substrates.

introduction of almost any functional group onto the surface. However, defects are inevitable and the functionality of the surface is only two dimensional, meaning functional groups are only present at the interface. To overcome these issues polymer brushes that exhibit a three dimensional configuration greatly enhance the functionality of the surface.

Polymer Brushes

Polymer brushes refer to an assembly of polymer chains tethered by one end to a surface or an interface, where the graft density of surface-attached polymers is sufficient enough to force the chains to stretch away from the surface avoiding overlap.[8] This stretched configuration of the polymer chains attached to the surface differs significantly from the random-walk configuration of polymer chains in solution, affecting the interfacial behavior of the tethered chains spawning many novel properties as a result.[9] The three dimensional brush conformation greatly extends the number of functional groups per unit of surface area due to the fact that each monomer unit is capable of carrying a functional moiety, ultimately, offering an opportunity to present functional

groups not only at the interface, but also throughout the interface.[10,11] Advantageous to surface engineering, modifying the interfacial properties of a material with polymer brushes does not sacrifice the underlying bulk properties. Polymer brushes can be used to control surface properties such as, but not limited to, biocompatibility, wettability, corrosion resistance, friction, affinity to a specific target molecule, and adsorption capacity.

"Grafting – To" Approaches

Methods of fabricating polymer brushes on solid substrates fall under two categories: 1) "grafting – to" or 2) "grafting – from" techniques.[8] Scheme 2 depicts the grafting – to and grafting – from approaches. These approaches are vastly superior to self-assembled monolayers where functionality is limited to the outermost edge of the interface. The grafting – to approach involves tethering pre-made chains to the surface, either by preferential physisorption[12-19] or via covalent attachment[20-24] between reactive surface sites and end-functionalized polymers. Grafting – from approaches, which will be discussed later, involve growing chains from surface – bound initiators.[25] As suggested in Scheme 2a, physisorption of amphiphilic block copolymers proceeds by adsorbing and self-assembling onto a substrate in the presence of selective solvents or surfaces, where one block interacts strongly with the surface and the other block extends from the surface generating a polymer layer.[26,27] The polymer brush structure resulting from this approach is dependent on the selectivities of the solvent or surface, the nature and architecture of the copolymers, the length of each block and the interactions between the blocks and the surface.[8] In these systems, solvent and surface choice is chosen carefully in order to collapse one block of the copolymer and allow for the maximum

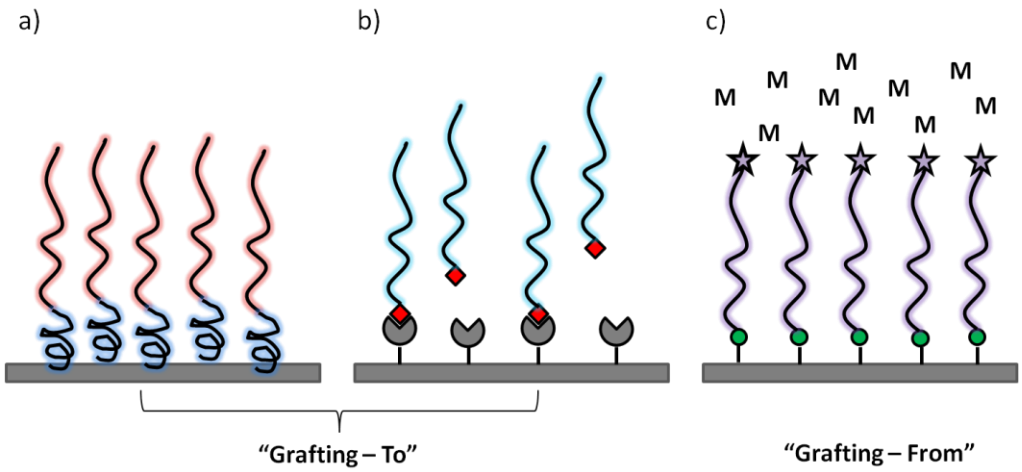

Scheme 2. Strategies for fabrication of polymer brushes: a) physisorption of amphiphilic diblock copolymers, b) covalent attachment of pre-made end-functionalized polymer chains, and c) surface-initiated polymerization.

preferential adsorption to the surface, respectively, while the other block is well-solvated and able to extend. However, the non-covalent adsorption renders the brush layer susceptible to thermal and solvent instabilities. Devising a way of covalently attaching the polymer chains to the surface overcomes the limitations of physisorption.

The tethering of polymer chains to surfaces, or covalent grafting – to approaches, involves reacting end-functionalized polymer chains with an appropriate complementary functionality on the surface (Scheme 2b).[20,28] The polymer brushes formed are robust and resistant to various chemical and physical environments due to covalent linkage formation between the surface and the polymer chains. Another salient feature of the grafting – to method is the fact that the chain size, composition and architecture can all be controlled and characterized before assembly onto the surfaces. Reviews by Azzaroni[29] and Luzinov et al.[30] have well-documented the preparation and application of polymer brushes via grafting – to methods. However, both the physisorption and covalent grafting – to approach suffer in terms of the maximum grafting density achievable. After

significant coverage of the surface with polymer chains, additional polymer molecules in solution are unable to effectively diffuse through to the reactive surface sites due to steric hinderance associated with the polymers already attached to the surface.[31,32] This hinderance halts the growth of the film resulting in low grafting density and film thickness on the surface.[33] To circumvent this issue, the grafting – from approach has become the method of choice to prepare thick, covalently attached polymer brushes with high grafting density.

"Grafting – From" Approaches

The grafting – from technique involves polymer brush formation in situ from surface-bound initiators.[25] Specifically, almost any planar or particle surface can be modified with initiator-bearing groups by choosing the anchoring functionality carefully (i.e. thiols on gold, silanes on glass, Si/SiO_2 and plasma oxidized materials) as previously described in the SAM approach. Upon initiator-immobilization, surface-initiated polymerization (SIP) is subsequently performed in the presence of a solution containing monomer in order to generate tethered polymer brushes (Scheme 2c).[8,32,34-36] Steric hinderance does not present any issues due to the fact that initiator and monomer species are relatively small as compared to macromolecular chains permitting brushes with high grafting density to be achieved.[37] SIP represents one of the most effective and versatile methods for tailoring the physicochemical properties of surfaces.[25,38] SIP offers a direct means to control the density, thickness, and functionality of ultrathin films by growing polymer chains directly from surface. The ability to endow a surface with 3D functionality has tremendous advantages for applications where high functional group densities are required, e.g. membranes and biosensor chips.[39] When properly designed,

polymer films fabricated by SIP are extremely stable under a variety of environmental conditions owing to the covalent interaction of the polymer chains with the substrate surface. Additionally, the ability to conformally modify substrates of any geometry with outstanding film homogeneity at nanometer thicknesses offers many advantages over solution cast films. Several recent reviews highlight the fabrication strategies and utility of SIP.[8,40] A variety of polymerization methods utilizing SIP techniques exist, including thermal[37,38] and photo-initiated[41,42] free-radical polymerizations, living anionic and cationic polymerizations,[43] and controlled radical polymerization (CRP) techniques,[44-46] to produce surface-tethered polymer layers via the grafting – from approach. Combining SIP with CRP techniques provides a means of growing precisely defined polymer structures from surfaces. The most widely used CRP method for growing surface brushes is surface-initiated atom radical transfer polymerization (SI-ATRP) which allows for polymer growth in a controlled fashion where each repeat unit bestows specific functionality.[11,25] SI-ATRP also has the benefit of allowing the synthesis of polymers with end groups capable of reinitiating polymerization, which is useful should copolymer structures with controlled block sizes be desired.

Post-polymerization Modification (PPM)

Despite recent advances in the SIP approach, there remains a large number of pendent functional groups that cannot be directly polymerized from the surface due to i) exorbitant cost of functional monomer synthesis and/or ii) intolerance of the functional moiety in the polymerization process (i.e. reactivity, steric bulk). This often necessitates the development of a modular approach to surface engineering in the form of post-polymerization modification (PPM). As schematically illustrated in Scheme 3, post-

polymerization modification of brushes can involve modification of polymer chain ends and/or side-chain functional groups with the potential for a combination of both. Among different techniques of functional soft surface engineering, the combination of SIP and PPM offers unique advantages where the latter provides an avenue to tailor the properties of the surface beyond what the original polymer brush possesses.[11,47-50] Surface-initiated polymerization opens the door to highly controlled polymer structures on the surface from a variety of commercially available monomers. Post-polymerization modification, on the other hand, is based on the direct polymerization of monomers bearing chemoselective handles that are inert towards the polymerization conditions, but can be quantitatively converted to a broad range of functional groups in a subsequent step.[51] PPM enables one to take full advantage of the versatility of the SIP technique while extending the range of functional groups that can be bestowed to the surface. As highlighted by recent reviews by Klok et al.,[40,51] a plethora of efficient, high-yield reactions under mild conditions can be used to modify polymer brushes. The next section focuses mainly on these recent advances utilizing click chemistry for post-modification of polymers covalently attached to surfaces.

Click Chemistry for Post-polymerization Modification

"Click" chemistries are known as "Robust, Efficient, Orthogonal" (REO) strategies to tailor-make polymeric materials with specific function. Tailoring the chemical composition of the material interface is a major impetus of surface engineering. In recent years, this impetus has been particularly driven by the desire to endow surfaces with well-defined chemical functionality, with high specificity and conversion, and with fine control over the spatial arrangement of the surface chemical composition. Among

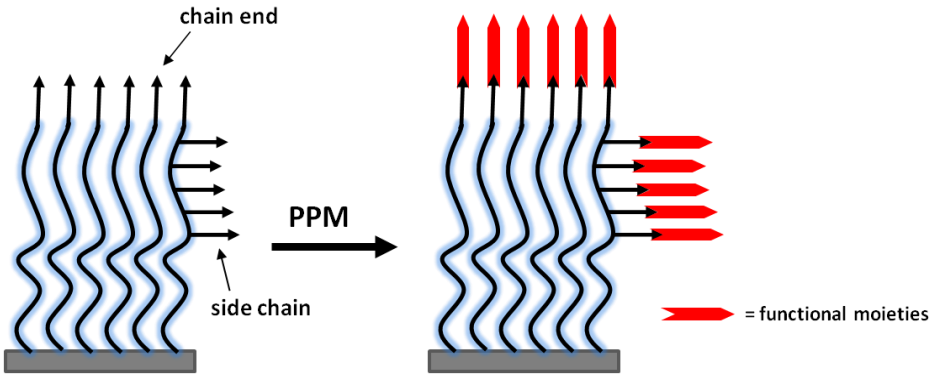

Scheme 3. Postmodification of polymer brushes: chain end and/or side chain functionalization.

several PPM strategies reported for surface modification, those that exploit "click" reactions, such as the archetypical copper catalyzed azide-alkyne Huisgen 1,3-dipolar cycloaddition (CuAAC),[52-56] are particularly attractive for transforming the aforementioned desires into the realities of precisely engineering the chemical composition of surfaces. The click approach to engineer surfaces circumvents several limitations often associated with conventional conjugation chemistries including poor conversions on the surface, harsh reaction conditions, side reactions, and the need for highly active reactants which often require extensive synthetic preparation. A recent review by Nebhani and Barner-Kowollik[55] highlighted the admirable characteristics of CuAAC for engineering a variety of functional surfaces. However, concern over the presence of residual metal impurities following copper-catalyzed click reactions has motivated the development of alternate, metal-free surface modification strategies. Consequently, a wide variety of metal-free click reactions – such as strain promoted azide-alkyne cycloadditions,[50,57-60] and Diels-Alder cycloadditions[61-65] – are increasingly becoming methods of choice to synthesize functional surfaces particularly in the realm of biomaterials.

In a complementary direction to those metal-free click reactions previously mentioned, thiol-based click reactions provide a powerful approach for engineering multifunctional surfaces in a modular fashion. Specifically, thiols readily react with electron rich alkenes (radical-mediated), alkynes (radical-mediated), electron poor alkenes (amine or phosphine catalyzed), isocyanates (amine catalyzed), epoxies (amine catalyzed SN_2 ring opening), and halogens[66-68] (amine catalyzed SN_2 nucleophilic substitution) creating a diverse thiol-click toolbox which exploits a large library of functional moieties for rapid manipulation of surface properties (Scheme 4).[69] The utility of the PPM strategy has been highlighted in several recent approaches implementing thiol-click reactions for the modification of the interfacial properties of materials without sacrificing bulk properties.[70-74]

Thiol-click reactions are advantageous for this purpose in that they proceed at room temperature with high efficiency and rapid kinetics, in the presence of oxygen/water, without expensive and potentially toxic catalysts, and are highly tolerant of a wide range of functional groups.[69,75-77] The efficacy and click-like characteristics of these reactions have been amply demonstrated in areas of macromolecular design,[78-82] post-polymerization modification,[83-90] hyperbranched polymers,[91,92] particle derivatization,[93-95] and even bioconjugation.[96-98] In many cases, these thiol-click transformations fulfill the robust-efficient-orthogonal (REO) strategy by proceeding orthogonally with one another (i.e. radical-mediated thiol-yne and base-catalyzed thiol-ene[99]) and with other click reactions such as the CuAAC and Diels-Alder cycloadditions providing a powerful approach to engineer surfaces with complex architectures and multicomponent chemistries.[100]

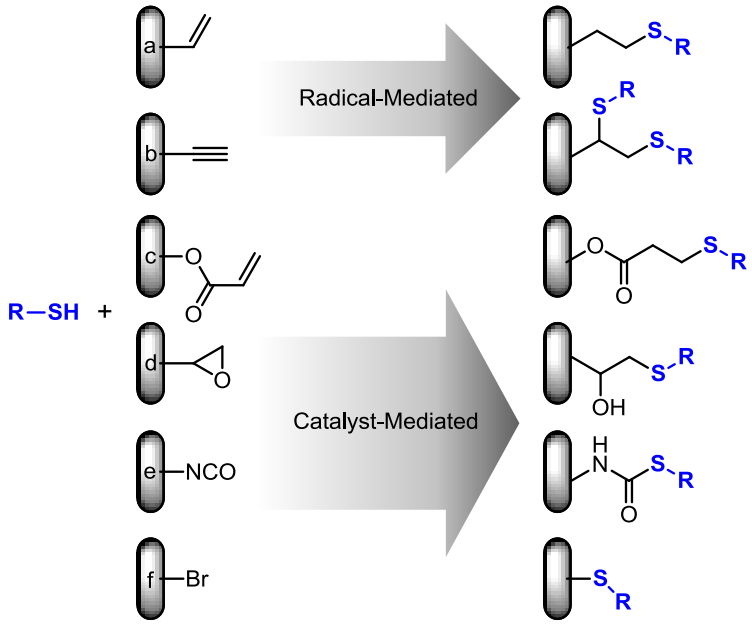

Scheme 4. Thiol-based reactions for surface engineering: a) radical-mediated thiol-ene, b) radical-mediated thiol-alkyne, c) base or phosphine catalyzed thiol-Michael addition, d) base catalyzed thiol-epoxy ring opening, e) base catalyzed thiol-isocyanate, and f) base catalyzed thiol-halogen substitution. The reverse configuration of reactants (i.e. thiol-functionalized surface) is also possible and is often exploited.

In the next section, the goal is to provide a comprehensive literature review of works illustrating simple, versatile, and modular synthetic methods for modifying surfaces based on thiol-click reactions. Rather than the specific type of thiol-click reaction used, the examples are organized based on the type of substrate surface being modified, including i) Monolayers and Other Ultrathin Films, ii) Polymer Surfaces, and iii) Microporous Membranes.

Thiol-click Surface Engineering

Monolayers and Other Ultrathin Films

Modifying the terminal group of self-assembled monolayers (SAMs) via thiol-click reactions offers a viable way to add two-dimensional functionality to either planar or curved surfaces enabling control over interfacial properties such as wetting and

adhesion, chemical resistance, bio-compatibility, sensitization, and molecular recognition for sensors and nano-fabrication.[101] To date, Michael-type thiol-ene[102-104] as well as radical-mediated thiol-ene[105-108] and thiol-yne[108] reactions have been utilized to modify the terminal group of SAMs creating complex functional surfaces used for microarrays to biochips. Inherent to SAMs, the surface-attached molecules have the ability to fully extend, maximizing packing density and Van der Waals interactions allowing for a dense distribution of desirable functionality at the air interface upon surface modification with thiol-click reactions.[7]

As an approach to engineer functional SAMs, Michael-type thiol-ene conjugations involving the reaction between thiols and maleimides have perhaps received the most attention in recent years – particularly for immobilization of biomolecules. The thiol-maleimide reaction exhibits several salient features that are particularly attractive for bio-immobilizations, including selectivity in the presence of multiple functional groups, rapid and quantitative conversions at low concentrations, and minimal synthetic modification of ligands prior to immobilization. In an early example, Schreiber et al.[109] exploited these features for the preparation of printed microarrays to probe protein-ligand interactions using maleimide-terminated SAMs to conjugate several cysteine-containing bio-ligands (i.e. biotin) to the surface. Similarly, Mrksich and coworkers fabricated peptide and carbohydrate biochips via Michael-type thiol-ene reactions of thiol-functionalized glycosides and peptides on maleimide-functionalized SAMs,[102] while Corn et al.[110] used thiol-terminated SAMs as a platform for the immobilization of maleimide-terminated nucleic acids. The key for successful biomolecule immobilization for microarray applications is preventing nonspecific interactions with biomolecules,

while enabling quantitative analysis of specific binding events. To improve deoxyribonucleic acid (DNA) hybridization from complex media for DNA microarray and biosensor applications, Castner and co-workers investigated the surface structure and performance of thiolated single-strand DNA (HS-ssDNA) immobilized onto maleimide-ethylene glycol disulfide (MEG) monolayers on gold.[103] The MEG thiolate monolayers were formed via a single-step solution self-assembly process, as opposed to a conventional approach involving the preparation of an amino-terminated layer followed by reaction with a bifunctional linker molecule that contains both an amino-reactive site and a maleimide group. The combination of surface-exposed maleimide functional moieties within a background of inert ethylene glycol units aided in selective and efficient reactivity toward HS-ssDNA end groups while providing resistance to nonspecific binding of DNA and proteins. Michael-type thiol-ene additions between maleimides and thiols are ideal due to being stable in aqueous environments as well as the inherent maleimide selectivity toward thiols.[103] In a similar approach, Magnusson and co-workers immobilized cysteine-functionalized chemoattractant peptides onto mixed SAMs composed of maleimide- and hydroxyl-terminated oligo(ethylene glycol) alkyldisulfides.[104] The mixed monolayer approach allowed for site-specific immobilization of peptides via Michael-type thiol-ene reactions along with spatial and temporal control of chemoattractant distribution to develop defined circumstances for recruitment and activation of cells.

Radical-mediated thiol-ene and thiol-yne reactions have also been demonstrated as versatile approaches to engineer the chemistry of SAM surfaces. In an early example, radical-mediated thiol-ene was employed to graft linseed oil onto a thiol functionalized

aluminum surface to investigate thin vegetable oil films for friction reduction.[106,111] The ability to initiate thiol-ene and thiol-yne reactions with light is particularly attractive as a way to fabricate multicomponent functional surfaces using photopatterning techniques.[105,107,108] Zuilhof and coworkers[107] developed radical-mediated thiol-ene click chemistry as an efficient, facile route to create patternable biofunctional monolayers on silicon hydride substrates – an approach advantageous for oxide-free silicon substrates useful for biofunctional electronic applications. H-terminated Si(111) surfaces were reacted with neat 1,13-tetradecadiene at 80 °C under an inert atmosphere for 16 h to facilitate the covalent attachment of an alkene-terminated monolayer. Under ambient atmosphere, the alkene-terminated monolayer was then exposed to 365 nm light in the presence of various thiols such as thioglycolic acid, 3-mercaptopropyl tetraacetate, 9-fluorenylmethoxy-carbonyl cysteine and a typical photoinitiator, 2,2-dimethoxy-2-phenylacetophenone (DMPA), at room temperature employing minimal amounts of solvent to solubilize the thiols. High surface coverage of the attached thiols was achieved (45 – 75%) for a wide variety of functional thiols, while maintaining oxide-free surfaces. Zuilhof and coworkers[107] extended their approach by combining photo-induced thiol-ene reactions with microcontact printing (μCP) to prepare chemical patterns on alkene-terminated oxide-free surfaces. In this approach, a PDMS stamp with pillar features was inked with thioglycolic acid and brought into conformal contact with the alkene-terminated monolayer. UV irradiation through the backside of the transparent stamp facilitated the thiol-ene reaction in the contacted area resulting in circular patterns of carboxylic acid groups. Ravoo and colleagues[112] extended the scope of photochemical μCP to include thiol-ene and thiol-yne reactions on alkene and alkyne-terminated alkoxy-

silane monolayers. In 2011, Ravoo et al.[108] further probed structure-reactivity relationships for a range of fluorescent thiols undergoing photoinduced thiol-ene or thiol-yne reactions with alkene or alkyne terminated SAMs, respectively, within the nanoconfined environment between the PDMS stamp and the substrate. Using fluorescence intensity of the modified SAM, the authors probed the reactivity of various thiol/ene and thiol/yne pairs (i.e. aromatic thiol versus aliphatic thiol) and found the structure-reactivity relationships for confined reactions were similar to those observed in solution (i.e. electron-poor alkynes react with thiols faster that electron-rich alkynes). The dependence of confined thiol-click reactions on irradiation conditions (i.e. UV vs. visible vs. dark) was also developed by monitoring the fluorescence intensity of the fluorescent thiol-modified alkene surfaces in respect to printing time and light conditions.[108] As expected, under irradiation with UV light the reaction rate was the highest, while under ambient light conditions, the yield was still remarkably high. However, the reactions proceeded very slowly in the dark suggesting that the confinement plays little role in mediating the thiol-click surface reactions.

Direct photomasking and writing strategies with radical-mediated thiol-ene reactions have also been demonstrated on other ultrathin film platforms. For example, Waldmann and coworkers used the thiol-ene reaction to pattern proteins and other biomolecule arrays onto surfaces using a biotin/streptavidin approach.[113,114] Silicon wafers were first modified with a thin film of COOH-terminated dendrimers followed by conversion to thiol or ene-modified surfaces. The thiol-terminated surface was coated with an olefin-modified biotin derivative (or vice versa for the ene-terminated surface) and then exposed to UV light through a photomask, yielding the thioether linkage and

biotin micropatterns. Exposure of the biotin-modified surfaces to Cy5-labeled streptavidin provided homogeneous protein patterns over centimeter-wide areas. The patterns were also used to demonstrate protein-protein interactions, indicating that the thiol-ene based immobilization strategy provided immobilized proteins with retention of their structure and function, as well as a preferred orientation.[97] Waldman et al. further demonstrated protein immobilization onto biotin line patterns using a laser scanned over the surface to directly facilitate the thiol-ene reaction between the thiol surface and the olefin-modified biotin derivative.[113]

Photolabile protecting groups (PPGs) can be removed upon exposure to light under neutral and reagent-free conditions to yield reactive functional groups (e.g. acids, alcohols, amines, and thiols).[115,116] As a stimulus for deprotection, light has the added benefit of spatial and temporal control when used for surface patterning. Smith et al.[117] employed the PPG approach to design "caged" thiol monolayers on amorphous carbon surfaces for thiol-click mediated biomolecule immobilization. In this approach, an *o*-nitrobenzyl-protected thiopropyl phosphoramidite moiety was immobilized onto a hydroxyl-terminated oligo(ethylene glycol) layer on ultrathin amorphous carbon (15 nm). Photolytic cleavage of the *o*-nitrobenzyl protecting group was performed using a maskless array synthesizer with programmed illumination locations generating thiol reactive functionality only in the light exposed areas. These reactive thiols enabled the attachment of biomolecules onto the surface pattern via thiol-maleimide reactions and disulfide exchange. This strategy enabled facile covalent attachment of biotin, DNA, and proteins while maintaining their biological activity.

Polymer Surfaces

This dissertation focuses on designing polymer brush platforms through SIP that bear specific pendent functional groups amenable to thiol-click PPMs. The research herein investigates radical mediated thiol-yne,[71] base-catalyzed thiol-isocyanate,[72] thiol-epoxy, and thiol-bromo chemistries[73] along with Michael-type thiol-ene reactions as modular PPM brush platforms fulfilling REO requirements for the rapid fabrication of highly functional, multicomponent surfaces. Other polymer surface modification strategies involving thiol-click reactions are revealed below. Using difunctional thiols and difunctional enes, the Bowman research group provided early examples of employing radical-mediated thiol-ene polymerization, base-catalyzed thiol-acrylate polymerization, and combinations thereof to fabricate polymer thin films by "grafting from" either thiol or ene terminated monolayers.[118-120] The click and step-growth mechanisms of these reactions was exploited to control film thickness in a self-limiting manner by small manipulations in diene to dithiol stoichiometric ratio. Similar approaches have been used to fabricate patterned thiol-ene thin films,[105,121] and films exhibiting gradients in composition and thickness.[122]

With an ongoing theme of biologically relevant surface modifications, peptide-functionalized thin films are of great interest and have been explored for an array of applications including biomedical,[123] anti-fouling,[124] inorganic/peptide hybrids,[125] and stimuli-responsive materials.[126] Polypeptide brushes are a unique class of surface-grafted polymers in that they allow the incorporation of structural motifs typical of those found in proteins, such as α-helices, β-sheets, and random coils. Like their native counterparts in proteins, these surface-grafted motifs can respond dynamically to changes in their

environment.[127] This feature presents an opportunity to control the brush structure, function, and response at a level difficult to achieve with conventional organic polymers. In this direction, our group has recently demonstrated nickel-mediated SIP of α-amino N-carboxyanhydrides, in particular NCA-S-tert-butylmercapto-L-cysteine, to facilitate PPM of thiol-clickable polypeptide brushes.[128] This approach demonstrates the versatility of thiol-click reactions by utilizing the pendent thiol of tethered poly(cysteine) brushes upon deprotection of the tert-butyl mercapto moieties with dithiothreitol in DMF at 60 °C. Michael-type thiol-ene reactions were employed to functionalize the poly(cysteine) brushes with a fluorine-labeled maleimide. The brush functionalization was characterized by X-ray photoelectron spectroscopy (XPS), which confirmed the attachment of the pendent maleimide. Although the maleimide used in this study was convenient for XPS analysis, the modification of the pendent thiol can easily be extended to other "enes" carrying pendent moieties useful for a broad range of applications, i.e., bioconjugation.

In most cases, the creation of functional surfaces via SAMs or SIP requires specific surface chemistry as anchoring groups as a first step, i.e. thiols on gold or silanes on oxides. The specificity of the anchoring step can potentially limit the types of surfaces that can be facilely modified in a post-modification approach. Chemical vapor deposition (CVD) polymerization decouples the polymerization process from the underlying substrate significantly broadening the range of materials that may serve as substrates.[129] Additionally, a number of unique attributes arise from the CVD process, such as coating conformity, film homogeneity, solvent-free environments, and absence of initiators and plasticizers.[130-132] In 2012, Chen and co-workers[133] combined CVD with thiol-ene and

thiol-yne post-modification processes to demonstrate a versatile, and substrate-independent route to functional polymer films. Alkene and alkyne functionalized polymers, poly(4-vinyl-p-xylylene-co-p-xylylene) and poly(4-ethynyl-p-xylylene-co-p-xylylene) were prepared via CVD polymerization of 4-vinyl[2.2]paracyclophane and ethynyl-[2.2]paracyclophane, respectively, onto various substrates (silver, titanium, stainless steel, polystyrene, poly(methyl methacrylate), silicon, glass, poly(dimethylsiloxane), and poly(tetrafluoroethylene)) to support thiol-ene and thiol-yne click reactions.[133] Thiol-terminated poly(ethylene glycol) molecules as well as cell-adhering peptides containing thiols were used to investigate click reactions for antifouling and protein adsorption applications on various substrates. The specific activation locations were resolved using a high-resolution photomask enabling activation of the thiol-ene/thiol-yne radical reactions only in light exposed areas.

Microporous Membranes

Microporous polymer membranes have found widespread use for various applications in industry, medicine, pharmacology, and for separation of particles, colloids, proteins, enzymes, and cells. For many membrane applications, it would be desirable to have straight forward surface engineering approaches that enable the simple alteration of surfaces, for example to prevent biofouling, without significantly altering the properties of the bulk membrane material. For example, the hydrophobic nature of common polymers (i.e. poly(vinylidene fluoride) (PVDF) and poly(propylene)) used in microporous membrane applications limit their practical use. In this sense, thiol-click reactions, particularly radical-mediated thiol-ene[134] and thiol-yne[135,136] processes, have proven to be a viable approach to improve membrane performance for purposes such as

fouling minimization, hydrophilicity/hydrophobicity modulation, biocompatibility, biomembrane mimicry, as well as providing bio- and/or chemical functionalities that differ from the bulk membrane composition.

Kang and co-workers[134] synthesized functional poly(vinylidene fluoride) (PVDF) copolymer membranes via thermally-induced graft copolymerization of allyl methacrylate (AMA) from ozone-preactivated PVDF chains (PVDF-g-PAMA). Microporous membranes were prepared from PVDF-g-PAMA by phase inversion from 15 wt. % polymer solutions (NMP solvent) in water. The (PVDF-g-PAMA) graft copolymer membranes with active allyl groups served as a platform for surface modification via radical-mediated thiol-ene and thiol-Michael reactions. PVDF-g-PAMA membranes were modified initially through thermally-induced radical-mediated thiol-ene coupling of 3-mercaptopropionic acid (MPA) or 1,6-hexanedithiol (HDT) in the presence of azobisisobutyronitrile, AIBN, at 70 °C under an argon atmosphere for 24 hours.[134] Successful immobilization of MPA and HDT onto PVDF-g-PAMA membranes was observed by XPS. The MPA-modified membranes exhibited pH-dependent permeability in aqueous solutions. Changes in the permeability were attributed to changes in the conformation of carboxylic acid functionalized graft chains on the membrane surface and within the pores upon changes in pH. Modification of the membrane with HDT resulted in excess thiol groups on the membrane surface, which served as reactive sites for thiol-Michael immobilization of N,N'-dimethy-(methylmethacryloyl ethyl) ammonium propanesulfonate (DMAPS) – a functional moiety known for excellent antimicrobial properties. DMAPS-modified membranes showed good antibacterial properties (S. epidermidis) under 1 mL/min flow conditions. Successful incorporation of DMAPS was

indicated by XPS and SEM, through observing changes in binding energy as well as antibacterial efficiency when exposing unmodified and modified copolymer membranes to S. epidermidis bacteria cells, respectively. Analogously, Kang and co-workers[135] demonstrated a modular membrane platform with "clickable" alkyne surfaces. The surface-enriched alkyne groups within the poly(vinylidene fluoride)-graft-poly(propargyl methacrylate) (PVDF-g-PPMA) copolymer membranes enabled tailoring of the surface via thiol-yne click reactions with thiols such as 3-mercapto-1-propanesulfonic acid (MPS), or alkyne-azide click reactions with azide-functionalized macromolecules such as azido-β-cyclodextrin (β-CD). The PDVF-g-PPMA membranes modified with MPS exhibited electrolyte-dependent permeability for aqueous solutions, while the membranes modified with azido-β-CD showed protein adsorption resistance.[135] Highly functionalized biomaterial surfaces for specific separation and purification of proteins were created by Xu and co-workers by glycosylating microporous polypropylene membranes (MPPMs) via thiol-yne click chemistry.[136] Carbohydrate-protein interactions are of great interest for mimicking the "glycoside cluster effect" by providing glycosylated or carbohydrate-decorated surfaces with a high density of saccharides for lectin recognition and affinity adsorption. Azide-alkyne click chemistry is a viable method to provide this "glycoside cluster effect" on MPPMs; however, the triazole moieties formed via the cycloaddition reaction show an affinity for the amino acid residues of proteins promoting hydrogen bonding and stacking interactions, which decrease the specific recognition capability of the glycosylated membrane.[54,137] As shown by Xu et al.,[136] the use of radical-mediated thiol-yne click chemistry yields membranes with high carbohydrate grafting densities while avoiding undesirable

interactions. UV-induced graft polymerization of acrylic acid from MPPMs provided carboxylic acid moieties on the membrane surface. The COOH groups were subsequently activated with 1-ethyl-3-[3-dimethylaminopropyl]carbodiimide hydrochloride/N-hydroxysuccinimide and reacted with propargylamine to give an alkyne-modified MPPM susceptible to reaction with 2,3,4,6-tetra-O-acetyl-β-D-glucopyranosyl thiol when exposed to UV irradiation in the presence of a photoinitiator.[136,137] The glycosylated membranes showed significant recognition specificity and affinity adsorption towards fluorescently labeled lectins (FITC-Con A).[136] Rapid modification of microporous membranes represents yet another niche were thiol-click reactions have impacted the development of specific bio-related surface functionalization without interference from the route used for immobilization.

In summary, thiol-click chemistry represents a powerful and versatile approach to engineer functional surfaces, as demonstrated by the broad scope of examples described in this section. The defining characteristics of thiol-click reactions – high efficiency, rapid kinetics, insensitivity to oxygen/water, and little to no byproduct formation – have propelled these reactions to the fore-front of surface modification strategies. It is envisioned that future research on this topic will continue to focus on optimizing existing thiol-click chemistries for application to a broader scope of substrate surfaces, as well as expand opportunities to create complex, multifunctional surfaces by combining thiol-click chemistry with numerous other click chemistries in an orthogonal fashion.

References

(1) Meguid, S. A. *Surface engineering*; Elsevier Applied Science: London; New York, 1990.

(2) Prashar, D. *Int. J. ChemTech. Res.* **2012**, *4*, 258 - 265.

(3) Samanta, D.; Sarkar, A. *Chem. Soc. Rev.* **2011**, *40*, 2567-2592.

(4) Ulman, A. *Chem. Rev.* **1996**, *96*, 1533 - 1554.

(5) Nuzzo, R. G.; Allara, D. L. *J. Am. Chem. Soc.* **1983**, *105*, 4481-4483.

(6) Love, J. C.; Estroff, L. A.; Kriebel, J. K.; Nuzzo, R. G.; Whitesides, G. M. *Chem. Rev.* **2005**, *105*, 1103-1170.

(7) Knieling, T.; Lang, W.; Benecke, W. *Sensors Actuat. B-Chem.* **2007**, *126*, 13-17.

(8) Zhao, B.; Brittain, W. J. *Prog. Polym. Sci.* **2000**, *25*, 677-710.

(9) Halperin, A.; Tirrell, M.; Lodge, T. P. *Adv. Poly. Sci.* **1992**, *100*, 31 - 71.

(10) Milner, S. T. *Science* **1991**, *251*, 905 - 914.

(11) Orski, S. V.; Fries, K. H.; Sontag, S. K.; Locklin, J. *J. Mater. Chem.* **2011**, *21*, 14135-14149.

(12) Brandani, P.; Stroeve, P. *Macromolecules* **2003**, *36*, 9492-9501.

(13) Brandani, P.; Stroeve, P. *Macromolecules* **2003**, *36*, 9502-9509.

(14) Brandani, P.; Stroeve, P. *Macromolecules* **2004**, *37*, 6640-6643.

(15) Elbert, D. L.; Hubbell, J. A. *Chem. Biol.* **1998**, *5*, 177-183.

(16) Huang, N.-P.; Michel, R.; Voros, J.; Textor, M.; Hofer, R.; Rossi, A.; Elbert, D. L.; Hubbell, J. A.; Spencer, N. D. *Langmuir* **2000**, *17*, 489-498.

(17) Kenausis, G. L.; Voros, J.; Elbert, D. L.; Huang, N.; Hofer, R.; Ruiz-Taylor, L.; Textor, M.; Hubbell, J. A.; Spencer, N. D. *J. Phys. Chem. B* **2000**, *104*, 3298-3309.

(18) Lee, S.; Voros, J. *Langmuir* **2005**, *21*, 11957-11962.

(19) Tsukruk, V. V. *Prog. Polym. Sci.* **1997**, *22*, 247-311.

(20) Luzinoz, I.; Julthongpiput, D.; Malz, H.; Pionteck, J.; Tsukruk, V. V. *Macromolecules* **2000**, *33*, 1043 - 1048.

(21) Minko, S.; Patil, S.; Datsyuk, V.; Simon, F.; Eichhorn, K.-J.; Motornov, M.; Usov, D.; Tokarev, I.; Stamm, M. *Langmuir* **2002**, *18*, 289-296.

(22) Papra, A.; Gadegaard, N.; Larsen, N. B. *Langmuir* **2001**, *17*, 1457-1460.

(23) Sofia, S. J.; Premnath, V.; Merrill, E. W. *Macromolecules* **1998**, *31*, 5059-5070.

(24) Tran, Y.; Auroy, P. *J. Am. Chem. Soc.* **2001**, *123*, 3644-3654.

(25) Edmondson, S.; Osborne, V. L.; Huck, T. S. *Chem. Soc. Rev.* **2004**, *33*, 14 - 22.

(26) Belder, G. F.; ten Brinke, G.; Hadziioannou, G. *Langmuir* **1997**, *13*, 4102-4105.

(27) Dhinojwala, A.; Granick, S. *Macromolecules* **1997**, *30*, 1079 - 1085.

(28) Penn, L. S.; Hunter, T. F.; Lee, Y.; Quirk, R. P. *Macromolecules* **2000**, *33*, 1105 - 1107.

(29) Azzaroni, O. *J. Polym. Sci., Part A: Polym. Chem.* **2012**, *50*, 3225-3258.

(30) Zdyrko, B.; Luzinov, I. *Macromol. Rapid Comm.* **2011**, *32*, 859-869.

(31) Balazs, A. C.; Singh, C.; Zhulina, E.; Chern, S.-S.; Lyatskaya, Y.; Pickett, G. *Prog. Surf. Sci.* **1997**, *55*, 181 - 269.

(32) Ruhe, J.; Knoll, W. J. *J. Macromol. Sci., Polym. Rev.* **2002**, *C42*, 91 - 138.

(33) Toomey, R.; Mays, J.; Tirrell, M. *Macromolecules* **2004**, *37*, 905 - 911.

(34) Advincula, R. C. *J. Dispersion Sci. Technol.* **2003**, *24*, 343 - 361.

(35) Jennings, G. K.; Brantley, E. L. *Adv. Mater.* **2004**, *16*, 1983-1994.

(36) Radhakrishnan, B.; Ranjan, R.; Brittain, W. J. *Soft Matter* **2006**, *2*, 386-396.

(37) Prucker, O.; Ruhe, J. *Macromolecules* **1998**, *31*, 592 - 601.

(38) Prucker, O.; Ruhe, J. *Langmuir* **1998**, *14*, 6893 - 6898.

(39) Senaratne, W.; Andruzzi, L.; Ober, C. K. *Biomacromolecules* **2005**, *6*, 2427-2448.

(40) Barbey, R.; Lavanant, L.; Paripovic, D.; Schüwer, N.; Sugnaux, C.; Tugulu, S.; Klok, H. A. *Chem. Rev.* **2009**, *109*, 5437-5527.

(41) Paul, R.; Schmidt, R.; Dyer, D. J. *Langmuir* **2002**, *18*, 8719 - 8723.

(42) Schmidt, R.; Zhao, T.; Green, J. B.; Dyer, D. J. *Langmuir* **2002**, *18*, 1281 - 1287.

(43) Advincula, R. *Adv. Poly. Sci.* **2006**, *197*, 107 - 136.

(44) Baum, M.; Brittain, W. J. *Macromolecules* **2002**, *35*, 610 - 615.

(45) Husseman, M.; Malmstrom, E. E.; McNamara, M.; Mate, M.; Mecerreyes, D.; Benoit, D. G.; Hedrik, J. L.; Mansky, P.; Huang, E.; Russell, T. P.; Hawker, C. J. *Macromolecules* **1999**, *32*, 1424 - 1431.

(46) Matyjaszewski, K.; Miller, P. J.; Shukla, N.; Immaraporn, B.; Gelman, A.; Luokala, B. B.; Siclovan, T. M.; Kickelbick, G.; Vallant, T.; Hoffman, H.; Pakula, T. *Macromolecules* **1999**, *32*, 8716 - 8724.

(47) Chen, G.; Tao, L.; Mantovani, G.; Geng, J.; Nystrom, D.; Haddleton, D. M. *Macromolecules* **2007**, *40*, 7513-7520.

(48) Li, Y.; Benicewicz, B. C. *Macromolecules* **2008**, *41*, 7986-7992.

(49) Murata, H.; Prucker, O.; Rühe, J. *Macromolecules* **2007**, *40*, 5497-5503.

(50) Orski, S. V.; Poloukhtine, A. A.; Arumugam, S.; Mao, L.; Popik, V. V.; Locklin, J. *J. Am. Chem. Soc.* **2010**, *132*, 11024-11026.

(51) Gauthier, M. A.; Gibson, M. I.; Klok, H. A. *Angew. Chem. - Int. Ed.* **2009**, *48*, 48-58.

(52) Im, S. G.; Bong, K. W.; Kim, B.-S.; Baxamusa, S. H.; Hammond, P. T.; Doyle, P. S.; Gleason, K. K. *J. Am. Chem. Soc.* **2008**, *130*, 14424-14425.

(53) Kolb, H. C.; Finn, M. G.; Sharpless, K. B. *Angew. Chem. Int. Ed.* **2001**, *40*, 2004-2021.

(54) Manetsch, R.; Krasinski, A.; Radic, Z.; Raushel, J.; Taylor, P.; Sharpless, K. B.; Kolb, H. C. *J. Am. Chem. Soc.* **2004**, *126*, 12809 - 12818.

(55) Nebhani, L.; Barner-Kowollik, C. *Adv. Mater.* **2009**, *21*, 3442-3468.

(56) Xu, H.; Hong, R.; Lu, T.; Uzun, O.; Rotello, V. M. *J. Am. Chem. Soc.* **2006**, *128*, 3162-3163.

(57) Baskin, J.; Prescher, J.; Laughlin, S.; Agard, N.; Chang, P.; Miller, I.; Lo, A.; Codelli, J.; Bertozzi, C. *Proc. Natl. Acad. Sci. U.S.A.* **2007**, *104*, 16793 - 19797.

(58) Jewett, J. C.; Sletten, E. M.; Bertozzi, C. R. *J. Am. Chem. Soc.* **2010**, *132*, 3688-3690.

(59) Kuzmin, A.; Poloukhtine, A.; Wolfert, M. A.; Popik, V. V. *Bioconjugate Chem.* **2010**, *21*, 2076-2085.

(60) Manova, R.; van Beek, T. A.; Zuilhof, H. *Angew. Chem. Int. Ed.* **2011**, *50*, 5428-5430.

(61) Arumugam, S.; Orski, S. V.; Locklin, J.; Popik, V. V. *J. Am. Chem. Soc.* **2011**, *134*, 179-182.

(62) Arumugam, S.; Popik, V. V. *J. Am. Chem. Soc.* **2011**, *133*, 15730-15736.

(63) Dirlam, P. T.; Strange, G. A.; Orlicki, J. A.; Wetzel, E. D.; Costanzo, P. J. *Langmuir* **2009**, *26*, 3942-3948.

(64) Pauloehrl, T.; Delaittre, G.; Winkler, V.; Welle, A.; Bruns, M.; Börner, H. G.; Greiner, A. M.; Bastmeyer, M.; Barner-Kowollik, C. *Angew. Chem. Int. Ed.* **2012**, *51*, 1071-1074.

(65) Sun, X.-L.; Stabler, C. L.; Cazalis, C. S.; Chaikof, E. L. *Bioconjugate Chem.* **2005**, *17*, 52-57.

(66) Rosen, B. M.; Lligadas, G.; Hahn, C.; Percec, V. *J. Polym. Sci. Part A: Polym. Chem.* **2009**, *47*, 3931-3939.

(67) Rosen, B. M.; Lligadas, G.; Hahn, C.; Percec, V. *J. Polym. Sci. Part A: Polym. Chem.* **2009**, *47*, 3940-3948.

(68) Xu, J.; Tao, L.; Boyer, C.; Lowe, A. B.; Davis, T. P. *Macromolecules* **2009**, *43*, 20-24.

(69) Hoyle, C. E.; Lowe, A. B.; Bowman, C. N. *Chem. Soc. Rev.* **2010**, *39*, 1355 - 1387.

(70) Gao, G.; Yu, K.; Kindrachuk, J.; Brooks, D. E.; Hancock, R. E. W.; Kizhakkedathu, J. N. *Biomacromolecules* **2011**, *12*, 3715-3727.

(71) Hensarling, R. M.; Doughty, V. A.; Chan, J. W.; Patton, D. L. *J. Am. Chem. Soc.* **2009**, *131*, 14673-14675.

(72) Hensarling, R. M.; Rahane, S. B.; LeBlanc, A. P.; Sparks, B. J.; White, E. M.; Locklin, J.; Patton, D. L. *Polym. Chem.* **2011**, *2*, 88-90.

(73) Rahane, S. B.; Hensarling, R. M.; Sparks, B. J.; Stafford, C. M.; Patton, D. L. *J. Mater. Chem.* **2012**, *22*, 932-943.

(74) Song, X.-J.; Hu, J.; Wang, C.-C. *Colloids Surf., A* **2011**, *380*, 250-256.

(75) Hoyle, C. E.; Bowman, C. N. *Angew. Chem. Int. Ed.* **2010**, *49*, 1540-1573.

(76) Hoyle, C. E.; Lee, T. Y.; Roper, T. *J. Polym. Sci., Part A: Polym. Chem.* **2004**, *42*, 5301-5338.

(77) Lowe, A. B.; Hoyle, C. E.; Bowman, C. N. *J. Mater. Chem.* **2010**, *20*, 4745-4750.

(78) Cortez, M. A.; Grayson, S. M. *Macromolecules* **2010**, *43*, 4081-4090.

(79) Javakhishvili, I.; Binder, W. H.; Tanner, S.; Hvilsted, S. *Polym. Chem.* **2010**, *1*, 506-513.

(80) Killops, K. L.; Campos, L. M.; Hawker, C. J. *J. Am. Chem. Soc.* **2008**, *130*, 5062-5064.

(81) Lluch, C.; Ronda, J. C.; Galia, M.; Lligadas, G.; Cadiz, V. *Biomacromolecules* **2010**, *11*, 1646-1653.

(82) Rissing, C.; Son, D. Y. *Organometallics* **2009**, *28*, 3167-3172.

(83) Boyer, C.; Granville, A.; Davis, T. P.; Bulmus, V. *J. Polym. Sci., Part A: Polym. Chem.* **2009**, *47*, 3773-3794.

(84) Campos, L. M.; Killops, K. L.; Sakai, R.; Paulusse, J. M. J.; Damiron, D.; Drockenmuller, E.; Messmore, B. W.; Hawker, C. J. *Macromolecules* **2008**, *41*, 7063-7070.

(85) DeForest, C. A.; Polizzotti, B. D.; Anseth, K. S. *Nat. Mater.* **2009**, *8*, 659-664.

(86) Flores, J. D.; Shin, J.; Hoyle, C. E.; McCormick, C. L. *Polym. Chem.* **2009**, *1*, 213-220.

(87) Geng, Y.; Discher, D. E.; Justynska, J.; Schlaad, H. *Angew. Chem. Int. Ed.* **2006**, *45*, 7578-7581.

(88) Nurmi, L.; Lindqvist, J.; Randev, R.; Syrett, J.; Haddleton, D. M. *Chem. Comm.* **2009**, 2727-2729.

(89) Sun, J.; Schlaad, H. *Macromolecules* **2010**, *43*, 4445-4448.

(90) ten Brummelhuis, N.; Diehl, C.; Schlaad, H. *Macromolecules* **2008**, *41*, 9946-9947.

(91) Konkolewicz, D.; Gray-Weale, A.; Perrier, S. *J. Am. Chem. Soc.* **2009**, *131*, 18075-18077.

(92) Semsarilar, M.; Ladmiral, V.; Perrier, S. b. *Macromolecules* **2010**, *43*, 1438-1443.

(93) Rutledge, R. D.; Warner, C. L.; Pittman, J. W.; Addleman, R. S.; Engelhard, M.; Chouyyok, W.; Warner, M. G. *Langmuir* **2010**, *26*, 12285-12292.

(94) van Berkel, K. Y.; Hawker, C. J. *J. Polym. Sci., Part A: Polym. Chem.* **2010**, *48*, 1594-1606.

(95) van der Ende, A. E.; Harrell, J.; Sathiyakumar, V.; Meschievitz, M.; Katz, J.; Adcock, K.; Harth, E. *Macromolecules* **2010**, *43*, 5665-5671.

(96) Lo Conte, M.; Pacifico, S.; Chambery, A.; Marra, A.; Dondoni, A. *J. Org. Chem.* **2010**, *75*, 4644-4647.

(97) Weinrich, D.; Lin, P.; Jonkheijm, P.; Nguyen, U.; Schroder, H.; Niemeyer, C.; Alexandrov, K.; Goody, R.; Waldmann, H. *Angew. Chem. Int. Ed.* **2010**, *49*, 1252-1257.

(98) Wittrock, S.; Becker, T.; Kunz, H. *Angew. Chem. Int. Ed.* **2007**, *46*, 5226-5230.

(99) Chan, J. W.; Hoyle, C. E.; Lowe, A. B. *J. Am. Chem. Soc.* **2009**, *131*, 5751-5753.

(100) Iha, R. K.; Wooley, K. L.; Nystrom, A. M.; Burke, D. J.; Kade, M. J.; Hawker, C. J. *Chem. Rev.* **2009**, *109*, 5620-5686.

(101) Schwartz, D. K. *Annu. Rev. Phys. Chem.* **2001**, *52*, 107-137.

(102) Houseman, B. T.; Gawalt, E. S.; Mrksich, M. *Langmuir* **2002**, *19*, 1522-1531.

(103) Lee, C.-Y.; Nguyen, P.-C. T.; Grainger, D. W.; Gamble, L. J.; Castner, D. G. *Anal. Chem.* **2007**, *79*, 4390-4400.

(104) Wettero, J.; Hellerstedt, T.; Nygren, P.; Broo, K.; Aili, D.; Liedberg, B.; Magnusson, K.-E. *Langmuir* **2008**, *24*, 6803-6811.

(105) Besson, E.; Gue, A.-M.; Sudor, J.; Korri-Youssoufi, H.; Jaffrezic, N.; Tardy, J. *Langmuir* **2006**, *22*, 8346-8352.

(106) Bexell, U.; Olsson, M.; Sundell, P. E.; Johansson, M.; Carlsson, P.; Hellsing, M. *Appl. Surf. Sci.* **2004**, *231-232*, 362-365.

(107) Campos, M.; Paulusse, J.; Zuilhof, H. *Chem. Comm.* **2010**, *46*, 5512-5514.

(108) Mehlich, J.; Ravoo, B. J. *Org. Biomol. Chem.* **2011**, *9*, 4108-4115.

(109) MacBeath, G.; Koehler, A. N.; Schreiber, S. L. *J. Am. Chem. Soc.* **1999**, *121*, 7967-7968.

(110) Smith, E. A.; Wanat, M. J.; Cheng, Y.; Barreira, S. r. V. P.; Frutos, A. G.; Corn, R. M. *Langmuir* **2001**, *17*, 2502-2507.

(111) Bexell, U.; Berger, R.; Olsson, M.; Grehk, T. M.; Sundell, P. E.; Johansson, M. *Thin Solid Films* **2006**, *515*, 838-841.

(112) Wendeln, C.; Rinnen, S.; Schulz, C.; Arlinghaus, H. F.; Ravoo, B. J. *Langmuir* **2010**, *26*, 15966-15971.

(113) Jonkheijm, P.; Weinrich, D.; Köhn, M.; Engelkamp, H.; Christianen, P. C. M.; Kuhlmann, J.; Maan, J. C.; Nüsse, D.; Schroeder, H.; Wacker, R.; Breinbauer, R.; Niemeyer, C. M.; Waldmann, H. *Angew. Chem. Int. Ed.* **2008**, *47*, 4421-4424.

(114) Weinrich, D.; Köhn, M.; Jonkheijm, P.; Westerlind, U.; Dehmelt, L.; Engelkamp, H.; Christianen, P. C. M.; Kuhlmann, J.; Maan, J. C.; Nüsse, D.; Schröder, H.; Wacker, R.; Voges , E.; Breinbauer, R.; Kunz, H.; Niemeyer, C. M.; Waldmann, H. *ChemBioChem.* **2010**, *11*, 235-247.

(115) Miguel, V. S.; Bochet, C. G.; del Campo, A. *J. Am. Chem. Soc.* **2011**, *133*, 5380-5388.

(116) Pelliccioli, A. P.; Wirz, J. *Photoch. Photobio. Sci.* **2002**, *1*, 441-458.

(117) Chen, S.; Smith, L. M. *Langmuir* **2009**, *25*, 12275-12282.

(118) Harant, A. W.; Khire, V. S.; Thibodaux, M. S.; Bowman, C. N. *Macromolecules* **2006**, *39*, 1461-1466.

(119) Khire, V.; Lee, T.; Bowman, C. *Macromolecules* **2008**, *41*, 7440-7447.

(120) Khire, V. S.; Lee, T. Y.; Bowman, C. N. *Macromolecules* **2007**, *40*, 5669-5677.

(121) Khire, V. S.; Harant, A. W.; Watkins, A. W.; Anseth, K. S.; Bowman, C. N. *Macromolecules* **2006**, *39*, 5081-5086.

(122) Khire, V. S.; Benoit, D. S. W.; Anseth, K. S.; Bowman, C. N. *J. Polym. Sci. Part A: Polym. Chem.* **2006**, *44*, 7027-7039.

(123) Curtin, S. A.; Deming, T. J. *J. Am. Chem. Soc.* **1999**, *121*, 7427-7428.

(124) Wang, J.; Gibson, M. I.; Barbey, R.; Xiao, S.-J.; Klok, H.-A. *Macromol. Rapid Comm.* **2009**, *30*, 845-850.

(125) Lunn, J. D.; Shantz, D. F. *Chem. Mater.* **2009**, *21*, 3638-3648.

(126) Mart, R. J.; Osborne, R. D.; Stevens, M. M.; Ulijn, R. V. *Soft Matter* **2006**, *2*, 822-835.

(127) Ito, Y.; Ochiai, Y.; Park, Y. S.; Imanishi, Y. *J. Am. Chem. Soc.* **1997**, *119*, 1619-1623.

(128) Sparks, B. J.; Ray, J. G.; Savin, D. A.; Stafford, C. M.; Patton, D. L. *Chem. Commun.* **2011**, *47*, 6245-6247.

(129) Alf, M. E.; Asatekin, A.; Barr, M. C.; Baxamusa, S. H.; Chelawat, H.; Ozaydin-Ince, G.; Petruczok, C. D.; Sreenivasan, R.; Tenhaeff, W. E.; Trujillo, N. J.; Vaddiraju, S.; Xu, J.; Gleason, K. K. *Adv. Mater.* **2010**, *22*, 1993-2027.

(130) Lahann, J. *Polym. Int.* **2006**, *55*, 1361-1370.

(131) Lahann, J. *Chem. Eng. Commun.* **2006**, *193*, 1457-1468.

(132) Lahann, J.; Langer, R. *Macromolecules* **2002**, *35*, 4380-4386.

(133) Wu, J.-T.; Huang, C.-H.; Liang, W.-C.; Wu, Y.-L.; Yu, J.; Chen, H.-Y. *Macromol. Rapid Comm.* **2012**, *33*, 922-927.

(134) Cai, T.; Wang, R.; Neoh, K. G.; Kang, E. T. *Polym. Chem.* **2011**, *2*, 1849-1858.

(135) Cai, T.; Neoh, K. G.; Kang, E. T. *Macromolecules* **2011**, *44*, 4258-4268.

(136) Wang, C.; Ren, P. F.; Huang, X. J.; Wu, J.; Xu, Z. K. *Chem. Commun.* **2011**, *47*, 3930-3932.

(137) Wang, C.; Wu, J.; Xu, Z.-K. *Macromol. Rapid Comm.* **2010**, *31*, 1078 - 1082.

CHAPTER II

RATIONALE AND OBJECTIVES

Rationale

Synthesis of polymer brushes to decorate a surface with desired functionality typically involves SIP of functional, but non-reactive monomers. This approach requires synthesizing sufficiently thick polymer brushes containing surface-attached polymer chains of high molecular weight at high grafting density to ensure full coverage of the surface such that the underlying surface itself has minimal or no influence on overall surface properties. In general, large quantities of monomer are required in this approach not only due to the kinetic consideration that molecular weight of the polymer chains (as manifest in the thickness of the brush) scales linearly with the monomer concentration, but also due to an obvious experimental requirement that the surface needs to be submerged completely in monomer solution. This need to use large amounts of monomer can render SIP of functional, but non-reactive monomers excessively expensive. Additionally, the brush growth mechanism does not tolerate all possible functionalities that might be of interest. As with any chain growth process, functional groups that act as terminating or chain transfer agents prevent the formation of dense, thick polymer brushes, and effectively limit the number of functional groups per unit area on the surface. For example, monomers containing thiol and amine moieties are not tolerated by radical polymerization and limit the molecular weight of chains. To circumvent these limitations, the decoration of surfaces with polymer chains bearing specific pendent functional groups amenable to post-polymerization modification is of interest. As shown in Scheme 5, the proposed strategy (referred to as an “universal” reactive brush precursor

approach) requires synthesis of polymer brushes by SIP from functional monomers with pendant moieties that are suitable for “click” or “click”-type reactions and are inert to radical polymerization.

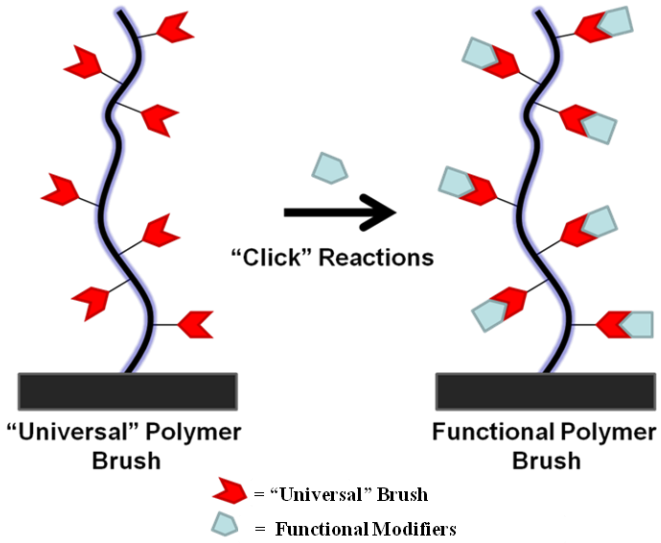

Scheme 5. “Universal” research brush precursor approach.

Objectives

As stated previously, the primary objective of this research is to exploit a specific class of click reactions for post-polymerization modification – “thiol-click” – to tackle practically unexplored areas in polymer surface engineering, ultimately leading to unprecendented control of surface functionality. Thiol-click reactions for surface modifications are ideal chemical platforms that (1) enable the rapid generation of a diverse library of functional surfaces from a single substrate precursor, (2) utilize a structurally diverse range of commercially available or easily attainable reagents, (3) proceed rapidly to quantitative conversions under mild conditions and (4) open the door to orthogonal and site-selective functionalization. With these design parameters in mind, the specific objectives of this research are briefly stated below:

1) synthesize “universal” polymer brush surfaces carrying pendent ‘reactive’ functionalities along the brush backbone amendable to post-polymerization modification (PPM) (i.e. alkynes, isocyanates, halides, epoxies, thiols, etc.);
2) design thiol-click post-polymerization modification strategies fulfilling robust-efficient-orthogonal (REO) strategies for fabrication of complex, multicomponent functional surfaces;
3) demonstrate UV light triggered deprotection strategies to spatially and temporally control PPM reactions via photolabile protecting group chemistries;
4) elucidate the surface constraints affecting the success of PPM processes (thiol-isocyanate click reactions used for this study); and
5) develope block copolymer brushes and tapered block copolymer brushes with unique surface properties unattainable from conventional synthetic techniques

CHAPTER III

"CLICKING" POLYMER BRUSHES WITH THIOL-YNE CHEMISTRY: INDOORS AND OUT

Introduction

Engineering the chemistry and topography of surfaces affords technological advancements for a variety of applications ranging from biosensors to microelectronics. This broad range of applications necessitates the development of a modular approach to surface engineering – ideally one that (1) enables the rapid generation of a diverse library of functional surfaces from a single substrate precursor, (2) utilizes a structurally diverse range of commercially available or easily attainable reagents, (3) proceeds rapidly to quantitative conversions under mild conditions and (4) opens the door to orthogonal and site-selective functionalization. These criteria are, of course, similar to those that define a class of reactions commonly known as "click" chemistry.[1] Click chemistry, particularly Cu-catalyzed azide-alkyne cycloaddition (CuAAC), has proven to be a powerful approach towards meeting the aforementioned criteria for surface engineering.[2-4] However, the biotoxicity of Cu and the limited availability of cycloalkynes used in Cu-free AAC[5] reactions may limit utility in certain arenas. Modular surface reactions that circumvent these issues while retaining click-like characteristics are highly desirable. In this chapter, we present thiol-yne chemistry as a modular approach towards surface engineering. Using this approach, we demonstrate the rapid generation of a library of highly functional, patterned and multicomponent polymer brush surfaces under ambient conditions from a single substrate precursor. We also demonstrate the practicality of this

approach by performing thiol-yne surface modifications using outdoor, ambient-air reactions with sunlight as the radiation source.

The recently highlighted utility and click-like characteristics of the radical-mediated thiol-yne reaction,[6-9] and the more thoroughly investigated thiol-ene reaction,[10,11] have been amply demonstrated in areas of macromolecular design,[12,13] post-polymerization modification[14-19] and even bioconjugation.[20] Thiol-ene reactions have also been demonstrated as a viable approach to surface modification by the Bowman[21,22] and Waldmann[23] groups; thiol-yne reactions, however, have yet to be explored for this purpose despite many common advantages. Notably, thiol-yne reactions proceed at room temperature with high efficiency and rapid kinetics, in the presence of oxygen/water, without expensive and potentially toxic catalysts, and are highly tolerant of a wide range of functional groups. Additionally, the thiol-yne reaction is orthogonal to a wide range of chemistries including the phosphine-catalyzed nucleophilic thiol-ene reaction.[6] The hydrothiolation reaction can also be photoinitiated in the UV-visible range (254 – 470 nm) affording both temporal and spatial control of the reaction site. The vast number of commercially available thiols is yet another advantage of this chemistry as a broadly applicable platform. Considering these attributes, we envisioned the fabrication of highly functional surfaces using thiol-yne reactions to modify the three-dimensional configuration of reactive "handles" expressed by densely tethered "yne"-containing polymer brushes. Similar post-modification of brush surfaces has been successfully demonstrated using pendant active esters[24] and azides modified nanoparticles.[25]

Experimental

Materials

All reagents and solvents were obtained at the highest purity available from Aldrich Chemical Company or Fisher Scientific and used without further purification unless otherwise specified. Methacryloyl chloride and 2-Hydroxy-4'-(2-hydroxyethoxy)-2-methylpropiophenone (Irgacure 2959) were purchased from Fluka and Ciba Specialty Chemicals, respectively. Mercaptopropylisobutyl Polyhedral Oligomeric Silsesquioxane (POSS)® was generously donated by Hybrid Plastics.

Characterization

A Varian Mercury Plus 200MHz NMR spectrometer operating at a frequency of 200.13 MHz with VNMR 6.1C software was used for proton analysis. Contact angle goniometry was performed using a Ramé-hart 200-00 Std.-Tilting B. goniometer. Static (θ_{sw}) contact angles were measured using 10 μL water droplets. Ellipsometric measurements were carried out using a Gaertner Scientific Corporation LSE ellipsometer with a 632.8 nm laser at 70° from the normal. Refractive indices of 3.89 for silicon, 1.46 for silicon oxide, 1.43 for initiator, and 1.5 for the polymer were used. ATR-FTIR spectra of surface polymers were carried out using a Digilab FTS 6000 with a PIKE ATR attachment using WIN-IR Pro software. A bare silicon wafer was used as the background. Spectra were taken with a resolution of 4 cm^{-1} by accumulating a minimum of 100 scans per run. Nitrogen was constantly purged through the attachment to reduce interference of carbon dioxide and water. Optical images of the micropatterns were taken using a Keyence VHX digital microscope with a multi-illumination lighting system.

Synthesis of 2-Hydroxy-4'-(2-allyloxyethoxy)-2-methyl-propiophenone (Allyloxy-HPP) (1)

Compound 1 was prepared according to literature.[26] All spectroscopic and characterization data match those values reported in the literature. 2-Hydroxy-4'-(2-hydroxyethoxy)-2-methylpropiophenone (Irgacure 2959) (4.0 g, 17.8 mmol, 1.0 eq) was dissolved in ~ 5 mL dry DMF along with NaOH powder (720 mg, 18.0 mmol, 1.0 eq) and KI (6.60 g, 40.0 mmol, 2.3 eq). To the stirred suspension allyl chloride (18.5 mL, 227 mmol, 12.8 eq) was added dropwise. The reaction was stirred at r.t. for 17 h, and subsequently poured into a solution of 15.0 g NaCl in 300 mL of water followed by extraction with diethylether (3 x 100 mL). The combined organic layers were dried over $MgSO_4$, filtrated and solvent was removed under reduced pressure. The product was purified using flash chromatography (silica gel, Hexane/EtOAc 5:1 → 2:1) to yield 1.85 g (6.99 mmol), 39.3% of 2-Hydroxy-4'-(2-allyloxyethoxy)-2-methyl-propiophenone (1). ^{1}H-NMR ($CDCl_3$; λ ppm, (see Appendix A)): 1.62 (s, 6H, ($C^{1}H_3$), 3.83 ($C^{9}H_2$), 4.10 ($C^{10}H_2$), 4.20 ($C^{8}H_2$), 5.25 ($C^{12}H_2$), 5.92 ($C^{11}H_2$), 6.96 (H_{Arom}), 8.04 (H_{Arom}); ^{13}C-NMR ($CDCl_3$; λ ppm, (see Appendix A)): 28.9, 67.8, 68.2, 72.6, 75.8, 114.28, 117.7, 126.2, 132.4, 134.6, 162.9, 202.9.

Protection of tertiary hydroxyl group (Acetate protected-HPP) (2)

Compound 2 was prepared according to literature.[26] All spectroscopic and characterization data match those values reported in the literature. Allyloxy-HPP (1) (1.85 g, 7.0 mmol, 1 eq) was dissolved in a solution of acetic acid anhydride (8.6 mL, 91.0 mmol, 13 eq) and pyridine (3.96 mL, 49.0 mmol, 7 eq) followed by being heated to reflux for 2 h. The excess reagents were evaporated in vacuo and the crude product was distilled with toluene (10 mL) to remove any acetic acid anhydride or pyridine leaving

pure product (2) behind. Product (2) was subsequently dried in vacuo to yield 2.14 g (6.9 mmol, 99.1%). ^{1}H-NMR ($CDCl_3$; λ ppm, (see Appendix A)): 1.69 (s, 6H, ($C^{3}H_3$), 1.94 (s, 3H, $C^{1}H_3$), 3.81 (t, 2H, $C^{11}H_2$), 4.09 (m, 2H, $C^{12}H_2$), 4.18 (t, 2H, $C^{10}H_2$), 5.26 (m, 2H, $C^{14}H_2$), 5.92 (m, 1H, $C^{13}H$), 6.91 (d, 2H, H_{Arom}), 8.0 (d, 2H, H_{Arom}); ^{13}C-NMR ($CDCl_3$; λ ppm, (see Appendix A)): 21.4, 25.3, 67.5, 68.2, 72.4, 84.3, 114.1, 117.5, 127.3, 130.8, 134.4, 162.1, 170.0, 197.5.

Synthesis of 2-hydroxy-4'-(2-hydroxyethoxy)-2-methylpropiophenone trichlorosilane HPP-$SiCl_3$ (3)

HPP-$SiCl_3$ (3) was prepared according to a modified literature procedure.[26] Under an inert atmosphere, the acetate protected Allyloxy-HPP (2) (0.51 g, 1.7 mmol, 1eq), ~ 4 mL toluene, ~ 2 mL trichlorosilane, and 5 – 6 drops of Pt-divinyl tetramethyl disiloxane complex in vinyl silicone was allowed to react overnight. The catalyst and any solids were removed by filtration and toluene and excess trichlorosilane were removed under vacuum yielding (3) as a mixture of the two markovnikov products (0.73 g, 99.2%). The product was used as obtained without additional purification. Dry toluene (6 mL) was added to (3) creating a stock 275 mM solution. ^{1}H-NMR ($CDCl_3$; λ ppm, (see Appendix A)): 0.06 (m, 1H), 0.77 – 1.54 (m, 3H), 1.68 (s, 6H), 1.93 (s, 3H, $C^{1}H_3$), 3.58 (t, 2H, $C^{12}H_2$), 3.78 (t, 2H, $C^{11}H_2$), 4.14 (t, 2H, $C^{10}H_2$), 6.90 (d, 2H, H_{Arom}), 8.01 (d, 2H, H_{Arom}); ^{13}C-NMR ($CDCl_3$; λ ppm, (see Appendix A)): 0.99, 9.50, 21.42, 22.59, 25.40, 32.93, 67.48, 68.65, 72.44, 84.33, 114.21, 117.84, 127.38, 130.87, 162.11, 170.26, 197.63.

Immobilization of HPP-$SiCl_3$ on SiO_2 Surfaces

Silicon wafers were cut into appropriate sized pieces and ultrasonically cleaned in acetone, ethanol, and toluene for 15 min. in each solvent. The substrates were dried

under a stream of N_2 and treated with UV-ozone for 45 min. HPP-$SiCl_3$ (3) (4 mM) in toluene was immobilized on the SiO_2 surface at room temperature using excess Et_3N as an acid scavenger for ~ 1 h. The samples were then cleaned by rinsing with toluene and methanol and dried under a stream of N_2. The functionalized silicon wafers were stored in toluene at -20 °C until use.

Deprotection of the tertiary hydroxyl group at the surface[26]

The acetate protection group was removed by immersing the wafers prepared above in a suspension of 240 mg K_2CO_3 in 12 mL methanol containing 150 µL H_2O for 1 h. The substrate was subsequently washed with water, methanol, and toluene followed by drying with a stream of N_2.

Synthesis of 3-Trimethylsilyl-2-propyn-1-ol (PgOH-TMS) (4)

PgOH-TMS (4) was prepared according to literature.[27,28] All spectroscopic and characterization data match those values reported in the literature. At -78 °C, a 2.5 M solution of n-BuLi in hexane (157.0 mL, 392.4 mmol, 2.2 eq) was added dropwise to a solution of propargyl alcohol (10 g, 10.5 mL, 178.0 mmol, 1 eq) in dry THF (200 mL). After stirring for 1 h, the yellow-colored suspension was allowed to warm to r.t. and subsequently cooled to -78 °C before the dropwise addition of trimethylchlorosilane (TMSCl) (49.6 mL, 392.4 mmol, 2.2 eq). After addition, the cooling bath was removed, and the reaction was stirred overnight. The reaction was cooled to 0 °C and quenched by the dropwise addition of 5.0 M sulfuric acid. The reaction was stirred for 1 h to ensure complete consumption of the TMS-ether. (TLC analysis: (TMS-ether), R_f 0.90 (9:1 Hexane/EtOAc), no UV, purple (vanillin)). The water layer was separated and extracted with Et_2O (2 x 100mL). The combined organic layers were washed with H_2O (1 x 100

mL) and brine (1 x 100 mL), dried over $MgSO_4$, filtrated and concentrated under reduced pressure. Purification by short path distillation (80 – 83 °C) afforded the TMS-propargyl alcohol (20.3 g, 88.7%) as a pale yellow oil. ^{1}H-NMR ($CDCl_3$; λ ppm, (see Appendix A)): 0.17 (s, 9H, $Si(CH_3)_3$), 1.79 (s, 1H, OH), 4.26 (s, 2H, CH_2); ^{13}C-NMR ($CDCl_3$; λ ppm, (see Appendix A)): 0.2, 51.5, 90.7, 103.8.

Synthesis of protected alkyne containing monomer, (3-trimethylsilylpropargyl) methacrylate (PgMA-TMS) (5)

PgMA-TMS (5) was synthesized according to literature,[29] although we modified the purification procedure as noted below. All spectroscopic and characterization data match those values reported in the literature. A solution of PgOH-TMS (4) (7 g, 54.6 mmol, 1 eq) and Et_3N (9.13 mL, 65.5 mmol, 1.2eq) in dry CH_2Cl_2 (100 mL) was cooled in an ice bath (0 °C). Then, methacryloyl chloride (6.34 mL, 65.5 mmol, 1.2 eq) in CH_2Cl_2 (10 mL) was added dropwise. The reaction was stirred at 0 °C for 10 min and then at r.t. overnight. The ammonium salts were removed by filtration and the organic layer was washed with H_2O (1 x 100 mL), sodium bicarbonate (2 x 100 mL), brine (1 x 100 mL), and dried over $MgSO_4$. Volatiles were removed under reduced pressure. The crude product was purified by column chromatography (silica gel: hexane:acetone 40:1; R_f = 0.67) to yield (4.2 g, 71.2%) a pale yellow product. ^{1}H-NMR ($CDCl_3$; λ ppm, (see Appendix A)): 0.19 (s, 9H, $Si(C^8H_3)_3$), 1.97 (s, 3H, C^3H_3), 4.76 (s, 2H, C^5H_2), 5.62 (s, 1H, C^1*H*H), 6.18 (s, 1H, C^1H*H*); ^{13}C-NMR ($CDCl_3$; λ ppm, (see Appendix A)): 1.76, 20.41, 55.1, 94.2, 101.3, 128.7, 137.9, 168.9.

Surface-Initiated Polymerization (SIP) of (5)

SIP reactions were carried out in a custom-built inert atmosphere (nitrogen) box using a microchannel reaction device (Fabricated from Norland 81 optical adhesive).

This approach permits the preparation of polymer brushes on wafer size substrates and requires a minimal amount of monomer solution (400 μL for microchannel + 600 μL for tubing = 1000 μL total volume). The initiator-functionalized silicon wafers were placed in a microchannel reaction device approximately 7" from the UV light source (λ_{max} = 365 nm, Omnicure Series 1000 with a 5 mm collimating adaptor). After purging the reaction chamber and monomer solution with N_2 for 30 min, a 1:1 volume % solution of (5) in toluene was injected into the microfluidic channel and subsequently exposed to UV light for 45 minutes. After polymerization, any physisorbed polymer was removed by Soxhlet extraction in toluene for a minimum of 24 h.

Deprotection of Polymer Brushes

The TMS group was removed by immersing the wafer in KOH (0.6 g) in methanol (12 mL) at ambient temperature for 1 h to afford the alkyne functionalized polymer brush. The substrate was subsequently washed with water, methanol, toluene, and dried under a stream of N_2.

Thiol-yne "Click" Reactions

All thiol-yne reactions were photoinitiated by UV irradiation (~12 mW/cm^2, λ_{max} = 365 nm) under ambient laboratory conditions (i.e. r.t. and normal atmosphere) unless otherwise specified. Reaction mixtures were not degassed prior to use. After thiol-yne reactions, the samples were washed extensively with THF, methanol, and toluene. Neat "click" reactions were performed when solubility of the thiol permitted. In some cases, a minimal amount of solvent was necessary to dissolve the thiol and/or solvate the brush. Details of the various thiol-yne reactions are given below. In all cases, a significant

change in wettability could be observed within seconds of initiation. However, reaction times were chosen to ensure complete conversion of the alkynes units on the surface.

3-mercaptoproprionic acid

Two wt. % (61.0 mg, 0.24 mmol) α,α-dimethoxy-α-phenylacetophenone (Irgacure 651) was dissolved in 3-mercaptoproprionic acid (2.5 mL, 28.7 mmol). The solution was placed into the reaction vessel containing the deprotected polymer brush and irradiated with UV light for 8 minutes.

1-dodecanethiol

Two wt. % (21.1 mg, 0.08 mmol) α,α-dimethoxy-α-phenylacetophenone (Irgacure 651) and 1-dodecanethiol (1.25 mL, 5.2 mmol) was dissolved in THF (1.25 mL). The solution was placed into the reaction vessel containing the deprotected polymer brush and irradiated with UV light for 8 minutes.

1-thioglycerol

Two wt. % (63.6 mg, 0.25 mmol) α,α-dimethoxy-α-phenylacetophenone (Irgacure 651) was dissolved in 1-thioglycerol (2.5 mL, 29.4 mmol). The solution was placed into the reaction vessel containing the deprotected polymer brush and irradiated with UV light for 8 minutes.

N-acetyl-L-cysteine

Two wt. % (5.3 mg, 0.02 mmol) α,α-dimethoxy-α-phenylacetophenone (Irgacure 651) and N-acetyl-L-cysteine (245.0 mg, 1.5 mmol) was dissolved in THF (1 mL) and DMF (0.5 mL). The solution was placed into the reaction vessel containing the deprotected polymer brush and irradiated with UV light for 30 minutes.

Benzyl mercaptan

Two wt. % (26.3 mg, 0.10 mmol) α,α-dimethoxy-α-phenylacetophenone (Irgacure 651) and benzyl mercaptan (1.25 mL, 9.7 mmol) was dissolved in THF (1.25 mL). The solution was placed into the reaction vessel containing the deprotected polymer brush and irradiated with UV light for 8 minutes.

1-adamantanethiol

Two wt. % (4.21 mg, 0.016 mmol) α,α-dimethoxy-α-phenylacetophenone (Irgacure 651) and 1-adamantanethiol (210.4 mg, 1.25 mmol) was dissolved in THF (2.5 mL). The solution was placed into the reaction vessel containing the deprotected polymer brush and irradiated with UV light for 30 minutes.

Thiocholesterol

Two wt. % (3.0 mg, 0.012 mmol) α,α-dimethoxy-α-phenylacetophenone (Irgacure 651) and thiocholesterol (150.0 mg, 0.37 mmol) was dissolved in THF (2.5 mL). The solution was placed into the reaction vessel containing the deprotected polymer brush and irradiated with UV light for 1 h.

Mercaptopropylisobutyl Polyhedral Oligomeric Silsesquioxane (POSS)®

Two wt. % (20.0 mg, 0.08 mmol) α,α-dimethoxy-α-phenylacetophenone (Irgacure 651) and mercaptopropylisobutyl POSS® (1.0 g, 1.1 mmol) was dissolved in THF (3.5 mL). The solution was placed into the reaction vessel containing the deprotected polymer brush and irradiated with UV light for 30 minutes. Longer reaction times were employed here due to poor solubility of POSS in THF.

Micropatterning and Sequential Thiol-yne Reactions

For patterning, a 300 mesh (58 μm hole, 25 μm bar) or a 2000 mesh (7.5 μm hole, 5 μm bar) copper grid was used as a photomask. Details of the procedure are given below.

Preparation of 3-mercaptopropionic acid/1-dodecanethiol and 1-dodecanethiol/ mercaptopropionic acid micropatterns

Two wt. % (30.5 mg, 0.12 mmol) α,α-dimethoxy-α-phenylacetophenone (Irgacure 651) and 3-mercaptopropionic acid (1.25 mL, 15.2 mmol) were dissolved in THF (1.25 mL). The solution was placed into the reaction vessel containing the deprotected polymer brush with a TEM grid in direct contact with the surface and irradiated with UV light for 8 minutes. The grid was then removed and the sample was washed with THF, methanol, and toluene followed by a sequential thiol-yne reaction with 1-dodecanethiol to backfill the unexposed portion of the pattern. Two wt. % (21.3 mg, 0.08 mmol) α,α-dimethoxy-α-phenylacetophenone (Irgacure 651) and 1-dodecanethiol (1.25 mL, 5.3 mmol) was dissolved in THF (1.25 mL). The solution was placed into the reaction vessel containing the patterned polymer brush and irradiated with UV light for 8 minutes. The inverted micropattern was prepared by reversing the order of reaction. Patterned substrates were exposed to 0.01 M KOH to deprotonate the carboxylic acid in order to improve the contrast in wettability for imaging.

3-Mercaptoproprionic acid/1-dodecanethiol in Sunlight

2 wt. % (73.2 mg, 0.3 mmol) α,α-dimethoxy-α-phenylacetophenone (Irgacure 651) and 3-mercaptopropionic acid (3.0 mL, 34.5 mmol) were dissolved in THF (3.0 mL). The reaction mixtures were not degassed prior to use. The solution was placed into a petri dish or scintillation vial containing a TEM grid in direct contact with the

deprotected polymer brush and subsequently exposed to sunlight for 1 h. The sunlight reactions were carried out in Hattiesburg, MS between 1 – 4 pm under partly cloudy skies (~ 4 mW/cm^2). The grid was removed and the samples were washed with THF, methanol, and toluene followed by a sequential thiol-yne reaction with 1-dodecanethiol. 2 wt. % (16.9 mg, 0.07 mmol) α,α-dimethoxy-α-phenylacetophenone (Irgacure 651) and 1-dodecanethiol (1 mL, 4.18 mmol) were dissolved in THF (1 mL). The solution was placed into the reaction vessel containing the patterned polymer brush and subsequently exposed to sunlight for 1 h. Homogeneous thiol-yne functionalization of surfaces in sunlight was performed as described for the reactions carried out in the lab.

Reversible pH-Responsive Polymer Brushes

Homogeneous mercaptopropionic acid functionalized brushes exhibited reversible wettability by depronating with 0.01 M KOH and subsequently protonating with 0.1 M HCl for 30 seconds each. Substrates were blown dry with N_2 prior to measuring water contact angles.

Results and Discussion

As shown in Scheme 6a, silicon substrates were first functionalized with a chlorosilane derivative of commercially available 2-hydroxy-4'-(2-hydroxyethoxy)-2-methylpropiophenone (Irgacure 2959) photoinitiator.[26] These substrates were then inserted into a microchannel reactor (see Appendix A) containing trimethylsilane-protected propargyl methacrylate (PgMA-TMS, 1:1 v/v in toluene), and surface-initiated by irradiating with $UV_{\lambda max=365nm\ light}$ (20 mW cm^{-2}, 45 min, ~25 nm). Notably, the fabrication of a 14 × 65 mm substrate using our microchannel reactor requires only 400 μL of monomer solution (additional solution required depending on volume of

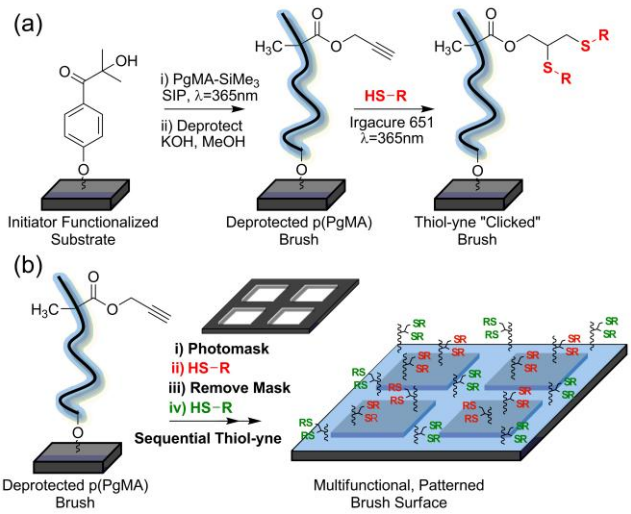

Scheme 6. (a) Schematic procedure of surface-initiated photopolymerization of TMS-protected propargyl methacrylate, deprotection, and subsequent thiol-yne functionalization. (b) Schematic procedure for photopatterning "yne"-containing polymer brush surfaces with sequential thiol-yne reactions.

connecting tubing), significantly reducing the cost of this approach. After Soxhlet extraction in toluene, the deprotection of the p(PgMA-TMS) brush in KOH/MeOH was followed by ATR-FTIR. Quantitative deprotection was confirmed by the disappearance of the protected alkyne C≡C stretch (~2185 cm^{-1}) and the appearance of the characteristic peaks of the unprotected alkyne (C−H 3288 cm^{-1}, C≡C 2131 cm^{-1}) (Figure 1).[30] The resulting "yne" functionalized polymer brush served as a "universal" reactive precursor for subsequent thiol-yne reactions eliminating the synthetic effort associated with the use of multiple functional monomers.

The radical-mediated reaction of a thiol with an alkyne generates a dithioether adduct as shown in Scheme 6a. The reaction occurs in a two step process involving the addition of the thiyl radical to the C≡C bond yielding an intermediate vinyl sulfide species that subsequently undergoes a second, formally thiol-ene reaction, yielding the 1,2-dithioether adduct.[8] To explore the efficacy of the thiol-yne reaction at surfaces, we

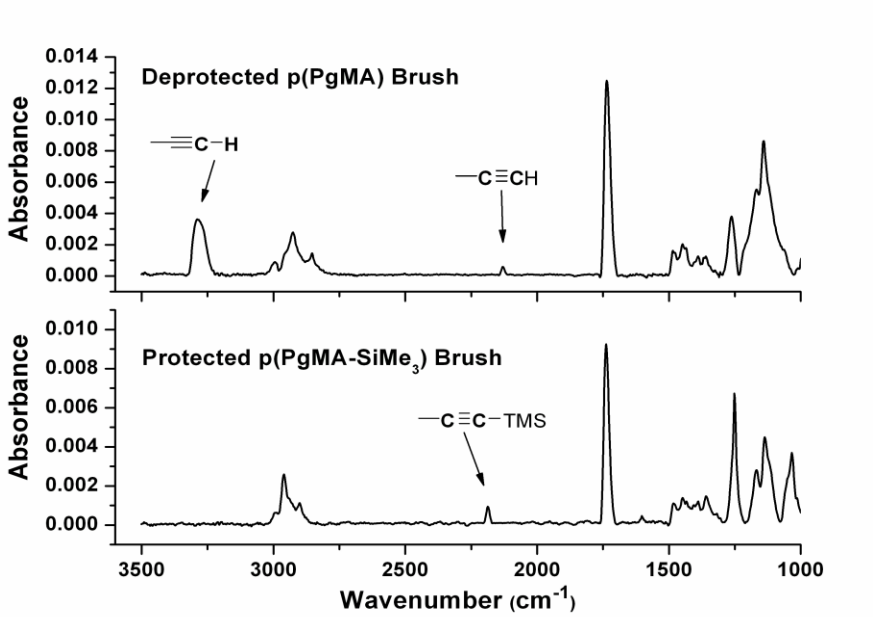

Figure 1. ATR-FTIR: (a) Deprotected p(PgMA) brush (b) Protected p(PgMA-TMS) brush.

selected a library of commercially available thiols (Figure 2), including 3-mercaptopropionic acid (MPA) of interest for pH responsive surfaces, N-acetyl-L-cysteine as a model for the attachment of peptide fragments to brush surfaces and thiocholesterol as a ubiquitous component of biomembrane structures.[31] Thiol-yne reactions were carried out in the presence of α,α-dimethoxy-α-phenylacetophenone (Irgacure 651, 2 wt% I:thiol) at 365 nm under ambient air, temperature and humidity conditions to afford the functional brushes. Reactions were performed solvent-free when possible, but in some cases, solvent was required to solubilize the thiol and/or solvate the brush. After the thiol-yne reaction, substrates were washed extensively with multiple solvents to remove any physisorbed species and then characterized by water contact angle and ATR-FTIR. Static water contact angles confirmed the expected changes in wettability associated with each functional moiety conjugated to the surface (Figure 3). ATR-FTIR was used to follow the thiol-yne functionalization of the brushes. Under

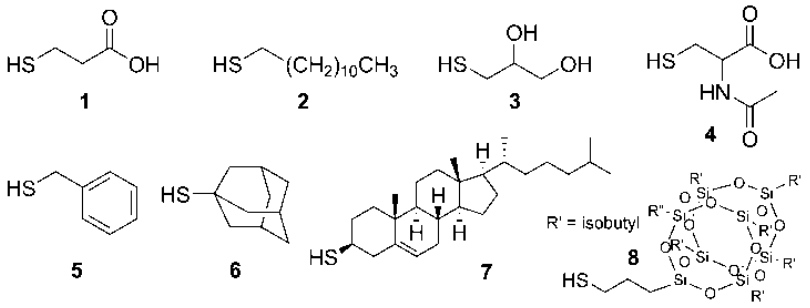

Figure 2. Commercially available thiols used for thiol-yne click reactions: mercaptopropionic acid (1), 1-dodecanethiol (2), 1-thioglycerol (3), N-acetyl-L-cysteine (4), benzyl mercaptan, (5), 1-admantanethiol (6), thiocholesterol (7), and 3-mercaptopropyl polyhedral oligomeric silsequioxane (POSS) (8).

these conditions, quantitative conversion of the tethered alkynes was observed within minutes (compared with hours typically required for CuAAC surface reactions) as indicated by disappearance of the peaks assigned to the alkyne (C−H 3288 cm^{-1}, C≡C 2131 cm^{-1}) for the entire series of functional brushes (Figure 4). Further, the spectra clearly show peaks that are indicative of the incorporated thiols (see Appendix A for additional spectra/peak assignments). For small MW thiols, we see little evidence for the vinyl sulfide species (~1609 cm^{-1}, position shown by blue marker in Figure 4)[8] that would result from monosubstitution of the alkyne indicating full conversion to the 1,2-dithioether adduct. However, full conversion to the disubstituted adduct may be more difficult to achieve as the MW (or steric bulk) of the thiol increases. As shown in Figure 4(g,h), there exists a very weak band at ~1609 cm^{-1} that could be assigned to the vinyl sulfide, but quantitative analysis is potentially complicated by weak absorbance and spectral overlap.

Further to this point, we observe an increase in brush thickness (Table 1), which is attributed to the increase in molar mass of the monomer repeat unit, and consequently, an increase in MW of the brush after functionalization.[24] We also note that other factors

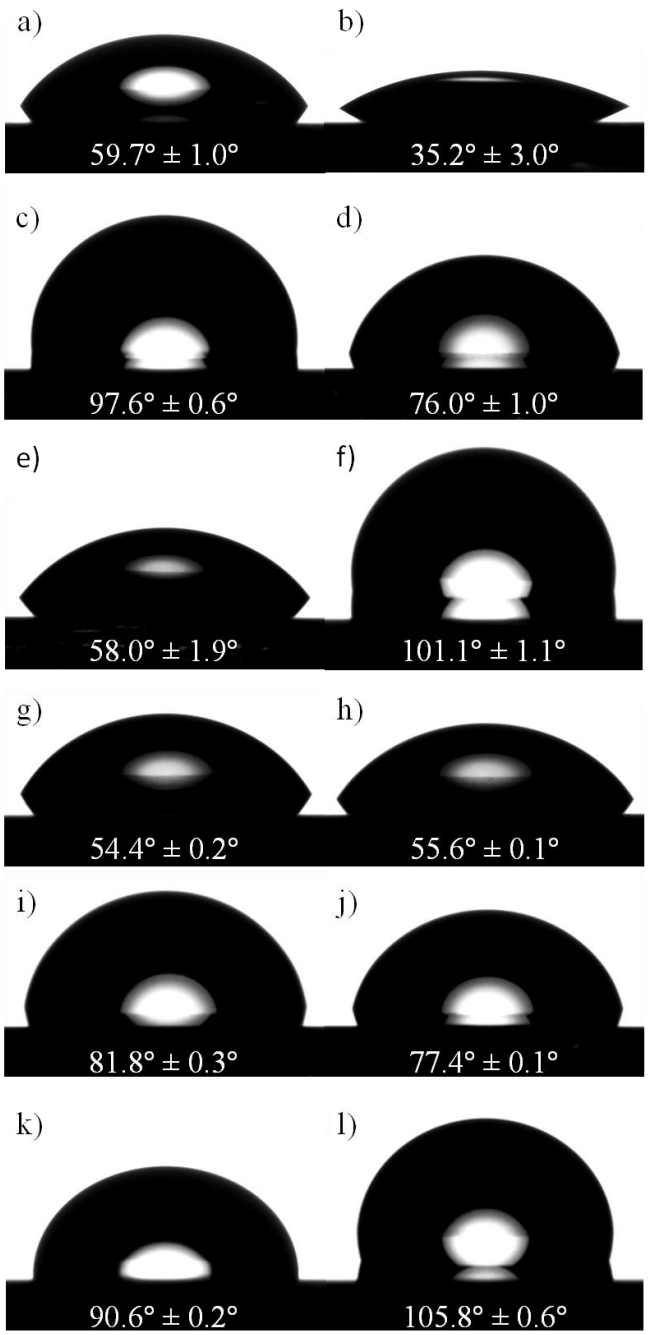

Figure 3. Static water contact angle (WCA): (a) protected initiator (b) deprotected initiator (c) Protected brush (d) Deprotected brush (e) 3-mercaptopropionic acid (f) 1-dodecanethiol (g) 1-thioglycerol (h) N-acetyl-L-cysteine (i) Benzyl mercaptan (j) 1-admantanethiol (k) Thiocholesterol (l) Mercaptopropylisobutyl POSS®.

may also contribute to the changes in film thickness observed, including molecular stacking, hydrophobicity effects, etc. From cursory analysis of film thickness increase

relative to the MW of the thiol derivatives (where the MW of the thiol would dictate a one or two-times increase in the molar mass of the monomer repeat depending on whether mono- or disubstitution occurs), it is apparent that larger MW thiols are not fully substituted to the 1,2-dithioether adduct. For example, the brush thickness increases by a factor of ~4.5 after functionalization with 1-dodecanethiol (DDT) and only by ~2.7 for thiocholesterol, despite DDT being half the molecular weight of the latter (202.4 g/mol and 402.72, respectively). A similar dependence of substitution efficiency on increasing MW of amines was observed with N-hydroxysuccinimide brushes.[24] In our case, the effect is exacerbated by the steric hindrance of adding a second bulky thiol per alkyne within the densely grafted polymer brush. Model studies using time resolved reactions and application of the relationships reported by Murata et al.[24] to calculate the predicted film thickness at full 1,2-adduct conversion are ongoing to better understand the efficacy of the thiol-yne reaction within the confinements of the brush surface. Ultimately, we believe this observation does little to affect the potential of the thiol-yne reaction as a platform for surface engineering.

To illustrate both the modularity and the versatility of our approach, we conducted sequential and area-selective thiol-yne/thiol-yne brush modifications using a simple photopatterning technique. The process is schematically shown in Scheme 6b. Copper grids (300 mesh, 58 μm holes/25 μm bars and 2000 mesh, 7.5 μm holes/5 μm bars) were used as photomasks. The grids were placed in direct contact with the brush surface, immersed in MPA containing 2 wt% Irgacure 651, and irradiated with $UV_{\lambda max=365nm}$ light (8 min) yielding a patterned MPA/"yne" surface. After removing the

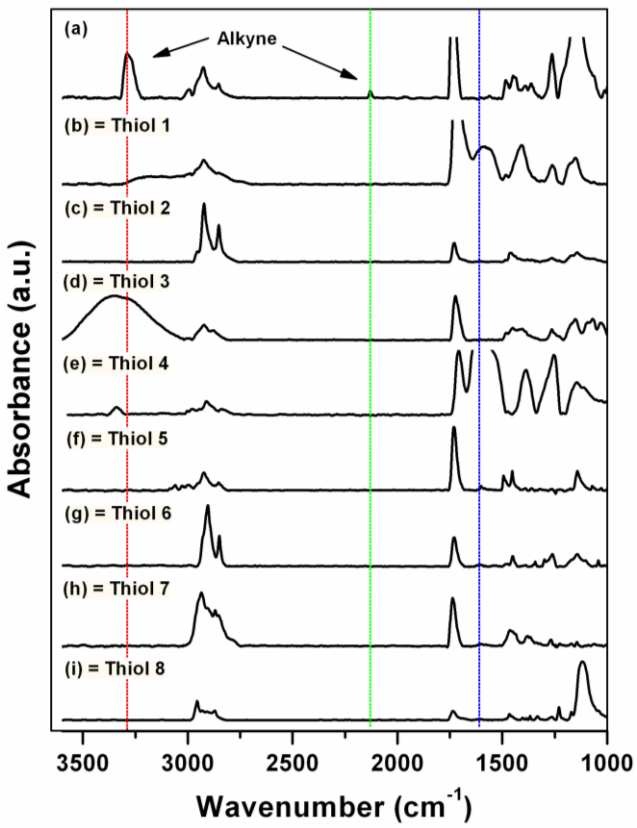

Figure 4. ATR-FTIR spectra of brushes on SiO_x substrates (key peaks are identified): (a) poly(propargyl methacrylate) brush (3283 cm^{-1} C≡C-H (red), 2129 cm^{-1}, C=C (green)) reacted with (b) 3-mercaptopropionic acid (3320-3000 cm^{-1}, COO-H) (c) 1-dodecanethiol (2955, 2922, 2852 cm^{-1}, C-H), (d) 1-thioglycerol (3600-3000 cm^{-1}), (e) N-acetyl-L-cysteine (3354 cm^{-1} CO-NH), (f) benzyl mercaptan (3061, 3028, 3000 cm^{-1}, =C-H; 1601 cm^{-1} C=C) (g) 1-adamantanethiol (2905, 2849 cm^{-1}, C-H), (h) thiocholesterol (2934, 2905, 2868, 2870 cm^{-1}, C-H), (i) 3-mercaptopropyl polyhedral oligomeric silsequioxane (1115 cm^{-1}, Si-O). The blue line indicates the position of the vinyl sulfide species (1609 cm^{-1}).

grid and washing with THF, the unexposed and unreacted "yne" was then subjected to a second thiol-yne reaction with DDT (8 min) affording the micropatterned, multicomponent surface. Figure 5 (a-b) shows the optical condensation images for the MPA/DDT patterned surface (see Appendix A for additional optical images). As shown, the hydrophilic MPA regions (deprotonated with 0.01 M KOH) preferentially nucleate condensation of water permitting facile visualization of the chemically patterned

surface.[32] The inverse pattern DDT/MPA was also demonstrated (Figure 5c). Well-defined edges and droplet confinement indicate a sharp interface between the hydrophilic MPA and hydrophobic DDT regions.

Since thiyl radicals can be generated close to visible wavelengths,[19] we further demonstrate the practicality of the thiol-yne approach for surface modification by

Table 1

Thickness measurements before/after thiol-yne "click" reactions

Ellipsometry Measurements (nm)	
Initiator	
Protected	Deprotected
2.3 ± 0.4	1.1 ± 0.3
Polymer Brush	
Protected	Deprotected
24.2 ± 2.7	12.8 ± 1.7

Thiol-yne "Click" Reactions[A]

Thiol Derivatives	Deprotected Brush (nm)	"Click" Rxn (nm)
3-mercaptopropionic acid	14.0 ± 0.3	29.3 ± 0.9
1-dodecanethiol	13.9 ± 0.5	64.0 ± 2.2
1-thioglycerol	14.4 ± 0.3	33.5 ± 3.1
N-acetyl-L-cysteine	11.0 ± 0.5	30.9 ± 1.5
Benzyl mercaptan	14.7 ± 0.4	32.1 ± 1.6
1-admantanethiol	11.4 ± 1.0	29.3 ± 3.7
Thiocholesterol	10.0 ± 0.4	26.6 ± 0.8
Mercaptopropylisobutyl POSS®	12.7 ± 0.4	56.8 ± 0.3

[A] Representative values from a single experiment, values represent avg. thickness and st.dev. calculated from a minimum of three points along each substrate.

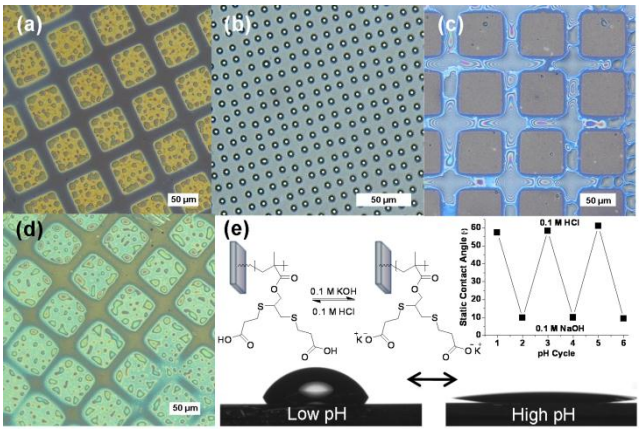

Figure 5. Condensation images of sequential thiol-yne micropatterned brushes showing water droplets selectively nucleating on the hydrophilic MPA areas: (a) MPA/DDT (square/bars), 300 mesh (b) MPA/DDT (squares/bars), 2000 mesh (c) Inverse DDT/MPA (squares/bars), 300 mesh (d) MPA/DDT modification in Sunlight (squares/bars) (e) Static water contact angle measurements showing pH responsive reversible wettability of MPA surfaces prepared outdoors in sunlight. Note: Color variations result from thin film interference under humid conditions.

performing homogeneous and patterned thiol-yne surface reactions outdoors using sunlight as a radiation source. Reactions were carried out in Petri dishes with non-purged thiol solutions. For consistency, we again used 2 wt% Irgacure 651 although photoinitiators that absorb further into the visible are readily available. Quantitative conversion of the tethered alkynes was observed within 1 h of sunlight exposure (Figure 6). Figure 5d shows the condensation image of the resulting sunlight patterned MPA/DDT brush. The results are analogous to those obtained in the lab suggesting the possibility of large scale surface modifications using renewable energy resources. As a final point, we show that homogeneous, pH responsive MPA functionalized brushes can easily be synthesized in sunlight. These surfaces exhibit reversible wettability upon protonation and deprotonation of the carboxylic acid functionalities as shown in Figure 5e.

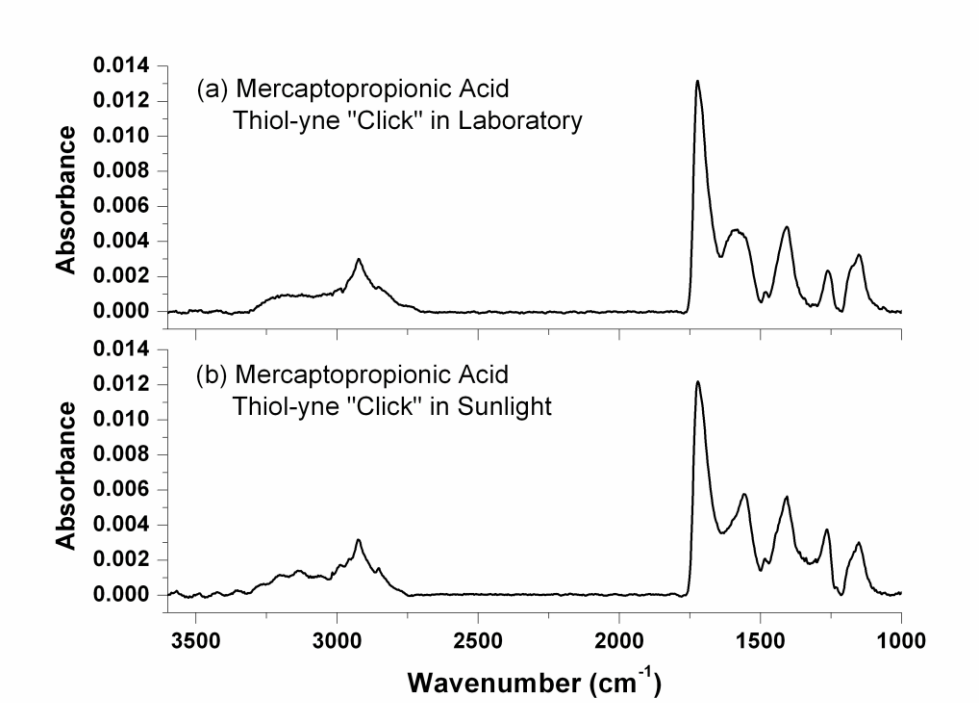

Figure 6. ATR-FTIR for (a) Sunlight vs. (b) Laboratory (Mercaptopropionic acid). The absence of the characteristic alkyne C≡C (2129 cm^{-1}) and C−H stretch (3283 cm^{-1}) indicate complete conversion of the brush pendant "yne" functionalities.

Conclusions

In summary, we have demonstrated thiol-yne chemistry as a modular platform for rapid and practical fabrication of highly functional, multicomponent surfaces. Although demonstrated here on polymer brushes, this approach is certainly extendable to a broad range of surfaces, including bio-related substrates. Considering the mild reaction conditions, rapid throughput, and compatibility with orthogonal chemistries, we expect this platform to find widespread use among the materials science community.

Acknowledgments

The financial support for this research was provided by the University of Southern Mississippi startup funds. We thank Ms. Megan Aumsuwan and Dr. Cathrin Corten of the Urban research group for help with ATR-FTIR and the Rawlins research group for

help with optical microscopy. This paper is dedicated to the late Prof. Charles E. Hoyle for his pioneering work in the field of photopolymerization and photochemistry.

References

(1) Kolb, H. C.; Finn, M. G.; Sharpless, K. B. *Angew. Chem. Int. Ed.* **2001**, *40*, 2004-2021.

(2) Im, S. G.; Bong, K. W.; Kim, B.-S.; Baxamusa, S. H.; Hammond, P. T.; Doyle, P. S.; Gleason, K. K. *J. Am. Chem. Soc.* **2008**, *130*, 14424-14425.

(3) Nebhani, L.; Barner-Kowollik, C. *Adv. Mater.* **2009**, *21*, 3442-3468.

(4) Xu, H.; Hong, R.; Lu, T.; Uzun, O.; Rotello, V. M. *J. Am. Chem. Soc.* **2006**, *128*, 3162-3163.

(5) Baskin, J.; Prescher, J.; Laughlin, S.; Agard, N.; Chang, P.; Miller, I.; Lo, A.; Codelli, J.; Bertozzi, C. *Proc. Natl. Acad. Sci. U.S.A.* **2007**, *104*, 16793 - 19797.

(6) Chan, J. W.; Hoyle, C. E.; Lowe, A. B. *J. Am. Chem. Soc.* **2009**, *131*, 5751-5753.

(7) Chan, J. W.; Zhou, H.; Hoyle, C. E.; Lowe, A. B. *Chem. Mater.* **2009**, *21*, 1579-1585.

(8) Fairbanks, B. D.; Scott, T. F.; Kloxin, C. J.; Anseth, K. S.; Bowman, C. N. *Macromolecules* **2008**, *42*, 211-217.

(9) Yu, B.; Chan, J. W.; Hoyle, C. E.; Lowe, A. B. *J. Polym. Sci., Part A: Polym. Chem.* **2009**, *47*, 3544-3557.

(10) Dondoni, A. *Angew. Chem. Int. Ed.* **2008**, *47*, 8995-8997.

(11) Hoyle, C. E.; Lee, T. Y.; Roper, T. *J. Polym. Sci., Part A: Polym. Chem.* **2004**, *42*, 5301-5338.

(12) Killops, K. L.; Campos, L. M.; Hawker, C. J. *J. Am. Chem. Soc.* **2008**, *130*, 5062-5064.

(13) Rissing, C.; Son, D. Y. *Organometallics* **2009**, *28*, 3167-3172.

(14) Boyer, C.; Granville, A.; Davis, T. P.; Bulmus, V. *J. Polym. Sci., Part A: Polym. Chem.* **2009**, *47*, 3773-3794.

(15) Campos, L. M.; Killops, K. L.; Sakai, R.; Paulusse, J. M. J.; Damiron, D.; Drockenmuller, E.; Messmore, B. W.; Hawker, C. J. *Macromolecules* **2008**, *41*, 7063-7070.

(16) DeForest, C. A.; Polizzotti, B. D.; Anseth, K. S. *Nat. Mater.* **2009**, *8*, 659-664.

(17) Geng, Y.; Discher, D. E.; Justynska, J.; Schlaad, H. *Angew. Chem. Int. Ed.* **2006**, *45*, 7578-7581.

(18) Nurmi, L.; Lindqvist, J.; Randev, R.; Syrett, J.; Haddleton, D. M. *Chem. Comm.* **2009**, 2727-2729.

(19) ten Brummelhuis, N.; Diehl, C.; Schlaad, H. *Macromolecules* **2008**, *41*, 9946-9947.

(20) Wittrock, S.; Becker, T.; Kunz, H. *Angew. Chem. Int. Ed.* **2007**, *46*, 5226-5230.

(21) Khire, V.; Lee, T.; Bowman, C. *Macromolecules* **2008**, *41*, 7440-7447.

(22) Khire, V.; Yi, Y.; Clark, N.; Bowman, C. *Adv. Mater.* **2008**, *20*, 3308-3313.

(23) Jonkheijm, P.; Weinrich, D.; Köhn, M.; Engelkamp, H.; Christianen, P. C. M.; Kuhlmann, J.; Maan, J. C.; Nüsse, D.; Schroeder, H.; Wacker, R.; Breinbauer, R.; Niemeyer, C. M.; Waldmann, H. *Angew. Chem. Int. Ed.* **2008**, *47*, 4421-4424.

(24) Murata, H.; Prucker, O.; Rühe, J. *Macromolecules* **2007**, *40*, 5497-5503.

(25) Li, Y.; Benicewicz, B. C. *Macromolecules* **2008**, *41*, 7986-7992.

(26) Schuh, C.; Santer, S.; Prucker, O.; Rühe, J. *Adv. Mater.* **2009**, *21*, 4706-4710.

(27) Hu, M.; Li, J.; Q. Yao, S. *Org. Lett.* **2008**, *10*, 5529-5531.

(28) Velcicky, J.; Lanver, A.; Lex, J.; Prokop, A.; Wieder, T.; Schmalz, H.-G. *Chem. Eur. J.* **2004**, *10*, 5087-5110.

(29) Ladmiral, V.; Mantovani, G.; Clarkson, G. J.; Cauet, S.; Irwin, J. L.; Haddleton, D. M. *J. Am. Chem. Soc.* **2006**, *128*, 4823-4830.

(30) Lin-Vien, D. *The Handbook of infrared and raman characteristic frequencies of organic molecules*; Academic Press: Boston, 1991.

(31) Cadenhead, G. *Structure and properties of cell membranes*; CRC Press: Boca Raton, FL, 1985; Vol. III.

(32) Brown, A. A.; Azzaroni, O.; Fidalgo, L. M.; Huck, W. T. S. *Soft Matter* **2009**, *5*, 2738-2745.

CHAPTER IV

THIOL-ISOCYANATE "CLICK" REACTIONS: RAPID DEVELOPMENT OF FUNCTIONAL POLYMERIC SURFACES

Introduction

Applications for advanced functional polymeric surfaces that possess precisely engineered properties are expanding rapidly. Such demands necessitate the development of fabrication methods for soft material surfaces with precise control over functionality, architecture, reactivity and domain size for an array of applications ranging from biosensors to microelectronics.[1] Among several surface functionalization strategies recently developed, those involving robust and efficient click reactions are particularly attractive for orthogonal and site-selective immobilization of functional moities.[2] Several outstanding examples involving conventional Cu-catalyzed azide-alkyne[3-5] and photoactivated Cu-free azide-alkyne cycloadditions[6] illustrate the power of click strategies for tailor-made surfaces. Additionally, we and others have demostrated thiol-click reactions, including thiol-ene[7-10] and thiol-yne,[11] as rapid, robust, and efficient immobilization strategies toward patterned, multicomponent surfaces. Our current efforts focus on expanding the "toolbox" of modular reactions that allow immobilization of functionally complex molecules onto solid substrates by exploiting efficient linking strategies. Herein, we report thiol-isocyanate (thiol-NCO) chemistry as a modular approach toward surface engineering by demonstrating the rapid generation of a library of functional, patterned, and multicomponent polymer brush surfaces using a single substrate precursor.

The base-catalyzed reaction of thiols with isocyanates yielding thiourethanes has been known for over 50 years,[12,13] but has only recently been recognized for its potential as a click reaction.[14,15] Despite impressive potential, these reactions have been scarcely exploited for polymer synthesis[16,17] and postmodification.[18,19] For functional surfaces, isocyanate chemistry has only been explored in a few instances that focused on reactions with amines (urethane linkages) for immobilizing functional moieties on self-assembled monolayers for biosurfaces,[20,21] photoswitchable wettability,[22] organometallic surfaces,[23] and self-cleaning/anti-fog surfaces.[24] Considering rapid kinetics, quantitative conversions, and vast libraries of commercially available and/or naturally occuring thiols, we envisioned the fabrication of highly functional surfaces using base-catalyzed thiol-NCO reactions to modify densely tethered NCO-containing polymer brush surfaces. As we will show, this approach works equally well with thiols or amines. This platform is analogus, but orthogonal to our recently reported radical-mediated thiol-yne click approach.[11] Additionally, the NCO group is inert to radical polymerization conditions eliminating any need and synthetic effort to protect the "clickable" moeity during surface-initiated photopolymerization (SIP).

Experimental

Materials

All reagents and solvents were obtained at the highest purity available from Aldrich Chemical Company or Fisher Scientific and used without further purification unless otherwise specified. Commercially available photoinitiator, 2-hydroxy-4'-(2-hydroxyethoxy)-2-methylpropiophenone (Irgacure 2959), was obtained from Ciba Specialty Chemicals and modified with trichlorosilane according to a previously reported

protocol (synthetic procedures found in Chapter III experimental).[11,25] Mercapto-propylisobutyl Polyhedral Oligomeric Silsesquioxane (POSS)® was generously donated by Hybrid Plastics. 2-Isocyanatoethyl methacrylate (NCOMA, (1)) was purchased from TCI America and passed through neutral alumina before use to remove the BHT inhibitor (See Appendix B for corresponding ^{1}H and ^{13}C-NMR, respectively).

Characterization

A Varian Mercury Plus 300 MHz NMR spectrometer operating at a frequency of 300 MHz with VNMR 6.1C software was used for proton and carbon analysis. Contact angle goniometry was performed using a Ramé-hart 200-00 Std.-Tilting B. goniometer. Static (θ_{sw}) contact angles were measured using 10 μL water droplets. Ellipsometric measurements were carried out using a Gaertner Scientific Corporation LSE ellipsometer with a 632.8 nm laser at 70° from the normal. Refractive indices of 3.89 for silicon, 1.46 for silicon oxide, 1.43 for initiator, and 1.5 for the polymer were used. ATR-FTIR spectra of surface polymers were carried out using a Nicolet 8700 with a gradient-angle ATR attachment using Omnic software. Spectra were taken with a resolution of 4 cm^{-1} by accumulating a minimum of 64 scans per run. Nitrogen was constantly purged through the attachment to reduce interference of carbon dioxide and water. Optical images of the micropatterns were taken using a Keyence VHX digital microscope with a multi-illumination lighting system. Fluorescent images were taken using a Nikon eclipse 80i with a fict filter, Plan-Fluor 20x/0.50 scope, and a photometrics coolsnap cf camera using NIS-Elements F software. AFM imaging was performed in tapping mode on a Multimode Nanoscope IIIa (Digital Instruments/Veeco Metrology Group) using silicon

AFM probes with a nominal spring constant of 40 N/m and a resonant frequency of 300 kHz. The scan rate used was 0.374 Hz.

Surface-Initiated Polymerization (SIP) of NCOMA (1)

SIP reactions were carried out in a custom-built inert atmosphere (nitrogen) box using a microchannel reaction device (Fabricated from Norland 81 optical adhesive). This approach permits the preparation of polymer brushes on wafer size substrates and requires a minimal amount of monomer solution (400 μL for microchannel + 600 μL for tubing = 1000 μL total volume). The initiator-functionalized silicon wafers were placed in a microchannel reaction device approximately 7" from the UV light source (λ_{max} = 365 nm, Omnicure Series 1000 with a 5 mm collimating adaptor). After purging the reaction chamber and monomer solution with N_2 for 30 min, a 1:6 volume % solution of (1) in THF was injected into the microfluidic channel and subsequently exposed to UV light for 20 minutes. After polymerization, any physisorbed polymer was removed by washing the substrate extensively with THF and toluene. Figure 7 shows the polymer brush thickness achieved as a function of polymerization time. The non-linear response of the thickness vs. polymerization time (or UV irradiation time) is the typical behavior observed for conventional free-radical surface-initiated photopolymerization. The behavior is also consistent with results reported by Schuh and coworkers[25] for other vinyl monomers using similar photoinitiator monolayers.

Thiol-Isocyanate "Click" Reactions

All thiol-isocyanate reactions were catalyzed using 1,8-diazabicyclo[5.4.0]undec-7-ene (DBU) under ambient laboratory conditions (i.e. r.t. and normal atmosphere) for 12 minutes unless otherwise specified. No catalyst was required for amine-isocyanate

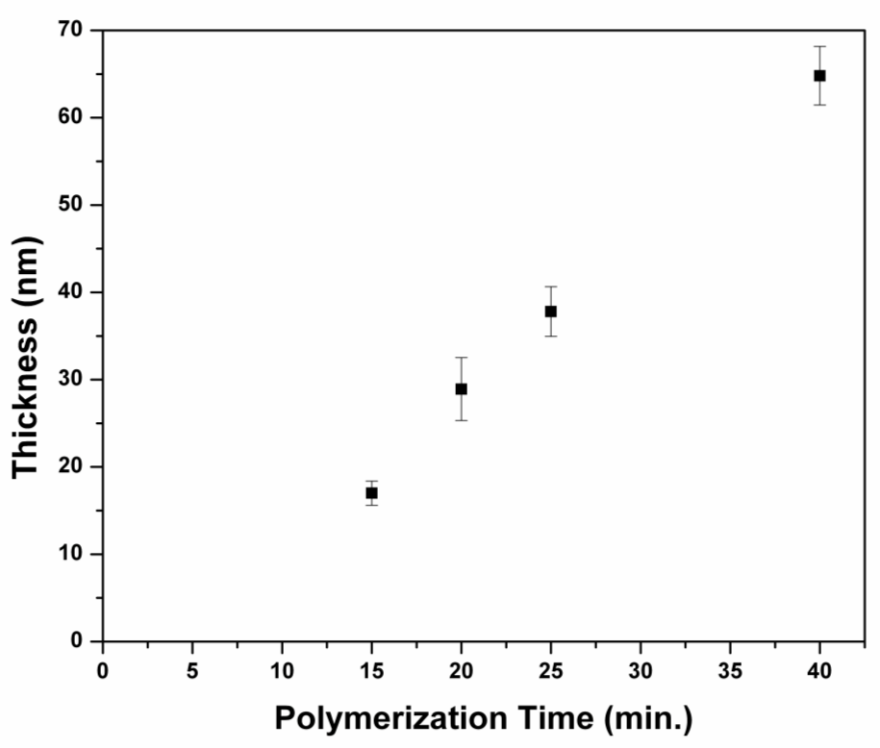

Figure 7. Isocyanate functionalized polymer brush thickness as a function of polymerization time.

reactions. Reaction mixtures were not degassed prior to use. After X-isocyanate (X = thiol or amine) reactions, the samples were washed extensively with THF, and toluene. Details of the various X-isocyanate reactions are given below. In all cases, a significant change in wettability could be observed within seconds of initiation. However, reaction times were chosen to ensure complete conversion of the isocyanate units on the surface.

3-mercaptoproprionic acid

A solution of 3-mercaptoproprionic acid (1.2 mL, 13.8 mmol) and THF (3.6 mL), 1:3 (v/v) ratio, was prepared. A 500:1 (mol/mol) ratio of thiol:DBU (4.12 µL DBU) was used to catalyze the reaction. The thiol solution was placed into the reaction vessel containing the isocyanate-functionalized polymer brush followed by the addition of the catalyst, and subsequently allowed to react for 12 minutes.

1-dodecanethiol

A solution of 1-dodecanethiol (1.5 mL, 6.3 mmol) and THF (4.5 mL), 1:3 (v/v) ratio, was prepared. A 500:1 (mol/mol) ratio of thiol:DBU (1.91 µL DBU) was used to catalyze the reaction. The thiol solution was placed into the reaction vessel containing the isocyanate-functionalized polymer brush followed by the addition of the catalyst, and subsequently allowed to react for 12 minutes.

1-thioglycerol

A solution of 1-thioglycerol (1.2 mL, 13.8 mmol) and THF (3.6 mL), 1:3 (v/v) ratio, was prepared. A 500:1 (mol/mol) ratio of thiol:DBU (4.13 µL DBU) was used to catalyze the reaction. The thiol solution was placed into the reaction vessel containing the isocyanate-functionalized polymer brush followed by the addition of the catalyst, and subsequently allowed to react for 12 minutes.

N-acetyl-L-cysteine

A solution of N-acetyl-L-cysteine (0.25 g, 1.5 mmol) and a 2:1 (v/v) THF:DMF (3.2 mL, 1.6 mL) was prepared. A 300:1 (mol/mol) ratio of thiol:DBU (0.75 µL DBU) was used to catalyze the reaction. The thiol solution was placed into the reaction vessel containing the isocyanate-functionalized polymer brush followed by the addition of the catalyst, and subsequently allowed to react for 12 minutes.

Benzyl mercaptan

A solution of benzyl mercaptan (1.2 mL, 9.3 mmol) and THF (3.6 mL), 1:3 (v/v) ratio, was prepared. A 500:1 (mol/mol) ratio of thiol:DBU (2.77 µL DBU) was used to catalyze the reaction. The thiol solution was placed into the reaction vessel containing

the isocyanate-functionalized polymer brush followed by the addition of the catalyst, and subsequently allowed to react for 12 minutes.

1-adamantanethiol

A solution of 1-adamantanethiol (0.25 g, 1.5 mmol) and THF (4.8 mL) was prepared. A 300:1 (mol/mol) ratio of thiol:DBU (0.71 µL DBU) was used to catalyze the reaction. The thiol solution was placed into the reaction vessel containing the isocyanate-functionalized polymer brush followed by the addition of the catalyst, and subsequently allowed to react for 12 minutes.

Thiocholesterol

A solution of thiocholesterol (0.15 g, 0.37 mmol) and THF (4.8 mL) was prepared. A 100:1 (mol/mol) ratio of thiol:DBU (0.56 µL DBU) was used to catalyze the reaction. The thiol solution was placed into the reaction vessel containing the isocyanate-functionalized polymer brush followed by the addition of the catalyst, and subsequently allowed to react for 12 minutes.

Mercaptopropylisobutyl Polyhedral Oligomeric Silsesquioxane (POSS)®

A solution of POSS (1.0 g, 0.001 mmol) and THF (4.8 mL) was prepared. A 300:1 (mol/mol) ratio of thiol:DBU (0.56 µL DBU) was used to catalyze the reaction. The thiol solution was placed into the reaction vessel containing the isocyanate-functionalized polymer brush followed by the addition of the catalyst, and subsequently allowed to react for 12 minutes.

Furfuryl mercaptan

A solution of furfuryl mercaptan (1.2 mL, 11.8 mmol) and THF (3.6 mL), 1:3 (v/v) ratio, was prepared. A 500:1 (mol/mol) ratio of thiol:DBU (3.53 µL DBU) was

used to catalyze the reaction. The thiol solution was placed into the reaction vessel containing the isocyanate-functionalized polymer brush followed by the addition of the catalyst, and subsequently allowed to react for 12 minutes.

Hexyl amine

A solution of hexyl amine (0.4 mL, 3.0 mmol) and THF (1.2 mL), 1:3 (v/v) ratio, was prepared. The amine solution was placed into the reaction vessel containing the isocyanate-functionalized polymer brush and allowed to react for 12 minutes.

Benzyl amine

A solution of benzyl amine (0.4 mL, 3.7 mmol) and THF (1.2 mL), 1:3 (v/v) ratio, was prepared. The amine solution was placed into the reaction vessel containing the isocyanate-functionalized polymer brush and allowed to react for 12 minutes.

Fluorescent Dye Functionalized Polymer Brush Preparation

Water contact angle measurements (see Appendix B) were the only means of determining the covalent attachment of each molecule synthesized onto the surface. Microscope cover glass slides were cut into appropriate sized pieces and ultrasonically cleaned in acetone, ethanol, and toluene for 15 min. in each solvent. The substrates were dried under a stream of N_2 and treated with UV-ozone for 45 min. Surface-initiated polymerization of (1) was facilitated according to our recent work with p(PgMA) polymer brushes.[11] A 1:6 vol.% solution of (1) in dry THF was injected into a microfluidic channel containing the initiator-immobolized substrate and subsequently exposed to UV light for 20 minutes. After polymer brush formation, a thiol-isocyanate "click" reaction with 3-mercapto-propionic acid was performed with subsequent deprotonation with 0.1 M KOH solution for 5 minutes. The deprotonated MPA

functionalized polymer brush was allowed to form ionic interactions with acridine orange (0.10 g, 0.4 mmol) in deionized water (10 mL) for 30 minutes with subsequent rinsing with deionized water before characterization. Fluorescent microscopy and UV-Vis spectroscopy was performed before/after functionalization with the fluorescent dye, acridine orange, in order to monitor the absorbance of the polymer brush without and with incorporation of the fluorescent molecule.

Micropatterning and Sequential Thiol-Isocyanate Reactions

For patterning, a PDMS stamp was made from a master nanostamp (linewidth 15.0 μm). Details of the procedure are given below.

PDMS stamp fabrication

Three to four drops of (1H, 1H, 2H, 2H-perfluorooctyl) silane was added to the bottom of a small vacuum chamber containing a single crystal nanostamp. Vacuum was applied for 1 h to create a monolayer of silane onto the nanostamp. A 10:1 mixture of Sylgard 184 silicone elastomer base (28.7 g) and Sylgard silicone elastomer curing agent (2.87 g) was mixed well in a disposable beaker followed by removing air bubbles by applying vacuum. Once the air bubbles are removed, the viscous Sylgard solution is poured over the silanated nanostamp in a plastic petri dish. The stamp is allowed to cure for 2 hours at room temperature followed by overnight exposure in an oven for 50 °C.

Preparation of 3-mercapto-1-propanesulfonic acid/1-dodecanethiol micropatterns

The PDMS stamp (linewidth 15.0 μm) previously made was placed onto an isocyanate-containing polymer brush and slight pressure was applied to ensure intimate contact between the stamp and surface. A solution of 3-mercapto-1-propanesulfonic acid (0.25 g, 1.0 mmol) in methanol (10.0 mL) was prepared. A 300:1 (mol/mol) ratio of

thiol:DBU (0.70 µL DBU) was used to catalyze the reaction. Once prepared, the thiol solution containing the catalyst was wicked into the crevices of the stamp and allowed to react for 12 minutes. The stamp was then removed and the sample was washed with methanol and toluene followed by a sequential thiol-isocyanate reaction with 1-dodecanethiol to backfill the unexposed portion of the pattern. 1-dodecanethiol (1.5 mL, 6.3 mmol) in THF (0.375 mL) with a 500:1 (mol/mol) ratio of thiol:DBU (1.91 µL DBU) was used for backfilling. Optical microscopy and AFM was used to analyze the micropatterned polymer brushes.

Results and Discussion

As shown in Scheme 7a, silicon substrates were first functionalized with a chlorosilane derivative of commercially available 2-hydroxy-4'-(2-hydroxyethoxy)-2-methylpropiophenone (Irgacure 2959) photoinitiator.[11,25] These substrates were subsquently inserted into a microchannel reactor containing NCOMA (1:6 v/v in dry THF) and irradiated with $UV_{\lambda max=365nm}$ light (~140 mW/cm^2, 20 min., ~28 nm brush thickness). For the fabrication of a 15 mm x 65 mm substrate only 1 mL of monomer solution was required to fill the microchannel reactor, drastically reducing the cost of this approach. After extensive washing in THF and toluene, the brush surfaces were analyzed by grazing-angle attenuated total reflection FTIR (GATR-FTIR), ellipsometry and water contact angle measuements. Polymer brush formation was confirmed by the presence of the asymmetric stretching vibration of the isocyanate group (2275 cm^{-1}) and carbonyl stretching vibration for esters (1729 cm^{-1}) (Figure 8).[26] The resulting isocyanate-containing polymer brushes served as a "universal" reactive precursor for subsequent thiol-NCO click reactions eliminating the synthetic effort associated with the use of

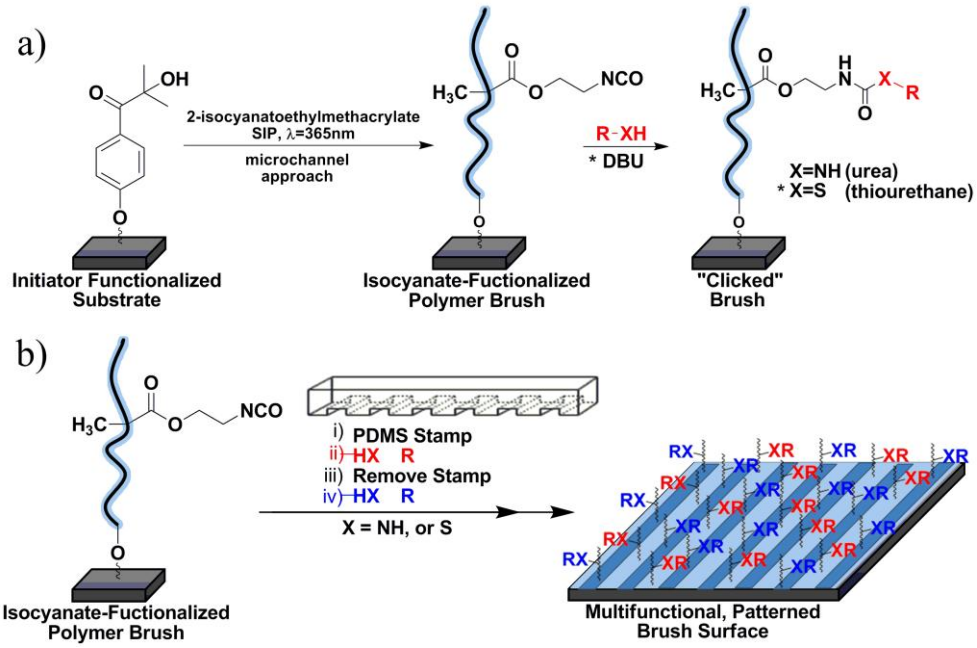

Scheme 7. (a) Schematic procedure for surface-initiated photopolymerization of 2-isocyanatoethyl methacrylate and subsequent X-isocyanate functionalization (X = thiol or amine), (b) Schematic procedure for patterning isocyanate-containing polymer brush surfaces with sequential X-isocyanate reactions.

multiple functional monomers. Despite the known sensitivity of NCO functional groups, no special handling of the substrates was required prior to thiol modification. NCO-modified surfaces could be stored up to two-weeks in nitrogen-flushed, septum-sealed test tubes with no observable loss in functionality or degradation in reactivity.

The nucleophilic addition of primary thiols or amines to isocyanates generates a thiourethane or urea linkage, respectively (Scheme 7a). Amine-NCO reactions are self-catalyzed while thiol-NCO reactions require the addition of a base catalyst – the identity of which is known to have a pronounced effect on the reaction kinetics.[17] Tertiary amine catalysts facilitate rapid reactions via generation of 1) a more electron deficient carbonyl carbon within the isocyanate moiety and 2) a strongly nucleophilic thiolate ion.[14,17] For thiol-NCO reactions herein, 1,8-diazabicyclo[5.4.0]undec-7-ene (DBU) (0.2 mol% with

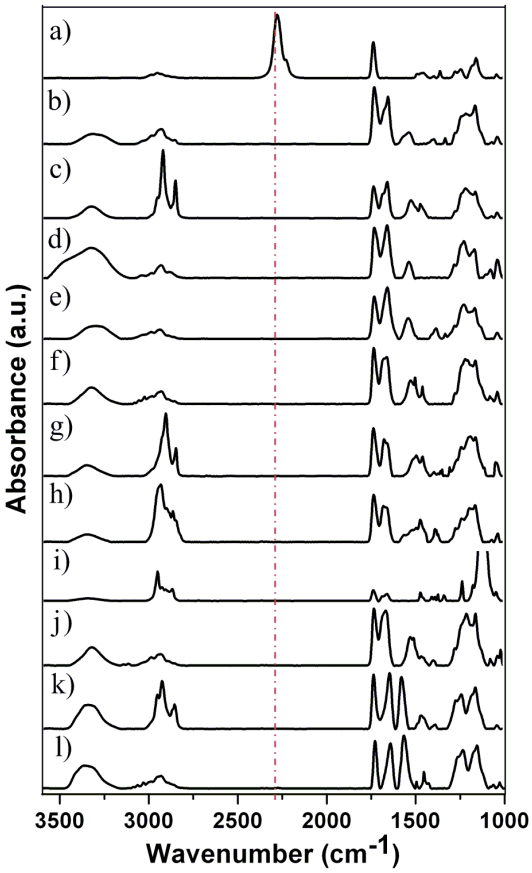

Figure 8. GATR-FTIR spectra of brushes on SiO_x substrates (key peaks are identified): (a) poly(2-isocyanatoethyl methacrylate) brush (2275 cm^{-1}, NCO) (red) reacted with (b) 3-mercaptopropionic acid (3320-3000 cm^{-1}, COO-H), (c) 1-dodecanethiol (2954, 2924, 2852 cm^{-1}, C-H), (d) 1-thioglycerol (3573-3125 cm^{-1}, OH), (e) N-acetyl-L-cysteine (3450-3162 cm^{-1}, CO-NH), (f) benzyl mercaptan (3084, 3058, 3025 cm^{-1}, =C-H; 1517, 1493, 1451 cm^{-1}, C=C), (g) 1-adamantanethiol (2906, 2850 cm^{-1}, C-H), (h) thiocholesterol (2936, 2903, 2865, 2850 cm^{-1}, C-H), (i) 3-mercaptopropyl polyhedral oligomeric silsequioxane (1109 cm^{-1}, Si-O), (j) furfuryl mercaptan (1204, 1156 cm^{-1}, C-O (cyclic), 1068 cm-1, C-O-C (5-membered rings), (k) hexyl amine (2954, 2930, 2856 cm^{-1}, C-H), (l) benzyl amine (3085, 3061, 3025 cm^{-1}, =C-H; 1565, 1493, 1451 cm^{-1}, C=C).

respect to thiol) was used as catalyst. To explore the efficacy of the isocyanate click reactions on surfaces, we selected a library of commerically available thiols and amines for functionalization (Figure 9): 3-mercaptopropionic acid (MPA) (pH responsive), 1-dodecanethiol (DDT) (hydrophobic), 1-thioglycerol (hydrophilic), N-acetyl-L-cysteine (model peptide attachment), benzyl mercaptan, 1-adamantanethiol, thiocholesterol (biomembrane attachment), 3-mercaptopropyl polyhedral oligomeric silsequioxane

(POSS), furfuryl mercaptan, hexyl amine, and benzyl amine. These reactions were carried out under ambient air, temperature, and humidity conditions to afford functional polymeric brushes. Subsequently, the substrates were washed extensively with multiple solvents to eliminate any physisorbed material prior to characterization. GATR-FTIR was used to follow the functionalization of the brushes with the various thiols and amines. For the entire series of functional brushes, quantitative conversion of the tethered isocyanates was observed within minutes as indicated by the disappearance of the peak associated with the isocyanate group (2275 cm^{-1}) (Figure 8) and appearance of peaks indicative of the incorporated thiols and amines (see Appendix B for additional peak assignments). Triethylamine also carried the thiol-NCO reaction to quantitative conversion, albeit in several hours rather than minutes as observed with DBU. Static water contact angles revealed expected changes in wettability related to the functional moieties incorporated into the polymer brushes (Figure 10). An increase in thickness of the polymer brushes was observed after functionalization with the various thiols and amines due to an increase in the molar mass of the monomer repeat unit, resulting in an increase in the molecular weight of the brush (Table 2). Additionally, to broaden the utility of this approach, fluorescent brushes were easily obtained by absorbing acridine orange (fluorescent dye) onto deprotonated MPA functionalized polymer brushes (see Appendix B). The fluorescent dye adheres to the functionalized polymer brush through an ionic interaction and demonstrates the potential use of orthogonal covalent/non-covalent interactions for fabrication of functional polymer surfaces.

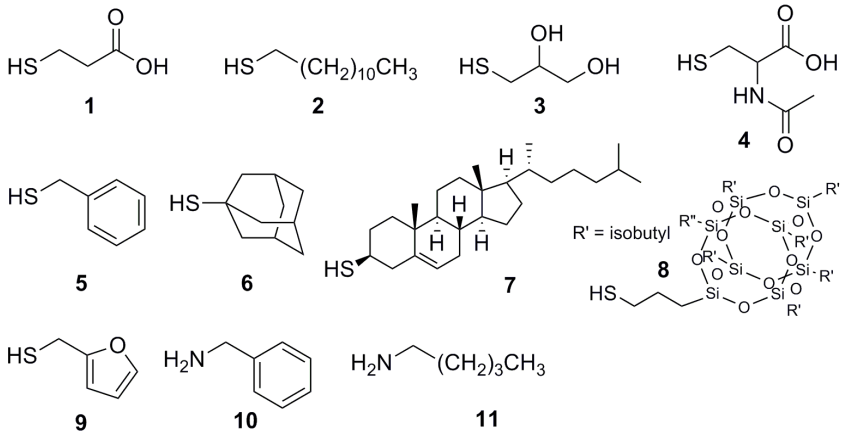

Figure 9. Commercially available thiols/amines used for X-isocyanate click reactions: mercaptopropionic acid (1), 1-dodecanthiol (2), thioglycerol (3), N-acetyl-L-cysteine (4), benzyl mercaptan (5), 1-adamantanethiol (6), thiochlolesterol (7), 3-mercaptopropyl polyhedral oligomeric silsequioxane (POSS) (8), furfuryl mercaptan (9), hexyl amine (10), and benzyl amine (11).

With the developement of thiol-NCO click reactions as a platform for surface engineering in mind, the modularity and versatility of our approach was demonstrated by conducting sequential/area-selective thiol-NCO brush modifications using an elastomeric microcapillary patterning process.[27] The process is schematically shown in Scheme 7b. A line-patterned PDMS stamp (linewidth: 15.0 μm) was used to create defined, micropatterned polymeric surfaces. The stamp was placed in direct contact with the brush surface and a solution of 3-mercapto-1-propanesulfonic acid (300:1 mol/mol thiol:DBU) in methanol was wicked in, subsequently reacting for 12 min yielding a patterned sulfonate/NCO surface. After removing the stamp and washing with methanol and toluene, the unexposed and unreacted isocyanate groups were then subjected to a second thiol-NCO click reaction with DDT (500:1 mol/mol thiol:DBU, 12 min) in THF followed by washing with THF and toluene affording the micropatterned, multi-component surface. Similar patterns could be obtained using sequential combinations of functional thiols and amines. Figure 11a shows the optical condensation image for the

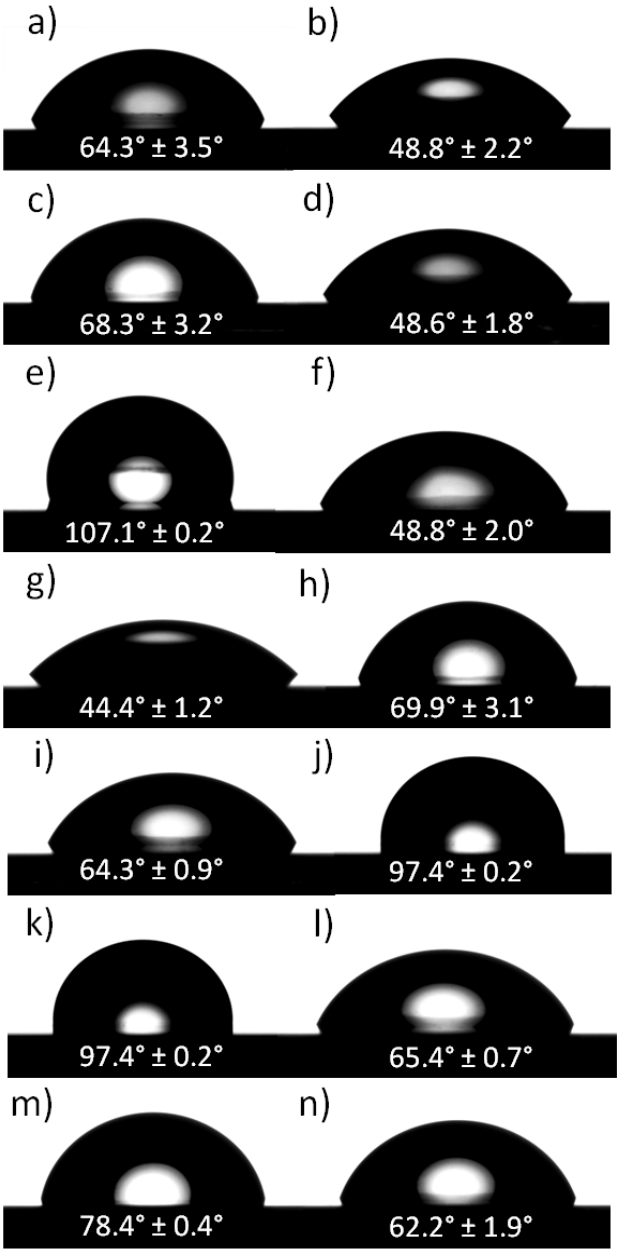

Figure 10. WCA: (a) Protected initiator, (b) Deprotected initiator, (c) 2-isocyanatoethyl methacrylate polymer brush, (d) 3-mercaptopropionic acid, (e) 1-dodecanethiol, (f) 1-thioglycerol, (g) N-acetyl-L-cysteine, (h) Benzyl mercaptan, (i) 1-admantanethiol, (j) Thiocholesterol, (k) Mercaptopropylisobutyl POSS®, (l) Furfuryl mercaptan, m) Hexyl amine, and n) Benzyl amine.

sulfonate/DDT patterned surface. As shown, the hydrophilic sulfonated domains preferentially nucleate condensation of water allowing visualization of the patterned surface.[11,28] To compliment these results, atomic force microscopy (AFM) imaging was

used (Figure 11b) showing height differences created by the incorporation of the two different functional molecules.

Table 2

Thickness measurements before/after X-isocyanate "click" reactions

Ellipsometry Measurements (nm)		
Initiator*		
Protected	Deprotected	
1.8 ± 0.6	0.9 ± 0.7	
Polymer Brush*		
28.2 ± 6.1		
Thiol-Isocyanate "Click" Reactions		
Thiol Derivatives	Polymer Brush**	"Click" Rxn
3-mercaptopropionic acid	37.8 ± 2.8	72.9 ± 1.6
1-dodecanethiol	18.3 ± 0.8	47.8 ± 1.5
1-thioglycerol	37.8 ± 2.8	71.3 ± 3.3
N-acetyl-L-cysteine	29.5 ± 1.9	69.5 ± 5.0
Benzyl mercaptan	19.2 ± 1.7	38.9 ± 2.2
1-admantanethiol	19.2 ± 1.7	44.5 ± 5.1
Thiocholesterol	28.9 ± 3.6	104.1 ± 1.1
Mercaptopropylisobutyl POSS®	28.9 ± 3.6	81.9 ± 1.1
Furfuryl mercaptan	29.5 ± 1.9	51.0 ± 3.1
Amine-Isocyanate "Click" Reactions		
Amine Derivatives	Polymer Brush**	"Click" Rxn
Benzyl amine	33.8 ± 0.6	55.6 ± 2.3
Hexyl amine	28.3 ± 0.4	53.6 ± 1.6

* Values indicative of all substrates used before "Click" Reactions

** Values indicative of individual Polymer Brush uniformity before functionalization

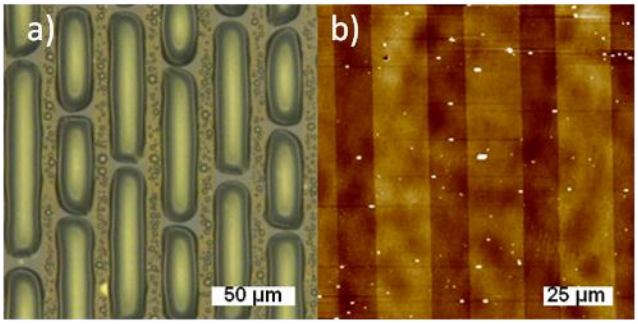

Figure 11. (a) Condensation image of sequential isocyanate-thiol micropatterned brushes (sulfonate/DDT) showing water droplets selectively nucleating on the hydrophilic sulfonated areas, (b) AFM image of sequential isocyanate-thiol micropatterned brushes (sulfonate/DDT), 100 × 100 µm, Z-scale = 50.0 nm.

Conclusions

In summary, we have demonstrated thiol-NCO click chemistry as a modular platform for rapid and robust fabrication of highly functional, multicomponent surfaces. Although demonstrated here on polymer brush modified planar substrates, this approach is certainly extendable to a broad range of surfaces, including three-dimensional particle substrates. As a functional handle for post-polymerization modification, we anticipate thiol-isocyanate click reactions to have a significant impact in many areas of polymer/materials chemistry.

Acknowledgments

Support for this research was provided by startup funds from USM, National Science Foundation (Grant #0917730), and fellowship support from the U.S. Dept. of Education GAANN program (#P200A090066). We thank Baobin Kang in the USM biology department for help with fluorescent microscopy.

References

(1) Barbey, R.; Lavanant, L.; Paripovic, D.; Schüwer, N.; Sugnaux, C.; Tugulu, S.; Klok, H. A. *Chem. Rev.* **2009**, *109*, 5437-5527.

(2) Iha, R. K.; Wooley, K. L.; Nystrom, A. M.; Burke, D. J.; Kade, M. J.; Hawker, C. J. *Chem. Rev.* **2009**, *109*, 5620-5686.

(3) Gonzalez-Campo, A.; Hsu, S.-H.; Puig, L.; Huskens, J.; Reinhoudt, D. N.; Velders, A. H. *J. Am. Chem. Soc.* **2010**, *132*, 11434-11436.

(4) Im, S. G.; Bong, K. W.; Kim, B.-S.; Baxamusa, S. H.; Hammond, P. T.; Doyle, P. S.; Gleason, K. K. *J. Am. Chem. Soc.* **2008**, *130*, 14424-14425.

(5) Krovi, S. A.; Smith, D.; Nguyen, S. T. *Chem. Comm.* **2010**, *46*, 5277-5279.

(6) Orski, S. V.; Poloukhtine, A. A.; Arumugam, S.; Mao, L.; Popik, V. V.; Locklin, J. *J. Am. Chem. Soc.* **2010**, *132*, 11024-11026.

(7) Campos, M.; Paulusse, J.; Zuilhof, H. *Chem. Comm.* **2010**, *46*, 5512-5514.

(8) Khire, V.; Lee, T.; Bowman, C. *Macromolecules* **2008**, *41*, 7440-7447.

(9) Khire, V.; Yi, Y.; Clark, N.; Bowman, C. *Adv. Mater.* **2008**, *20*, 3308-3313.

(10) Weinrich, D.; Lin, P.; Jonkheijm, P.; Nguyen, U.; Schroder, H.; Niemeyer, C.; Alexandrov, K.; Goody, R.; Waldmann, H. *Angew. Chem. Int. Ed.* **2010**, *49*, 1252-1257.

(11) Hensarling, R. M.; Doughty, V. A.; Chan, J. W.; Patton, D. L. *J. Am. Chem. Soc.* **2009**, *131*, 14673-14675.

(12) Arnold, R. G.; Nelson, J. A.; Verbanc, J. J. *Chem. Rev.* **1957**, *57*, 47 - 76.

(13) Dyer, E.; Glenn, J. F.; Lendrat, E. G. *J. Org. Chem.* **1961**, *26*, 2919-2925.

(14) Hoyle, C. E.; Lowe, A. B.; Bowman, C. N. *Chem. Soc. Rev.* **2010**, *39*, 1355 - 1387.

(15) Kolb, H. C.; Finn, M. G.; Sharpless, K. B. *Angew. Chem. Int. Ed.* **2001**, *40*, 2004-2021.

(16) Shin, J.; Matsushima, H.; Chan, J. W.; Hoyle, C. E. *Macromolecules* **2009**, *42*, 3294-3301.

(17) Shin, J.; Matsushima, H.; Comer, C. M.; Bowman, C. N.; Hoyle, C. E. *Chem. Mater.* **2010**, *22*, 2616-2625.

(18) Flores, J. D.; Shin, J.; Hoyle, C. E.; McCormick, C. L. *Polym. Chem.* **2009**, *1*, 213-220.

(19) Li, H.; Yu, B.; Matsushima, H.; Hoyle, C. E.; Lowe, A. B. *Macromolecules* **2009**, *42*, 6537-6542.

(20) Perzyna, A.; Zotto, C. d.; Durand, J.-O.; Granier, M.; Smietana, M.; MeInyk, O.; Stara, I. G.; stary, I.; Kepetarova, B.; Saman, D. *Eur. J. Org. Chem.* **2007**, 4032-4037.

(21) Vigano, M.; Suriano, R.; Levi, M.; Turri, S.; Chiari, M.; Damin, F. *Surf. Sci.* **2007**, *601*, 1365-1370.

(22) Delorme, N.; Bardeau, J. F.; Bulou, A.; Poncin-Epaillard, F. *Langmuir* **2005**, *21*, 12278-12282.

(23) McDonald, A. R.; Dijkstra, H. P.; Suijkerbuijk, B. M. J. M.; van Klink, G. P. M.; van Koten, G. *Organometallics* **2009**, *28*, 4689-4699.

(24) Howarter, J. A.; Youngblood, J. P. *Adv. Mater.* **2007**, *19*, 3838-3843.

(25) Schuh, C.; Santer, S.; Prucker, O.; Rühe, J. *Adv. Mater.* **2009**, *21*, 4706-4710.

(26) Socrates, G. *Infrared and Raman Characteristics Group Frequencies*; 3rd ed. ed.; John Wiley & Sons Ltd.: Chichester, 2001.

(27) Kaufmann, T.; Ravoo, B. *Polym. Chem.* **2010**, *1*, 371-387.

(28) Brown, A. A.; Azzaroni, O.; Fidalgo, L. M.; Huck, W. T. S. *Soft Matter* **2009**, *5*, 2738 - 2745.

CHAPTER V

SYNTHESIS OF MULTIFUNCTIONAL POLYMER BRUSH SURFACES VIA SEQUENTIAL AND ORTHOGONAL THIOL-CLICK REACTIONS

Introduction

Multicomponent surfaces – where all components synergistically control the surface properties – are ubiquitous in natural biological systems. For example, the unique superhydrophobic properties of lotus leaves, butterfly wings, and rose petals result from not only multi-scale surface topographies, but also cooperative interactions of these features with multicomponent chemical compositions.[1] The allure of mimicking nature's approach to surface engineering – particularly the ability to install multiple chemical functionalities on surfaces in a controlled fashion – has recently attracted significant attention in terms of strategies leading to multifunctional surfaces and advanced applications in biosensors, self-cleaning surfaces, etc. Among several immobilization strategies reported for surface modification, those that exploit "click" reactions, such as the azide-alkyne Huisgen 1,3-dipolar cycloaddition,[2,3] Diels-Alder,[4-6] and thiol-click,[7-10] as well as other high efficiency transformations like activated ester-amine reactions,[11-14] are particularly attractive for the fabrication of multifunctional surfaces. These reactions – due to the possibility of orthogonal reaction conditions – permit sequential and/or simultaneous modifications resulting in the ability to control the number and spatial location of multiple functional groups on the surface.[3,11,15] Orthogonal modification of surfaces using Cu(I)-catalyzed azide-alkyne Huisgen 1,3-dipolar cycloaddition (CuAAC) has been demonstrated by several groups. For example, Murphy et al.[16] simultaneously immobilized amine and acetylene-terminated peptides onto a mixed self-assembled

monolayer containing complementary carboxylate and azide groups via orthogonal carbodiimide condensation and CuAAC chemistry to create multifunctional surfaces that present distinct peptides to stem cells on a bioinert background. These surfaces enabled a better understanding of multiple, distinct extracellular factors that work in concert to regulate stem cell adhesion at interfaces. Im et al.[17] used orthogonal acetylene and amine functionalized thin films obtained by plasma enhanced chemical vapor deposition for synthesis of multifunctional nanopatterned surfaces via an elegant one-pot transformation using CuAAC and carbodimide/activated ester chemistries. Concern over the presence of residual metal impurities following copper-catalyzed click reactions has motivated the development of alternate, metal-free surface modification strategies. Consequently, a wide variety of metal-free click reactions – such as strain promoted azide-alkyne cycloadditions,[18-21] and Diels-Alder cycloadditions[4-6] – are increasingly becoming methods of choice to synthesize multifunctional surfaces via orthogonal transformations. For example, Orski and coworkers[22] used cyclopropenone-masked dibenzocyclooctynes tethered on a brush surface for light-activated and orthogonal immobilization of two azides via sequential copper-free [3+2] cycloaddition click reactions. Similarly, a route to bio-orthogonal multifunctional surface modification using copper-free azide-alkyne click with electron-deficient alkynes was recently demonstrated by Deng et al.[23]

Alternatively, we and others have shown thiol-based click reactions – such as thiol-ene,[24-28] thiol-yne[28-33] and thiol-isocyanate[34-37] – to be a powerful approach for engineering multifunctional materials and surfaces in a modular fashion. Thiol-click reactions are advantageous for this purpose in that they proceed at room temperature with high efficiency and rapid kinetics, in the presence of oxygen/water, without expensive

and potentially toxic catalysts, and are highly tolerant of a wide range of functional groups. Additionally, thiol-click reactions are orthogonal to a wide range of chemistries.[38] Notably, one only has to look within the thiol-click class of reactions to realize a powerful set of orthogonal transformations that enable the installation of multiple chemical functionalities on a surface with high efficiency and modularity. Herein, we describe a versatile post-polymerization modification strategy to synthesize multifunctional polymer brush surfaces via combination of surface-initiated photopolymerization (SIP) and orthogonal thiol-click reactions. One of the principal advantages of the post-modifiable brush platform is that it provides a much larger number of modifiable sites per unit area of substrate as compared to conventional self-assembled monolayers (SAMs), while decoupling the polymer synthesis step from the immobilization of sensitive functional groups on the surface thereby avoiding expensive monomer synthesis and reducing potential side reactions.[39] Specifically, we demonstrate two routes to multifunctional brush surfaces: In the first approach, alkyne-functionalized homopolymer brushes are simultaneously modified with multiple thiols via a statistical, radical-mediated thiol-yne co-click reaction; and in the second approach, copolymer brushes carrying two distinctly-addressable reactive moieties are sequentially modified via orthogonal base-catalyzed thiol-X (where X represents an isocyanate, epoxy,[40] or α-bromoester[41-43]) and radical-mediated thiol-yne reactions. In both cases, we show that surface properties, in the form of wettability as a model example, can be easily tuned over a wide range by judicious choice of brush composition and thiol functionality.

Experimental

Materials

All the solvents and reagents were obtained at the highest purity available from Aldrich Chemical Company or Fisher Scientific and were used as received unless otherwise specified. Silicon wafers polished only on one side were purchased from University Wafers. Commercially available photoinitiator, 2-hydroxy-4'-(2-hydroxyethoxy)-2-methylpropiophenone (Irgacure 2959), was obtained from Ciba Specialty Chemicals and modified with trichlorosilane according to a previously reported protocol.[29,44]

Monomers, glycidyl methacrylate (GMA; Acros Organics, 97%), hydroxyethyl-methacrylate (HEMA, 98% Aldrich), and 2-isocyanatoethyl methacrylate (NCOMA; TCI America, 98%), were passed through basic and vacuum-dried neutral alumina columns, respectively, to remove the inhibitor. Protected propargyl alcohol, 3-trimethylsilyl-2-propyn-1-ol (PgOH-TMS; 98%), was purchased from GFS Chemicals and was used as received. All thiols were obtained at the highest available purity from Aldrich Chemical Company and were used without any further purification. Reagents, 1,8-diazabicyclo-[5.4.0]undec-7-ene (DBU) and 2,2-dimethoxy-2-phenyl acetophenone (DMPA), for thiol-click reactions were also obtained from Aldrich and used as received.

Characterization

Chemical structures of synthesized monomers were confirmed using a Varian Mercury Plus 200 MHz NMR spectrometer operating at a frequency of 200.13 MHz. VNMR 6.1C software was used for proton and carbon analysis. Ellipsometric measurements were carried out using a Gaertner Scientific Corporation LSE ellipsometer

with a 632.8 nm laser at 70° from the normal. Refractive index values of 3.86, 1.45, 1.43 and 1.5 for silicon, oxide layer, photoinitiator monolayer and all polymer layers, respectively, were used to build the layer model and calculate layer thicknesses.[44,45] Wettability of the polymer brush surfaces modified with various functionalities was tracked by measuring static water contact angles using a ramé-hart 200-00 Std.-Tilting B with 10 μL water droplets. The static contact angle goniometer was operated in combination with accompanying DROPimage Standard software. The chemical nature of the polymer brush surfaces was characterized by Fourier transform infrared spectroscopy (FTIR) in grazing-angle attenuated total reflectance mode (GATR-FTIR) using a ThermoScientific FTIR instrument (Nicolet 8700) equipped with a VariGATR™ accessory (grazing angle 65°, germanium crystal; Harrick Scientific). Spectra were collected with a resolution of 4 cm^{-1} by accumulating a minimum of 128 scans per sample. All spectra were collected while purging the VariGATR™ attachment and FTIR instrument with N_2 gas along the infrared beam path to minimize the peaks corresponding to atmospheric moisture and CO_2. Spectra were analyzed and processed using Omnic software. XPS measurements were performed using a Kratos Axis Ultra Spectrometer (Kratos Analytical, Manchester, UK) with a monochromatic Al K X-ray source (1486.6 eV) operating at 150 W under 1.0×10^{-9} Torr. Measurements were performed in hybrid mode using electrostatic and magnetic lenses, and the pass energy of the analyzer was set at 420 eV for high-resolution spectra and 160 eV for survey scans, with energy resolutions of 0.1 eV and 0.5 eV, respectively. Generally, total acquisition times of 180 s and 440 s were used to obtain high resolution and survey spectra, respectively. All XPS spectra were recorded using the Kratos Vision II software; data files were translated to

VAMAS format and processed using the CasaXPS software package (v. 2.3.12). Binding energies were calibrated with respect to C 1s at 285 eV.

Synthesis of protected alkyne containing monomer, (3-trimethylsilylpropargyl) methacrylate (PgMA-TMS)

PgMA-TMS was synthesized according to a previously reported protocol.[29] Briefly, PgMA-TMS was synthesized by reacting 1 equivalent of PgOH-TMS with 1.2 equivalents of methacryloyl chloride in presence of 1.2 molar equivalents of triethylamine in CH_2Cl_2. First, methacryloyl chloride was added dropwise to the mixture of PgOH-TMS and triethyl amine cooled in an ice bath. The reaction mixture was stirred for 1 h at 0 °C and then at room temperature overnight. The salt byproducts were filtered and the filtrate was washed with deionized water, saturated sodium carbonate and brine, and the organic layer was dried over $MgSO_4$. The product was finally concentrated using rotavap distillation and purified by column chromatography (silica gel column with 40:1 hexane:acetone as eluent) to obtain pure PgMA-TMS (73% yield). ^{1}H-NMR ($CDCl_3$; λ ppm, (see Appendix C)): 0.19 (s, 9H, Si(C^8H_3)$_3$), 1.97 (s, 3H, C^3H_3), 4.76 (s, 2H, C^5H_2), 5.62 (s, 1H, C^1*H*H), 6.18 (s, 1H, C^1H*H*); ($CDCl_3$; λ ppm, (see Appendix C)): 1.76, 20.41, 55.1, 94.2, 101.3, 128.7, 137.9, 168.9. Anal. Calculated for $C_{10}H_{16}O_2Si$: C, 61.18; H, 8.21; O, 16.30; Si, 14.31; Found: C 60.96; H 8.19. (+ESI-MS) m/z (%): 219 [M+Na] (100), 197 [MH+] (40). IR (neat): ν ~ = 2960, 1723, 1638, 1452, 1366, 1314, 1292, 1251, 1147, 1035, 971, 942, 842, 813, 761 cm^{-1}.

Synthesis of α-bromoester containing monomer, 2-(2-bromopropanoyloxy) ethyl methacrylate (BrMA)

BrMA was synthesized by reacting 1 equivalent of HEMA with 1.1 equivalents of 2-bromopropionyl bromide in presence of 1 molar equivalents of triethylamine in anhydrous CH_2Cl_2. First, 2-bromopropionyl bromide was added dropwise to the mixture

of HEMA and triethylamine cooled in an ice bath. The reaction mixture was stirred for 1 h at 0 °C and then at room temperature for 4 h. The salt byproducts were filtered and the filtrate was washed with deionized water and saturated sodium carbonate, and the organic layer was dried over $MgSO_4$. The product was finally concentrated using rotavap distillation and purified by column chromatography (silica gel column with 3:1 v/v hexane: ethyl acetate as eluent) to obtain pure BrMA in 70% yield. ^{1}H-NMR ($CDCl_3$; λ ppm, (see Appendix C)): 1.82 (d, 3H); 1.93 (s, 3H); 4.38 (m, 5H); 5.59 (s, 1H); 6.13 (s, 1H). ^{13}C-NMR (CDCl3; λ ppm, (see Appendix C)): 18.5, 21.8, 39.8, 62.1, 63.6, 126.5, 136.0, 167.3, 170.2. Anal. Calculated for $C_9H_{13}BrO_4$: C, 40.78; H, 4.94; Found: C 40.62; H, 5.09. IR (neat): ν ~ = 2929, 1147, 1718, 1388, 940, 645 cm^{-1}.

Immobilization of 2-hydroxy-4'-(2-hydroxyethoxy)-2-methylpropiophenone trichlorosilane (HPP-$SiCl_3$) on SiO_2 Surfaces

Silicon wafers were cut into appropriate sized pieces and ultrasonically cleaned in acetone, ethanol, and toluene for 15 minutes in each solvent. The substrates were dried under a stream of N_2 and treated with UV-ozone for 45 minutes. HPP-$SiCl_3$ (4 mM) in toluene was immobilized on the SiO_2 surface at room temperature using excess Et_3N as an acid scavenger for ~ 1 h. The samples were then cleaned by extensively rinsing with toluene and methanol and dried under a stream of N_2. The acetate protection group was removed by immersing the wafers prepared above in a suspension of 240 mg K_2CO_3 in 12 mL methanol containing 150 µL H_2O for 1 h. The substrate was subsequently washed with water, methanol, and toluene followed by drying with a stream of N_2. The functionalized silicon wafers were stored in toluene at -20 °C until use. Ellipsometric thickness of the immobilized photoinitiator was 1.1 nm ± 0.3 nm.

Synthesis of (Co)Polymer Brushes by Surface-Initiated Photopolymerization

All (co)polymer brushes were synthesized by surface-initiated photo-polymerization from a solution of the monomer or a mixture of monomers in an appropriate solvent in a custom-built and inert (nitrogen) atmosphere using a microchannel reaction device (fabricated from Norland 81 optical adhesive). This microchannel device uses only 400 μL of monomer solution for a 10 mm × 60 mm substrate and is especially useful for expensive and custom-made monomers. For the sake of brevity, the details of this microchannel-SIP procedure are described elsewhere.[29,46] SIP was carried out using a UV light source (λ_{max} = 365 nm, Omnicure Series 1000 with a 5 mm collimating adaptor) at a light intensity of 150 mW/cm^2 for a specified time. The synthesized (co)polymer brushes were typically sonicated in a good solvent to remove any physisorbed (co)polymer chains, dried with a stream of nitrogen and stored until further use. A brush thickness of 25 nm was targeted to allow facile characterization by GATR-FTIR. For trimethylsilyl-protected poly(propargyl methacrylate) brushes (p(PgMA-TMS)), the TMS group was removed by immersing the wafer in KOH (0.6 g) in methanol (12 mL) at ambient temperature for 1 h to afford the alkyne functionalized polymer brush. The substrate was subsequently washed with water, methanol, toluene, and dried under a stream of N_2. Similarly, silver triflate (AgOTf) in THF/water (1:1 v/v) was used to remove the TMS group from brush substrates with base labile linkages (i.e. thiourethanes).

Thiol-click Reactions on (Co)Polymer Brushes

All thiol-click reactions were conducted under ambient air, temperature and humidity conditions as described in our previous publications.[29,34] DBU (500:1

thiol:DBU mol/mol) was used as a catalyst for all base-catalyzed thiol-click reactions and DMPA (2 % by mass with respect to the thiol) was used as a source of radicals for all the light-induced thiol-yne reactions. Unless otherwise specified, nucleophile-mediated thiol-click reactions were conducted overnight, only to ensure complete reaction. All thiol-yne reactions were conducted using a UV light source (λ_{max} = 365 nm, Omnicure Series 1000 with a 5 mm collimating adaptor) at a light intensity of 40 mW/cm^2 for a specified time. The (co)polymer brushes were sonicated in THF after thiol-click reactions to remove unreacted thiols.

Results and Discussion

One-Pot Thiol-Yne Reactions for Dual-/Multifunctional Surfaces

Scheme 8 shows the general schematic for the synthesis of dual-functional polymer brush surfaces using a one-pot thiol-alkyne functionalization of a poly(propargyl methacrylate) p(PgMA) brush in the presence of a mixture of thiols. This facile synthesis of dual-functional polymer surfaces is accessible due to the similar reactivity of various thiols with the pendant alkyne groups of the p(PgMA) brush. Fairbanks et al.[47] recently showed no statistical difference between the reaction rates of aliphatic thiols and mercaptopropionates with various alkynes under photopolymerization conditions; thus, a one-pot approach would enable a simple route to obtain dual-functional polymer brush surfaces where the final composition of the brush surface depends on the composition of the initial functional thiol mixture used in the thiol-yne reaction. This approach, using a single thiol, was demonstrated previously by our group where it was observed that model thiols reacted quantitatively with alkyne groups within 8 min under the investigated

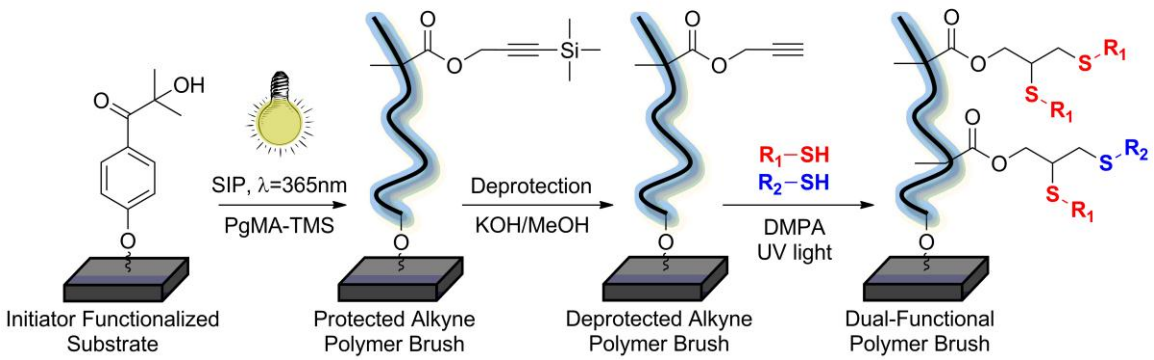

Scheme 8. General schematic for dual-functional polymer brushes by one-pot thiol-yne co-click reactions from p(PgMA) brushes (DMPA = 2,2-Dimethoxy-2-phenylacetophenone). Based on similar thiol reactivities, the thiol-yne co-click likely yields a distribution of 1,2-homo and 1,2-hetero dithioether adducts within the brush surface.

conditions. Similar reaction conditions were adopted here in the case of multiple thiol compositions.

p(PgMA-TMS) brushes were synthesized by surface-initiated photo-polymerization as previously described using the trimethylsilyl-protected alkyne monomer and subsequently deprotected using KOH/methanol to give the terminal alkyne.[29] Figure 12a and 12b show the GATR-FTIR spectra for p(PgMA) brush with pendent alkyne groups in protected and deprotected forms, respectively. The peak at 2189 cm^{-1} for the protected alkyne group in Figure 12a, and the peaks at 2125 and 3280 cm^{-1} for the deprotected alkyne in Figure 12b are consistent with our previous work and confirm the successful synthesis of the p(PgMA) brush. The deprotected p(PgMA) brush was further functionalized via radical-mediated thiol-yne click by exposing the surface to UV light in the presence of a photoinitiator and a mixture of desired thiols (thiol:THF, 50/50 v/v). All thiol-yne reactions were conducted for 4 h at 40 mW/cm^2. The reaction time of 4 h was selected to ensure complete conversion of alkyne groups of p(PgMA) regardless of the fact that the actual time required for complete conversion may be

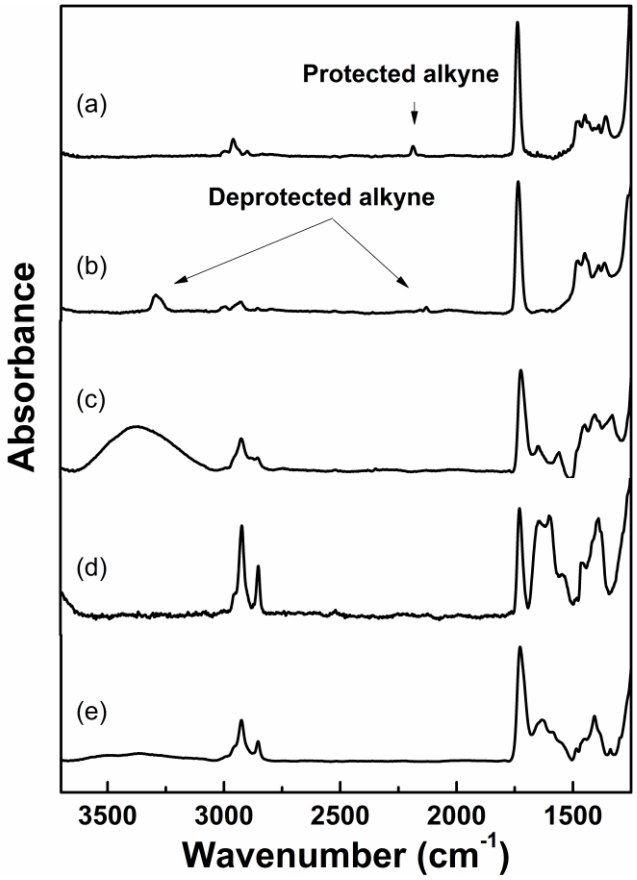

Figure 12. Poly(PgMA) brush (a) protected, 23.7 nm ± 1.1 nm; (b) deprotected, 11.4 nm ±1.1 nm; (c) clicked with an equimolar mixture of thioglycerol and dodecanethiol, 26.1 nm ±3.0 nm; (d) clicked with an equimolar mixture of dodecanethiol and N-acetyl cysteine, 26.9 nm ± 2.3 nm; and (e) clicked with an equimolar mixture of dodecanethiol, mercaptopropionic acid and N-acetyl cysteine, 26.8 nm ±2.8 nm.

significantly shorter than 4 h. Indeed, quantitative conversion of the alkyne groups was observed following thiol-yne click reactions with equimolar mixtures of various thiols as indicated by the disappearance of the peaks corresponding to deprotected alkyne at 2125 cm^{-1} and 3280 cm^{-1} (GATR-FTIR spectra in Fig. 5.1 (c – e). The p(PgMA) brushes showed an expected increase in thickness after thiol-yne reactions with all of the thiol mixtures due to increase in molecular mass of repeat units and was consistent with previous results.[29] Figure 12c shows the GATR-FTIR spectrum for a p(PgMA) brush after thiol-yne click from an equimolar mixture of dodecanethiol and thioglycerol. As

shown in Figure 12c, the broad peak between 3600 and 3100 cm^{-1} corresponding to the hydroxyl groups of thioglycerol, and peaks at 2955, 2922 and 2853 cm^{-1} corresponding to the aliphatic chain of dodecanethiol appear indicating that both thiols simultaneously undergo thiol-yne click reaction with p(PgMA) brush. The concentration of the hydrophilic hydroxyl and hydrophobic aliphatic groups in the clicked brush can be easily controlled by simply varying the concentration of respective thiols to control the wettability of the surface. As a second example, we selected a binary mixture of N-acetyl cysteine, a biologically relevant thiol, and dodecanethiol to perform the one-pot thiol-yne click reaction with a p(PgMA) brush. Figure 12d shows the GATR-FTIR spectrum of a p(PgMA) brush clicked with the equimolar mixture of N-acetyl-cysteine and dodecanethiol. Peaks at 1643 cm^{-1} and 1605 cm^{-1} for the secondary amine groups of N-acetyl cysteine, and peaks at 2955 cm^{-1}, 2922 cm^{-1} and 2853 cm^{-1} corresponding to the aliphatic chains of dodecanethiol appear suggesting successful simultaneous thiol-yne click reaction of both the thiols. The one-pot thiol-yne click approach can be further extended to more complex model systems via use of ternary thiol mixtures. Figure 12e shows the GATR-FTIR spectrum of p(PgMA) functionalized with an equimolar ternary mixture of thiols containing dodecanethiol to impart hydrophobic character, 3-mercaptopropionic acid (MPA) to impart hydrophilic character and N-acetyl cysteine as a model biological thiol. As can be observed in Figure 12e, each of the thiols was successfully coupled with the p(PgMA) brush in one-pot fashion: peaks at 2955 cm^{-1}, 2922 cm^{-1} and 2853 cm^{-1} confirm the functionalization with dodecanethiol; the broad peak at 3250 cm^{-1} confirms the functionalization with 3-mercaptopropionic acid; and peaks at 1643 cm^{-1} and 1605 cm^{-1} confirm the successful coupling of N-acetyl cysteine.

In principle, this ternary brush surface constitutes a model for a biological molecule embedded in a microenvironment with tunable wettability by virtue of the facile control over the proportion of MPA and dodecanethiol in the ternary thiol mixture.

To demonstrate control over brush composition and ultimately wettability, we modified the p(PgMA) brush via thiol-yne reactions with mixtures containing different molar ratios of 3-mercaptopropionic acid and dodecanethiol (DDT). Figure 13 (a – c) shows the GATR-FTIR spectra for polymer brushes clicked with different concentrations of dodecanethiol and 3-mercaptopropionic acid; (a) 3:1 MPA/dodecanethiol, (b) 1:1 MPA/dodecanethiol and (c) 1:3 MPA/dodecanethiol. The characteristic bands for hydroxyl groups within the carboxylic acid moieties of clicked MPA (peak between 3650 and 3050 cm^{-1}) and aliphatic groups (peaks at 2955, 2922 and 2853 cm^{-1}) of dodecanethiol clearly show the differences in the surface composition obtained at various thiol ratios. Quantitatively, the peak area ratio of peaks corresponding to hydroxyl groups within the carboxylic acid moieties (COOH) of MPA to the peaks corresponding to aliphatic groups of dodecanethiol ($A_{Peak,MPA}/A_{Peak,DDT}$) was observed to be 3.13, 0.71 and 0.14 for p(PgMA) functionalized with a mixture of MPA and dodecanethiol in the molar proportions of 3:1, 1:1, and 1:3. While $A_{Peak,MPA}/A_{Peak,DDT}$ values do not reflect the accurate concentrations of pendant COOH and aliphatic groups due to the contribution of aliphatic groups of p(PgMA) main chain and different extinction coefficients of the COOH and aliphatic groups, the relative comparison of $A_{Peak,MPA}/A_{Peak,DDT}$ values qualitatively suggest that it is straightforward to control the concentration of the functional groups, and in turn, the surface properties (wettability in our case) of p(PgMA)

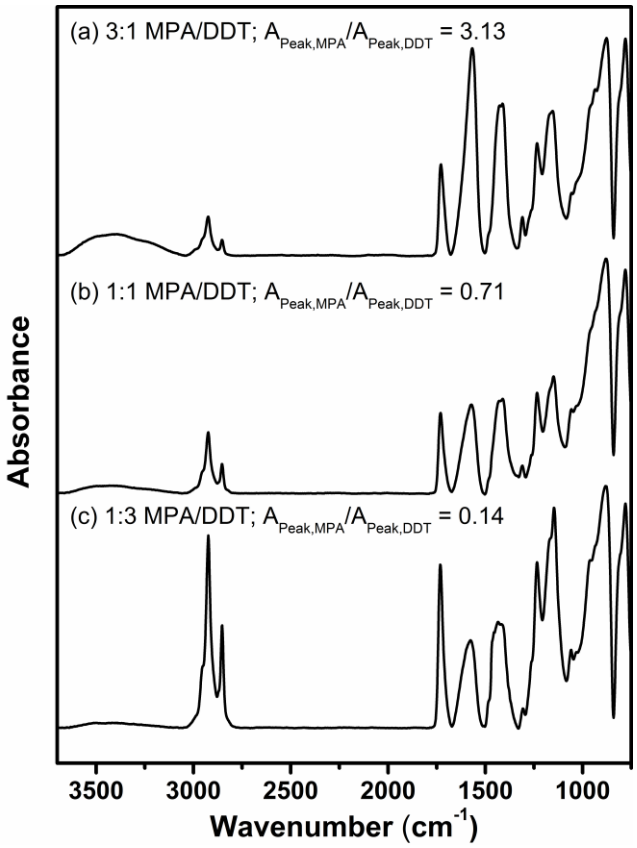

Figure 13. Poly(PgMA) brush clicked with a mixture of mercaptopropionic acid (MPA) and dodecanethiol (DDT) in the ratio of (a) 3:1, 32.1 nm ± 7.3 nm; (b) 1:1, 38.3 nm ± 4.3 nm; and (c) 1:3, 53.0 nm ±1.7 nm.

brush after thiol-yne reaction by simply varying the concentration of component thiols in the initial mixture.

Figure 14 shows the wettability of the clicked polymer brush as a function of the initial MPA/dodecanethiol molar concentrations evaluated by water contact angle measurements after a final THF rinse. As expected, water contact angles of the dually-clicked MPA/dodecanethiol polymer brush lie between the water contact angles of polymer brushes clicked individually with MPA (52°) and dodecanethiol (101°), and decrease as the concentration of MPA in the MPA/dodecanethiol reaction mixture increases. Additionally, methanol as a final rinse induces rearrangement of the top

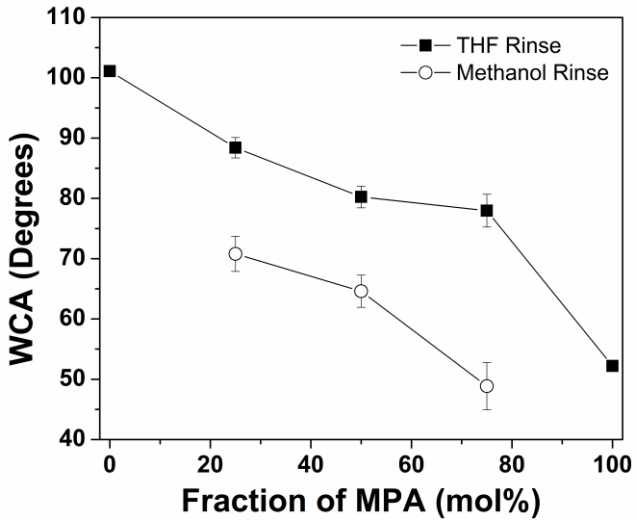

Figure 14. Water contact angle of p(PgMA) brushes functionalized with 3-mercaptopropionic acid and dodecanethiol via one-pot thiol-yne reactions as a function of molar fraction of 3-mercaptopropionic acid in the thiol mixture. Error bars represent one standard deviation of the data, which is taken as the experimental uncertainty of the measurement.

surface of the dual-functional brush, which exposes COOH groups at the surface. Thus, the water contact angles after the methanol rinse are lower than the water contact angles after THF rinsing treatment across the compositional series, but in general, both follow similar trends. Though the one-pot approach is an extremely simple method to synthesize dual or multi-functional brushes with tunable surface properties, it suffers from a limitation that one-pot thiol-yne reactions are random and non-specific, i.e. both functional groups are arranged randomly within the polymer brush and as a mixture of 1,2-homo and 1,2-hetero dithioether adducts. Additionally, the only control over surface composition of the clicked functional groups in this approach is the molar ratio of the thiols in the initial reaction mixture. In many cases, particularly where site-specific modifications are of interest and warranted, i.e. block copolymers, gradients, and patterned brush surfaces, it would be advantageous to explore sequential and/or orthogonal surface modification schemes.

Sequential/Orthogonal Click Reactions for Synthesis of Multifunctional Polymer Brushes

Due to different mechanisms for reactions within the thiol-click toolbox, it is expected that nucleophile-mediated and radical-mediated reactions of thiols with various functional groups can be conducted in an orthogonal fashion. Indeed, the orthogonal nature of thiol-click reactions, in combination with other chemistries, has been previously harnessed by several authors to fabricate functional polymers,[48,49] surfaces,[50] dendrimers[51,52] and several other polymer architectures.[38,53] In this work, we specifically used the orthogonal nature of thiol-click reactions to fabricate dual-functional polymer brushes. Close examination of the thiol-click toolbox suggests that several pairs of thiol-clickable monomers can be used to synthesize dual-functional polymer brushes. Synthesis of these dual-functional brushes, as shown in Scheme 9, was performed by first synthesizing copolymer brushes via copolymerization of monomers containing two different thiol-clickable functional groups, followed by sequential and orthogonal thiol-click reactions. Taking advantage of the orthogonal nature of the radical-mediated thiol-yne reaction and nucleophilic reaction of thiols with isocyanates, alkylhalides, and epoxides, we synthesized copolymer brushes via SIP from mixtures of PgMA-TMS with 2-isocyanatoethyl methacrylate (NCOMA), 2-(2-bromopropanoyloxy) ethyl methacrylate (BrMA) and glycidyl methacrylate (GMA) to form p(NCOMA-stat-PgMA), p(BrMA-stat-PgMA) and p(GMA-stat-PgMA), respectively. In all cases, the nucleophilic thiol-isocyanate, thiol-halogen and thiol-epoxy reactions were performed first followed by deprotection of alkyne group and thiol-yne click reaction. It should be noted that protection of the alkyne group was necessary only to eliminate radical-mediated side reactions during the synthesis of copolymer brushes by SIP.

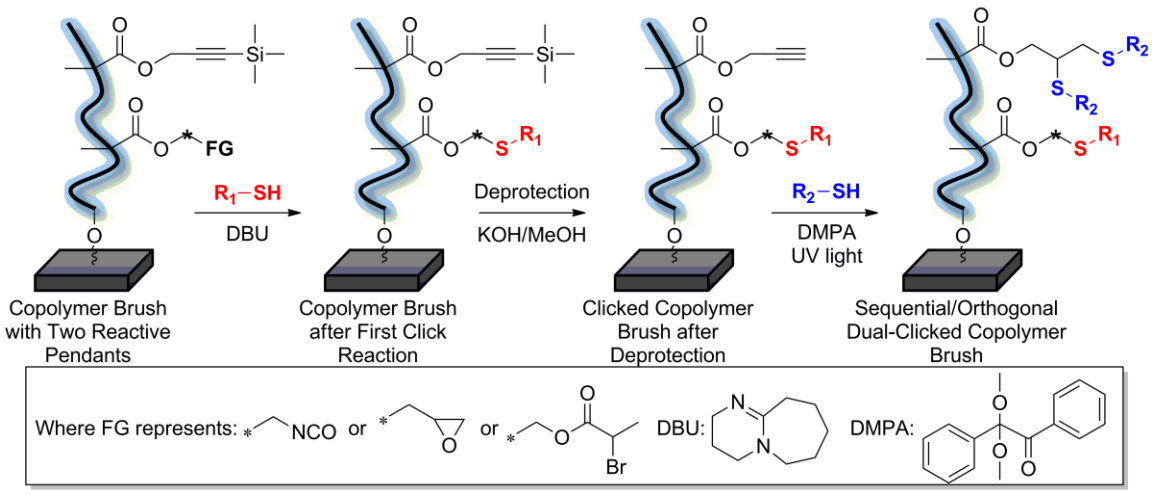

Scheme 9. Schematic for synthesis of dual-functional polymer brushes by sequential and orthogonal and thiol-based click reactions.

Orthogonal Thiol-Isocyanate and Thiol-Yne Functionalization to form Dual-Functional Polymer Brushes

SIP of NCOMA and PgMA-TMS was performed for 45 min at 150 mW/cm^2 to synthesize p(NCOMA-stat-PgMA). Figure 15a shows the GATR-FTIR spectrum for unmodified p(NCOMA-stat-PgMA). Peaks at 2180 cm^{-1} and 2275 cm^{-1} are attributed to the protected alkyne and isocyanate groups, respectively, confirming the presence of both alkyne and isocyanate groups in the statistical copolymer brush. While the ratio of isocyanate and alkyne groups in the copolymer brush could be varied simply by changing the ratio of NCOMA and PgMA-TMS in the monomer mixture, quantifying the ratios in the copolymer brush is beyond the scope of this study and will not be discussed in detail here. Due to the reactivity of isocyanate groups towards moisture, the p(NCOMA-stat-PgMA) surfaces were stored under nitrogen at room temperature until ready for further modification. Additionally, all thiol-isocyanate click reactions were performed using dry solvents. Tertiary amine catalysts facilitate rapid reactions via generation of 1) a more electron deficient carbonyl carbon within the isocyanate moiety and 2) a strongly

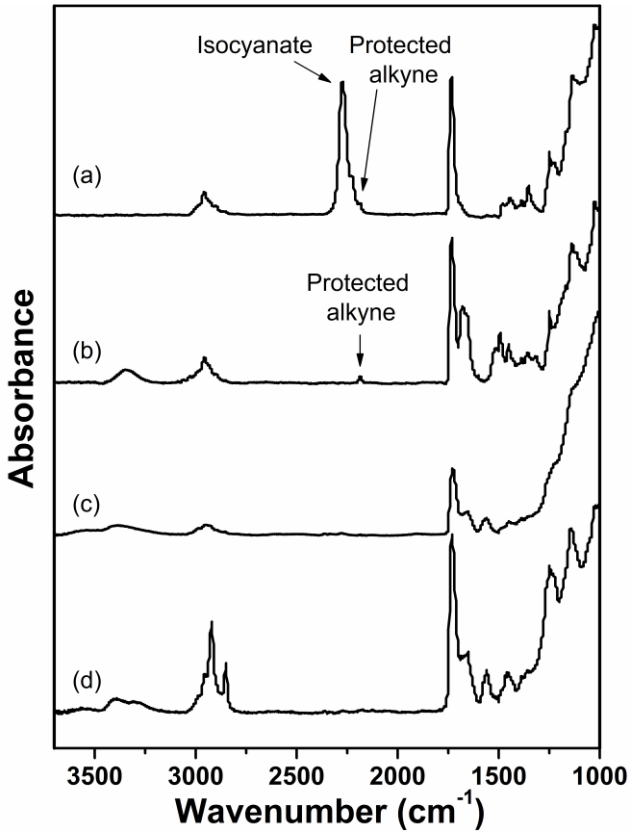

Figure 15. (a) GATR-FTIR spectra for p(NCOMA-stat-PgMA-TMS) synthesized by SIP of 1:6 v/v PgMA:NCOMA, 76.4 nm ± 2.8 nm; (b) after thiol-isocyanate click with benzyl mercaptan, 125.9 nm ± 1.2 nm; (c) after deprotection using AgOTf, 101.7 nm ± 1.8 nm; and (d) after thiol-yne click with dodecanethiol,127.1 nm ± 0.3 nm.

nucleophilic thiolate ion.[9,54] In the first click reaction, benzyl mercaptan was reacted with isocyanate groups in the copolymer brush for 1 h. Figure 15b shows the FTIR spectrum of p(NCOMA-stat-PgMA) brush after the thiol-isocyanate click reaction. The disappearance of the peak associated with the isocyanate group (2275 cm^{-1}) and appearance of peaks indicative of the thiourethane linkage (3326 cm^{-1} (NH-CO)) and incorporated benzyl mercaptan (3018 and 3030 cm^{-1} (=C-H); 1517, 1493 and 1451 cm^{-1} (C=C)) confirm the successful thiol-isocyanate reaction. Notably, the peak at 2180 cm^{-1} corresponding to the protected alkyne group was found to be intact following the thiol-isocyanate click reaction suggesting that thiol-isocyanate transformations do not affect

the protected alkyne groups and can be utilized for further transformations to form a dual-functional polymer brush.

To perform the sequential thiol-yne reaction, alkyne groups must be deprotected to remove the trimethylsilyl functionality. Deprotection of the alkyne moieties under caustic conditions using KOH in methanol was first attempted. However, it was found that the thiourethane bonds resulting from the initial thiol-isocyanate click reaction are labile under these caustic conditions leading to loss of tethered functionality. To eliminate thiourethane cleavage, we adapted an alternate mild strategy to deprotect the alkyne group. In this method, p(NCOMA-stat-PgMA) brushes clicked with benzyl mercaptan were treated with silver triflate (AgOTf) overnight using THF/water (1:1 v/v) as solvent.[55] Figure 15c shows the p(NCOMA-stat-PgMA) after the AgOTf-mediated deprotection step. The peak corresponding to the protected alkyne at 2180 cm^{-1} disappears after the treatment with AgOTf; however, the peak expected for deprotected alkyne at 2210 cm^{-1} was not observed. While the disappearance of the peak corresponding to the protected alkyne can be attributed to the formation of silver acetylide complex, it is crucial to understand the mechanism of AgOTf-mediated deprotection to understand the absence of deprotected alkyne peaks. Typically, in an AgOTf-mediated silyl deprotection shown in Scheme 10, the silver acetylide complex and triflic acid are formed upon silver activation of the alkyne and hydrolysis of the resulting Me_3SiOTf. This triflic acid then hydrolyzes the silver acetylide complex to give a deprotected alkyne and regenerates AgOTf.[55] However, in the case of deprotection of surface-tethered protected alkyne groups, we speculate triflic acid generated during the deprotection step quickly diffuses away from the polymer brush surface into solution

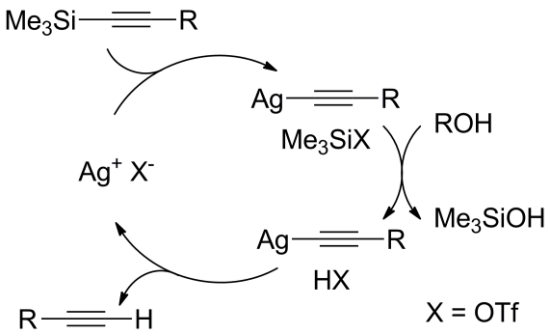

Scheme 10 . General mechanism for Ag-mediated deprotection of trimethylsilyl-protected alkynes.[55] Diffusion of triflic acid out of the brush surface would result in incomplete deprotection and the presence of brush-bound silver acetylide.

resulting in incomplete deprotection leaving alkyne groups in a silver acetylide form. High resolution XPS indeed shows the presence of silver with an Ag3d binding energy of 368.25 eV (Figure 16). We posit that regardless of the exact nature of the alkyne group after AgOTf-mediated deprotection, it should still be reactive in the subsequent thiol-yne reactions. To prove this, we performed the sequential radical-mediated thiol-yne reaction using dodecanethiol and DMPA on the AgOTf treated brushes. Figure 15d shows the GATR-FTIR spectrum after thiol-yne reaction with dodecanethiol. As shown in Figure 15d, the appearance of peaks corresponding to aliphatic groups of dodecanethiol at 2955 cm^{-1}, 2922 cm^{-1} and 2853 cm^{-1} confirms the successful thiol-yne reaction (regardless of the speculated silver acetylide complex) and the successful sequential thiol-isocyanate/thiol-yne transformations of the p(NCOMA-stat-PgMA) brush. Although not ideal due to the fact that residual silver remains in the film even after thiol-yne modification (Figure 16), these results suggest that AgOTf-mediated deprotection of surface-tethered functional groups can be used as an alternative in cases where highly caustic conditions might pose a problem.

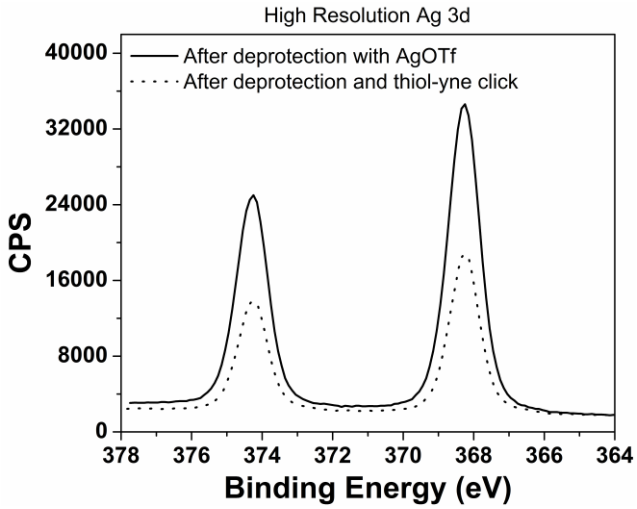

Figure 16 . High resolution Ag3d XPS spectra of p(NCOMA-stat-PgMA-TMS) after clicking p(NCOMA) with benzyl mercaptan and TMS deprotection with AgOTf (solid line) and after thiol-yne click with dodecanethiol. The presence of silver supports the formation of a silver acetylide complex within the brush, but also shows that residual silver remains even after thiol-yne click.

Orthogonal Thiol-Bromo and Thiol-Yne Functionalization to form Multifunctional Polymer Brushes

A methodology similar to that described previously for sequential thiol-isocyanate/thiol-yne surface reactions was adapted for the synthesis of statistical copolymer brushes comprised of 2-(2-bromopropanoyloxy) ethyl methacrylate (BrMA) and TMS-protected propargyl methacrylate allowing for sequential thiol-bromo and thiol-yne transformations. In the case of thiol-bromo/thiol-yne surfaces reactions, the weak FTIR signature of the secondary bromine in p(BrMA) prevents the confirmation of the incorporated bromo functionality using GATR-FTIR spectroscopy. Rather, XPS was performed to follow the sequence of reactions for this system. Figure 17a shows the survey and corresponding high resolution C1s, S2p, and Br3d spectra for a copolymer brush prepared via SIP from a 1:1 mixture of 2-(2-bromopropanoyloxy) ethyl methacrylate (BrMA) and PgMA in THF (p(BrMA-stat-PgMA)). The C1s (285 eV), O1s

531 eV) and particularly the presence of bromine (Br3d, 70 eV; Br3p, 182 eV; Br3s, 257 eV) confirms the successful surface-initiated copolymerization. Due to the thickness (10.9 nm for the unmodified brush) of the polymer brush samples, signals from the silicon substrate (Si2p, 100 eV; Si2s, 149 eV) are also present. Evidence for the presence of the TMS-protected alkyne was confirmed by GATR-FTIR as previously described (see Appendix C). Next, the α-bromo functional groups of p(BrMA-stat-PgMA) brush surface were modified with dodecanethiol under base-catalyzed (DBU) conditions. The disappearance of the peaks associated with bromine (Br3d, 70 eV; Br3p, 182 eV; Br3s, 257 eV) and the appearance of peaks attributed to sulfur (S2p, 163.4 eV; S2s, 229 eV) provide evidence for a successful replacement of bromine with the thioether (Figure 17b). An expected increase in the C/O ratio was also observed as a result of the incorporation of aliphatic dodecanethiol molecules. Again, the presence of the protected alkyne was confirmed by FTIR. After deprotection of the alkyne under KOH/methanol conditions, the alkyne pendants were modified by radical-mediated thiol-yne with N- acetyl cysteine as indicated by the appearance of the nitrogen N1s peak (400 eV) in Figure 17c. It is noteworthy that the preliminary investigations of thiol-bromo surface reactions were much slower when conducted under similar conditions of the thiol-isocyanate click reaction which reflects the difference in reactivity between the α-bromoester and isocyanate. Nonetheless, both systems reach quantitative conversion (within the sensitivity of our surface measurements) given sufficient reaction time.

Orthogonal Thiol-Epoxy and Thiol-Yne Functionalization to form Multifunctional Polymer Brushes

The thiol-epoxy reaction has recently been demonstrated as an efficient route to polymer modification.[40] Here, sequential thiol-epoxy and thiol-yne reactions on p(GMA-

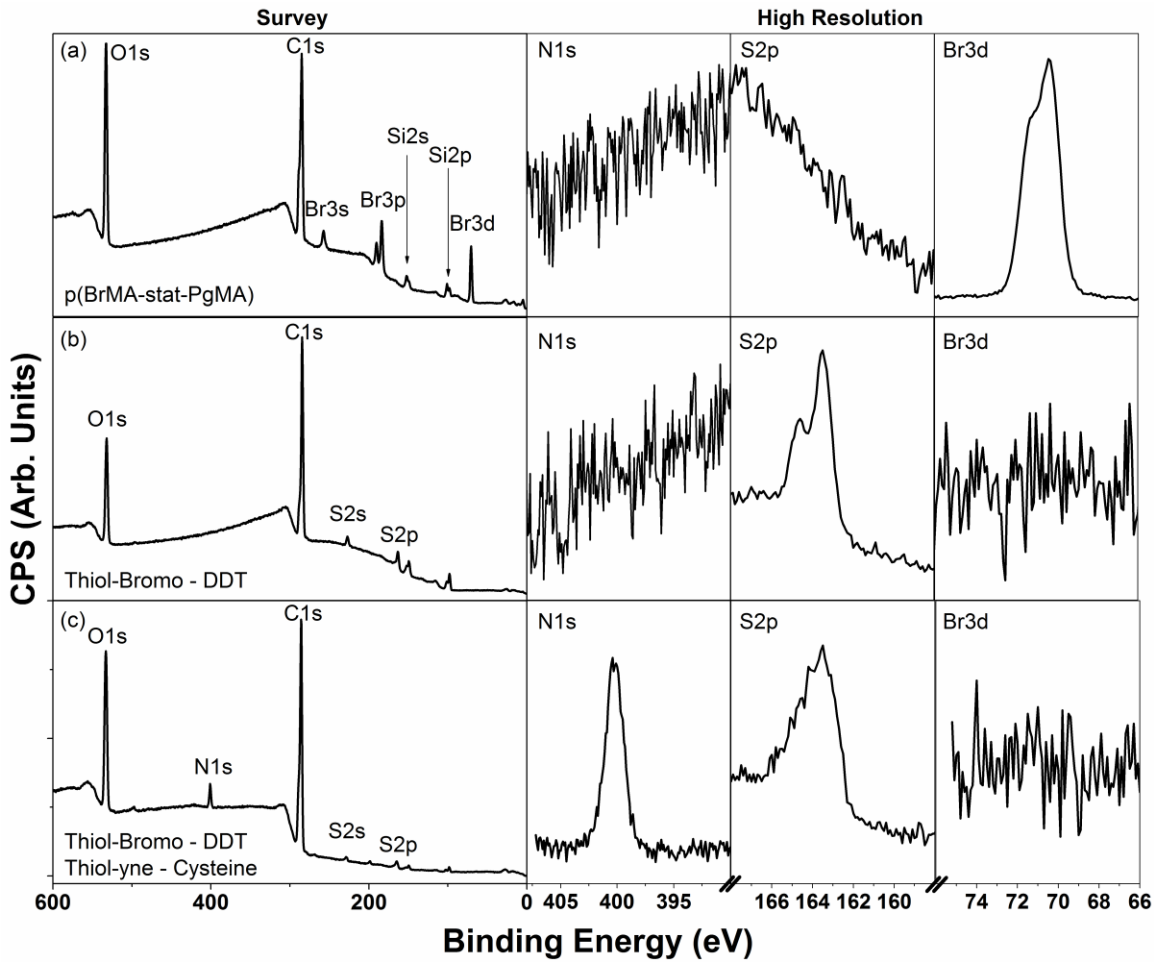

Figure 17. Survey and N1s, S2p, and Br3d high-resolution XPS spectra for (a) unmodified statistical copolymer brush p(BrMA-stat-PgMA), 10.9 nm ± 1.2 nm; (b) p(BrMA-stat-PgMA) with α-bromoesters clicked with dodecanethiol (DDT), 25.5 nm ± 5.6 nm; and (c) p(BrMA-stat-PgMA) with α-bromoesters clicked with dodecanethiol and alkynes sequentially clicked with N-acetyl cysteine, 28.2 nm ± 4.8 nm.

stat-PgMA) brushes were carried out under identical conditions as described above for the sequential thiol-bromo/thiol-yne system. p(GMA-stat-PgMA) brushes were synthesized by SIP from a mixture of GMA and PgMA-TMS. Varying the thickness and composition of the brushes was easily achieved by changing the time of SIP and composition of monomer mixture, respectively. Figure 18a shows the GATR-FTIR spectrum of p(GMA-stat-PgMA) synthesized by SIP from a equimolar mixture of GMA and PgMA in THF. The spectrum shows the characteristic peaks corresponding to epoxy

ring at 906 cm^{-1} and protected alkyne at 2180 cm^{-1} confirming the presence of both epoxy and alkyne clickable moieties in the copolymer brush. Similar to the case of p(BrMA-stat-PgMA) and p(NCOMA-stat-PgMA), the tertiary amine-catalyzed thiol-epoxy transformation was performed first using thioglycerol and DBU. Figure 18b shows the GATR-FTIR spectrum for thioglycerol-modified p(GMA-stat-PgMA) brush in which the thiolysis of the epoxy was confirmed by disappearance of an epoxy ring stretch at 930 cm^{-1}, and appearance of a strong, broad peak at 3400 cm^{-1} attributable to the hydroxyl groups of thioglycerol. Again, the peaks corresponding to the protected alkyne at 2180 cm^{-1} remain intact after the thiol-epoxy reaction. The thioglycerol-modified p(GMA-stat-PgMA) brush was then exposed to KOH/methanol to deprotect the TMS-alkyne group. Figure 18c shows the p(GMA-stat-PgMA) after deprotection step indicating the disappearance of the protected alkyne group at 2180 cm^{-1} and appearance of peaks corresponding to the deprotected alkyne appear at 2230 cm^{-1} confirming successful deprotection under caustic conditions. Additionally, peaks corresponding to thioglycerol hydroxyl groups remain intact after deprotection step indicating that the thioether bond resulting from the thiol-epoxy reaction is stable under the caustic conditions, unlike the thiourethane bond discussed previously. Subsequently, the deprotected pendent alkyne groups were transformed by thiol-yne reaction using dodecanethiol as a model thiol. Figure 18d shows the spectrum for the p(GMA-stat-PgMA) after final thiol-yne modification. The GATR-FTIR spectrum clearly confirms the thiol-yne click showing the sharp peaks at 2955, 2922 and 2853 cm^{-1} corresponding to aliphatic groups of dodecanethiol along with loss of peaks at 2125 and 3280 cm^{-1} corresponding to deprotected alkyne groups. Thus, a dual-functional brush containing hydroxyl and

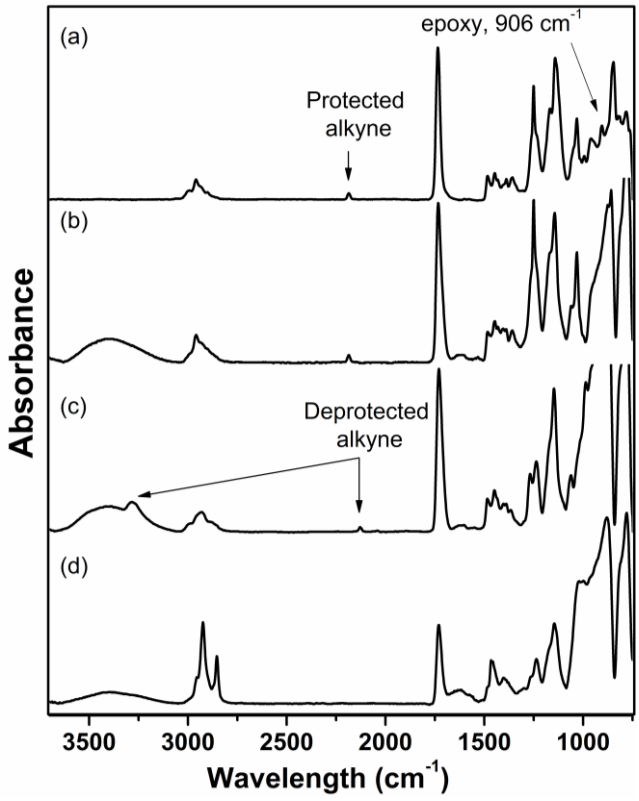

Figure 18. GATR-FTIR spectrum for p(GMA-stat-PgMA) (a) synthesized by SIP of 1:3 v/v GMA:PgMA, 73.5 nm ± 4.5 nm; (b) after thiol-epoxy click with thioglycerol, 122.7 nm ±1.1 nm; (c) after deprotection using KOH in methanol, 92.9 nm ± 5.8 nm; and (d) after thiol-yne click with dodecanethiol, 126.2 nm ± 4.4 nm.

aliphatic groups was synthesized by sequential thiol-based reactions starting with a p(GMA-stat-PgMA) copolymer brush.

Taken together, these studies of functionalizing the copolymer brushes containing two thiol-clickable groups prove, in concept, that orthogonal thiol-click reactions can be conducted in a sequential manner to yield dual-functional polymer brushes. Though, for all three systems, only one type of thiol was used for each of the click reactions, it has been shown previously by numerous researchers that these thiol-click reactions can be conducted with a multitude of thiols imparting the desired properties to the polymer brush. Additionally, with the choice of two thiols, the properties of the surface can be

tuned by varying the composition of copolymer brush (concentration of one thiol-clickable group relative to another thiol-clickable group). To demonstrate tunability of the copolymer brushes, we synthesized dual-functional polymer brushes of varying wettability by sequential and orthogonal click reactions from p(GMA-stat-PgMA).

Tuning Surface Properties via Orthogonal Click Transformations

We have already demonstrated facile tunability of the composition and wetting properties of polymer brush surfaces using a one-pot thiol-yne approach with binary and ternary thiol mixtures. Similarly, it should be possible to impart tunability by controlling the functional monomer feed ratios used in the statistical copolymerization from the surface, which in turn dictates the final composition and properties of the surface upon sequential click reactions at full functional group conversion. To explore this concept, statistical copolymer brushes containing varying concentrations of epoxy and alkyne functionality were synthesized by SIP from different monomer feed ratios of GMA and PgMA. Figure 19 (a – c) shows the FTIR spectra for copolymer brushes synthesized by SIP from different GMA/PgMA feed ratios containing 25% v/v, 50% v/v and 75% v/v GMA, respectively. As the concentration of GMA in monomer feed increases, the concentration of epoxy functionality relative to the alkyne functionality in the copolymer brush increases as indicated by an increase in the height of the peak at 906 cm^{-1} corresponding to the epoxy group and decrease in the height of the peak at 2180 cm^{-1} corresponding to the protected alkyne group. The trend in the concentration of epoxy and alkyne functionality in the copolymer brush was confirmed by calculating peak area ratios for epoxy and alkyne peaks ($A_{Peak,GMA}/A_{Peak,PgMA}$) in each of the FTIR spectra. As the fraction of GMA in monomer feed increases, $A_{Peak,GMA}/A_{Peak,PgMA}$ was calculated to be

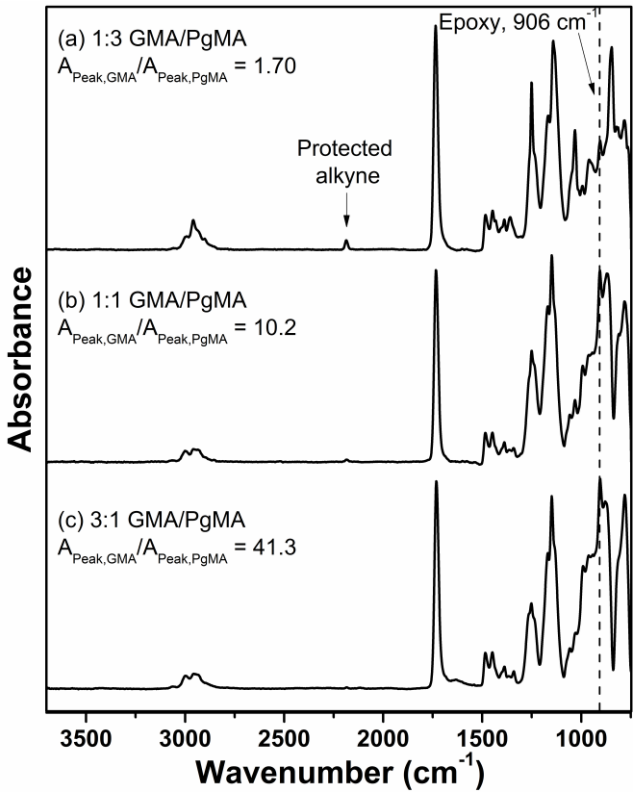

Figure 19. GATR-FTIR spectra for p(GMA-stat-PgMA-TMS) synthesized by SIP of (a) 1:3 v/v GMA:PgMA-TMS, 73.5 nm ± 4.5 nm; (b) 1:1 v/v GMA:PgMA-TMS, 40.9 nm ± 2.1 nm; and (c) 3:1 v/v GMA:PgMA-TMS, 68.2 nm ± 3.8 nm.

1.70, 10.2, and 41.3 for copolymer brushes synthesized from 25% v/v, 50% v/v and 75% v/v GMA fractions, respectively. The variation in epoxy/alkyne composition in the copolymer brush was also characterized by water contact angle analysis. As shown in Figure 20, the water contact angle of copolymer brush decreases from the observed value for pure p(PgMA) (96°) down to the observed for pure p(GMA) (56°) as the fraction of GMA in the monomer feed increases. This trend in the water contact angle is expected due to higher hydrophilicity of p(GMA) as compared to p(PgMA). These p(GMA-stat-PgMA) surfaces were then employed as platforms for sequential thiol-epoxy and thiol-yne modifications in the same manner previously described. Due to the orthogonal nature of radical-mediated thiol-yne and base-catalyzed thiol-epoxy transformations, the

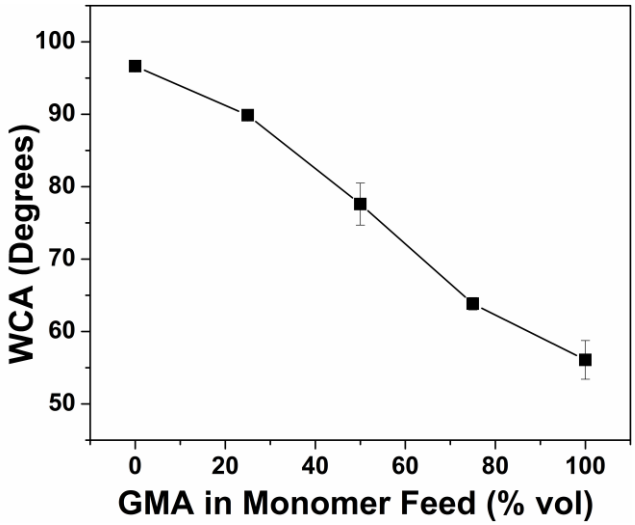

Figure 20. Water contact angle of p(GMA-stat-PgMA) brushes as a function of GMA in the GMA/PgMA comonomer feed used for SIP. Error bars represent one standard deviation of the data, which is taken as the experimental uncertainty of the measurement.

p(GMA-stat-PgMA) copolymer brush can be modified with independent thiol-click reactions. To demonstrate control of surface properties, pendent epoxy groups were modified with hydrophilic thioglycerol, and pendent alkynes were modified with hydrophobic dodecanethiol. Figure 21 shows the GATR-FTIR spectra of p(GMA-stat-PgMA) brushes clicked with thioglycerol and dodecanethiol via orthogonal thiol-epoxy and thiol-yne transformations, respectively. As the GMA fraction in the parent p(GMA-stat-PgMA) brush increases, the intensity of peaks corresponding to the hydroxyl groups at 3400 cm^{-1} increase as a result of the thiolysis of pendent epoxy moieties with thioglycerol. In contrast, after sequential thiol-yne click with dodecanethiol, the intensity of peaks corresponding to aliphatic groups at 2955, 2922 and 2853 cm^{-1} of dodecanethiol decreases as the fraction of GMA in the brush increases. Accordingly, as shown in Figure 22, the water contact angle of the sequentially clicked copolymer brush surfaces decreases as the GMA fraction in the parent p(GMA-stat-PgMA) brush increases, indicating that the amount of hydrophilic thioglycerol and hydrophobic dodecanethiol

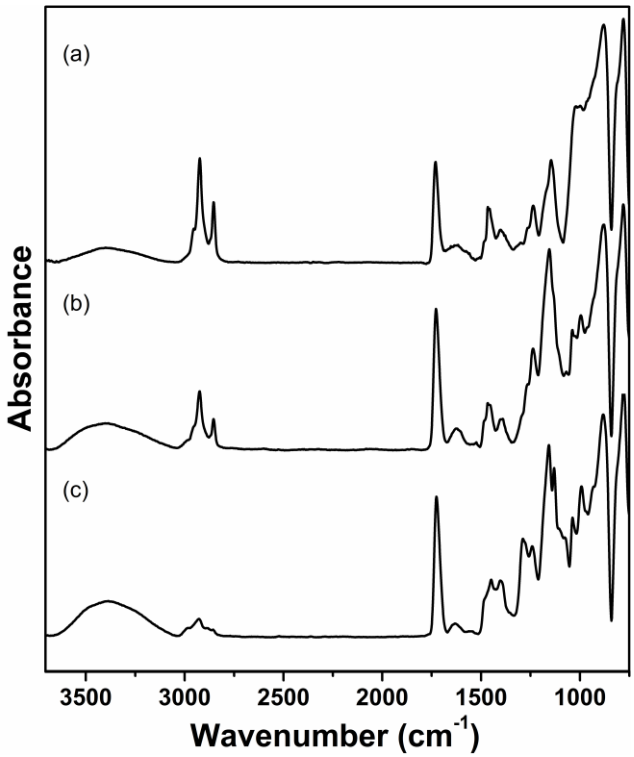

Figure 21. GATR-FTIR spectra of p(GMA-stat-PgMA) after sequential thiol-epoxy and thiol-yne with thioglycerol and dodecanethiol, respectively. p(GMA-stat-PgMA) brushes are synthesized by SIP of (a) 1:3 v/v GMA:PgMA, 54.2 nm ±2.7 nm (b) 1:1 v/v GMA:PgMA, 43.6 nm ±1.2 nm; and (c) 3:1 v/v GMA:PgMA, 48.4 nm ± 3.1 nm.

incorporated in the brush is dictated simply from the composition of the parent polymer brush (assuming complete conversion of the epoxy and alkyne groups). Also shown in Figure 22, the modified brush surfaces undergo rearrangement as a result of various solvent treatments. THF likely exposes a greater fraction of dodecanethiol at the surface, and vice versa, methanol likely exposes a greater fraction of thioglycerol. Although some degree of rearrangement is expected, we are particularly interested in probing the distribution of these functional groups in the depth direction of the polymer brush to learn more about the possibilities of creating unique polymer brush architectures with compositional gradients by exploiting size-dependent exclusion inherent to polymer brush systems.

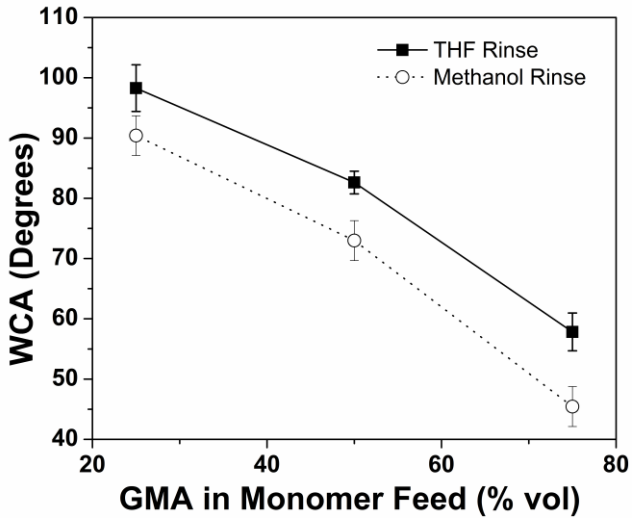

Figure 22. Water contact angle of p(GMA-stat-PgMA) brushes clicked sequentially with thioglycerol and dodecanethiol via thiol-epoxy and thiol-yne reactions as a function of volume fraction of GMA in the GMA/PgMA monomer feed used for SIP. Error bars represent one standard deviation of the data, which is taken as the experimental uncertainty of the measurement.

Conclusions

In summary, we successfully demonstrated a versatile post-polymerization modification strategy to synthesize multifunctional polymer brush surfaces via combination of surface-initiated photopolymerization and orthogonal thiol-click reactions, namely the base-catalyzed thiol-isocyanate, thiol-epoxy, or thiol-bromo reactions in sequential combination with the radical-mediated thiol-yne reaction. Initially, the applicability of the radical-mediated thiol-yne reaction was extended to include one-pot, statistical, co-click reactions of brush pendent alkyne groups with multiple thiols. This simple one-pot approach was successfully applied to various mixtures of thiols including a combination of thioglycerol and dodecanethiol, which bestow hydrophilic hydroxyl and hydrophobic aliphatic groups to the polymer brush, respectively, and a combination of N-acetyl-cysteine and dodecanethiol to form a model polymer coating with a biologically relevant molecule. The one-pot approach was also

shown to be easily extendable to a mixture of three thiols. The ability to control the surface properties (hydrophilicity in this work) by facile control over relative concentration of thiols in a thiol mixture also exhibits the robustness and versatility of the one-pot approach. Additionally, sequential and orthogonal thiol-click reactions were successfully applied to synthesize dual-functional polymer brushes by post-polymerization modification of p(NCOMA-stat-PgMA), p(GMA-stat-PgMA) and p(BrMA-stat-PgMA) via nucleophile-mediated thiol-isocyanate, thiol-epoxy or thiol-bromo, respectively, in combination with radical-mediated thiol-yne reactions. Generally, the base-catalyzed reactions were conducted first, and observe to have no effect on the alkyne groups, enabling the sequential thiol-yne reaction. In this case, surface properties were tailored by controlling the relative concentrations of monomers in the monomer feed during the SIP, which in turn dictates the composition of the thiol-clicked surface. While we demonstrated our strategy with model and commercially available thiols, we fully expect that this approach will be extended to fabrication of multiplexed biomolecules, i.e. proteins, DNA strands, antibodies, as well as to the fabrication of complex polymer brush architectures, i.e. mixed and block copolymer brushes.

Acknowledgments

This work was supported in part by NSF CAREER (DMR-1056817) and the Office of Naval Research (Award N00014-07-1-1057) and fellowship support from the U.S. Department of Education GAANN program (Award #P200A090066).

References

(1) Sanchez, C.; Arribart, H.; Giraud Guille, M. M. *Nat. Mater.* **2005**, *4*, 277-288.

(2) Hartmuth, C.; Finn, M.; Sharpless, B. *Angew. Chem. Int. Ed.* **2001**, *40*, 2004-2021.

(3) Nebhani, L.; Barner-Kowollik, C. *Adv. Mater.* **2009**, *21*, 3442-3468.

(4) Arumugam, S.; Popik, V. V. *J. Am. Chem. Soc.* **2011**, *133*, 15730-15736.

(5) Dirlam, P. T.; Strange, G. A.; Orlicki, J. A.; Wetzel, E. D.; Costanzo, P. J. *Langmuir* **2009**, *26*, 3942-3948.

(6) Sun, X.-L.; Stabler, C. L.; Cazalis, C. S.; Chaikof, E. L. *Bioconjugate Chem.* **2005**, *17*, 52-57.

(7) Hoyle, C. E.; Bowman, C. N. *Angew. Chem. Int. Ed.* **2010**, *49*, 1540-1573.

(8) Hoyle, C. E.; Lee, T. Y.; Roper, T. *J. Polym. Sci., Part A: Polym. Chem.* **2004**, *42*, 5301-5338.

(9) Hoyle, C. E.; Lowe, A. B.; Bowman, C. N. *Chem. Soc. Rev.* **2010**, *39*, 1355 - 1387.

(10) Lowe, A. B.; Hoyle, C. E.; Bowman, C. N. *J. Mater. Chem.* **2010**, *20*, 4745-4750.

(11) Christman, K. L.; Schopf, E.; Broyer, R. M.; Li, R. C.; Chen, Y.; Maynard, H. D. *J. Am. Chem. Soc.* **2008**, *131*, 521-527.

(12) Kessler, D.; Nilles, K.; Theato, P. *J. Mater. Chem.* **2009**, *19*, 8184-8189.

(13) Murata, H.; Prucker, O.; Rühe, J. *Macromolecules* **2007**, *40*, 5497-5503.

(14) Orski, S. V.; Fries, K. H.; Sheppard, G. R.; Locklin, J. *Langmuir* **2010**, *26*, 2136-2143.

(15) Iha, R. K.; Wooley, K. L.; Nystrom, A. M.; Burke, D. J.; Kade, M. J.; Hawker, C. J. *Chem. Rev.* **2009**, *109*, 5620-5686.

(16) Hudalla, G. A.; Murphy, W. L. *Langmuir* **2010**, *26*, 6449-6456.

(17) Im, S. G.; Bong, K. W.; Kim, B.-S.; Baxamusa, S. H.; Hammond, P. T.; Doyle, P. S.; Gleason, K. K. *J. Am. Chem. Soc.* **2008**, *130*, 14424-14425.

(18) Baskin, J.; Prescher, J.; Laughlin, S.; Agard, N.; Chang, P.; Miller, I.; Lo, A.; Codelli, J.; Bertozzi, C. *Proc. Natl. Acad. Sci. U.S.A.* **2007**, *104*, 16793 - 19797.

(19) Jewett, J. C.; Sletten, E. M.; Bertozzi, C. R. *J. Am. Chem. Soc.* **2010**, *132*, 3688-3690.

(20) Kuzmin, A.; Poloukhtine, A.; Wolfert, M. A.; Popik, V. V. *Bioconjugate Chem.* **2010**, *21*, 2076-2085.

(21) Manova, R.; van Beek, T. A.; Zuilhof, H. *Angew. Chem. Int. Ed.* **2011**, *50*, 5428-5430.

(22) Orski, S. V.; Poloukhtine, A. A.; Arumugam, S.; Mao, L.; Popik, V. V.; Locklin, J. *J. Am. Chem. Soc.* **2010**, *132*, 11024-11026.

(23) Deng, X.; Friedmann, C.; Lahann, J. *Angew. Chem. Int. Ed.* **2011**, *50*, 6522-6526.

(24) Cai, T.; Wang, R.; Neoh, K. G.; Kang, E. T. *Polym. Chem.* **2011**, *2*, 1849-1858.

(25) Jonkheijm, P.; Weinrich, D.; Köhn, M.; Engelkamp, H.; Christianen, P. C. M.; Kuhlmann, J.; Maan, J. C.; Nüsse, D.; Schroeder, H.; Wacker, R.; Breinbauer, R.; Niemeyer, C. M.; Waldmann, H. *Angew. Chem. Int. Ed.* **2008**, *47*, 4421-4424.

(26) Li, M.; De, P.; Li, H.; Sumerlin, B. S. *Polym. Chem.* **2010**, *1*, 854-859.

(27) Sparks, B. J.; Ray, J. G.; Savin, D. A.; Stafford, C. M.; Patton, D. L. *Chem. Commun.* **2011**, *47*, 6245-6247.

(28) Wendeln, C.; Rinnen, S.; Schulz, C.; Arlinghaus, H. F.; Ravoo, B. J. *Langmuir* **2010**, *26*, 15966-15971.

(29) Hensarling, R. M.; Doughty, V. A.; Chan, J. W.; Patton, D. L. *J. Am. Chem. Soc.* **2009**, *131*, 14673-14675.

(30) Huang, Y.; Zeng, Y.; Yang, J.; Zeng, Z.; Zhu, F.; Chen, X. *Chem. Commun.* **2011**, *47*, 7509-7511.

(31) Konkolewicz, D.; Gaillard, S.; West, A. G.; Cheng, Y. Y.; Gray-Weale, A.; Schmidt, T. W.; Nolan, S. P.; Perrier, S. *Organometallics* **2011**, *30*, 1315-1318.

(32) Naik, S. S.; Chan, J. W.; Comer, C.; Hoyle, C. E.; Savin, D. A. *Polym. Chem.* **2011**, *2*, 303-305.

(33) Wang, C.; Ren, P. F.; Huang, X. J.; Wu, J.; Xu, Z. K. *Chem. Commun.* **2011**, *47*, 3930-3932.

(34) Hensarling, R. M.; Rahane, S. B.; LeBlanc, A. P.; Sparks, B. J.; White, E. M.; Locklin, J.; Patton, D. L. *Polym. Chem.* **2011**, *2*, 88-90.

(35) Li, H.; Yu, B.; Matsushima, H.; Hoyle, C. E.; Lowe, A. B. *Macromolecules* **2009**, *42*, 6537-6542.

(36) Flores, J. D.; Shin, J.; Hoyle, C. E.; McCormick, C. L. *Polym. Chem.* **2009**, *1*, 213-220.

(37) Flores, J. D.; Treat, N. J.; York, A. W.; McCormick, C. L. *Polymer Chemistry* **2011**, *2*, 1976-1985.

(38) Chan, J. W.; Hoyle, C. E.; Lowe, A. B. *J. Am. Chem. Soc.* **2009**, *131*, 5751-5753.

(39) Barbey, R.; Lavanant, L.; Paripovic, D.; Schüwer, N.; Sugnaux, C.; Tugulu, S.; Klok, H. A. *Chem. Rev.* **2009**, *109*, 5437-5527.

(40) Harvison, M. A.; Davis, T. P.; Lowe, A. B. *Polym. Chem.* **2011**, *2*, 1347-1354.

(41) Rosen, B. M.; Lligadas, G.; Hahn, C.; Percec, V. *J. Polym. Sci. Part A: Polym. Chem.* **2009**, *47*, 3931-3939.

(42) Rosen, B. M.; Lligadas, G.; Hahn, C.; Percec, V. *J. Polym. Sci. Part A: Polym. Chem.* **2009**, *47*, 3940-3948.

(43) Xu, J.; Tao, L.; Boyer, C.; Lowe, A. B.; Davis, T. P. *Macromolecules* **2010**, *43*, 20-24.

(44) Schuh, C.; Santer, S.; Prucker, O.; Rühe, J. *Adv. Mater.* **2009**, *21*, 4706-4710.

(45) Beinhoff, M.; Frommer, J.; Carter, K. R. *Chem. Mater.* **2006**, *18*, 3425-3431.

(46) Xu, C.; Wu, T.; Drain, C. M.; Batteas, J. D.; Beers, K. L. *Macromolecules* **2004**, *38*, 6-8.

(47) Fairbanks, B. D.; Sims, E. A.; Anseth, K. S.; Bowman, C. N. *Macromolecules* **2010**, *43*, 4113-4119.

(48) Campos, L. M.; Killops, K. L.; Sakai, R.; Paulusse, J. M. J.; Damiron, D.; Drockenmuller, E.; Messmore, B. W.; Hawker, C. J. *Macromolecules* **2008**, *41*, 7063-7070.

(49) Kempe, K.; Hoogenboom, R.; Jaeger, M.; Schubert, U. S. *Macromolecules* **2011**, *44*, 6424-6432.

(50) Goldmann, A. S.; Walther, A.; Nebhani, L.; Joso, R.; Ernst, D.; Loos, K.; Barner-Kowollik, C.; Barner, L.; Müller, A. H. E. *Macromolecules* **2009**, *42*, 3707-3714.

(51) Antoni, P.; Robb, M. J.; Campos, L.; Montanez, M.; Hult, A.; Malmström, E.; Malkoch, M.; Hawker, C. J. *Macromolecules* **2010**, *43*, 6625-6631.

(52) Killops, K. L.; Campos, L. M.; Hawker, C. J. *J. Am. Chem. Soc.* **2008**, *130*, 5062-5064.

(53) Han, J.; Zhao, B.; Gao, Y.; Tang, A.; Gao, C. *Polym. Chem.* **2011**, *2*, 2175-2178.

(54) Shin, J.; Matsushima, H.; Comer, C. M.; Bowman, C. N.; Hoyle, C. E. *Chem. Mater.* **2010**, *22*, 2616-2625.

(55) Orsini, A.; Vitérisi, A.; Bodlenner, A.; Weibel, J.-M.; Pale, P. *Tetrahedron Lett.* **2005**, *46*, 2259-2262.

CHAPTER VI

CONTROLLED HETEROGENEITY WITHOUT CONTROLLED POLYMERIZATION: ENGINEERING TAPERED BLOCK COPOLYMER BRUSHES VIA POST-POLYMERIZATION MODIFICATION

Introduction

An ultimate goal of polymer surface engineering is the ability to deliberately tailor the composition, distribution, and spatial arrangement of functional groups on a surface using facile and efficient chemistries. Advances in controlled surface-initiated polymerization (SIP) techniques have certainly provided polymer chemists with a toolset to tailor these parameters given knowledge of reaction conditions, reactivity ratios, and order of monomer addition, but challenges remain particularly regarding direct polymerization of monomers with complex pendent functionality.[1,2] In this regard, post-polymerization modification of polymer surfaces, when combined with SIP, has evolved as a powerful approach to engineer polymer surfaces with complex functionality.[3,4] PPM circumvents limitations associated with direct polymerization of functional monomers due to intolerance of many functional groups with the polymerization mechanism and/or reaction conditions (i.e. reactivity, steric hindrance, temperature/light sensitivity).[5] Presently, a broad range of chemical and biological moieties has been installed on brush surfaces via the PPM methodologies providing surfaces for catalysis,[6,7] separations,[8] patterning,[9-11] barrier properties,[12] and biological activity.[13-15]

PPM of reactive polymer surfaces in the brush regime – where polymer chains are densely grafted to a surface such that the polymer chains overlap, experience strong segmental repulsion and accordingly stretch perpendicular to the surface – is particularly

challenging.[16-18] The stretching of the tethered chains reduces chain conformational entropy rendering the penetration of the brush by reactive modifiers from solution highly unfavorable. Thus, the efficacy, depth of penetration, and homogeneity of the PPM process in the brush regime are ultimately dependent on parameters associated with i) the reaction conditions (i.e. reaction efficiency, solvent quality) ii) the tethered polymer brush (i.e. grafting density and thickness) and iii) the physical properties of the unbound, reactive modifier (i.e. molecular weight (MW), steric bulk). It can be assumed that increases in brush thickness, grafting density, and MW of the modifier will lead to decreased efficacy and depths of penetration and increased heterogeneity. Whereas heterogeneous modification may be undesirable in some applications, exploiting the limited ability of modifiers to penetrate reactive brush surfaces will undoubtedly provide opportunities to design complex brush structures unattainable by direct polymerization.

Despite widespread implementation of PPM for brush modification, the interplay of the previously mentioned parameters is largely undefined and a complete understanding of the spatial distribution of functional modifiers throughout the thickness of the brush is lacking. Recently, Schuh and Rühe evaluated the reaction and penetration of active ester brush surfaces with amine-functionalized poly(ethylene glycol) (PEG-NH_2).[19] The authors developed an insightful model describing the strong dependence of PPM on the MW of PEG-NH_2, and the relatively weak dependence on grafting density, molecular weight, and active ester content of the brush. Recent work by Schuwer et al.[20] demonstrated an elegant use of neutron reflectivity (NR) to probe the vertical distribution of functional groups in PPM of activated poly(hydroxyethyl methacrylate) (pHEMA) brushes with amino acids, and in contrast to Schuh and Rühe,[19] showed that efficacy of

the PPM process depends on brush thickness, grafting density, and polarity of the amino acid modifier. More importantly, their work provided one of the first high resolution experimental insights into the concentration gradients and heterogeneity of post-modified brush surfaces present even for low molecular weight modifiers. However, a significant drawback of Schuwer and coworkers' system was the need for "pre-activation" of the pHEMA brush hydroxyl moieties with p-nitrophenyl chloroformate (NPC) – a PPM process itself determined to be less than quantitative – prior to the PPM aminolysis reaction with amino acids. Thus, the extent of penetration and the spatial distribution of amino acids observed by NR were directly dependent on and limited by the extent of NPC activation – leaving a complete picture of the PPM process on a fully reactive brush system unresolved.

Recently, our group demonstrated base-catalyzed thiol-isocyanate reactions as a modular PPM brush platform for rapid fabrication of highly functional, multicomponent surfaces.[21,22] Advantageously, this PPM strategy is a rapid one-step reaction requiring no "pre-activation" of the tethered isocyanate-functionalized brush (pNCO), and as such, represents an ideal platform to provide better insight into the spatial distribution of modifiers within the brush as a result of the PPM process. In this chapter, we employ neutron reflectometry to investigate the thiol-isocyanate PPM of pNCO brush surfaces using low molecular weight deuterated thiols as modifiers. We determine the depth of penetration and spatial distribution within the brush of two chemically identical *d*-thiols differing only in molecular weights (d_7-propanethiol (d_7-PPT) and d_{25}-dodecanethiol (d_{25}-DDT)). With knowledge of vertical composition profiles as a function of thiol MW at hand, we exploit the steric and mass transport aspects of PPM to intentionally generate

tapered block copolymer brush surfaces using a two-step PPM process – wherein a pNCO brush is first reacted with the larger MW d_{25}-DDT and then backfilled with the lower MW d_7-PPT. To our knowledge, this represents the first tapered block copolymer brush synthesized via a PPM process, and more specifically, without the use of sequential monomer addition by controlled SIP techniques.

Experimental

Materials

All reagents and solvents were obtained at the highest purity available from Aldrich Chemical Company or Fisher Scientific and used without further purification unless otherwise specified. 2-Hydroxy-4'-(2-hydroxyethoxy)-2-methylpropiophenone (Irgacure 2959) was purchased from Ciba Specialty Chemicals. 2-Isocyanatoethyl methacrylate was purchased from TCI America and passed through neutral alumina before use to remove the BHT inhibitor. d_7-propanethiol (d_7-PPT) and d_{25}-dodecanethiol (d_{25}-DDT) was purchased from CDN Isotopes and used as received. Silicon wafers polished only on one side were purchased from University Wafers.

Characterization

A Varian Mercury Plus 300MHz NMR spectrometer operating at a frequency of 300 MHz with VNMR 6.1C software was used for proton and carbon analysis. Wettability of the unmodified and modified polymer brushes was measured using a Ramé-hart 200-00 Std.-Tilting B. goniometer. Static (θ_{sw}) contact angles were measured using 10 μL water droplets in combination with DROPimage Standard software. Ellipsometric measurements were carried out using a Gaertner Scientific Corporation LSE ellipsometer with a 632.8 nm laser at 70° from the normal. Refractive index values

of 3.86, 1.45, 1.43 and 1.5 for silicon, oxide layer, photoinitiator monolayer and all polymer layers, respectively, were used to build the layer model and calculate layer thicknesses.[23,24] The chemical nature of the polymer brush surfaces was characterized by Fourier transform infrared spectroscopy (FTIR) in grazing-angle attenuated total reflectance mode (GATR-FTIR) using a ThermoScientific FTIR instrument (Nicolet 8700) equipped with a VariGATR™ accessory (grazing angle 65°, germanium crystal; Harrick Scientific). Spectra were collected with a resolution of 4 cm^{-1} by accumulating a minimum of 128 scans per sample. All spectra were collected while purging the VariGATR™ attachment and FTIR instrument with N_2 gas along the infrared beam path to minimize the peaks corresponding to atmospheric moisture and CO_2. Spectra were analyzed and processed using Omnic software. Atomic force microscopy was performed using a Bruker Icon in contact mode. The samples were scanned with T300R-25 probes (Bruker AFM Probes) with a spring constant of 40 N/m. Neutron reflectivity measurements were conducted at the Spallation Neutron Source (SNS) at Oak Ridge National Laboratory using the Liquids Reflectometer (LR) under standard collection parameters. The LR collects specular reflectivity data for low Q values ($Q = 4\pi \sin\theta/\lambda$) in continuous 3.5-Å-wide wavelength bands measured at an incident angle θ=0.6° over central wavelengths of 15, 13.24, 11.08, 8.9, 6.67, and 4.39 Å (0.008 $Å^{-1} < Q < 0.050$ $Å^{-1}$). Higher Q values are accessed using a fixed wavelength band centered at 4.25 Å (the brightest portion of the spectrum) at incident angles θ= 0.9, 1.12, and 1.97°. Data were collected at each setting with incident-beam slits set to maintain a constant relative wave vector resolution of $\delta Q/Q = 0.045$, allowing the data to be stitched together into a single reflectivity curve spanning 0.008 $Å^{-1} < Q < 0.173$ $Å^{-1}$. The neutron refractive index

depends on the scattering length density (SLD), Σ, which is determined using the equation $\Sigma = b/V$, where b is the monomer scattering length (sum of scattering lengths of constituent atomic nuclei) and V is the monomer volume. Model fits to the reflectivity profiles were performed using a six layer model where the layer thicknesses, scattering length densities, and interfacial widths were adjusted to minimize the χ^2 between the measured and calculated reflectivities. The layer models consisted of six layers: bulk Si, SiO_x, initiator, unmodified polymer, modified polymer with deuterated molecules, and hydrated polymer (isocyanate hydrolysis rendering amine groups that are unreactive, only present at the brush-air interface). The scattering length density (SLD) profiles were obtained by fitting the experimental data. The thicknesses of the various polymer brushes were obtained from ellipsometry and the fitted reflectivity data (Table 3). Experimental and theoretical SLD values used for all the fittings are shown in Appendix D.

Table 3

Thickness measurements of polymer brushes

	Thickness Measurements (nm)	
Polymer Brush Samples	before modification	after modification
unmodified p(NCO)	119.3	---
modified p(NCO)-d_7-PPT	77.3	150.7
modified p(NCO)-d_7-PPT	128.8	234.2
modified p(NCO)-d_{25}-DDT	123.4	261
tapered block copolymer – d_{25}-DDT/d_7-PPT	107.6	241.4/265.2
sequential modification with DDT/MPA	115.9	205.2/233.0
Sequential modification with DDT/benzyl amine	104.9	199.9/217.6

Silicon wafer cleaning procedure

Silicon wafers were cut into appropriate sized pieces and ultrasonically cleaned in DP2300 ultra-high performance general purpose cleaner and degreaser (Branson Ultrasonics Corp.) for 5 minutes. The wafers were then wiped gently with lens paper or a cotton-tipped applicator to remove silicon dust from the wafer dicing process. After wiping, the wafers were ultrasonicated for an additional 10 min, rinsed multiple times with DI water, and ultrasonicated in deionized water for 15 minutes. The wafers were then placed into a RCA-1 solution (5 parts deionized H_2O, 1 part 27% ammonium hydroxide, 1 part 30% hydrogen peroxide) for 15 min at 70 °C to remove any organic residues before initiator immobilization. The wafers were rinsed thoroughly with DI water, dried under a stream of N_2, and treated with UV ozone for 1 h before storing in an oven at 140 °C. Silicon wafers (2" diameter) used for neutron reflectivity studies were used as received with the exception of being treated with UV ozone.

Immobilization of HPP-trichlorosilane (Irgacure 2959) photoinitiator

HPP-trichlorosilane photoinitiator was synthesized according to previous literature procedures.[10,21,24] The silicon wafers were transferred into an acrylic glove box where they were placed into a toluene solution of HPP-trichlorosilane (4 mM) at room temperature for 3 h including an excess of triethylamine without stirring. The wafers were removed from the solution, rinsed extensively with toluene, dichloromethane, and dimethylformamide before drying under a stream of N_2. The initiator-functionalized silicon wafers were stored in toluene at -20 °C until use.

Deprotection of the tertiary hydroxyl group at the surface

The acetate protecting group was removed by immersing the wafers prepared above in a suspension of 240 mg K_2CO_3 in 12 mL methanol containing 150 µL H_2O for 1 h. The substrate was subsequently washed with water, methanol, and toluene followed by drying with a stream on N_2.

Synthesis of p(NCO) brush surfaces by surface-initiated polymerization (SIP)

The photoinitiator functionalized substrates were inserted into a microchannel reactor containing 2-isocyanatoethyl methacrylate (NCO) (3.5 M in dry THF) and irradiated with $UV_{\lambda max=365nm}$ light (~140 mW/cm^2) under an inert atmosphere for various time intervals to achieve desired brush thicknesses. After extensive washing in THF and toluene, the brush surfaces were analyzed by GATR-FTIR, ellipsometry, static water contact angle measurements, atomic force microscopy, and neutron reflectivity.

Thiol-Isocyanate (Thiol-NCO) "Click" Reactions

All thiol-isocyanate reactions were catalyzed using 1,8-diazabicyclo[5.4.0]undec-7-ene (DBU) under ambient laboratory conditions (i.e. r.t. and normal atmosphere). Reaction mixtures were not degassed prior to use. After extensive washing in THF and toluene, the brush surfaces were analyzed by GATR-FTIR, ellipsometry, water contact angle measurements, atomic force microscopy, and neutron reflectivity. Details of the various thiol-NCO reactions used for reaction kinetics and neutron reflectivity studies are given below.

Thiol-NCO post-polymerization modification for neutron reflectivity studies

Solutions of either d_7-PPT or d_{25}-DDT and DBU catalyst (thiol:DBU (M); 0.01:2x10^{-3}) in THF were prepared and placed into the reaction vessel containing the

isocyanate-functionalized polymer brush and subsequently allowed to react for at least 1 h unless otherwise specified to facilitate functionalization via thiol-isocyanate click reactions. For the creation of tapered block copolymer brushes, a solution of d_{25}-DDT and DBU catalyst (thiol:DBU (M) $0.01{:}2\text{x}10^{-3}$) in THF was prepared and placed into the reaction vessel containing the isocyanate-functionalized polymer brush and subsequently allowed to react for 15 min before removing the substrate and washing with THF and toluene followed by drying under a stream of N_2. Subsequently, a solution of d_7-PPT and DBU catalyst (thiol:DBU (M) $0.01{:}2\text{x}10^{-3}$) in THF was prepared and allowed to react with any remaining pendent isocyanate functionalities for 4 h before washing with THF and toluene and drying under a stream of N_2. The longer reaction time upon the latter modification process allows sufficient time for the smaller molecules (i.e. propanethiol) to penetrate through the outer layer previously functionalized with dodecanethiol. See Appendix D for the RMS roughness values obtained by AFM for the unmodified and modified polymer brush samples used for neutron reflectivity. The same reagent conditions and reaction times from above were used for the sequential incorporation of non-identical chemical functionalities.

Results and Discussion

pNCO brush samples were synthesized by surface-initiated photopolymerization of 2-isocyanatoethyl methacrylate from photoinitiator-modified silicon substrates (50 mm × 0.5 mm) as described in our previous work.[10,21,22] Grafting density and thickness of the pNCO brushes were held constant using fixed polymerization time and monomer concentration, respectively. After thoroughly removing unbound polymer, the average thickness of the unmodified pNCO brush samples, as measured by ellipsometry, was

determined to be 120 nm ± 3 nm. The surface topography of the p(NCO) brushes before modification was characteristic of polymer brush structures exhibiting low geometric roughness which is crucial for neutron reflectivity studies (see Appendix D). pNCO brush samples were then post-modified using thiol-isocyanate as modifiers to investigate the effect of probe MW on depth of penetration and distribution in post-modified brushes, while minimizing effects due to changes in the reactivity and polarity of the thiol. For homofunctionalization (Scheme 11a), pNCO brushes were exposed to a 0.01M solution of *d*-thiol in dry THF for 1 h, using 1,8-diazabicyclo[5.4.0]undec-7-ene (DBU) as a catalyst (thiol:DBU (M); $0.01{:}2x10^{-3}$).

Neutron reflectometry, conducted at Oak Ridge National Lab's Spallation Neutron Source, was used to determine the structure of the post-modified brushes. Figure 23a shows the reflectivity data (inset, multiplied by Q^4) and the scattering length density (SLD) profiles obtained by fitting the experimental data for dry films of an unmodified pNCO brush (120 nm), a d_7-PPT modified pNCO brush (234 nm), and a d_{25}-DDT modified pNCO brush (265 nm). The SLD model consisted of six layers including bulk Si/SiO_2/initiator/unmodified pNCO/postmodified pNCO/hydrated pNCO. The hydrated pNCO layer (< 5 nm in thickness) was necessary to account for minor hydrolysis of the isocyanate functionality at the brush/air interface. The experimental SLD values of the pNCO, d_7-PPT modified pNCO brush, and a d_{25}-DDT modified pNCO converged to 1.87×10^{-6} Å^{-2}, $3.07x10^{-6}$ Å^{-2}, and $4.60x10^{-6}$ Å^{-2}, respectively. These values compare relatively well with theoretical SLD values calculated using the National Institute of Standards and Technology online SLD calculator (see Appendix D). The SLD profile for unmodified pNCO shows two abrupt transitions at the Si/SiO_2 and

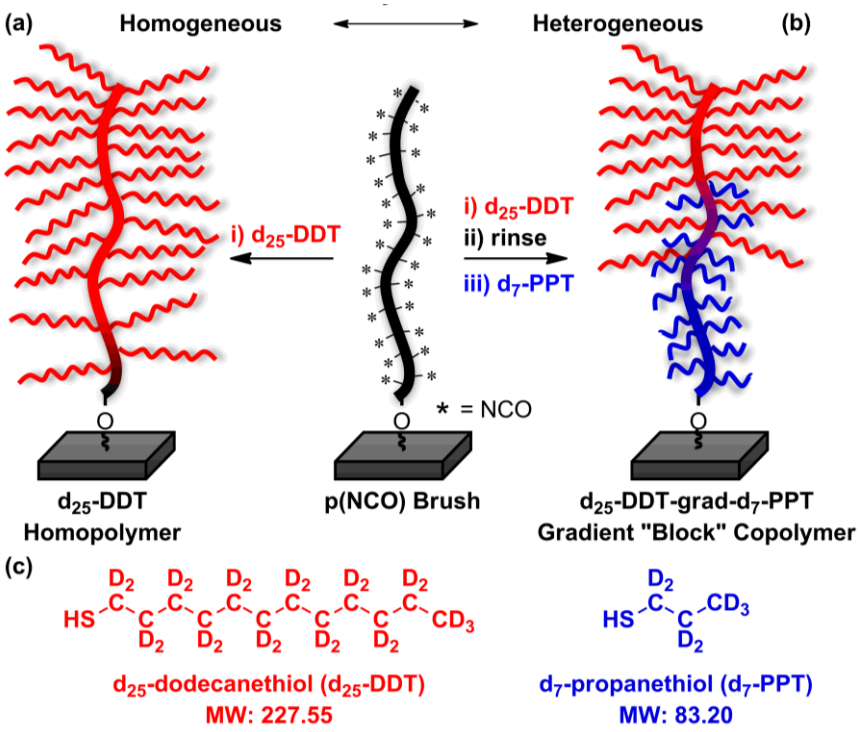

Scheme 11. Synthetic routes to a) homogeneous and b) heterogeneous, complex architecture polymer brush surfaces via post-polymerization modification using thiol-isocyanate click chemistry, and c) structures of d_{25}-DDT and d_7-PPT modifiers.

SiO_2/initiator interfaces, followed by a convergence to a constant SLD value (1.87×10^{-6} $Å^{-2}$) until a smooth brush to air transition is observed. Following PPM of the pNCO brush with d_7-PPT, the SLD profile displays a gradual increase in the SLD value over a 51 nm region extending from the initiator/brush interface before reaching a maximum constant SLD value ($3.07\text{x}10^{-6}$ $Å^{-2}$) that extends to the air interface. The gradual increase in the SLD in the near substrate region suggests the presence of a d_7-PPT concentration gradient moving from partially modified pNCO to fully modified pNCO-d_7-PPT. The experimental fit of the reflectivity data indicates that ~78% (182 nm) of the total film thickness is fully modified with d_7-PPT, while ~22% (51 nm) exhibits a concentration gradient. Upon PPM of a pNCO brush with the larger MW d_{25}-DDT probe, greater

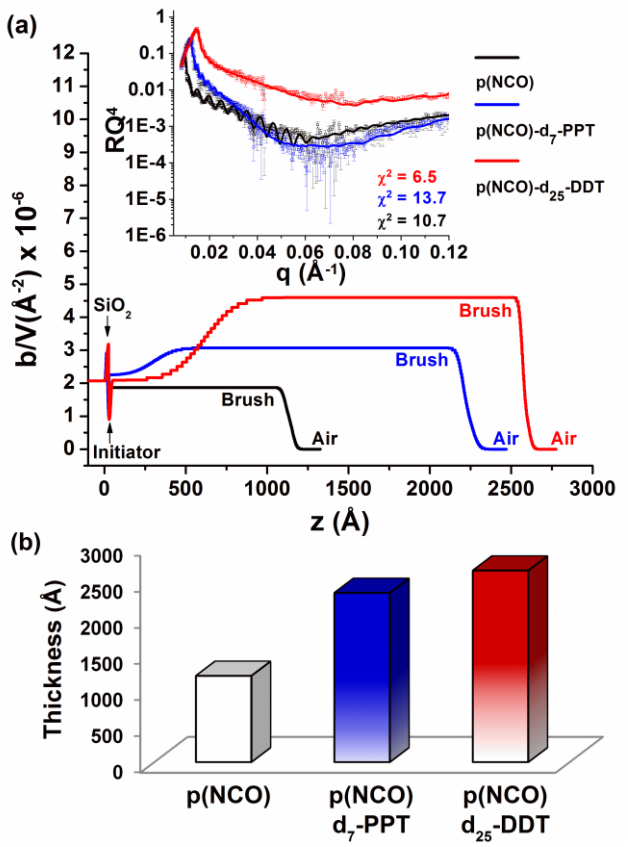

Figure 23. Probing penetration depth of incoming molecules into p(NCO) brushes via neutron reflectivity: a) experimental reflectivity data (open squares) and the corresponding fits for unmodified p(NCO) (black line), p(NCO) modified with d_7-PPT (blue line), and p(NCO) modified with d_{25}-DDT (red line) (inset, multiplied by Q^4) with corresponding SLD profiles, b) bar graphs representing concentration gradient profiles for p(NCO) modification with d_7-PPT and d_{25}-DDT. The initial p(NCO) brush thickness before modification is represented by the white bar graph.

heterogeneities in the SLD profile were observed with the SLD value increasing in a more gradual manner in the near substrate region before reaching a maximum value (4.60×10^{-6} Å^{-2}). With d_{25}-DDT, the concentration gradient region spans ~31% (81 nm) of the nearest substrate region, whereas only ~69% (180 nm) of the total brush thickness was fully modified with d_{25}-DDT. The concentration gradient profiles for d_7-PPT and d_{25}-DDT are summarized in a more visual manner in Figure 23b. Although only a snapshot of one reaction time (1 h), these results, in agreement with trends reported by

Schuwer et al.[20] and Schuh et al.,[19] clearly reflect the effect of thiol MW on depth of penetration into the brush, as well as the slope of the composition gradient observed at increasing penetration depths upon PPM. Work is on-going in our lab to provide a complete picture of governing parameters (thickness, grafting density, reaction time, etc.) in PPM processes to enable the preparation of homogeneous, fully functionalized polymer brushes.

While achieving homogeneity in polymer brush structure is certainly important, our results point to more exciting possibilities in terms of controlled design of heterogeneous, multicomponent brush structures. Given that the rate of the thiol-isocyanate reaction is exceedingly fast, the overall progression of PPM throughout the brush is ultimately dominated by the diffusion of the thiol modifier from solution into the brush – a process which becomes increasingly hindered as the PPM reaction progresses due to increasing segmental repulsion. Thus, for a given set of brush structural parameters, reaction time becomes a simple and convenient handle for controlling the depth of modifier penetration. Here, we use reaction time and differences in the depths of penetration of d_7-PPT and d_{25}-DDT to synthesize a tapered block copolymer brush.

Tapered block copolymer brushes were synthesized using a sequential PPM process with d_7-PPT and d_{25}-DDT as shown in Scheme 11b. pNCO brush surfaces were first exposed to a THF solution containing 0.01M d_{25}-DDT and 0.002 M DBU for 15 min. After rinsing with THF, the same surfaces were exposed to a THF solution containing 0.01 M d_7-PPT and 0.002 M DBU for 4 h to react the NCO groups remaining at greater penetration depths. Figures 24a and 24b show the reflectivity data and

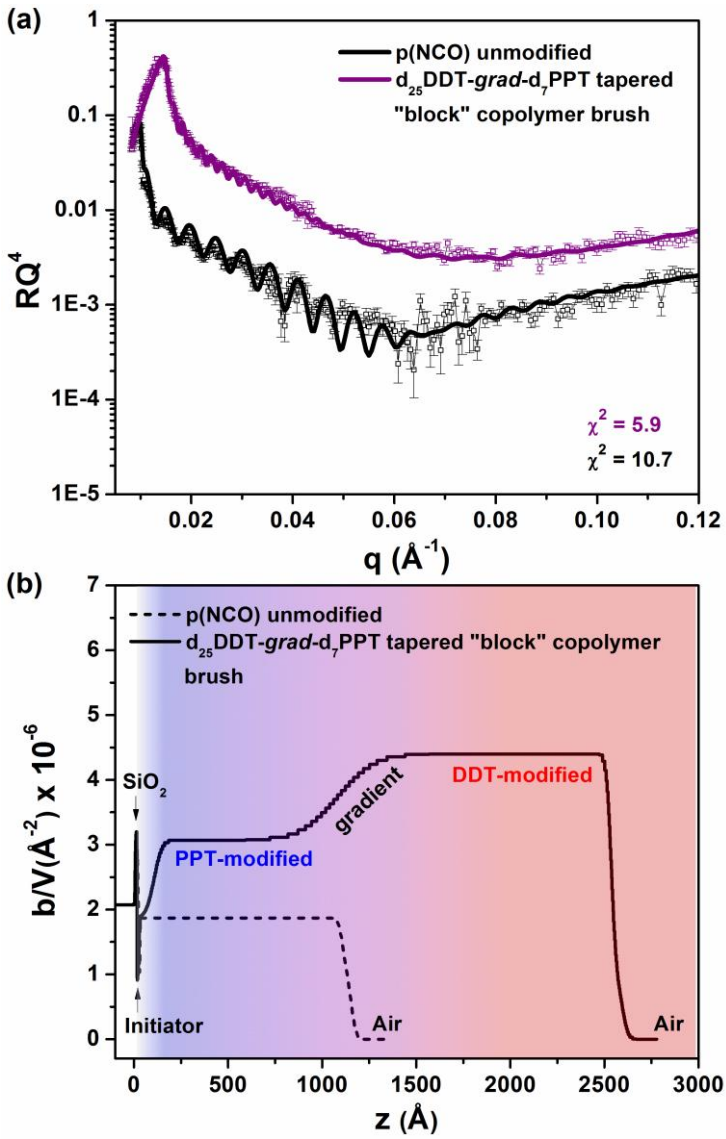

Figure 24. Neutron reflectivity data of tapered block copolymer brushes: a) experimental reflectivity data (open squares) and the corresponding fits for unmodified p(NCO) (black line) (used as a reference) and p(NCO) modified with d_{25}-DDT followed by d_7-PPT (purple line) (inset, multiplied by Q^4) and b) corresponding SLD profiles.

corresponding SLD profiles for a representative brush sample after sequential PPM. For reference, the pNCO brush prior to modification is also shown. Notably, the SLD value for the outermost 133 nm (50%) of the sequentially modified brush is consistent with a homogeneous layer fully modified with d_{25}-DDT. At a penetration depth of 133 nm, the SLD profile gradually decreases over a range of 62 nm (24%), and tapers to another 56

nm (21%) homogeneous layer consistent with d_7-PPT modification. In the near substrate region, the SLD rapidly decreases and approaches that of the hydrogenous pNCO value, suggesting that a thin d_7-PPT gradient (14 nm, 5%) of the total brush thickness) remains after 4 h of the second PPM reaction. Overall, the SLD profile described in Figure 24 is consistent with a tapered block copolymer structure. Remarkably, we have shown that complex brush architectures with controlled heterogeneity can be successfully synthesized without the use of controlled polymerization techniques. Replacing d_7-PPT with d_6-mercaptopropionic acid in the second PPM step enabled the synthesis of tapered block copolymer brushes containing a pH responsive block. We are particularly interested in how the presence and slope of a concentration gradient affects the stimuli-responsive behavior of the surfaces. Once gradient architectures are identified via NR (pending beamtime at ORNL), the stimuli-responsive behavior as a function of pH will be investigated by exploring the brush conformation (via NR using a liquid cell) and by following changes in surface energy. Preliminary studies suggest that non-identical chemical functionalities can be used to create tapered block copolymer brushes. The diffusion of lower molecular weight functional modifiers, as previously described, through the pre-existing modified brush layers to the unreacted portion of the brush can be facilitated as indicated by GATR-FTIR through monitoring the consumption of isocyanate functionalities. Figure 25 shows the GATR-FTIR spectra of the p(NCO) brushes before and after sequential PPMs with non-identical functional modifiers. Thus the conversion of the PPM was determined by taking the ratio of the integrated peak area associated with the isocyanate group (2275 cm^{-1}) before and after modification. The carbonyl band (C=O, 1730 cm^{-1}) was used as a reference peak as the area of this peak

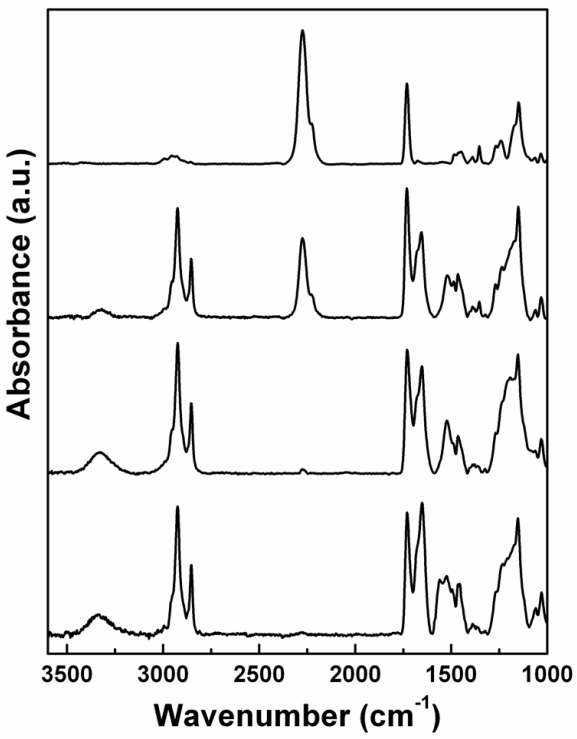

Figure 25. GATR-FTIR spectra of a) unmodified p(NCO) brush, b) partially modified p(NCO) with 1-dodecanethiol, c) pseudo-block (co)polymer brushes modified with 1-dodecanethiol followed by 3-mercaptopropionic acid and d) pseudo-block (co)polymer brushes modified with 1-dodecanethiol followed by benzyl amine.

remained constant during the surface modifications, (i.e. the C=O peak associated with formation of a thiourethane (-S-CO-NH-) linkage upon the thiol-NCO reaction appears at 1650 cm^{-1}).[25] According to GATR-FTIR, modification of a p(NCO) brush (~110 nm) with dodecanethiol (DDT) for 15 min consumes approximately 60 % of the isocyanate moieties. Upon modification with DDT, the peak associated with the isocyanate group (2275 cm^{-1}) decreases while the peaks associated with thiourethane formation (-S-CO-NH-, and N-H, 1650 cm^{-1} and 3200 – 3420 cm^{-1}, respectively) and incorporation of dodecyl units (C-H, 2852, 2924, 2954 cm^{-1}) increases (Figure 25b).[25] After extensive washing with THF and toluene followed by drying under a stream of N_2, the substrates were submerged into a solution of either 3-mercaptopropionic acid (MPA) or benzyl

amine and allowed to react overnight. The reaction time was increased to allow the incoming molecules sufficient time to diffuse through the existing functionalized polymer brushes. GATR-FTIR revealed the incorporation of MPA (Figure 25c) and benzyl amine (Figure 25d) by the appearance of peaks associated with MPA (COO-H, 3200 – 3420 cm^{-1}) and benzyl amine (C=C, 1458, 1494, 1563 cm^{-1}) as well as an increase in peaks associated with thiourethane formation along with complete disappearance of the peak associated with the isocyanate group.[25] The stretching vibrations for carboxylic acids associated with MPA incorporation appear in the same region as N-H stretching vibrations, but in either case an increase in the peak absorption suggests successful incorporation. Also, the thickness increases upon sequential modification steps validating the successful incorporation of the two non-identical functional modifiers (Table 3). However, GATR-FTIR only confirms the incorporation of the functional modifiers into the polymer brushes with no regard to the distribution of those functional groups throughout the brush. Through NR studies, a better understanding of the transition from one chemical species to another in the z-direction of the polymer brush can be determined. Ultimately, we aim to correlate brush composition and gradient block architecture identified by neutron reflectometry with brush surface properties (i.e. rearrangement of blocks due to environmental changes in solvent quality, pH, etc.).

Conclusions

In conclusion, we have provided a high resolution map of the vertical distribution of deuterated thiols following post-polymerization modification of isocyanate-functionalized polymer brush surfaces using thiol-isocyanate click chemistry. Using neutron reflectometry, we have shown that the molecular weight of the thiol plays an

important role on the depth of penetration into the reactive brush, and on the width of the concentration gradient observed at depths approaching the near substrate region under equivalent reaction conditions. Using this information, we demonstrated a straight-forward, yet unconventional route for the synthesis of complex block copolymer brush architectures using a sequential post-polymerization modification approach. The structure of the first tapered block copolymer brush surface prepared without the use of controlled polymerization techniques was confirmed by NR. By exploiting the limited mass transport of reactive modifiers into brush surfaces, these results exemplify exciting opportunities to design complex polymer surfaces with controlled heterogeneity – surfaces with structure and functionality unattainable by conventional routes that may exhibit new and unique properties.

Acknowledgments

The authors gratefully acknowledge financial support from the National Science Foundation (NSF CAREER DMR-1056817). RMH and EAH acknowledge fellowship support from the U.S. Dept. of Education GAANN program (P200A090066) and NSF GRFP, respectively. Travel assistance to ORNL was provided by JINS EPSCoR Neutron Travel Fellowship Program. We thank Drs. Bradley Lokitz and John Ankner of ORNL for helpful discussions.

References

(1) Barbey, R.; Lavanant, L.; Paripovic, D.; Schüwer, N.; Sugnaux, C.; Tugulu, S.; Klok, H. A. *Chem. Rev.* **2009**, *109*, 5437-5527.

(2) Ayres, N. *Polym. Chem.* **2010**, *1*, 769-777.

(3) Arnold, R. G.; Nelson, J. A.; Verbanc, J. J. *Chem. Rev.* **1957**, *57*, 47 - 76.

(4) Galvin, C. J.; Genzer, J. *Prog. Polym. Sci.* **2011**, *37*, 871-906.

(5) Gauthier, M. A.; Gibson, M. I.; Klok, H. A. *Angew. Chem. - Int. Ed.* **2009**, *48*, 48-58.

(6) Proch, S.; Mei, Y.; Villanueva, J. M. R.; Lu, Y.; Karpov, A.; Ballauff, M.; Kempe, R. *Adv. Synth. Catal.* **2008**, *350*, 493-500.

(7) Tam, T. K.; Zhou, J.; Pita, M.; Ornatska, M.; Minko, S.; Katz, E. *J. Am. Chem. Soc.* **2008**, *130*, 10888-10889.

(8) Sun, L.; Dai, J.; Baker, G. L.; Bruening, M. L. *Chem. Mater.* **2006**, *18*, 4033-4039.

(9) Arumugam, S.; Orski, S. V.; Locklin, J.; Popik, V. V. *J. Am. Chem. Soc.* **2011**, *134*, 179-182.

(10) Hensarling, R. M.; Doughty, V. A.; Chan, J. W.; Patton, D. L. *J. Am. Chem. Soc.* **2009**, *131*, 14673-14675.

(11) Orski, S. V.; Poloukhtine, A. A.; Arumugam, S.; Mao, L.; Popik, V. V.; Locklin, J. *J. Am. Chem. Soc.* **2010**, *132*, 11024-11026.

(12) Brantley, E. L.; Holmes, T. C.; Jennings, G. K. *Macromolecules* **2005**, *38*, 9730-9734.

(13) Cullen, S. P.; Liu, X.; Mandel, I. C.; Himpsel, F. J.; Gopalan, P. *Langmuir* **2007**, *24*, 913-920.

(14) Glinel, K.; Jonas, A. M.; Jouenne, T.; Leprince, J.; Galas, L.; Huck, W. T. S. *Bioconjug. Chem.* **2009**, *20*, 71-77.

(15) Paripovic, D.; Hall-Bozic, H.; Klok, H. A. *J. Mater. Chem.* **2012**, *22*, 19570-19578.

(16) Zhao, H.; Sterner, E. S.; Coughlin, E. B.; Theato, P. *Macromolecules* **2012**, *45*, 1723 - 1736.

(17) Chen, W. Y.; Zheng, J. X.; Cheng, S. Z. D.; Li, C. Y.; Huang, P.; Zhu, L.; Xiong, H.; Ge, Q.; Guo, Y.; Quirk, R. P.; Lotz, B.; Deng, L.; Wu, C.; Thomas, E. L. *Physical Review Letters* **2004**, *93*, 028301.

(18) Milner, S. T. *Science* **1991**, *251*, 905 - 914.

(19) Schuh, C.; Ruhe, J. *Macromolecules* **2011**, *44*, 3502-3510.

(20) Schuwer, N.; Geue, T.; Hinestrosa, J. P.; Klok, H.-A. *Macromolecules* **2011**, *44*, 6868-6874.

(21) Hensarling, R. M.; Rahane, S. B.; LeBlanc, A. P.; Sparks, B. J.; White, E. M.; Locklin, J.; Patton, D. L. *Polym. Chem.* **2011**, *2*, 88-90.

(22) Rahane, S. B.; Hensarling, R. M.; Sparks, B. J.; Stafford, C. M.; Patton, D. L. *J. Mater. Chem.* **2012**, *22*, 932-943.

(23) Beinhoff, M.; Frommer, J.; Carter, K. R. *Chem. Mater.* **2006**, *18*, 3425-3431.

(24) Schuh, C.; Santer, S.; Prucker, O.; Rühe, J. *Adv. Mater.* **2009**, *21*, 4706-4710.

(25) Socrates, G. *Infrared and Raman Characteristics Group Frequencies*; 3rd ed. ed.; John Wiley & Sons Ltd.: Chichester, 2001.

CHAPTER VII

PHOTOCAGED PENDENT THIOL POLYMER BRUSH SURFACES FOR POST-POLYMERIZATION MODIFICATIONS VIA THIOL-CLICK CHEMISTRY

Introduction

Engineering polymer surfaces with precise control over polymer architecture, chemical functionality, and spatial orientation of functional groups throughout the interface represents a grand challenge for polymer chemistry – particularly as demand increases for surfaces presenting complex chemistries and morphologies. A rapidly growing strategy to address this challenge involves post-polymerization modification (PPM) of polymer surfaces.[1] PPM of surfaces is a process based on the polymerization of monomers with functional groups that are inert under the polymerization and/or film formation conditions, but can subsequently be quantitatively converted into a broad range of other functional groups. Thus, PPM enables the versatile and modular transformation of physiochemical properties of surfaces, and has been demonstrated using modification chemistries ranging from activated esters[2,3] and ring-opening[4-7] to more efficient and robust chemistries based on the "click" family of reactions.[8,9] "Click" reactions – with the copper assisted azide-alkyne cycloaddition (CuAAC) reaction being the prominent example[10] – exhibit salient features such as high yields, fast reaction kinetics, orthogonal reactivity, and are tolerant to a broad range of reaction conditions. Successful utilization of CuAAC for PPM of surfaces has provided the impetus for continued development of click-based PPM strategies;[11] however, concern over the presence of residual metal impurities following copper-catalyzed click reactions has driven the development of alternate, metal-free surface modification strategies. Consequently, metal-free click

reactions – such as strain-promoted azide-alkyne cycloadditions,[12] Diels-Alder cycloadditions,[13-17] and thiol-based reactions[18] – are rapidly becoming methods of choice for post-polymerization surface modification strategies.

Our group, along with others, has demonstrated thiol-based click reactions – including thiol-ene,[19-22] thiol-yne,[22-25] and thiol-isocyanate[26] – as efficient and modular strategies towards engineering multifunctional surfaces.[27] Thiol-click reactions are advantageous for PPM of surfaces in that they proceed at room temperature with high efficiency and rapid reaction rates, in the presence of oxygen and water, without expensive and/or toxic catalysts, and exhibit high tolerance towards a broad range of functional groups.[28-30] In addition, we have recently exploited the orthogonal nature of radical-mediated thiol-yne reactions in sequential combination with base-catalyzed thiol-isocyanate, thiol-epoxy, and thiol-bromo reactions for the design of multifunctional polymer brush surfaces with controlled surface compositions and wetting properties.[31] Furthermore, thiol-click reactions also have a significant advantage in that a large number of functional thiols are commercially available eliminating the need for multistep synthesis of post-modifiers often encountered in other click-based strategies. In order to exploit the library of commercially available thiols, most examples of thiol-click PPM of surfaces have relied on the immobilization of alkenes, alkynes, or isocyanates as thiol-reactive handles on the surface. However, by employing the reverse scenario whereby thiols are immobilized as the reactive handle on the surface, one could easily take advantage of the vast libraries of commercially available maleimides, acrylates, isocyanates, etc. – all of which are attainable carrying a broad range of pendent functionalities. Such approach would vastly broaden the thiol-click toolbox for post-

modification of surfaces. Aside from serving as a handle for PPM, well-defined polymer surfaces with polyfunctional pendent thiols may also be of interest for immobilization of metallic nanoparticles and for heavy metal capture and remediation applications.

Unfortunately, the desirable characteristics of thiols – i.e. high reactivity and efficiency towards an array of functional groups – also make them intolerable under radical polymerization conditions. The large chain transfer constants of thiols in vinyl polymerizations, self-association via disulfide linkages, and numerous other side reactions eliminate any possibility of incorporating unprotected thiols into macromolecules by direct polymerization. While there are numerous examples of polymer pendent polyfunctional thiols,[32,33] researchers often resort to protection/deprotection schemes that require harsh reaction conditions to yield the thiol (i.e. conversion of halogens to thioesters followed by extended reflux under basic conditions). For engineering functional surfaces based on tethered thiols, particularly those with delicate underlying substrates, milder synthetic conditions towards the thiol are desirable.

"Caged" compounds, or structures containing photolabile protecting groups (PPGs), are well established in the areas of organic chemistry[34] and biochemistry as mild alternatives to chemically-induced deprotections.[35] PPGs can be removed by exposure to ultraviolent (UV) light under neutral and reagent-free conditions to yield a variety of reactive functional groups including acids, alcohols, and amines. Light can be used in a direct fashion to immediately trigger a desired modification or indirectly to release a reactive moiety that will then participate in a given activity or modification process such as post-polymerization modification. In this way, PPGs have been utilized for initiator,[36]

end group[37] and side chain polymer modifications,[38-41] block copolymers,[41-43] monolayers,[44-47] two-dimensional surface modifications[48-50] and polymer brushes.[51] PPG strategies have also been reported for the efficient photolysis of protected thiols based on 2-nitrobenzyl,[52] phenacyl,[53,54] benzoinyl,[55] and coumarinyl[52] protecting groups; however, these examples are mostly related to biochemistry applications with fewer examples describing photodeprotection of thiols for polymer or surface modifications. Recently, Barner-Kowollik et al. demonstrated *o*-nitrobenzyl protected thiols as latent pendents on methacrylate-based homopolymers[40] and acrylamide-based copolymers[38] rendering the thiol functionality inert during controlled radical polymerization, but amendable via sequential light-triggered deprotection and thiol-ene PPM process. Wosnick and Shoichet[56] covalently modified agarose hydrogels with a 6-bromo-7-hydroxycoumarin sulfide derivative which upon photo-triggered deprotection and thiol-Michael reaction with maleimide-functionalized biomolecules enabled the development of three-dimensional chemical patterns within the hydrogel. Examples utilizing surface-bound photolabile protected thiols as reactive handles for post-modification of surfaces have been limited to self-assembled monolayers.[44,45,49] For example, Chen et al.[49] described photopatterning of biomolecules on planar surfaces upon photolysis of an *o*-nitrobenzyl protected thiol monolayer. Upon exposure of the thiol, biomolecules were immobilized via disulfide and thiol-Michael reactions. Wavelength-selective PPGs have also been used to expose thiols as reactive head groups on monolayers by exploiting wavelength-selective photolysis of various PPG derivatives enabling independently addressable functional moieties.[44,45] Aside from our own example demonstrating the post-polymerization modification of pendent thiols via thiol-Michael on cysteine-containing

polypeptide brushes,[21] we are currently unaware of any literature reporting the synthesis of well-defined polymer brush surfaces bearing pendent thiols for modular post-polymerization modification.

In the present work, we report a post-polymerization surface modification approach that provides pendent thiol functionality along the polymer brush backbone using the photolabile protection chemistry of both *o*-nitrobenzyl (*o*-NB) and *p*-methoxyphenacyl (*p*-MP) thioethers. Addressing the protecting groups with light enables a plethora of thiol-mediated transformations with isocyanates and maleimides providing a versatile route to create complex, functional polymer surfaces. The experiments described in this article were performed using poly(hydroxyethyl methacrylate) (pHEMA) brushes synthesized via surface-initiated atom transfer radical polymerization (SI-ATRP), which were esterified with 3-(2-nitrobenzylthio)propanoic acid or 3-(2-(4-methoxyphenyl)-2-oxoethylthio)propanoic acid to provide the photolabile protected pendent thiols. SI-ATRP of HEMA was chosen for this work as it serves as a model brush platform allowing excellent control over film thickness and it enables facile synthesis of block copolymer brushes for investigation of photolysis and thiol-click PPM processes on more advanced brush architectures. A principal advantage of the post-modifiable brush platform is that it provides a larger number of modifiable sites per unit area of substrate as compared to conventional self-assembled monolayers (SAMs), while also decoupling the polymer synthesis step from the immobilization of sensitive functional groups on the surface, thereby avoiding expensive monomer synthesis and reducing potential side reactions.

Experimental

Materials

All reagents and solvents were obtained at the highest purity available from Aldrich Chemical Company or Fisher Scientific and used without further purification unless otherwise specified. Single-side polished silicon wafers were purchased from University Wafers. Monomers, 2-hydroxyethyl methacrylate (HEMA, 97% Aldrich, ^{1}H NMR (see Appendix E) and ^{13}C NMR (see Appendix E)) and 2-(dimethylamino)ethyl methacrylate (DMAEMA, 99% Aldrich, ^{1}H NMR (see Appendix E) and ^{13}C NMR (see Appendix E)), were passed through a neutral alumina column to remove the inhibitor. Reagents, 1,8-diazabicyclo[5.4.0]undec-7-ene (DBU), dimethylphenylphosphine (DMPP) and anhydrous triethylamine (TEA) for deprotection and thiol-click reactions were also obtained from Aldrich and used as received. Cyanophenyl maleimide was synthesized according to reported literature procedures (^{1}H NMR (see Appendix E) and ^{13}C NMR (see Appendix E)).[57,58]

Characterization

A Varian Mercury Plus 300MHz NMR spectrometer operating at a frequency of 300 MHz with VNMR 6.1C software was used for proton and carbon analysis. Wettability of the unmodified and modified polymer brushes was measured using a Ramé-hart 200-00 Std.-Tilting B. goniometer. Static (θsw) contact angles were measured using 10 μL water droplets in combination with DROPimage Standard software. Ellipsometric measurements were carried out using a Gaertner Scientific Corporation LSE ellipsometer with a 632.8 nm laser at 70° from the normal. Refractive index values of 3.86, 1.45, 1.43 and 1.5 for silicon, oxide layer, photoinitiator monolayer and all

polymer layers, respectively, were used to build the layer model and calculate layer thicknesses.[59,60] The chemical nature of the polymer brush surfaces was characterized by Fourier transform infrared spectroscopy (FTIR) in grazing-angle attenuated total reflectance mode (GATR-FTIR) using a ThermoScientific FTIR instrument (Nicolet 8700) equipped with a VariGATR™ accessory (grazing angle 65°, germanium crystal; Harrick Scientific). Spectra were collected with a resolution of 4 cm^{-1} by accumulating a minimum of 128 scans per sample. All spectra were collected while purging the VariGATR™ attachment and FTIR instrument with N_2 gas along the infrared beam path to minimize the peaks corresponding to atmospheric moisture and CO_2. Spectra were analyzed and processed using Omnic software. Atomic force microscopy was performed using a Bruker Icon in tapping mode. The samples were scanned with T300R-25 probes (Bruker AFM Probes) with a spring constant of 40 N/m. Confocal microscopy was performed on fluorescently patterned surfaces using a Zeiss LSM 710 operating with two lasers (433 nm and 548 nm) correlating to the absorption of fluorescein and rhodamine. The fluorescent images were processed using ZEN software.

Synthesis of 10-undecen-1-yl 2-bromo-2-methylpropionate (ATRP initiator precursor)

10-undecen-1-yl 2-bromo-2-methylpropionate was synthesized according to literature procedures.[61] Pyridine (2.1g, 26.5 mmol) was added to ω-undecylenyl alcohol (4.27g, 25.1 mmol) in 25 mL anhydrous tetrahydrofuran (THF) and subsequently cooled to 0 °C followed by the dropwise addition of 2-bromoisobutyryl bromide (6.1g, 26.5 mmol). The reaction was stirred overnight at r.t. followed by dilution with hexanes (50 mL) and washing with 2N HCl (2x) and deionized H_2O (2x). The organic phase was dried with $MgSO_4$, filtered, and concentrated via rotary evaporation. The colorless oily

residue was purified using flash chromatography (5:1 hexanes:ethyl acetate, $R_f = 0.7$) to give 7.25 g (91%) of the ester as a colorless oil. ^{1}H NMR ($CDCl_3$, δ ppm, (see Appendix E)): 1.28 – 1.72 (br m, 14H), 1.93 (s, 6H), 2.05 (q, 2H), 4.16 (t, 2H), 4.9 – 5.02 (m, 2H), 5.74 – 5.87 (m, 1H); ^{13}C NMR ($CDCl_3$, δ ppm, (see Appendix E)): 25.93, 28.50, 29.07, 29.23, 29.30, 29.52, 29.56, 30.95, 33.95, 56.16, 66.36, 114.25, 139.34, 171.89.

Synthesis of (11-(2-bromo-2-methyl)propionyloxy)undecyltrichlorosilane (ATRP initiator-tricholorsilane)

In a glovebox under a N_2 atmosphere, 10-undecen-1-yl 2-bromo-2-methyl-propionate (0.27g, 0.84 mmol, 1 eq), trichlorosilane (0.57g, 4.2 mmol, 5 eq), ~ 3 mL anhydrous toluene, and 5 – 6 drops of Pt-divinyl tetramethyl disiloxane complex in vinyl silicone were allowed to react overnight. Toluene and excess trichlorosilane were removed under vacuum to yield (11-(2-bromo-2-methyl)propionyloxy)undecyl-trichlorosilane (0.37g, 96.9%). Dry toluene (3.1 mL) was added creating a stock 271 mM solution. The catalyst and any solids were removed by a syringe filter before use. ^{1}H NMR ($CDCl_3$, δ ppm, (see Appendix E)): 1.23 – 1.45 (br m, 16H), 1.54 – 1.75 (m, 4H), 1.93 (s, 6H), 4.16 (t, 2H); ^{13}C NMR ($CDCl_3$, δ ppm, (see Appendix E)): 22.16, 24.22, 25.69, 28.26, 29.07, 29.22, 29.38, 30.71, 55.88, 66.02.

Immobilization of ATRP initiator-trichlorosilane on SiO_2 surfaces

Silicon wafers were cut into appropriate sized pieces and ultrasonically cleaned in DP2300 ultra-high performance general purpose cleaner and degreaser (Branson Ultrasonics Corp.) for 5 minutes. The wafers were then wiped gently with lens paper or a cotton-tipped applicator to remove silicon dust from the wafer dicing process. After wiping, the wafers were ultrasonicated for an additional 10 min, rinsed multiple times with DI water, and ultrasonicated in deionized water for 15 minutes. The wafers were

then placed into a RCA-1 solution (5 parts deionized H_2O, 1 part 27% ammonium hydroxide, 1 part 30% hydrogen peroxide) for 15 min at 70 °C to remove any organic residues before initiator immobilization. The wafers were rinsed thoroughly with DI water, dried under a stream of N_2, and transferred into an acrylic glove box where they were placed into a toluene solution of (11-(2-bromo-2-methyl)propionyloxy)undecyl-trichlorosilane (4 mM) at room temperature for 16 h without stirring. The wafers were removed from the solution, rinsed extensively with toluene, dichloromethane, and dimethylformamide before drying under a stream of N_2. The initiator-functionalized silicon wafers were stored in toluene at -20 °C until use.

Synthesis of 3-(2-nitrobenzylthio) propanoic acid (o-NB)

3-mercaptopropionic acid (2.95g, 23.1 mmol) and anhydrous TEA (1.83g, 18.1 mmol) were added to 2-nitrobenzyl bromide (2.5g, 11.6 mmol) in anhydrous acetone (150 mL) under a N_2 atmosphere and allowed to react overnight. The salt by-product was filtered and the crude product was isolated via rotary evaporation. The crude product was redissolved in ethyl acetate (100 mL), washed with 0.5 M HCl (4x, 75 mL/wash) and brine (1x, 75 mL), dried using $MgSO_4$. After filtration, the product was concentrated via rotary evaporation. The product crystallized upon removing excess solvent. The crystalline product was finally washed with hexanes and dried under vacuum (1.9g, 68.1%). ^{1}H NMR ($CDCl_3$, δ ppm, (see Appendix E)): 2.59 – 2.64 (t, 2H), 2.70 – 2.74 (t, 2H), 4.10 (s, 2H), 7.26 – 7.59 (m, 3H), 7.96 – 7.99 (d, 1H), 11.12 (b s, 1H); ^{13}C NMR ($CDCl_3$, δ ppm, (see Appendix E)): 26.64, 33.86, 34.47, 125.76, 128.76, 132.1, 133.37, 134.0, 149.01, 177.94.

Synthesis of 3-(2-(4-methoxyphenyl)-2-oxoethylthio) propanoic acid (p-MP)

3-mercaptopropionic acid (2.32g, 21.8 mmol) and anhydrous TEA (1.44g, 14.2 mmol) were added to 2-bromo-4'-methoxyacetophenone (2.5g, 10.9 mmol) in anhydrous acetone (150 mL) under an N_2 atmosphere and allowed to react overnight. The salt by-product was filtered and crude product was isolated via rotary evaporation. The crude product was redissolved in ethyl acetate (100 mL), washed with 0.5 M HCl (4x, 75 mL/wash) and brine (1x, 75 mL), dried using $MgSO_4$ followed by concentration of the product via rotary evaporation. The product crystallized upon placing into freezer at -20 °C. The crystalline product was washed with hexanes to remove any residue impurities and dried under vacuum (2.6g, 88.7%). ^{1}H NMR ($CDCl_3$, δ ppm, (see Appendix E)): 2.70 – 2.73 (d, 2H), 2.81 – 2.87 (d, 2H), 3.79 (s, 2H), 3.88 (s, 2H), 6.92 – 6.97 (d, 2H), 7.93 – 7.97 (d, 2H), 11.12 (b s, 1H); ^{13}C NMR ($CDCl_3$, δ ppm, (see Appendix E)): 26.81, 34.15, 36.93, 55.65, 114.14, 128.18, 131.39, 164.14, 177.27, 193.43.

Synthesis of pHEMA brush surfaces by SI-ATRP

SI-ATRP was carried out in vacuum purged test tubes equipped with rubber septa. In one tube, HEMA and a water/methanol mixture (1:4 v/v) were degassed by bubbling through with N_2 for 45 min. In a second tube, 2,2'-bipyridyl, and copper(I)bromide (40:1:0.5 mol% monomer/ligand/Cu(I)Br) were degassed by three vacuum/N_2 purge cycles. The monomer solution was transferred by cannula to the tube containing the ligand/Cu(I)Br and the mixture was stirred for 45 min or until a deep-red, homogeneous solution was obtained. The monomer/catalyst complex was then transferred by cannula into a degassed tube containing the initiator modified silicon substrate. The reaction proceeded at room temperature. Reaction times were varied to obtain the desired

thickness of pHEMA brushes. pHEMA modified substrates were rinsed extensively with water and methanol following polymerization.

Carbodiimide-mediated esterification of pHEMA brush surface with o-NB and p-MP protected thiols

The pendent hydroxyl groups of the pHEMA brushes were modified in anhydrous DMF (6 mL) with *o*-nitrobenzyl (3-(2-nitrobenzylthio)propanoic acid) or phenacyl (3-(2-(4-methoxyphenyl)-2-oxoethylthio)propanoic acid) derivatives (0.3 mmol) using 4-dimethylaminopyridine (DMAP) (7.3mg, 0.06 mmol) and N,N'-diisopropyl carbodiimide (DIPC) (57mg, 0.45 mmol). DIPC in anhydrous DMF (1 mL) was added dropwise over 5 minutes before placing the reaction on a shaker for 16 h. The substrates were rinsed extensively with DMF, THF, and toluene and dried under a stream of N_2.

Photodeprotection of brush pendent o-NB and p-MP protected thiols

Deprotection of the protected thiols was facilitated by irradiating the substrates with UV light (365 nm, 70 mW/cm^2, 2 h) in N_2 purged anhydrous dichloromethane with or without catalytic amounts of DMPP ($3.5x10^{-5}$ M). GATR-FTIR was used to monitor the disappearance of the *o*-nitrobenzyl and *p*-methoxyphenacyl groups.

One-pot photodeprotection and thiol-click modification

Protected substrates were irradiated with UV light under the above conditions to facilitate photolysis of the *o*-NB or *p*-MP moieties. The light source was turned off followed by the addition of reagents to facilitate Michael-type thiol-ene and base-catalyzed thiol-isocyanate surface modifications. Modification of the thiol with various functionalities was monitored by ellipsometry, GATR-FTIR and static water contact angle. Details for each set of thiol-click reactions are given below.

Thiol-Isocyanate modification

A N_2 purged solution consisting of 2-nitrophenyl isocyanate (98.5mg, 0.6 mmol, 0.1 M), 4-methoxybenzyl isocyanate (85.7 µL, 0.6 mmol, 0.1 M), dodecyl isocyanate (144.6 µL, 0.6 mmol, 0.1 M), furfuryl isocyanate (64.3 µL, 0.6 mmol, 0.1 M), or 1-adamantyl isocyanate (0.11 mg, 0.6 mmol, 0.1 M) in anhydrous DCM (6 mL) was added to the reaction vessel containing the reactive pendent thiol polymer brushes. For rapid reaction kinetics, 1,8-diazabicyclo[5.4.0]undec-7-ene (DBU) (0.3 mol% with respect to isocyanate) was used as catalyst. The reaction was allowed to react overnight to ensure completion; however, our group has previously reported quantitative base-catalyzed thiol-isocyanate reactions within minutes.[26]

Thiol-Michael modification

The reactive pendent thiol polymer brushes were submerged into a N_2 purged anhydrous dichloromethane (6 mL) solution containing cyanophenyl maleimide (0.1 M, 118.9mg, 0.6 mmol) with 5 eq. TEA (0.5 M, 418 µL, 3 mmol) with respect to maleimide. The reaction was allowed to react overnight to ensure completion, however, reactions times are known to be much faster.[29]

Surface patterning via photodeprotection and orthogonal thiol-click chemistries

Photomasks (copper grids, 200 mesh, hole width: 90 µm, bar width: 37 µm) were placed directly on top of *o*-NB protected thiol polymer brushes and secured in place with a microscope cover glass slide. The glass slide ensured the photomasks were in intimate contact with the surface as well as limited the mobility of the photomasks upon the addition of solvent. For photodeprotection, the substrates were irradiated with UV light (365 nm, 70 mW/cm^2) for 1 h in anhydrous dimethylformamide (DMF) to facilitate the

photolysis of the *o*-NB moieties. The photomask was removed and the sample was extensively washed in DMF, THF and toluene followed by reaction of the newly generated reactive pendent thiols with fluorescein isothiocyanate. Only areas exposed to UV light generate free thiols that are available for reaction. A solution of fluorescein isothiocyanate (9.9mg, 12.7 mM) and DBU (0.127 mM, 100:1 mol/mol % isothiocyanate:DBU) in anhydrous DMF (2 mL) was placed into the reaction vessel containing the polymer brushes and allowed to react for 1 h. After washing the substrate with DMF, THF and toluene the areas within the polymer brush still in a protected state were deprotected to form additional free thiols available for reaction by irradiating the sample with UV light (365 nm, 70 mW/cm^2) for 1 h in anhydrous DMF followed by reaction with Texas Red® C_2 maleimide. A solution of Texas Red® C_2 maleimide (0.1 mM) and TEA (0.5 mM, 5 eq. in respect to maleimide) in anhydrous DMF (2 mL) was purged with N_2 and subsequently added to the reaction vessel containing the polymer brushes and allowed to react for 1 h. The substrates were extensively washed with DMF, THF and toluene before confocal microscopy was performed.

Synthesis, photodeprotection, and thiol-click modification of block copolymer brush surfaces

pHEMA-b-pDMAEMA and pDMAEMA-b-pHEMA brush surfaces were prepared in an analogous manner as previously described for the homopolymer pHEMA brush surfaces using 2,2'-bipyridyl and copper(I)bromide (40:1:0.5 mol% monomer/ligand/Cu(I)Br). pHEMA or pDMAEMA brushes served as macroinitiator substrates for the chain extension reactions. Reaction times were varied to obtain the desired thickness of outer pDMAEMA or pHEMA blocks. The pendent hydroxyl groups of the pHEMA block within the block copolymer brushes were modified with *o*-

nitrobenzyl thioether units as previously described. For AFM studies, the modified block copolymers were submerged into a 0.01 M HCl aqueous solution for 30 minutes to protonate the pDMAEMA domains within the block copolymer.

Results and Discussion

Synthesis of pendent thiol polymer brushes

Scheme 12a shows the general approach for the synthesis of photolabile protected pendent thiol polymer brushes. Silicon substrates were first functionalized with a chlorosilane ATRP initiator derivative, 11-(2-bromo-2-methyl) propionyloxy-undecenyltrichlorosilane.[61] p(HEMA) brushes were then prepared using SI-ATRP of HEMA in a water/methanol mixture, followed by carbodiimide-mediated esterification with 3-(2-nitrobenzylthio)propanoic acid (**1**) (*o*-NB) or 3-(2-(4-methoxyphenyl)-2-oxoethylthio)-propanoic acid (**2**) (*p*-MP) to provide the polymer brushes with pendent photolabile protected thiols. Conversion to the desired ester derivatives was confirmed by GATR-FTIR (vide infra). Attempts to incorporate the *o*-NB functional group in the brush by direct SI-ATRP of an *o*-NB functional methacrylate monomer were successful; however, this approach yielded miniscule film thickness (<10 nm) presumably due to the inhibitory effects of the $-NO_2$ group.[62] The inhibition effect is likely amplified given the low concentration of propagating chains relative to monomer concentration in surface-initiated polymerizations. In contrast, SI-ATRP of a *p*-MP methacrylate monomer enabled a direct polymerization approach providing an evident advantage over the *o*-NB derivative, but for comparative purposes, the carbodiimide esterification route was adopted for both systems.

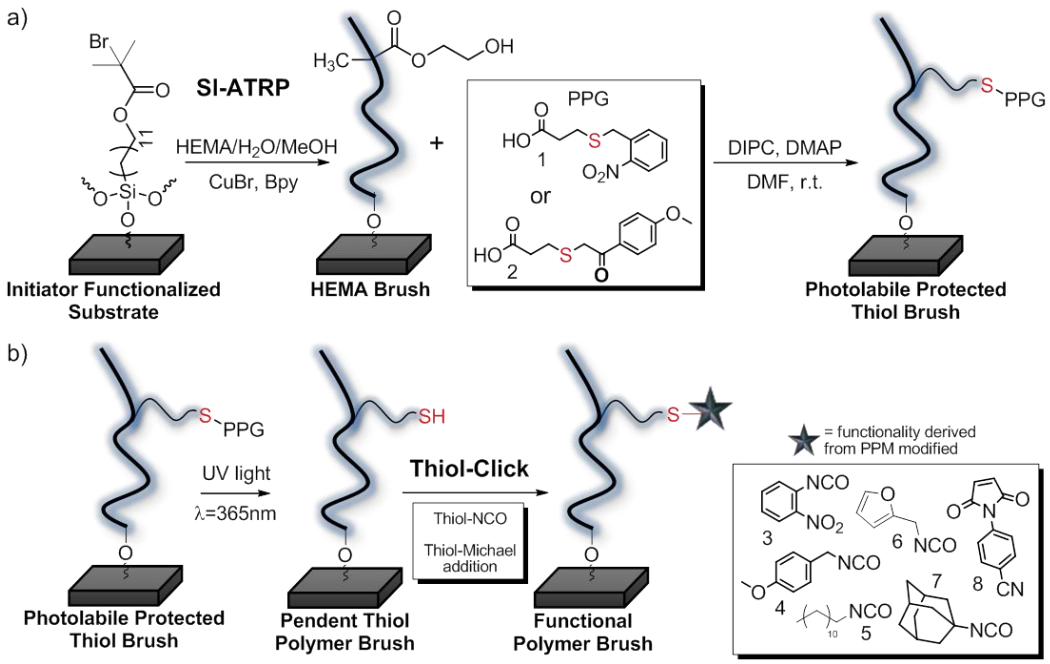

Scheme 12. a) General approach for the synthesis of polymer brush surfaces with pendent photolabile protected thiols and b) subsequent photodeprotection and thiol-click modification.

As shown in Scheme 12b, the *o*-NB and *p*-MP moieties are cleaved by irradiation with UV light at 365 nm yielding pendent thiol brush precursors. The resulting pendent thiol moieties along the polymer brush backbone then serve as reactive handles for subsequent thiol-click reactions. In the following sections, we describe the results of photodeprotection of both *o*-NB and *p*-MP PPGs and post-modification via base-catalyzed thiol-isocyanate reactions and thiol-Michael additions with maleimides. The reactions were carried out in a one-pot reaction, meaning that the UV light was turned off following deprotection, and base-catalyzed thiol-isocyanate reactions or Michael-type thiol-ene additions were facilitated in the same pot by syringing in solutions of either an isocyanate or a maleimide along with the respective catalysts.

Photodeprotection of o-NB and p-MP protected thiol brushes and one-pot thiol-click modificaton

Scheme 13 and Scheme 14 show the commonly accepted routes for photodeprotecton reactions of *o*-NB and *p*-MP derivatives (shown as thiol derivatives for relevance to the current work). A brief discussion of these schemes provides insight for the ensuing photodeprotection studies to yield pendent thiols on the brush platforms. Photodeprotection of *o*-nitrobenzyl derivatives (**9**) is known to be initiated by the abstraction of benzylic hydrogen from an excited nitro group producing aci-nitro intermediates (**10**) and (**11**).[35,63,64] Irreversible cyclization to the benzisoxazoline intermediate (**12**) through the neutral nitronic acid (**10**) followed by ring opening yields (**13**) and ultimately the products 2-nitrosobenzaldehyde (**14**) and R-SH (**15**).[35,64] A strong solvent and pH dependence has also been shown for the photodeprotection of *o*-nitrobenzyl derivatives.[65] The reaction of the deprotected thiol (**15**) with the nitroso moiety of 2-nitrosobenzaldehyde (**14**) should be noted as a potential side reaction[66] which would reduce the available thiol concentration within the brush. Much less is known about the detailed photodeprotection mechanism of *p*-methoxyphenacyl derivatives (**16**). Givens et al.[67,68] indicated the photodeprotection proceeded via a triplet-excited state and a spiroketone intermediate (not shown), which may account for byproduct (**20**) in the case of *p*-MP protected thiols, as (**20**) would result from a nucleophilic ring opening of the spiroketone by a thiol.[54] A more recent study by An et al.[69] suggested a concerted triplet deprotection and solvolytic rearrangement with little observation of a spiroketone intermediate to provide the deprotected thiol moiety (**17**) and a series of byproducts (**18**, **19**).

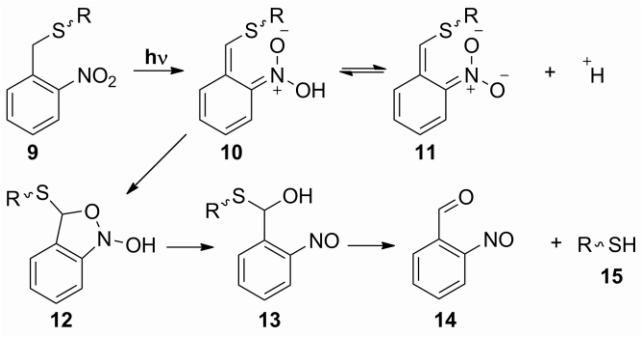

Scheme 13. Photodeprotection of *o*-nitrobenzyl (*o*-NB) protected thioether.

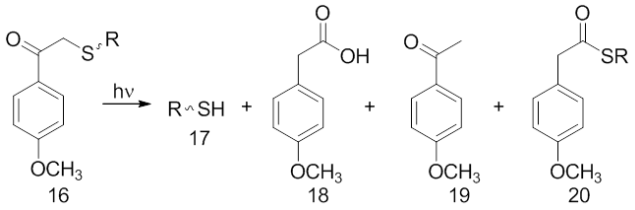

Scheme 14. Photodeprotection of *p*-methoxyphenacyl (*p*-MP) protected thioether.

Photo-induced deprotection of the caged thiols was investigated under various conditions to facilitate complete removal of the photolabile protecting groups while maximizing thiol yield. Pauloehrl and coworkers[40] previously showed that DMPP, when added in catalytic amounts, prevented the formation of disulfides during photo-deprotection of *o*-NB thioethers eliminating the need for a separate reduction step, thus we adopted similar conditions. The photodeprotection reaction was monitored with GATR-FTIR by observing the disappearance of the asymmetric and symmetric NO_2 stretching vibrations inherent to the aromatic nitro derivative at 1527 cm^{-1} and 1350 cm^{-1} for the *o*-nitrobenzyl PPG, and the aromatic C=C stretching vibrations of the phenacyl derivative at 1600 cm^{-1}, 1576 cm^{-1}, and 1515 cm^{-1} for the *p*-methoxyphenacyl PPG.[70] The formation of thiol upon deprotection could not be monitored by GATR-FTIR due to the band for S-H stretching vibration being very weak in the region of 2540 – 2600

cm^{-1}.[70] Figure 26 shows the GATR-FTIR spectra for the photolabile caged *o*-NB and *p*-MP protected pendent thiol polymer brushes upon just photodeprotection and also one-pot photodeprotection and sequential thiol-isocyanate click reactions. The *o*-NB protected thiol polymer brushes (Figure 26a) were subsequently deprotected by exposing the surface to UV_{365nm} light irradiation (70 mW/cm^2) for 2 h in N_2 purged anhydrous DCM in the presence of a catalytic amount of DMPP. Successful deprotection to the thiol was indicated by the complete disappearance of the NO_2 stretching vibrations in the GATR-FTIR (Figure 26b) and a decrease in polymer brush thickness (ca. 9 nm ± 1 nm). Similar results were obtained for the photodeprotection of the *p*-MP modified brush surfaces. As shown in Fig. 7.1d, the aromatic C=C stretching vibrations of the phenacyl derivative at 1600 cm^{-1}, 1576 cm^{-1}, and 1515 cm^{-1} present in the protected form were no longer observed following photodeprotection (Fig. 7.1e). In both cases, the surface becomes more hydrophilic upon deprotection and conversion from the aromatic PPG to the pendent thiol (i.e. water contact angle decreases from 73° to 52° for *o*-NB surface and from 74° to 49° for *p*-MP surface) (see Appendix E).

In order to gain better insight and provide a route to quantify the yield of thiol functionality on the surface following photodeprotection, the pendent thiols were "tagged" with isocyanates bearing a structural resemblance to the cleaved PPG via the base-catalyzed thiol-isocyanate reaction. Namely, thiols produced from the photodeprotection of *o*-NB and *p*-MP groups were subsequently tagged with 2-nitrophenyl isocyanate (**3**) and 4-methoxybenzyl isocyanate (**4**), respectively, in a one-pot fashion. Thus, using GATR-FTIR, the ratio of the $–NO_2$ peak (or the $–OCH_3$ peak) before photodeprotection and after thiol-isocyanate click will provide insight into the

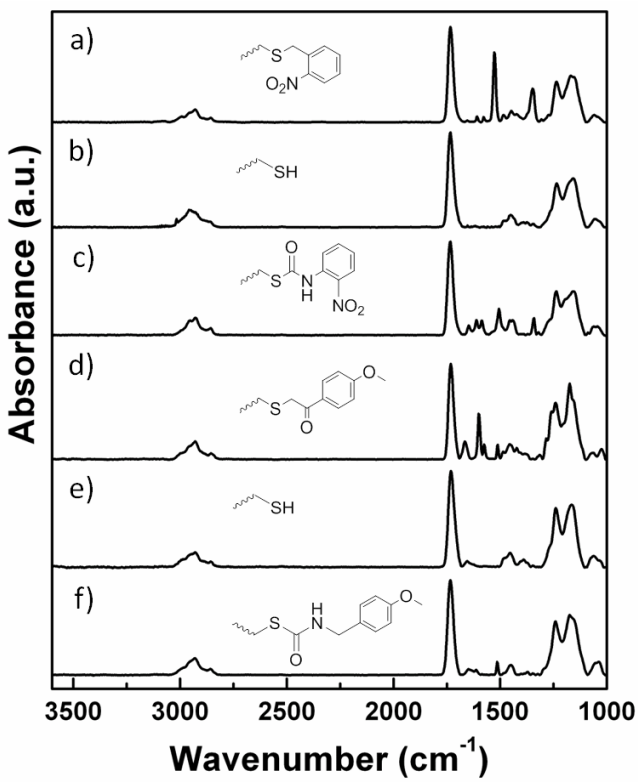

Figure 26. GATR-FTIR spectra of photolabile caged *o*-NB and *p*-MP protected pendent thiol polymer brushes, subsequent deprotection and thiol-isocyanate click reactions: a) photolabile *o*-NB protected pendent thiol polymer brush b) deprotected pendent thiol polymer brush ($3.5x10^{-5}$ M DMPP in DCM) c) one-pot photodeprotection and thiol-isocyanate reaction with 2-nitrophenyl isocyanate (**3**) (0.3 mol% DBU in respect to isocyanate) d) *p*-MP protected pendent thiol polymer brush e) deprotected pendent thiol polymer brush ($3.5x10^{-5}$ M DMPP in DCM) and f) one-pot photodeprotection and thiol-isocyanate reaction with 4-methoxybenzyl isocyanate (**4**) (0.3 mol% DBU in respect to isocyanate).

quantity of thiols available for modification. Importantly, we have previously shown that thiol-isocyanate post-modification of brush surfaces proceeds rapidly to full conversion, so we are confident this approach will tag any available thiols for analysis.[26] Figure 26 shows the GATR-FTIR spectra of *o*-NB (Figure 26a) and *p*-MP (Figure 26d) protected pendent thiol polymer brushes and subsequent one-pot photodeprotection and thiol-isocyanate click reactions with 2-nitrophenyl isocyanate (Figure 26c) or 4-methoxybenzyl isocyanate (Figure 26f). Photochemical conversion to free thiol was

estimated by taking the ratio of the integrated peak area of the NO_2 symmetric stretching vibration (1350 cm^{-1}) for the *o*-NB brushes before photodeprotection and after thiol-isocyanate click, and the integrated peak area of the aromatic phenacyl C=C stretching vibration (1515 cm^{-1}) before photodeprotection and after thiol-isocyanate click for the *p*-MP brushes. The carbonyl band (C=O, 1730 cm^{-1}) was used as a reference peak as the area of this peak remained constant during the surface modifications, (i.e. the C=O peak associated with formation of a thiourethane linkage (-S-CO-NH-) upon the thiol-isocyanate click reaction appears at 1650 cm^{-1}).[70] Accordingly, the photolabile *o*-NB and *p*-MP protected pendent thiol polymer brushes yield 77% ± 2% and 88% ± 3% reactive free thiols, respectively, upon photodeprotection when performed in the presence of a catalytic amount of DMPP as a reducing agent. Additionally, an increase in brush thickness was observed upon one-pot photodeprotection and thiol-isocyanate click in both *o*-NB and *p*-MP protected samples, where an increase from 21.4 ± 0.2 nm (*o*-NB protected) to 24.2 ± 0.1 nm (clicked with **3**) and from 19.1 ± 0.8 nm (*p*-MP protected) to 24.1 ± 0.2 nm (clicked with **4**) was measured, respectively (see Appendix E). The slight increase in brush thickness despite less than quantitative availability of thiol can be attributed to the replacement of the thioether linked *o*-NB and *p*-MP pendent groups with the larger molecular weight thiourethane linked pendent groups derived from **3** and **4**. Despite the use of DMPP, the formation of disulfides or other adventitious side products resulting from the photodeprotection precludes the possibility of achieving quantitative yields of reactive free thiol on the brush surface. For comparison, the formation of free thiols for both *o*-NB and *p*-MP protected polymer brushes decreased to 63% ± 1% and 75% ± 2%, respectively, when reducing agent was not used during photodeprotection.

GATR-FTIR spectra of samples with and without DMPP during the photodeprotection are available in the appendix E.

Upon optimization of the photodeprotection and thiol-click modifications of the brush surfaces, the scope of the thiol-click reactions was broadened to include other functionalities. Photodeprotection of the *o*-NB and *p*-MP protected brushes was facilitated as previously described in the presence of catalytic amounts of DMPP ($3.5x10^{-5}$ M). Figures 27 and 28 show the GATR-FTIR of the photolabile *o*-NB and *p*-MP protected thiol polymer brushes after modification via one-step photodeprotection and thiol-click reactions. For brevity, the thiol-click reactions for the *o*-NB and *p*-MP derivatives will be discussed collectively as the results were similar in each case. The polymer brushes before and after one-pot photodeprotection and thiol-click surface modification were characterized by GATR-FTIR, ellipsometry, and water contact angle measurements. Figure 27a-c and Figure 28a-c show the GATR-FTIR following thiol-isocyanate click of the pendent thiols produced from *o*-NB and *p*-MP cleavage, respectively, in the presence of DBU (0.3 mol% in respect to isocyanate) with dodecyl isocyanate (**5**), furfuryl isocyanate (**6**) and adamantyl isocyanate (**7**). In each case, FTIR confirms a successful thiol-click modification due to the appearance of peaks indicative of the functional isocyanates, for instance, aliphatic C-H stretching vibrations (2954, 2924, 2852 cm^{-1}) was observed for dodecyl isocyanate (Figure 27a and 28a) and for adamantyl isocyanate (Figure 27c and 28c). For modification with furfuryl isocyanate, C-H and =C-H stretching vibrations occur between 3000 – 2800 cm^{-1}; however, spectral overlap of the polymer backbone in the ether region (C-O-C asymmetric stretch, 1270 – 1060 cm^{-1}) makes explicit confirmation of a successful thiol-isocyanate modification with

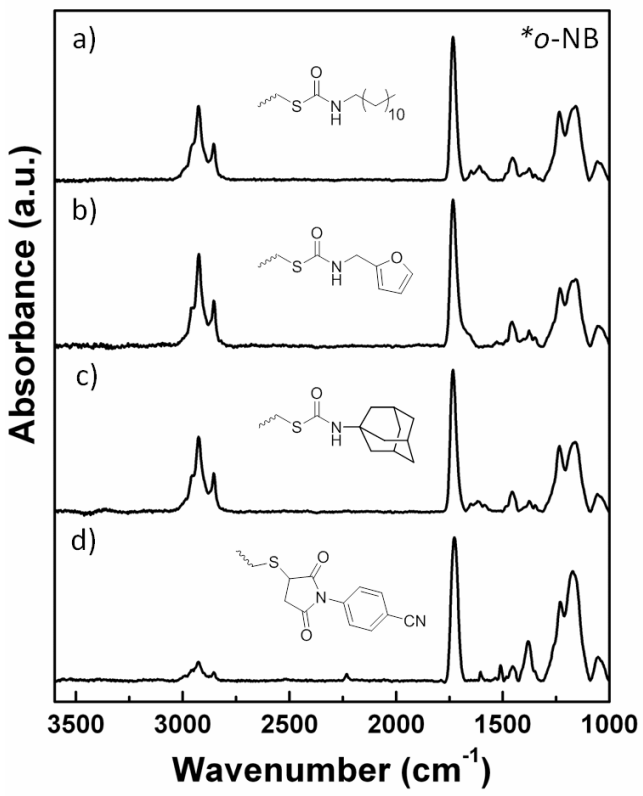

Figure 27. GATR-FTIR spectra after one-pot photodeprotection and thiol-click modifications (base-catalyzed thiol-isocyanate and Michael-type thiol-ene) of *o*-NB protected pendent thiol polymer brushes with a) dodecyl isocyanate, b) furfuryl isocyanate, c) adamantyl isocyanate, and d) cyanophenyl maleimide.

furfuryl isocyanate by GATR-FTIR difficult (Figure 27b and 28b). Lastly, Figure 27d and Figure 28d show the GATR-FTIR spectra for polymer brushes modified with cyanophenyl maleimide (**8**) via Michael-type thiol-ene reactions in the presence of 5 eq. of TEA. The incorporation of cyanophenyl maleimide in the brush was evident by the appearance of a C≡N stretching vibration at 2227 cm^{-1} and aromatic C=C stretching vibrations at 1610 cm^{-1} and 1510 cm^{-1}. All one-pot reactions show expected water contact angles and increases in film thickness upon modification (see Appendix E).

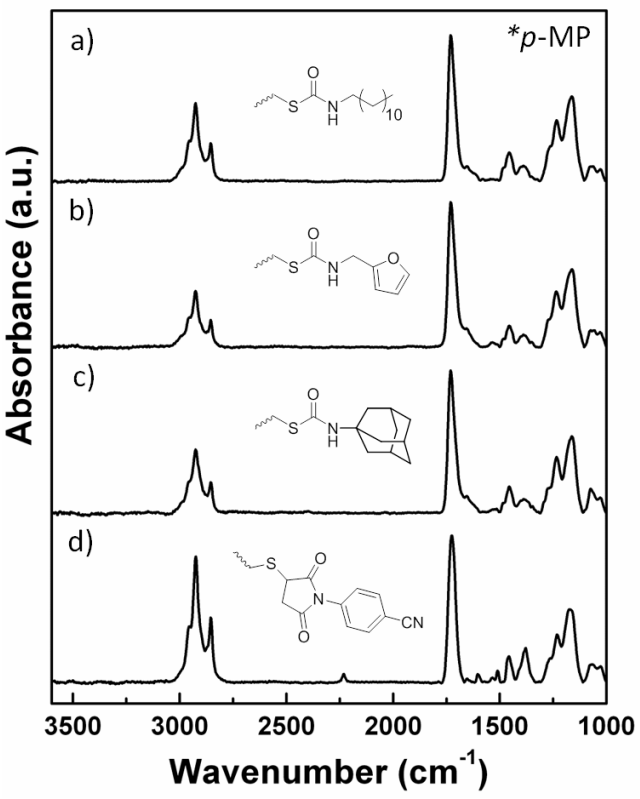

Figure 28. GATR-FTIR spectra after one-pot photodeprotection and thiol-click modifications (base-catalyzed thiol-isocyanate and Michael-type thiol-ene) of *p*-MP protected pendent thiol polymer brushes with a) dodecyl isocyanate, b) furfuryl isocyanate, c) adamantyl isocyanate, and d) cyanophenyl maleimide.

Surface patterning via photodeprotection and orthogonal thiol-click chemistries

As a stimulus for deprotection, light has the added benefit of spatial and temporal control useful for surface patterning. To demonstrate this control, we conducted sequential/area-selective orthogonal surface reactions via base-catalyzed thiol-isothiocyanate and thiol-Michael additions with fluorescein isothiocyanate and Texas Red® C_2 maleimide, respectively, using a simple photopatterning technique. Photomasks (copper grids, hole width: 90 μm, bar width: 37 μm) were placed in contact with the brush surface, immersed in anhydrous DMF and irradiated with UV light for 1 h (365 nm, 70 mW/cm^2) to facilitate the photolysis of the *o*-NB moieties only in the light

exposed areas. After exposure, substrates were immersed in a solution of fluorescein isothiocyanate/DBU for 1 h. The initial click reaction immobilized fluorescein on the brush surface only in the light exposed areas creating a well-defined pattern as shown by fluorescence microscopy (see Appendix E). The remaining *o*-NB protecting moieties were subsequently cleaved by UV flood exposure liberating free thiols available for further functionalization. Texas Red® C_2 maleimide was then immobilized onto the surface in the presence of TEA to generate multi-functional micropatterns in a sequentially orthogonal fashion. Figure 29 shows the fluorescence microscopy images of the fluorescein/Texas Red® C_2 micropatterns under illumination with two lasers (433 nm and 548 nm). Well-defined edges (Figure 29b) indicate a sharp interface between the two domains illustrating spatially resolved patterns can be achieved via cleavage of PPGs and PPM thiol-click processes.

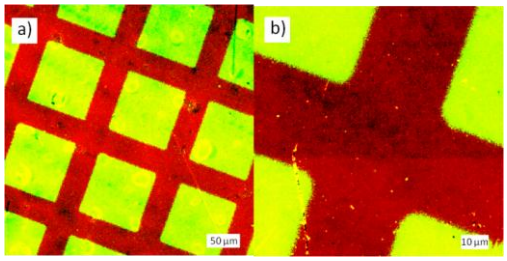

Figure 29. Fluorescence microscopy images of polymer brushes patterned with fluorescein isothiocyanate (squares) and Texas Red® C_2 maleimide (bars) with 433 nm and 548 nm lasers, respectively, at magnifications of a) 5x and b) 20x.

Post-polymerization Modification of Block Copolymer Brushes

With the retention of the bromine end group from SI-ATRP, chain extension enables preparation of block copolymer brushes containing photolabile thiol moieties available for post-modification within the upper or lower block (Scheme 15). Relatively few reports have demonstrated the post-polymerization modification of block copolymer

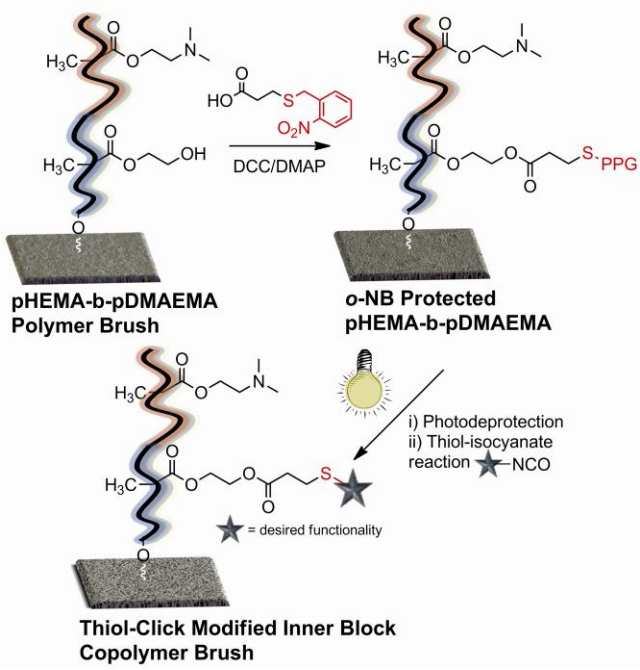

Scheme 15. General approach for block copolymer synthesis, one-pot photodeprotection and thiol-click modification. The analogous inverse block sequence (pendent thiol upper block) was also synthesized, but is not shown.

brush surfaces despite the potential of using the block copolymer brush architecture to control access and the microenvironment of pendent functional groups.[3,71] Block copolymer brushes with *o*-NB protected thiols in the inner block were synthesized using pHEMA with a thickness of 14.6 ± 0.4 nm as a macroinitiator for polymerization of DMAEMA. The thickness of the DMAEMA block was 22.1 ± 0.3 nm after 40 min of polymerization at room temperature. Block copolymers with *o*-NB protected thiols in the outer block were prepared analogously using instead a pDMAEMA macroinitiator for chain extension with HEMA. In both cases, the *o*-NB protected thiol was added via esterification of the pHEMA as described for the homopolymer brush samples resulting in a net thickness increase of ~15 nm.

Figure 30 shows the GATR-FTIR spectra of the block copolymer surfaces with *o*-NB pendent thiol in the inner (Figure 30a) and outer (Figure 30c) blocks. Both surfaces

show the characteristic peaks for the $–NO_2$ asymmetric and symmetric stretching vibrations (1527 cm^{-1} and 1350 cm^{-1}) of the *o*-NB block and for aliphatic amine N-C-H stretching vibrations, 2820 cm^{-1} and 2770 cm^{-1}, and C-N stretching vibration 1270 cm^{-1} of the DMAEMA block. When the outer block consisted of DMAEMA units, protonation in 0.01 M HCl (pH 2) resulted in a weak NH^+ stretching vibration at 2250 cm^{-1}. Upon one-pot photodeprotection and thiol-isocyanate click with dodecyl isocyanate, both samples show the disappearance of the NO_2 stretching vibrations and appearance of C-H stretching vibrations at 2989, 2930, 2860 cm^{-1} and $(CH2)_n$ 1470 cm^{-1} indicative of dodecyl moieties within inner (Figure 30b) and outer (Figure 30d) blocks. The corresponding GATR-FTIR spectra for the homopolymer brushes can be found in Appendix E.

Changes in the morphology of the block copolymer surfaces as a result of thiol-click modifications of the inner and outer blocks as well as solvent treatment were characterized by AFM in tapping mode. The height images show the geometric roughness of the surface while the phase images reveal the distribution of different polymer domains present at the brush interface. The DMAEMA block was protonated to create a more hydrophilic domain compared to the more hydrophobic pendent dodecyl-modified block. After protonation with 0.1 M HCl, the surfaces were dried, rinsed with toluene and finally dried with a stream of N_2. In order to better understand the morphological changes of the block copolymer surfaces, the height and phase images of each system are shown in Figure 31. For comparison, the AFM images for unmodified and modified homopolymer brushes and the unprotonated block copolymers are given in appendix E. Figure 31a,c show the topography and phase images for the block

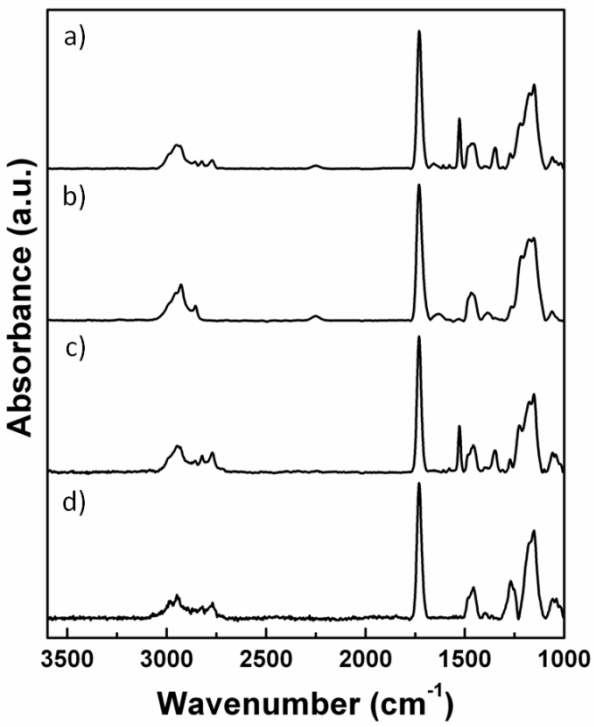

Figure 30. GATR-FTIR of block copolymers (p(inner block)-b-p(outer block)) after PPG modification and thiol-click reaction with dodecyl isocyanate: a) photolabile *o*-NB pendent thiol modified pHEMA-b-pDMAEMA polymer brush (protonated), b) pHEMA pendent thiol-b-pDMAEMA polymer brush clicked with dodecyl isocyanate (protonated), c) pDMAEMA-b-NB pendent thiol modified pHEMA polymer brush (protonated), d) pDMAEMA-b-pHEMA pendent thiol polymer brush clicked with dodecyl isocyanate (protonated).

copolymer surfaces with *o*-NB protected pendent thiol in the inner and outer blocks, respectively. These surfaces do not show a significant change in morphology when DMAEMA is in a deprotonated (see Appendix E) vs. protonated state (Figure 31a,c) (i.e. the differences in hydrophobicity of the protonated DMAEMA and the *o*-NB blocks are not significant). However, upon photodeprotection and functionalization with dodecyl isocyanate (Figure 31b,d), the height images reveal an increase in roughness and more pronounced domain-like morphology. The phase images also show a greater contrast between domains, particularly when comparing samples containing an *o*-NB inner block and protonated DMAEMA outer block (Figure 31a) with the equivalent structure

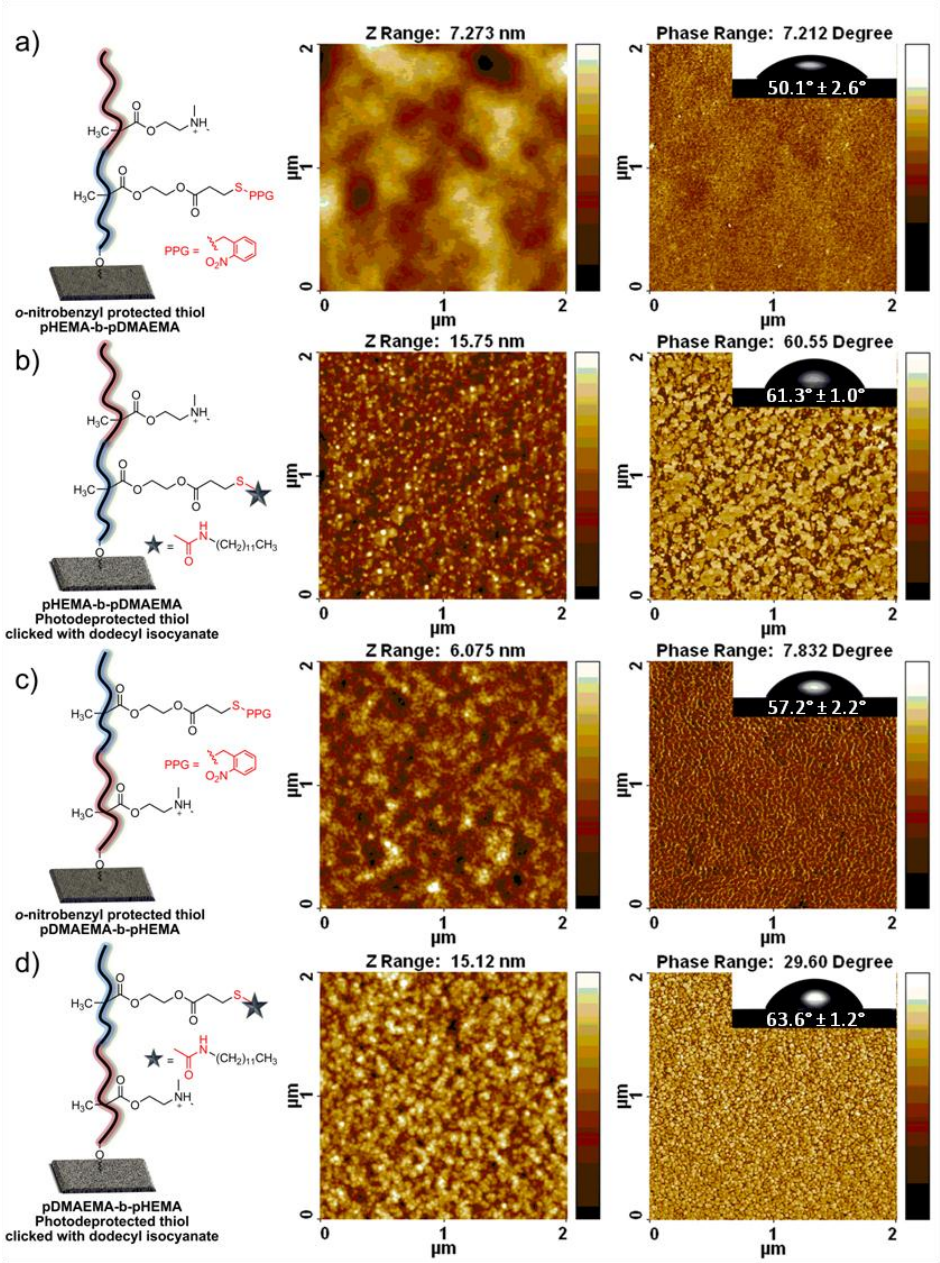

Figure 31. Tapping mode AFM images (height/phase) of block copolymers: a) photolabile *o*-NB pendent thiol modified pHEMA-b-pDMAEMA polymer brush (protonated), b) pHEMA pendent thiol-b-pDMAEMA polymer brush click with dodecyl isocyanate (protonated), c) pDMAEMA-b-photolabile *o*-NB pendent thiol modified pHEMA polymer brush (protonated), and d) pDMAEMA-b-pHEMA pendent thiol polymer brush clicked with dodecyl isocyanate (protonated).

containing an inner block modified with dodecyl isocyanate. (Figure 31b). The observed changes in topography and phase are likely derived not only from the greater contrast in

hydrophobicity among dodecyl and protonated tertiary amine-containing blocks, but also from the final solvent treatment with toluene before imaging. In comparison, samples containing dodecyl-pendent groups in the outer block (Figure 31d) show little rearrangement due to toluene exposure, as the solvated block already dominates the interface as in the case of the dodecyl-modified HEMA homopolymer (see Appendix E). Water contact angle measurements of the block copolymer surfaces, shown as insets in Figure 31, also indicate the presence of a mixed phase morphology at the brush-air interface. Samples containing protonated DMAEMA as the outer block with *o*-NB and dodecyl-modified inner blocks showed water contact angles of 50.1° and 61.3°, respectively. These values are much higher than the protonated pDMAEMA homopolymer brush (13.5°), indicating that both the inner and outer blocks contribute to the observed wettability. Similarly, the reverse scenario, where protonated DMAEMA units formed the inner block with the outer block consisting of *o*-NB and dodecyl moieties showed water contact angles of 57.2° and 63.6°, respectively – values slightly lower than either the *o*-NB or dodecyl-modified homopolymers. The static water contact angles for all combinations of block copolymer brushes can be found in Appendix E. Combined, these results show that post-polymerization modification of pendent thiols via thiol-click reactions can be successfully employed to tailor the functionality of complex polymer brush architectures – including the inner and outer blocks of a block copolymer brush surface.

Conclusions

We have demonstrated a post-polymerization surface modification approach that provides pendent thiol functionality along the polymer brush backbone using the

photolabile protection chemistry of both *o*-nitrobenzyl and *p*-methoxyphenacyl thioethers. Addressing the protecting groups with light enables a plethora of thiol-mediated transformations with isocyanates and maleimides providing a versatile route to create complex, functional polymer surfaces. GATR-FTIR analysis showed that greater than 70% of the protected pendent thiols are available for post-modification following photodeprotection. Also, the generation of reactive free thiols was controlled spatially during photodeprotection with photomasks affording patterned, multifunctional surfaces via orthogonal thiol-click chemistries. One-pot modification processes combining photodeprotection and sequential thiol-click of the brush surface were explored. This concept was extended to block copolymer architectures enabling the modification of the chemical functionality of both the inner and outer blocks of the block copolymer surface. The combination of photo-triggered thiol-click functionalization and controlled radical surface-initiated polymerization provides an attractive and modular approach to tailor the chemical functionality and architecture of polymer surfaces. The approach described also enables spatial immobilization of functional groups in multiple dimensions, i.e. laterally via photolithography and vertically via architectural design of block copolymer brushes; efforts in these directions are ongoing.

Acknowledgments

The authors gratefully acknowledge financial support from the National Science Foundation (NSF CAREER DMR-1056817). Funding from the Office of Naval Research (Award N00014-07-1-1057) enabled the acquisition of the AFM equipment. R.H. thanks the US Dept. of Education GAANN Fellowship Program (Award

#P200A090066) for financial support. We thank Michael Blanton and Kevin Davis of the Rawlins research group for help with confocal microscopy.

References

(1) Galvin, C. J.; Genzer, J. *Prog. Polym. Sci.* **2011**, *37*, 871-906.

(2) Murata, H.; Prucker, O.; Rühe, J. *Macromolecules* **2007**, *40*, 5497-5503.

(3) Orski, S. V.; Fries, K. H.; Sheppard, G. R.; Locklin, J. *Langmuir* **2010**, *26*, 2136-2143.

(4) Barbey, R.; Klok, H.-A. *Langmuir* **2010**, *26*, 18219-18230.

(5) Barringer, J. E.; Messman, J. M.; Banaszek, A. L.; Meyer, H. M.; Kilbey, S. M. *Langmuir* **2008**, *25*, 262-268.

(6) Lokitz, B. S.; Messman, J. M.; Hinestrosa, J. P.; Alonzo, J.; Verduzco, R.; Brown, R. H.; Osa, M.; Ankner, J. F.; Kilbey, S. M. *Macromolecules* **2009**, *42*, 9018-9026.

(7) Soto-Cantu, E.; Lokitz, B. S.; Hinestrosa, J. P.; Deodhar, C.; Messman, J. M.; Ankner, J. F.; Kilbey Ii, S. M. *Langmuir* **2011**, *27*, 5986-5996.

(8) Iha, R. K.; Wooley, K. L.; Nystrom, A. M.; Burke, D. J.; Kade, M. J.; Hawker, C. J. *Chem. Rev.* **2009**, *109*, 5620-5686.

(9) Mansfeld, U.; Pietsch, C.; Hoogenboom, R.; Becer, C. R.; Schubert, U. S. *Polym. Chem.* **2010**, *1*, 1560-1598.

(10) Kolb, H. C.; Finn, M. G.; Sharpless, K. B. *Angew. Chem. Int. Ed.* **2001**, *40*, 2004-2021.

(11) Nebhani, L.; Barner-Kowollik, C. *Adv. Mater.* **2009**, *21*, 3442-3468.

(12) Orski, S. V.; Poloukhtine, A. A.; Arumugam, S.; Mao, L.; Popik, V. V.; Locklin, J. *J. Am. Chem. Soc.* **2010**, *132*, 11024-11026.

(13) Arumugam, S.; Orski, S. V.; Locklin, J.; Popik, V. V. *J. Am. Chem. Soc.* **2011**, *134*, 179-182.

(14) Arumugam, S.; Popik, V. V. *J. Am. Chem. Soc.* **2011**, *133*, 15730-15736.

(15) Dirlam, P. T.; Strange, G. A.; Orlicki, J. A.; Wetzel, E. D.; Costanzo, P. J. *Langmuir* **2009**, *26*, 3942-3948.

(16) Pauloehrl, T.; Delaittre, G.; Winkler, V.; Welle, A.; Bruns, M.; Börner, H. G.; Greiner, A. M.; Bastmeyer, M.; Barner-Kowollik, C. *Angew. Chem. Int. Ed.* **2012**, *51*, 1071-1074.

(17) Sun, X.-L.; Stabler, C. L.; Cazalis, C. S.; Chaikof, E. L. *Bioconjugate Chem.* **2005**, *17*, 52-57.

(18) Arumugam, S.; Popik, V. V. *J. Am. Chem. Soc.* **2012**, *134*, 8408-8411.

(19) Cai, T.; Wang, R.; Neoh, K. G.; Kang, E. T. *Polym. Chem.* **2011**, *2*, 1849-1858.

(20) Jonkheijm, P.; Weinrich, D.; Köhn, M.; Engelkamp, H.; Christianen, P. C. M.; Kuhlmann, J.; Maan, J. C.; Nüsse, D.; Schroeder, H.; Wacker, R.; Breinbauer, R.; Niemeyer, C. M.; Waldmann, H. *Angew. Chem. Int. Ed.* **2008**, *47*, 4421-4424.

(21) Sparks, B. J.; Ray, J. G.; Savin, D. A.; Stafford, C. M.; Patton, D. L. *Chem. Commun.* **2011**, *47*, 6245-6247.

(22) Wendeln, C.; Rinnen, S.; Schulz, C.; Arlinghaus, H. F.; Ravoo, B. J. *Langmuir* **2010**, *26*, 15966-15971.

(23) Hensarling, R. M.; Doughty, V. A.; Chan, J. W.; Patton, D. L. *J. Am. Chem. Soc.* **2009**, *131*, 14673-14675.

(24) Huang, Y.; Zeng, Y.; Yang, J.; Zeng, Z.; Zhu, F.; Chen, X. *Chem. Commun.* **2011**, *47*, 7509-7511.

(25) Wang, C.; Ren, P. F.; Huang, X. J.; Wu, J.; Xu, Z. K. *Chem. Commun.* **2011**, *47*, 3930-3932.

(26) Hensarling, R. M.; Rahane, S. B.; LeBlanc, A. P.; Sparks, B. J.; White, E. M.; Locklin, J.; Patton, D. L. *Polym. Chem.* **2011**, *2*, 88-90.

(27) DeForest, C. A.; Anseth, K. S. *Angew. Chem. Int. Ed.* **2012**, *51*, 1816-1819.

(28) Hoyle, C. E.; Bowman, C. N. *Angew. Chem. Int. Ed.* **2010**, *49*, 1540-1573.

(29) Hoyle, C. E.; Lowe, A. B.; Bowman, C. N. *Chem. Soc. Rev.* **2010**, *39*, 1355 - 1387.

(30) Lowe, A. B. *Polym. Chem.* **2010**, *1*, 17-36.

(31) Rahane, S. B.; Hensarling, R. M.; Sparks, B. J.; Stafford, C. M.; Patton, D. L. *J. Mater. Chem.* **2012**, *22*, 932-943.

(32) Kihara, N.; Kanno, C.; Fukutomi, T. *J. Polym. Sci. A: Polym. Chem.* **1997**, *35*, 1443-1451.

(33) Kihara, N.; Tochigi, H.; Endo, T. *J. Polym. Sci. A: Polym. Chem.* **1995**, *33*, 1005-1010.

(34) Bochet, C. G. *J. Chem. Soc., Perkin Trans. 1* **2002**, 125-142.

(35) Pelliccioli, A. P.; Wirz, J. *Photoch. Photobio. Sci.* **2002**, *1*, 441-458.

(36) Rikkou, M. D.; Patrickios, C. S. *Prog. Polym. Sci.* **2011**, *36*, 1079-1097.

(37) Taniguchi, A.; Skwarczynski, M.; Sohma, Y.; Okada, T.; Ikeda, K.; Prakash, H.; Mukai, H.; Hayashi, Y.; Kimura, T.; Hirota, S.; Matsuzaki, K.; Kiso, Y. *ChemBioChem* **2008**, *9*, 3055-3065.

(38) Delaittre, G.; Pauloehrl, T.; Bastmeyer, M.; Barner-Kowollik, C. *Macromolecules* **2012**, *45*, 1792-1802.

(39) Gumbley, P.; Koylu, D.; Thomas, S. W. *Macromolecules* **2011**, *44*, 7956-7961.

(40) Pauloehrl, T.; Delaittre, G.; Bastmeyer, M.; Barner-Kowollik, C. *Polym. Chem.* **2012**, *3*, 1740 - 1749.

(41) Zhao, H.; Sterner, E. S.; Coughlin, E. B.; Theato, P. *Macromolecules* **2012**, *45*, 1723 - 1736.

(42) Jiang, J.; Tong, X.; Morris, D.; Zhao, Y. *Macromolecules* **2006**, *39*, 4633-4640.

(43) Woodcock, J. W.; Wright, R. A. E.; Jiang, X.; O'Lenick, T. G.; Zhao, B. *Soft Matter* **2010**, *6*, 3325-3336.

(44) Kikuchi, Y.; Nakanishi, J.; Shimizu, T.; Nakayama, H.; Inoue, S.; Yamaguchi, K.; Iwai, H.; Yoshida, Y.; Horiike, Y.; Takarada, T.; Maeda, M. *Langmuir* **2008**, *24*, 13084-13095.

(45) Miguel, V. S.; Bochet, C. G.; del Campo, A. *J. Am. Chem. Soc.* **2011**, *133*, 5380-5388.

(46) Stegmaier, P.; Alonso, J. M. a.; Campo, A. n. d. *Langmuir* **2008**, *24*, 11872-11879.

(47) Wirkner, M.; Alonso, J. M.; Maus, V.; Salierno, M.; Lee, T. T.; Garcia, A. J.; Campo, A. D. *Adv. Mater.* **2011**, *23*, 3907 - 3910.

(48) Alang Ahmad, S. A.; Wong, L. S.; ul-Haq, E.; Hobbs, J. K.; Leggett, G. J.; Micklefield, J. *J. Am. Chem. Soc.* **2011**, *133*, 2749-2759.

(49) Chen, S.; Smith, L. M. *Langmuir* **2009**, *25*, 12275-12282.

(50) Kawano, Y.; Takada, T.; nakamura, M.; Yamana, K. *Nucleic Acids Symposium Series No. 53* **2009**, 173 - 174.

(51) Brown, A. A.; Azzaroni, O.; Huck, W. T. S. *Langmuir* **2009**, *25*, 1744-1749.

(52) Kotzur, N.; Briand, B. t.; Beyermann, M.; Hagen, V. *J. Am. Chem. Soc.* **2009**, *131*, 16927-16931.

(53) Arabaci, G.; Guo, X.-C.; Beebe, K. D.; Coggeshall, K. M.; Pei, D. *J. Am. Chem. Soc.* **1999**, *121*, 5085-5086.

(54) Specht, A.; Loudwig, S.; Peng, L.; Goeldner, M. *Tetrahedron Lett.* **2002**, *43*, 8947-8950.

(55) Jones, P. B.; Pollastri, M. P.; Porter, N. A. *J. Org. Chem.* **1996**, *61*, 9455-9461.

(56) Wosnick, J. H.; Shoichet, M. S. *Chem. Mater.* **2007**, *20*, 55-60.

(57) Elsabee, M. Z.; Bamezai, R. K.; Hempel, E.; Kresse, H. *J. Polym. Res.* **2005**, *12*, 61- 66.

(58) Salman, I. A.; Al-Sagheer, F. A.; Elsabee, M. Z. *J. Macromol. Sci., Pure Appl. Chem.* **1997**, *34*, 1207 - 1220.

(59) Beinhoff, M.; Frommer, J.; Carter, K. R. *Chem. Mater.* **2006**, *18*, 3425-3431.

(60) Schuh, C.; Santer, S.; Prucker, O.; Rühe, J. *Adv. Mater.* **2009**, *21*, 4706-4710.

(61) Matyjaszewski, K.; Miller, P. J.; Shukla, N.; Immaraporn, B.; Gelman, A.; Luokala, B. B.; Siclovan, T. M.; Kickelbick, G.; Vallant, T.; Hoffman, H.; Pakula, T. *Macromolecules* **1999**, *32*, 8716 - 8724.

(62) Schumers, J.-M.; Fustin, C.-A.; Can, A.; Hoogenboom, R.; Schubert, U. S.; Gohy, J.-F. *J. Polym. Sci., Part A: Polym. Chem.* **2009**, *47*, 6504-6513.

(63) Morrison, H.; Migdalof, B. H. *J. Org. Chem.* **1965**, *30*, 3996.

(64) Walbert, S.; Pfleiderer, W.; Steiner, U. E. *HeIv. Chim. Acta* **2001**, *84*, 1601-1611.

(65) Il'ichev, Y. V.; Schwuer, M. A.; Wirz, J. *J. Am. Chem. Soc.* **2004**, *126*, 4581-4595.

(66) Zuman, P.; Shah, B. *Chem. Rev.* **1994**, *94*, 1621-1641.

(67) Givens, R. S.; Athey, P. S.; Matuszewski, B.; Kueper, L. W.; Xue, J.; Fister, T. *J. Am. Chem. Soc.* **1993**, *115*, 6001-6012.

(68) Givens, R. S.; Kueper, L. W. *Chem. Rev.* **1993**, *93*, 55-66.

(69) An, H.-Y.; Kwok, W. M.; Ma, C.; Guan, X.; Kan, J. T. W.; Toy, P. H.; Phillips, D. L. *J. Org. Chem.* **2010**, *75*, 5837-5851.

(70) Socrates, G. *Infrared and Raman Characteristics Group Frequencies*; 3rd ed. ed.; John Wiley & Sons Ltd.: Chichester, 2001.

(71) Pirri, G.; Chiari, M.; Damin, F.; Meo, A. *Anal. Chem.* **2006**, *78*, 3118-3124.

CHAPTER VIII

CONCLUSIONS AND RECOMMENDATIONS

Conclusions

The research presented in this dissertation describes the merging of surface-initiated polymerization (SIP) and post-polymerization modification (PPM) techniques as a versatile platform for polymer surface engineering. Radical-mediated and base-catalyzed thiol-click reactions are leveraged as ideal, efficient chemistries to achieve unprecedented control of surface functionality. Chapter I gives a general overview of recent progress surrounding surface property manipulation as well as post-polymerization modifications. The most prevalent surface modification strategies, such as self-assembled monolayers and polymer brush formation via "grafting – to" and "grafting – from" techniques are discussed with emphasis placed on the latter. Also, post-polymerization modifications are reviewed highlighting "click"-type reactions as they relate to each of the following chapters. Chapter II supports the reasoning behind our approach and outlines the specific objectives accomplished. The conclusions of each study are overviewed in the following paragraphs.

In Chapter III and IV, radical-mediated thiol-yne and base-catalyzed thiol-isocyanate post-polymerization modification reactions are demonstrated as modular platforms for the rapid and robust fabrication of highly functional, multicomponent surfaces under ambient conditions. As a functional handle for post-polymerization modification, the efficacy of the thiol-click reactions was explored with a plethora of commercially available thiols, ultimately, proving to exhibit high efficiency and short reaction times. For thiol-yne reactions, upon irradiation with UV light the quantitative

conversion of the tethered alkynes was observed within a matter of *minutes* even in the presence of sunlight suggesting the possibility of large scale modifications using renewable energy resources. For thiol-isocyanate reactions, increasing the basicity of the tertiary amine catalyst used (i.e. DBU as compared to TEA) reduced the reaction time from several *hours* to a matter of *mintues*. Also, well-defined surface patterns on the sub-micron scale were achieved on both PPM platforms through sequential, area-selective brush modifications using straightforward photolithography and PDMS microcapillary patterning techniques, respectively. Considering the mild reaction conditions, rapid throughput, and compatibility with orthogonal chemistries, these studies set the groundwork for further investigations involving SIP and PPM processes.

Chapter V describes two routes to multifunctional brush surfaces utilizing orthogonal thiol-click reactions based on the nature of previously mentioned modification processes. In the first approach, the applicability of the radical-mediated thiol-yne reaction was extended to include one-pot statistical co-click reactions of brush pendent alkyne groups with multiple thiols. The one-pot approach was easily extendable to a mixture of thiols, including biological relevant molecules, allowing for facile control of the surface properties based on the relative concentration of thiols in a thiol mixture. In the second approach, statistical copolymer brushes exhibiting two distinctly-addressable reactive moieties were sequentially modified via orthogonal base-catalyzed thiol-X (where X represents an isocyanate, epoxy, or α-bromoester) and radical-mediated thiol-yne reactions. The surface properties were tailored by controlling the relative concentration of monomers in the monomer feed during the SIP, which in turns dictates the composition of the thiol-clicked surface. In either case, the surface properties,

manifested in the form of wetability, were easily tuned over a wide range by judicious choice of brush composition and thiol functionality.

Chapter VI provides a high resolution map of the vertical distribution of deuterated thiols following post-polymerization modification of isocyanate-functionalized polymer brush surfaces using thiol-isocyanate click chemistry. Using neutron reflectometry, we have shown that the molecular weight of the thiol plays an important role on the depth of penetration into the reactive brush and on the width of the concentration gradient observed at depths approaching the near substrate region under equivalent reaction conditions. Using this information, opportunities to form hierarchical multilayer polymer brushes were discovered based on the initial penetration depth results using a sequential post-polymerization modification process to create complex block copolymer architectures. Intentionally introducing heterogeneity in the z-direction of the polymer brush was exploited due to the limited mass transport of reactive modifiers into brush surfaces, allowing the creation of tapered block copolymer brushes unattainable by conventional, direct polymerization methods such as controlled polymerization techniques.

Thus far, thiol-click PPM of surfaces have relied on the immobilization of alkenes, alkynes, isocyanates, halogens or epoxides as thiol-reactive handles on the surface. However, in Chapter VII the reverse scenario is applied whereby thiols are immobilized as the reactive handles on the surface, therefore allowing one to take advantage of the vast libraries of commercially available maleimides, acrylates, isocyanates, etc. – all of which are attainable carrying a broad range of pendent functionalities. The photolabile protection chemistry of both *o*-nitrobenzyl and *p*-

methoxyphenacyl thioethers provides pendent thiol functionality along the polymer brush backbone amendable to PPM upon photodeprotection. Addressing the protecting groups with light not only affords spatial control of reactive thiol functionality but also enables a plethora of one-pot thiol-mediated transformations with isocyanates and maleimides providing a modular route to create functional polymer surfaces. Through the combination of photo-triggered thiol-click functionalization and controlled radical surface-initiated polymerization, block copolymer brush architectures were formed enabling the modification of the chemical functionality of both the inner and outer blocks of the block copolymer surface.

Recommendations

The findings reported in this dissertation have broadened the scope and applicability of polymer surface engineering through surface-initiated polymerization coupled with post-polymerization modifications. The following recommendations, especially in the field of hierarchical multilayer polymer brushes, are suggested to advance the work reported in this dissertation:

1) Preliminary studies in Chapter VI involving the formation of tapered block copolymer brushes from a single "universal" reactive brush precursor suggests that the composition of vertical concentration gradients of functional groups can be tuned. In the current work, no efforts were made to control the factors contributing to the vertical distribution of functional modifiers upon sequential PPM processes besides judicious choice of modifiers used. However, the same factors contributing to the initial penetration depth results (i.e. reagent concentrations, initial 'reactive' brush thickness, molecular weight of incoming modifier and proximity between surface

reactive functionalities) should be applied in combination with one another to demonstrate control of the vertical distribution of functional modifiers creating precisely engineered hierarchical multilayer polymer brushes. In doing so, it is expected that brush surfaces containing concentration gradient profiles will exhibit unique surface properties (i.e. surface rearrangement) as a function of gradient chain structure.

2) The continuation of work presented in Chapter VII is currently underway in our laboratory. Synthetic strategies exploiting SIP, PPM, and photo-induced reactions to engineer soft material interfaces with compositional complexity in three-dimensions are being investigated. More powerful than the single-deprotection strategies described in Chapter VII, however, are multi-deprotection strategies via wavelength-selective photolabile protecting groups (PPGs). Multi-deprotection strategies combined with wavelength-selective PPGs can impart orthogonality to otherwise incompatible species and increase the degree and diversity of functionalization. Harnessing the capabilities of wavelength-selective photolabile protecting groups will allow for intentional introduction of heterogeneity in the z-direction along the polymer backbone and precise surface patterning in the xy-direction of the brush surfaces. This method should prove to be a very effective and efficient means of fabricating complex, multidimensional surface architectures with "on demand" properties. Exploring photo-induced reactions in combination with SIP and PPM processes has the potential to open many avenues to better engineer polymeric surfaces and to remove synthetic barriers that limit advances in many new technologies.

APPENDIX A

"CLICKING" POLYMER BRUSHES WITH THIOL-YNE CHEMISTRY: INDOORS AND OUT

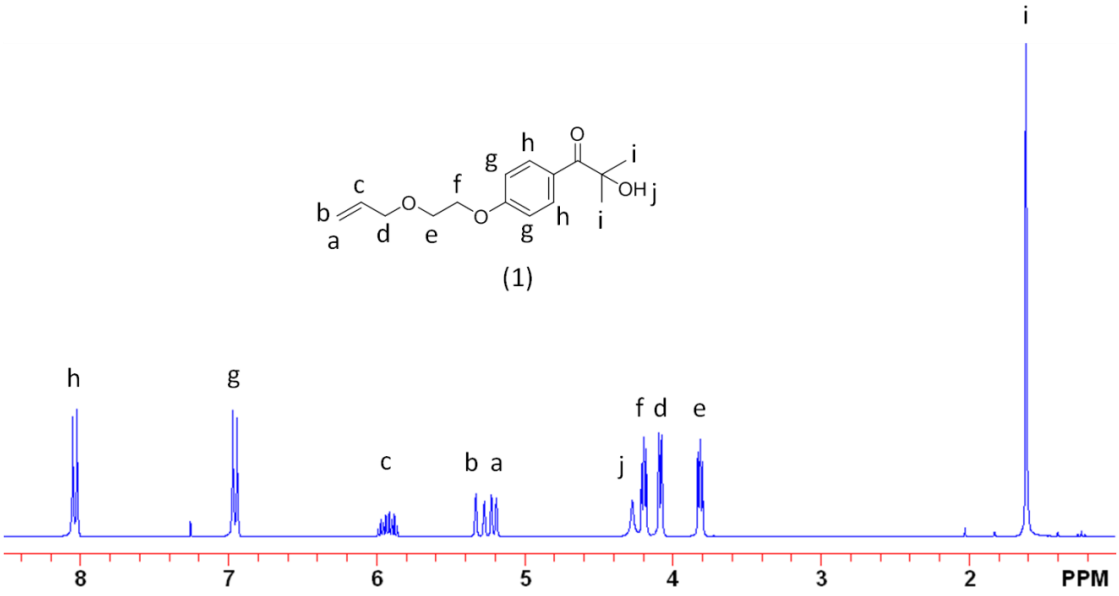

(1)

^{1}H-NMR spectrum of 2-Hydroxy-4'-(2-allyloxyethoxy)-2-methyl-propiophenone (Allyloxy-HPP) (1).

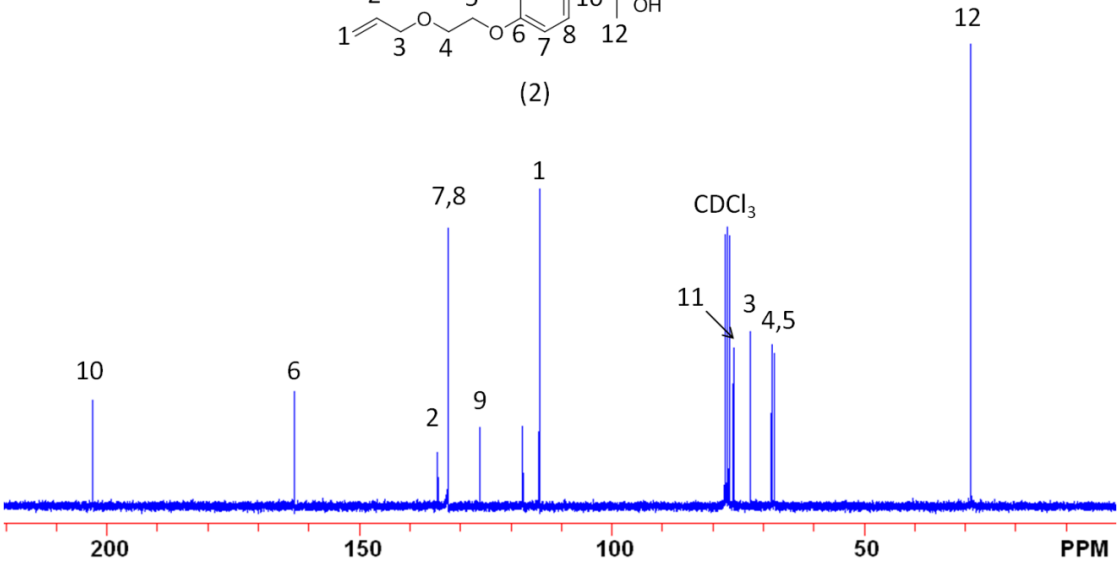

(2)

^{13}C-NMR spectrum of 2-Hydroxy-4'-(2-allyloxyethoxy)-2-methyl-propiophenone (Allyloxy-HPP) (1).

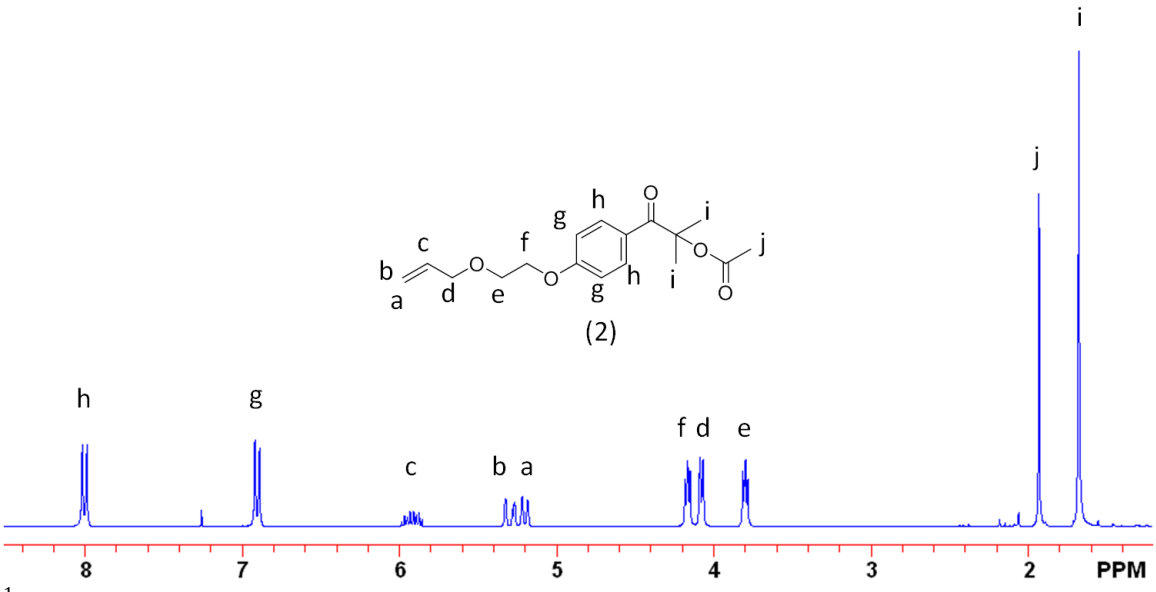

^{1}H-NMR spectrum of (Acetate protected-HPP) (2).

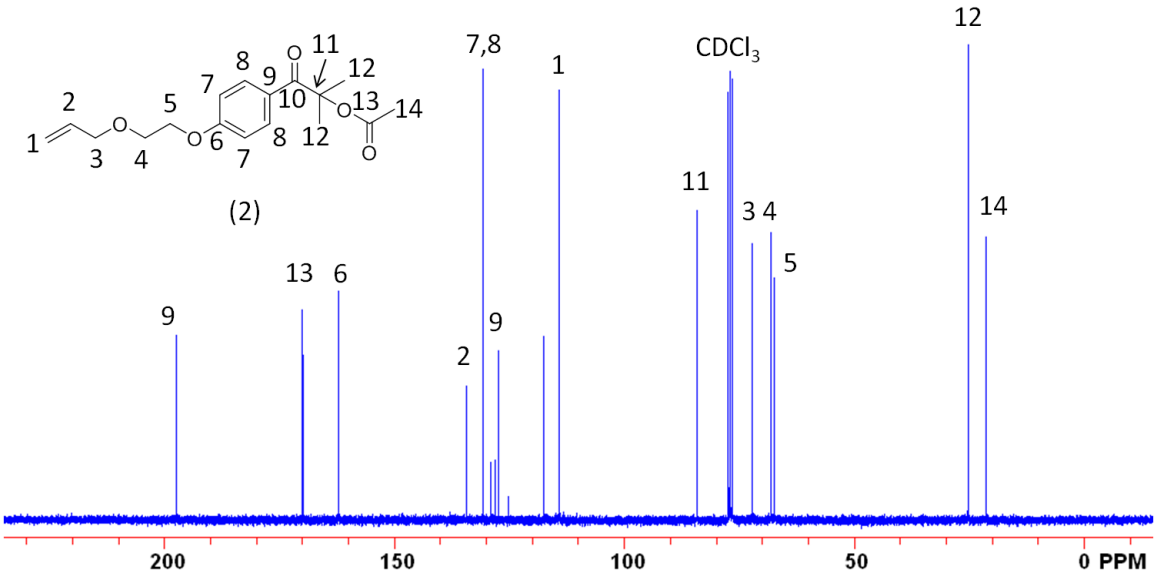

^{13}C-NMR spectrum of (Acetate protected-HPP) (2).

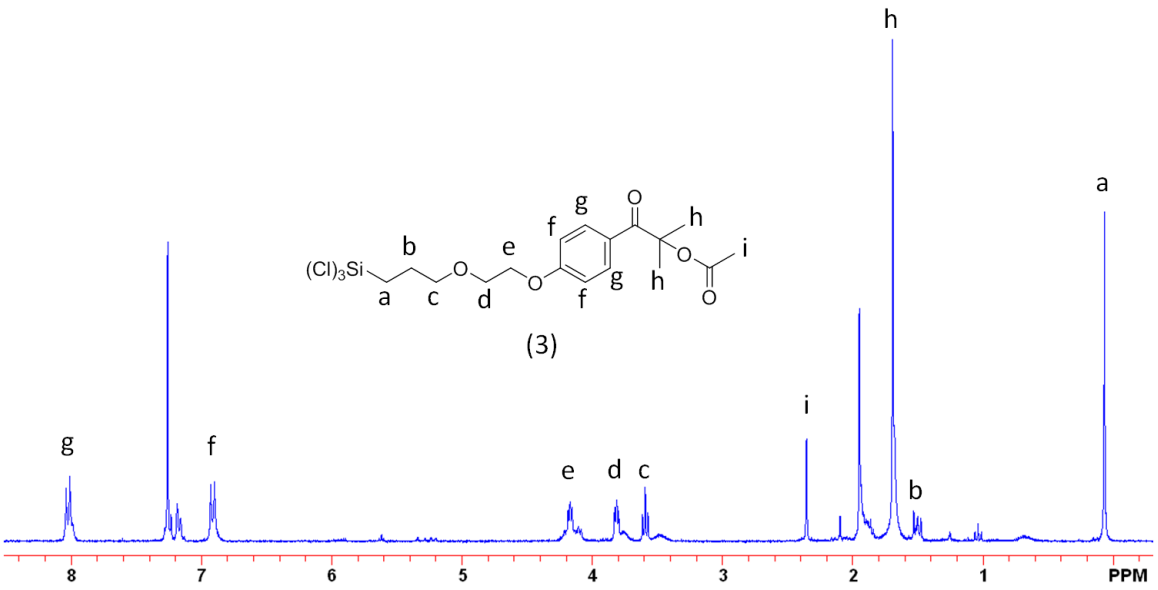

^{1}H-NMR spectrum of 2-hydroxy-4'-(2-hydroxyethoxy)-2-methyl propiophenone trichlorosilane (HPP-$SiCl_3$) (3).

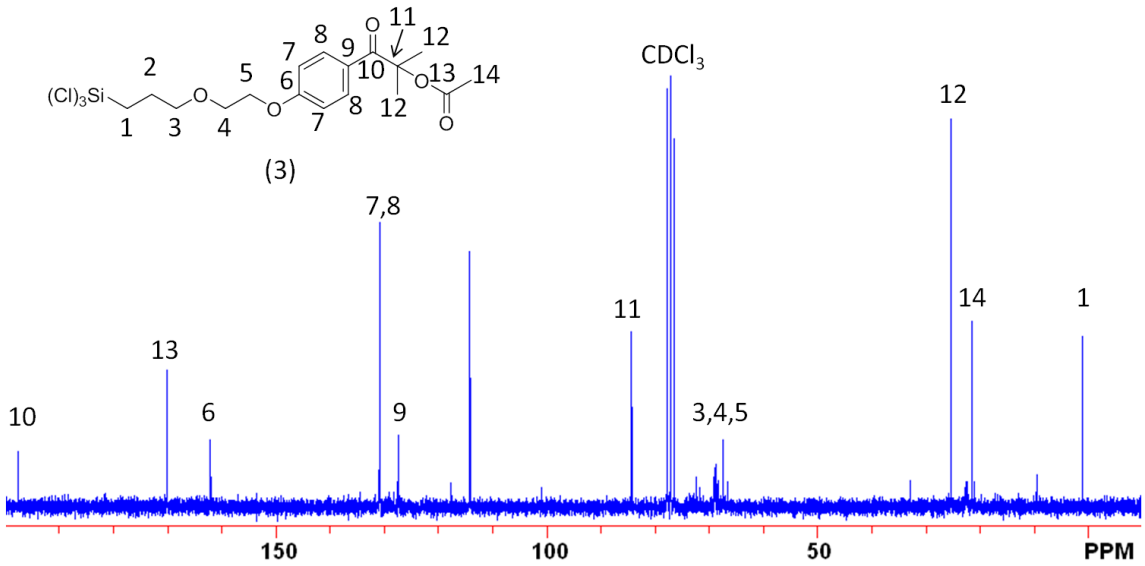

^{13}C-NMR spectrum of 2-hydroxy-4'-(2-hydroxyethoxy)-2-methyl propiophenone trichlorosilane (HPP-$SiCl_3$) (3).

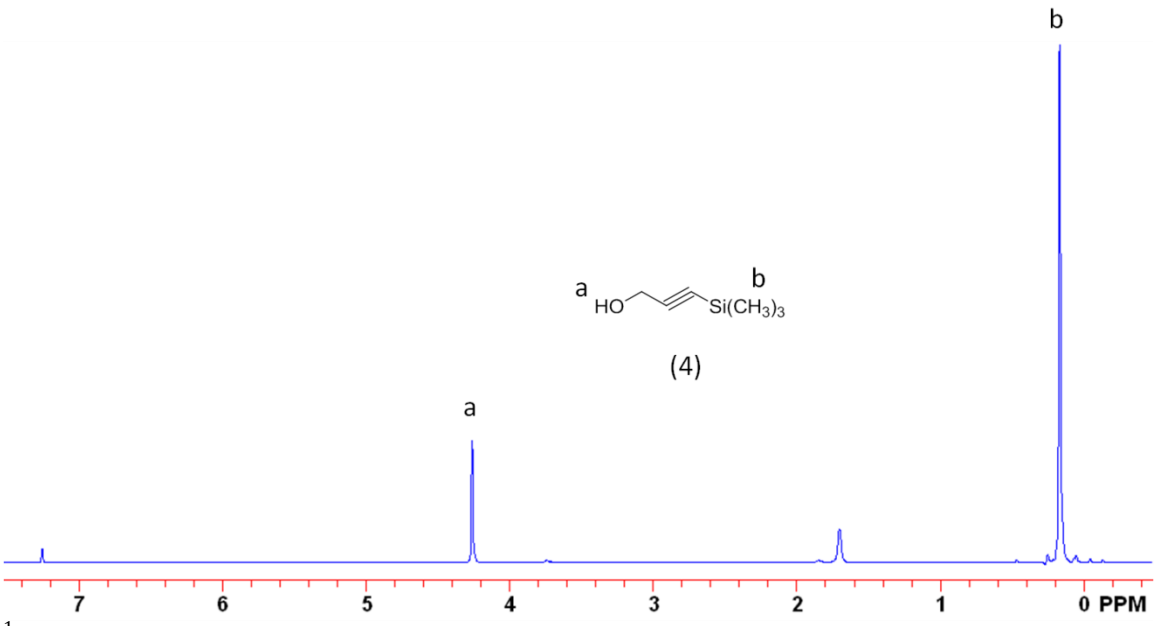

^{1}H-NMR spectrum of 3-Trimethylsilyl-2-propyn-1-ol (PgOH-TMS) (4).

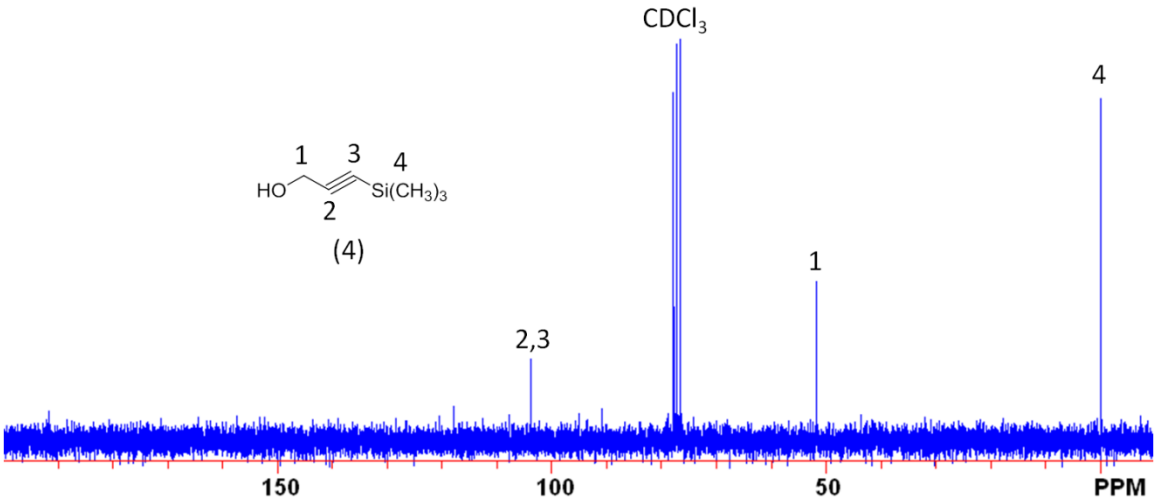

^{13}C-NMR spectrum of 3-Trimethylsilyl-2-propyn-1-ol (PgOH-TMS) (4).

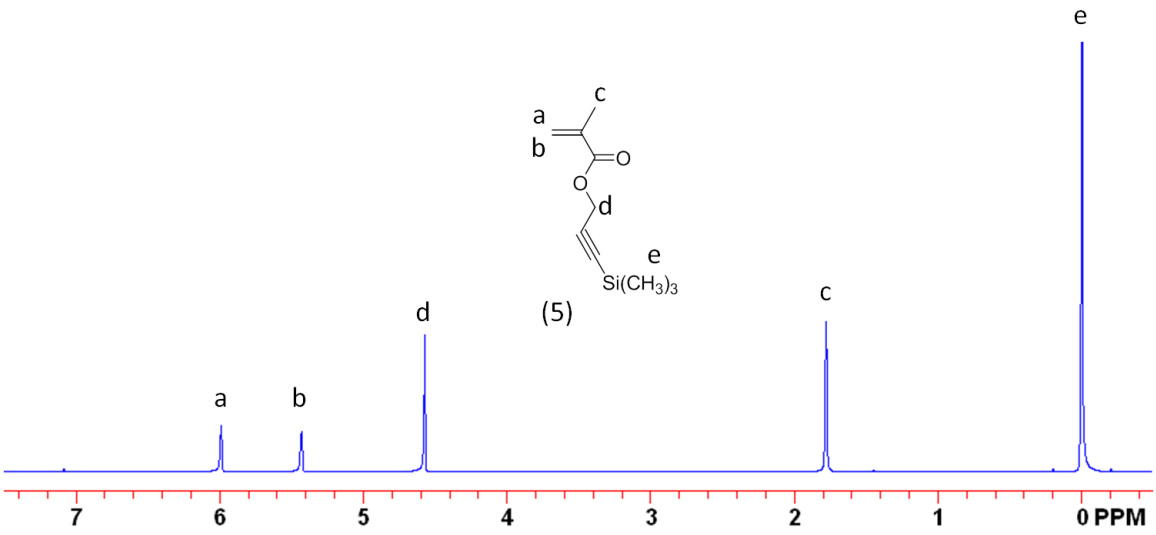

^{1}H-NMR spectrum of (3-trimethylsilylpropargyl) methacrylate (PgMA-TMS) (5).

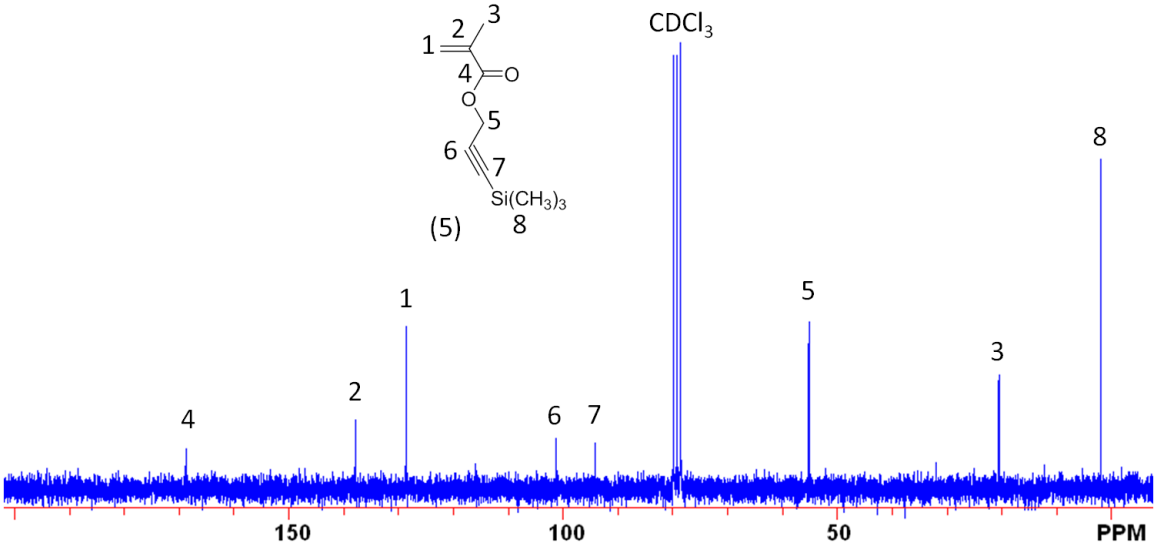

^{13}C-NMR spectrum of (3-trimethylsilylpropargyl) methacrylate (PgMA-TMS) (5).

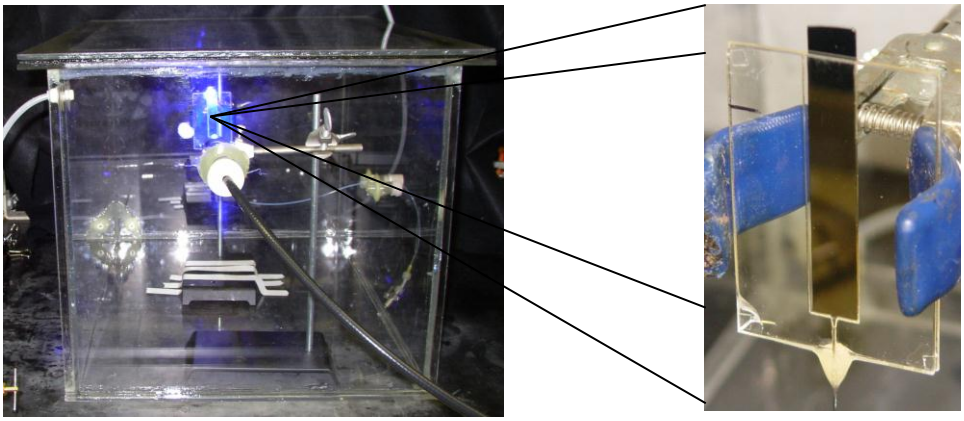

Acrylic box and microchannel setup.

IR Absorption Bands of "Functional" Polymer Brushes via Thiol-yne Reactions.[147] *Peak assignments are given here for*

Figure	Description	Absorption (cm^{-1})	Peak Assignment
4(a)	Deprotected p(PgMA) Brush	3283	C≡C-H
		2995, 2928, 2853	C-H
		2129	C≡C
		1738	C=O; ester
4(b)	3-mercaptopropionic acid	3320 – 3000	O-H (associated w/ COOH)
		2926	C-H
		1720	C=O; ester
4(c)	1-dodecanethiol	2955, 2922, 2853	C-H
		1728	C=O; ester
		1464	$(CH_2)_n$
4(d)	1-thioglycerol	3600 – 3000	O-H
		2922, 2880	C-H
		1724	C=O; ester
4(e)	N-acetyl-L-cysteine	3354	CO-NH
		2954, 2855	C-H
		1720	C=O; ester
		1618	$NHCOCH_3$
1(b)	Protected p(PgMA-$SiMe_3$) Brush	2995, 2961, 2900	C-H
		2185	C≡C
		1738	C=O; ester

(continued).

4(f)	Benzyl mercaptan	3061, 3028, 3000	=C-H
		2924, 2853	C-H
		1730	C=O; ester
		1601	C=C
4(g)	1-admantanethiol	2905, 2849	C-H
		1730	C=O; ester
4(h)	Thiocholesterol	2934, 2905, 2868, 2851	C-H
		1734	C=O; ester
4(i)	Mercaptopropylisobutyl POSS®	2953, 2926, 2907, 2870	C-H
		1732	C=O; ester
		1115	Si-O
6(a,b)	3-MPA sunlight/lab	3320 – 3000	O-H (associated w/ COOH)
		2926	C-H
		1720	C=O; ester

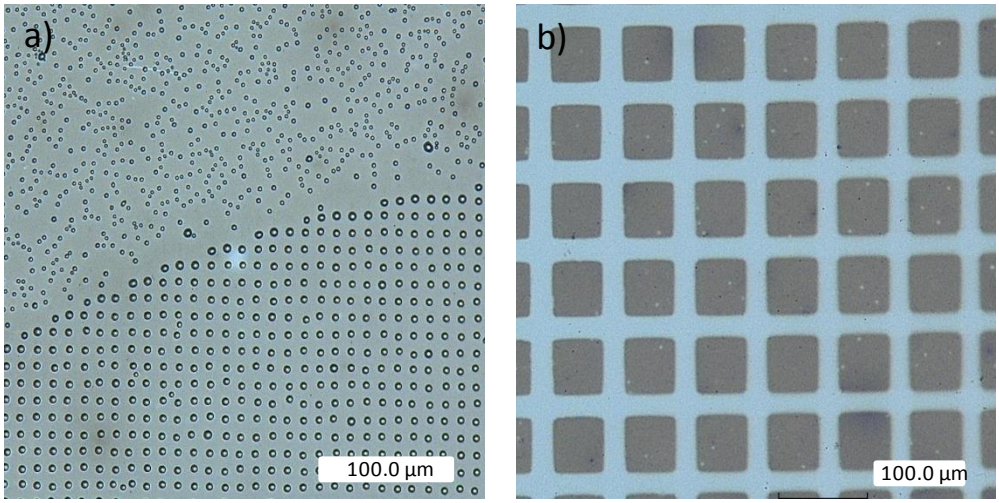

(a) Optical condensation images for 2000 mesh MPA squares/DDT bars. The patterned area creates a regular array of water droplets in contrast to the random droplets on the unpatterned area. (b) 300 mesh micropatterned DDT squares/"yne" bars. The image contrast is given by the difference in thickness of the DDT functionalized areas.

APPENDIX B

THIOL-ISOCYANATE "CLICK" REACTIONS: RAPID DEVELOPMENT OF FUNCTIONAL POLYMERIC SURFACES

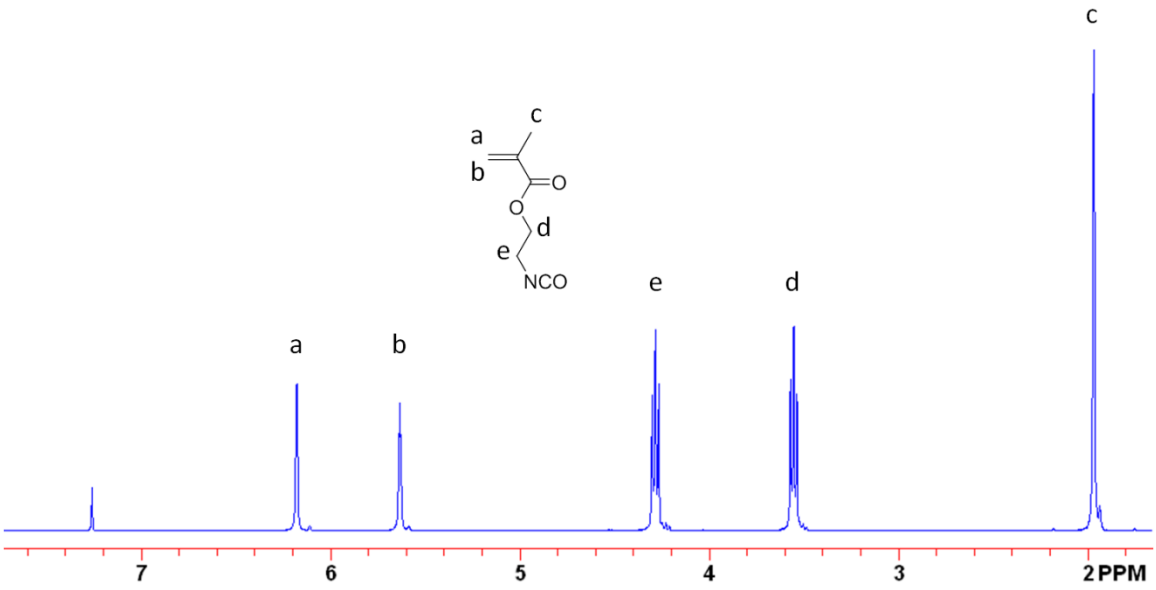

^{1}H-NMR spectrum of 2-Isocyanatoethyl methacrylate (NCOMA, (1).

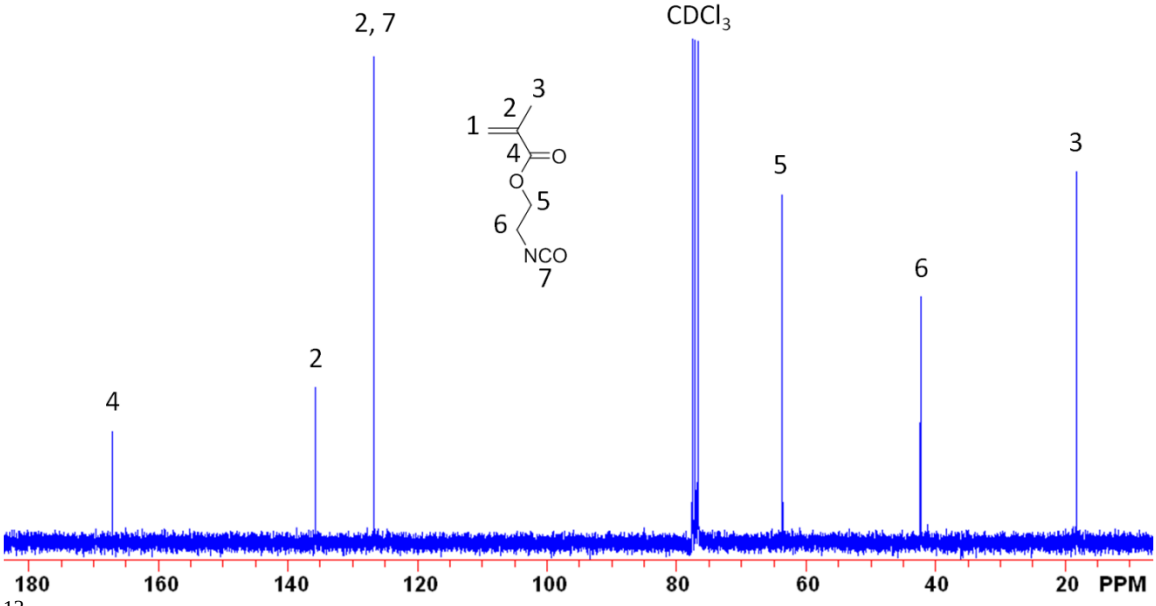

^{13}C-NMR spectrum of 2-Isocyanatoethyl methacrylate (NCOMA, (1)).

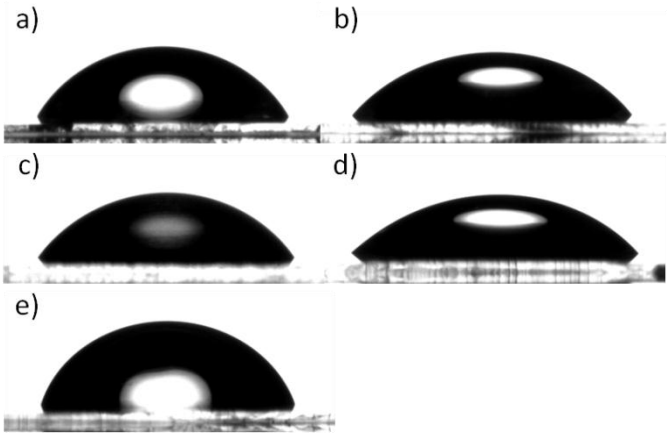

WCA: (a) Protected initiator (64.3° ± 3.5°), (b) Deprotected initiator (48.8° ± 2.2°), (c) Protonated MPA polymer brush (48.9° ± 2.1°), (d) Deprotonated MPA polymer brush (29.4° ± 1.7°), (e) Acridine orange functionalized polymer brush (73.8° ± 3.5°).

IR Absorption Bands of "Functional" Polymer Brushes via Thiol-isocyanate Reactions.[162] *Peak assignments provided:*

Figure	Description	Absorption (cm^{-1})	Peak Assignment
8a)	p(isocyanatoethyl methacrylate) Brush	2275	N=C=O
		1729	C=O; ester
8b)	3-mercaptopropionic acid	3430 - 3174	NH-CO
		3430 - 3174	O-H (associated w/ COOH)
		2930	C-H
		1725	C=O; ester
		1650	NH-CO-S
		1528	NH-CO (amide band II)
8c)	1-dodecanethiol	3442 - 3215	NH-CO
		2954, 2924, 2852	C-H
		1731	C=O; ester
		1653	NH-CO-S
		1516	NH-CO (amide band II)
		1463	(CH_2)=
8d)	1-thioglycerol	3573 - 3125	O-H
		3573 - 3125	NH-CO
		2930, 2882	C-H
		1725	C=O; ester
		1650	NH-CO-S
		1528	NH-CO (amide band II)

(continued).

8e)	N-acetyl-L-cysteine	3450 - 3162	NH-CO
		3450 - 3162	NH-CO-CH_3
		2989, 2942	C-H
		1725	C=O; ester
		1654	NH-CO-S
		1531	NH-CO (amide band II)
8f)	benzylmercaptan	3326	NH-CO
		3084, 3058, 3025	=C-H
		2942, 2859	C-H
		1725	C=O/ ester
		1657	NH-CO-S
		1517, 1493, 1451	C=C
8g)	1-admantanethiol	3350	NH-CO
		2906, 2850	C-H
		1731	C=O; ester
		1669	NH-CO-S
8h)	Thiocholesterol	3350	NH-CO
		2936, 2903, 2865, 2850	C-H
		1728	C=O;ester
		1671	NH-CO-S
		1556	NH-CO (amide band II)
8i)	Mercaptopropylisobutyl POSS®	3347	NH-CO
		2954, 2927, 2905, 2870	C-H
		1731	C=O; ester
		1665	NH-CO-S
		1109	Si-O

(continued).

8j)	Furfurylmercaptan	3326	NH-CO
		2987, 2939	C-H
		1728	C=O; ester
		1663	NH-CO-S
		1523	NH-CO (amide band II)
		1204, 1156	C-O (cyclic ether)
		1068	C-O-C (cyclic ethers: 5 membered ring
8k)	Hexyl amine	3344	NH-CO
		2954, 2980, 2856	C-H
		1731	C=O; ester
		1573	NH-CO-NH
		1460	$(CH_2)_n$
8l)	Benzyl amine	3353	NH-CO
		3085, 3061, 3025	=C-H
		2983, 2868	C-H
		1728	C=O; ester
		1567	NH-CO-NH
		1565, 1493, 1451	C=C

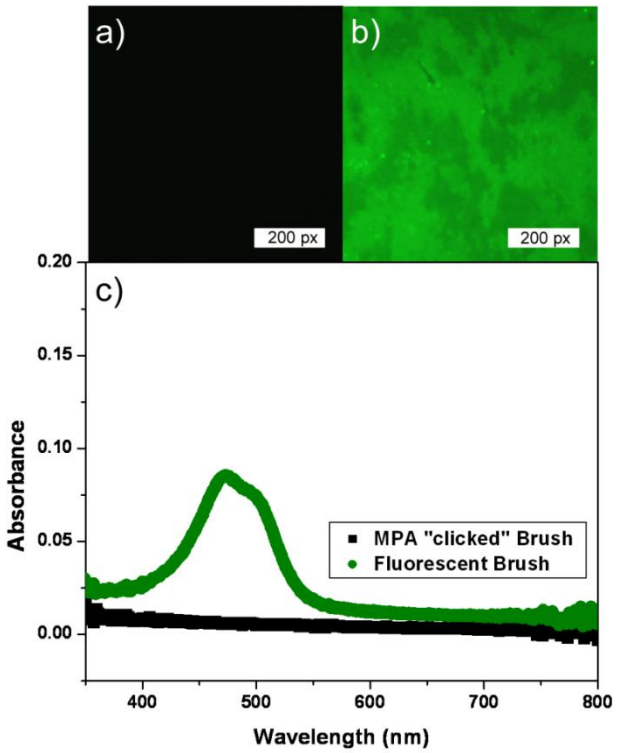

(a) Fluorescence microscopy before functionalization with fluorescent dye (b) Fluorescence microscopy after functionalization with fluorescent dye (c) UV-Vis spectroscopy of "MPA" clicked polymer brush vs. polymer brush after functionalization with fluorescent dye.

APPENDIX C

SYNTHESIS OF MULTIFUNCTIONAL POLYMER BRUSH SURFACES VIA SEQUENTIAL AND ORTHOGONAL THIOL-CLICK REACTIONS

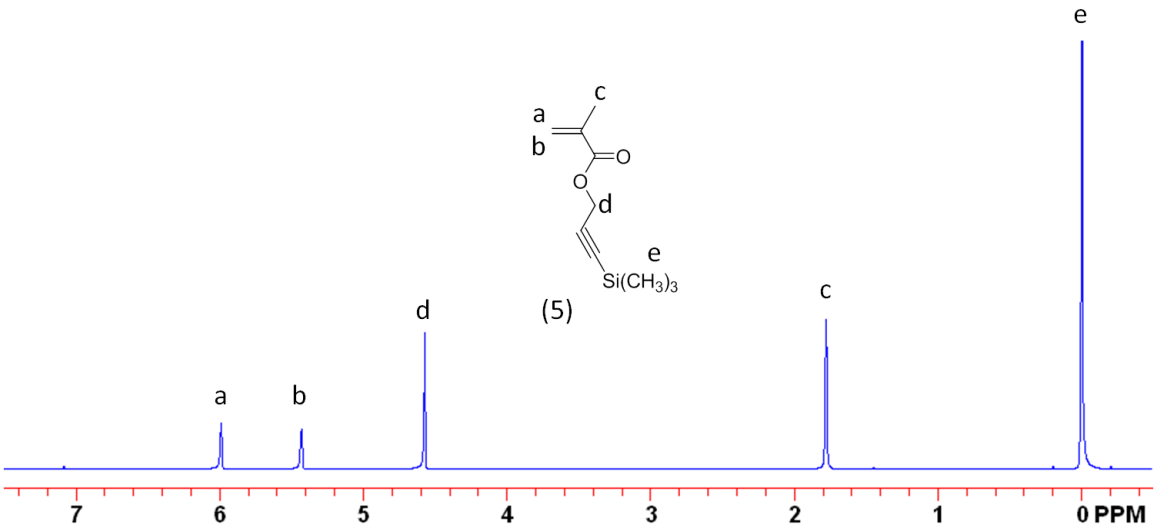

^{1}H-NMR spectrum of (3-trimethylsilylpropargyl) methacrylate (PgMA-TMS).

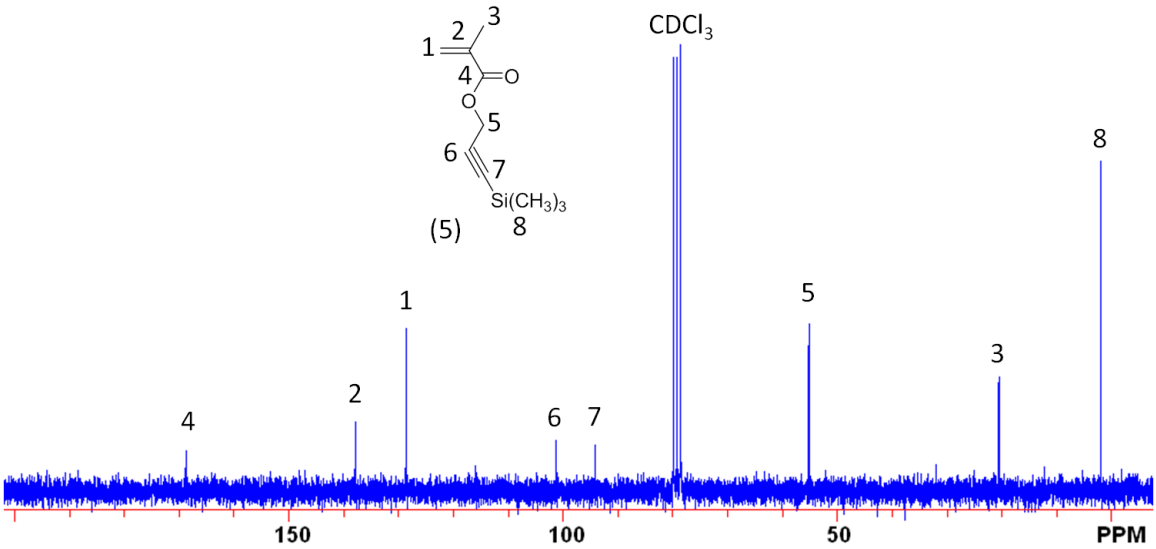

^{13}C-NMR spectrum of (3-trimethylsilylpropargyl) methacrylate (PgMA-TMS).

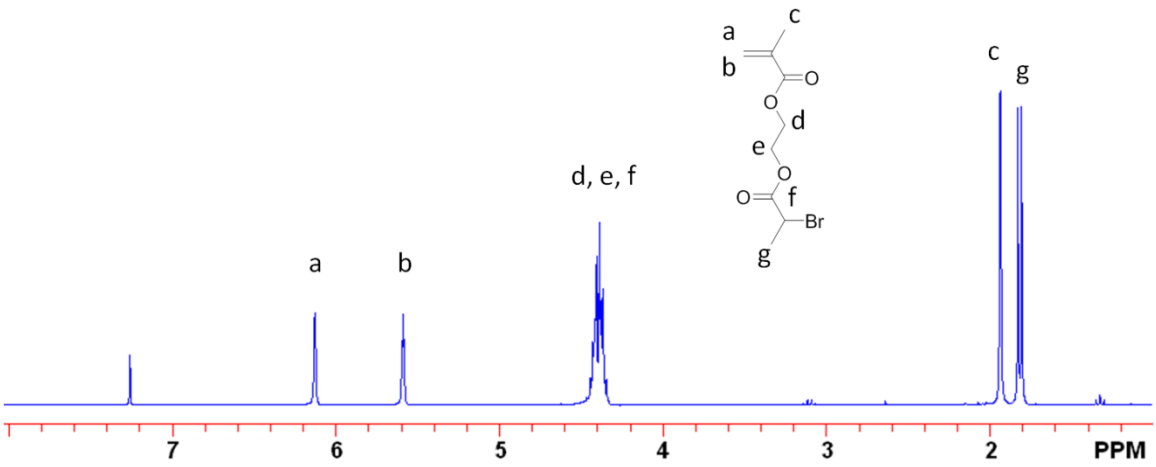

^{1}H-NMR spectrum of 2-(2-bromopropanoyloxy) ethyl methacrylate (BrMA).

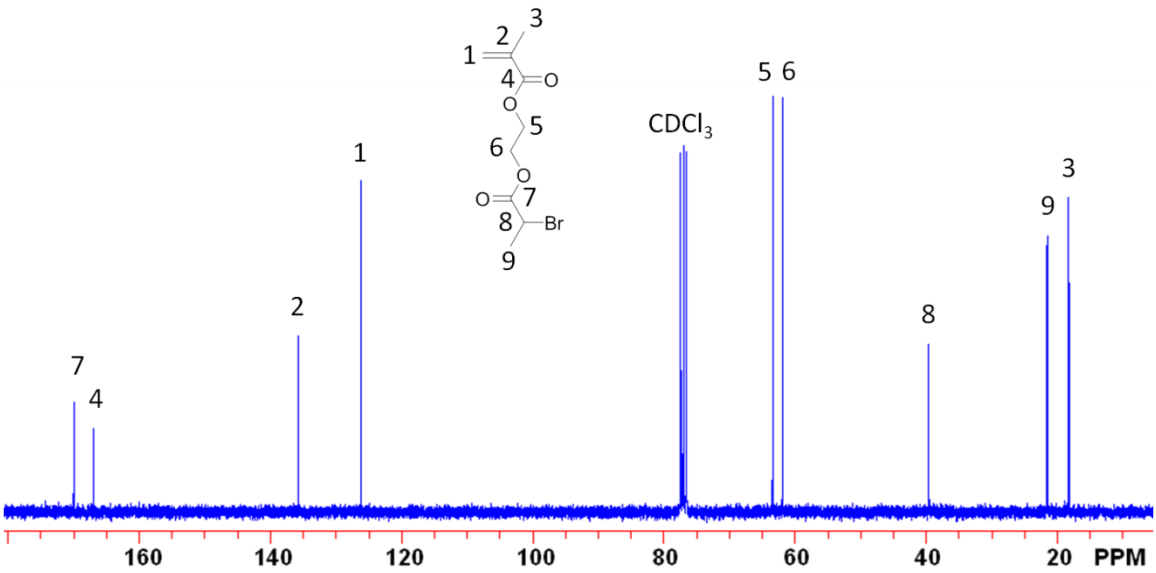

^{13}C-NMR spectrum of 2-(2-bromopropanoyloxy) ethyl methacrylate (BrMA).

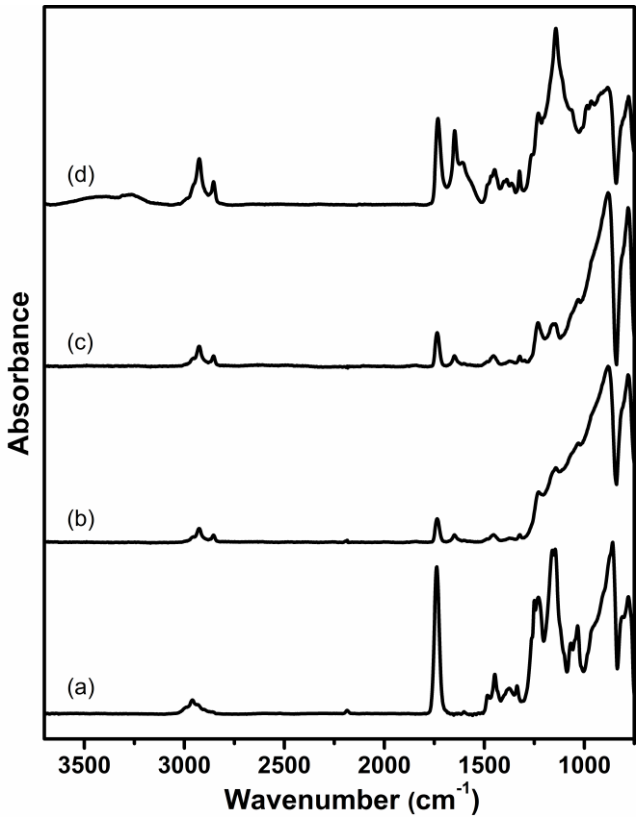

GATR-FTIR spectrum for p(BrMA-stat-PgMA) (a) synthesized by SIP of 1:1 v/v BrMA:PgMA; (b) after thiol-bromo click with dodecanethiol; (c) after deprotection using AgOTf; and (d) after thiol-yne click with N-acetyl cysteine.

APPENDIX D

CONTROLLED HETEROGENEITY WITHOUT CONTROLLED POLYMERIZATION: ENGINEERING TAPERED BLOCK COPOLYMER BRUSHES VIA POST-POLYMERIZATION MODIFICATION

Experimental and Theoretical Scattering Length Density values

Scattering Length Density (SLD) values

Layer	Experimental SLD ($Å^{-2}$)	Theoretical SLD ($Å^{-2}$)
bulk Si	$2.07x10^{-6}$	$2.07x10^{-6}$
SiO_x	$3.20x10^{-6}$	$3.14x10^{-6}$
Initiator	$8.89x10^{-7}$	$8.89x10^{-7}$
p(NCO) unmodified	$1.87x10^{-6}$	$1.54x10^{-6}$
p(NCO) mod d_{25}-DDT	$4.60x10^{-6}$	$4.49x10^{-6}$
p(NCO) mod d_7-PPT	$3.07x10^{-6}$	$2.66x10^{-6}$
hydrated p(NCO)	$9.50x10^{-7}$	$9.56x10^{-7}$

RMS Roughness Measurements

Roughness Measurements

Layer	RMS Roughness (nm)
unmodified p(NCO)	1.6 ± 0.2
modified p(NCO)-d_7-PPT	2.8 ± 0.4
modified p(NCO)-d_7-PPT	1.1± 0.2
modified p(NCO)-d_{25}-DDT	1.0 ± 0.2

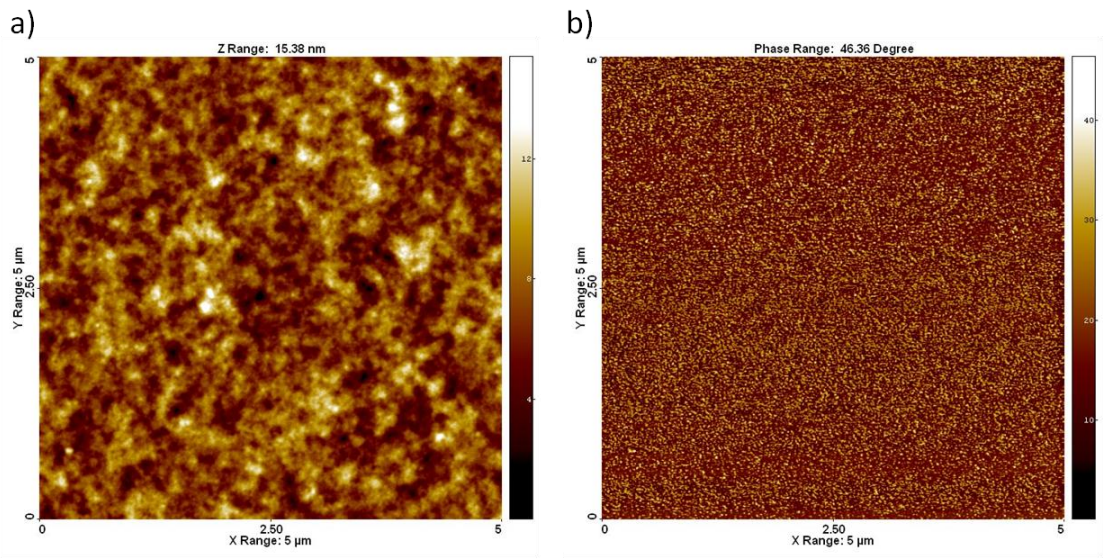

AFM images of unmodified p(NCO): a) height and b) phase.

APPENDIX E

PHOTOCAGED PENDENT THIOL POLYMER BRUSH SURFACES FOR POST-POLYMERIZATION MODIFICATIONS VIA THIOL-CLICK CHEMISTRY

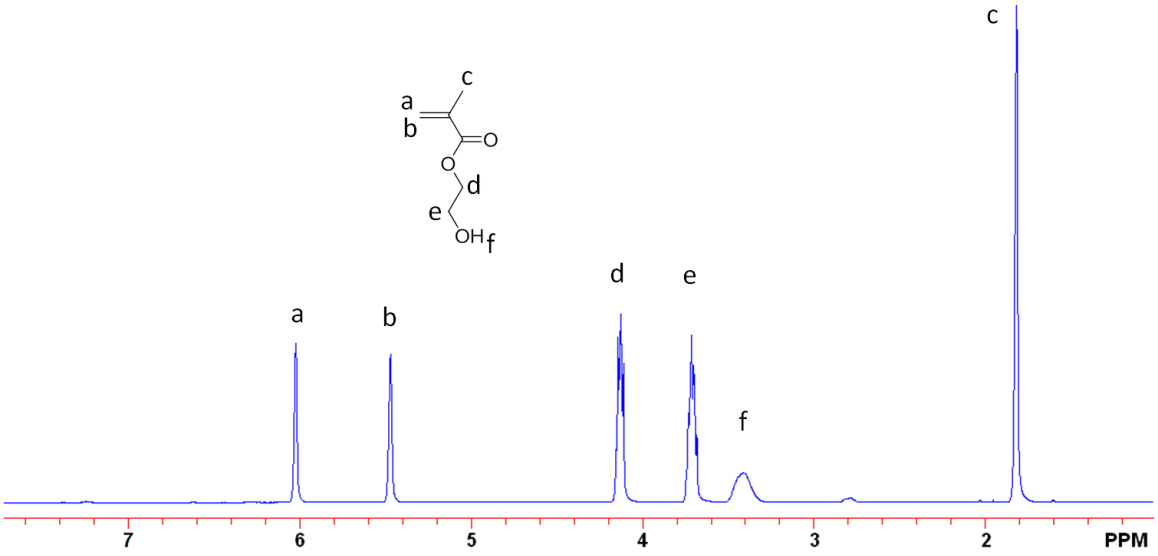

^{1}H NMR spectrum of 2-hydroxyethyl methacrylate (HEMA).

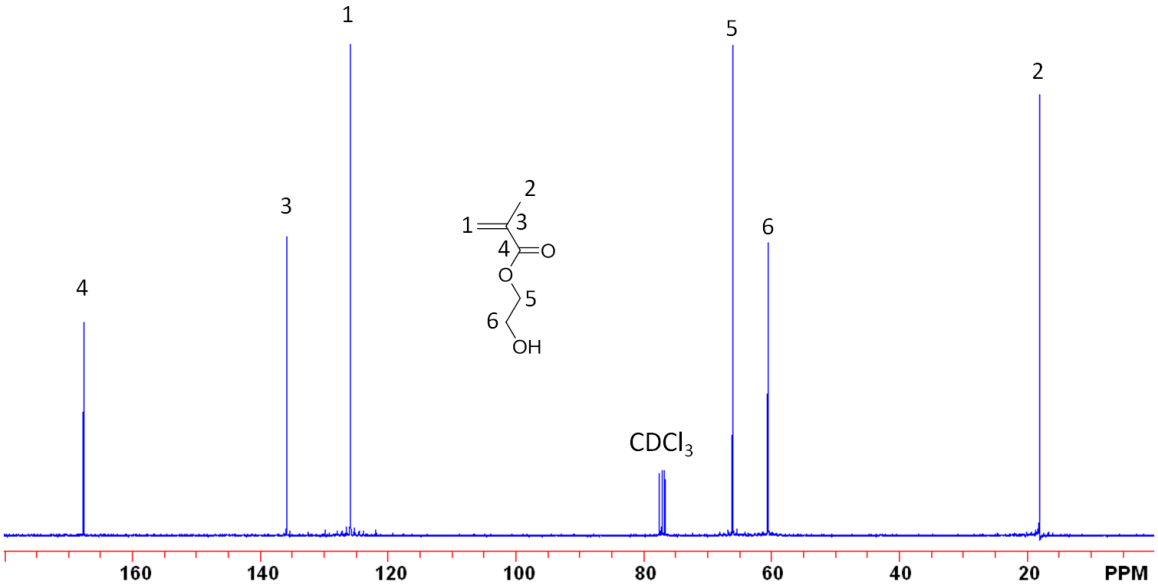

^{13}C NMR spectrum of 2-hydroxyethyl methacrylate (HEMA).

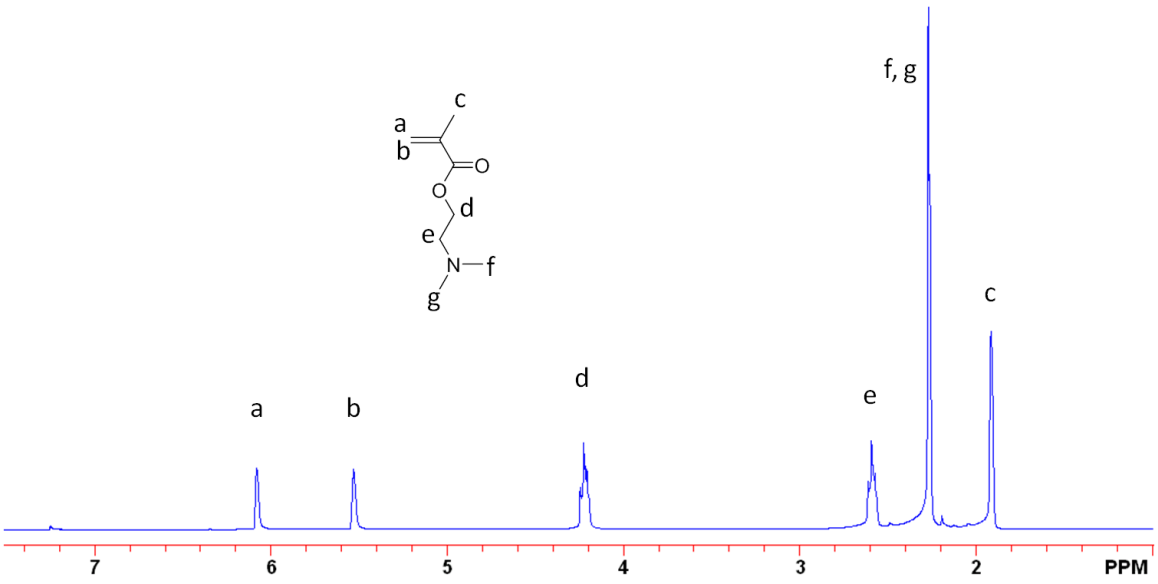

^{1}H NMR spectrum of 2-(dimethylamino)ethyl methacrylate (DMAEMA).

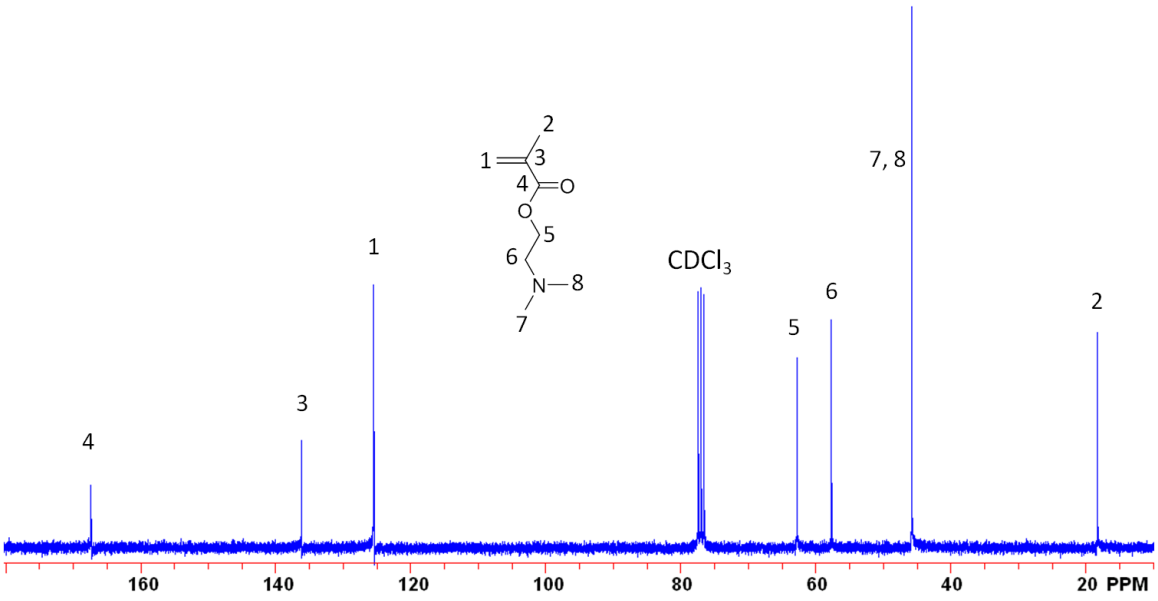

^{13}C NMR spectrum of 2-(dimethylamino)ethyl methacrylate (DMAEMA).

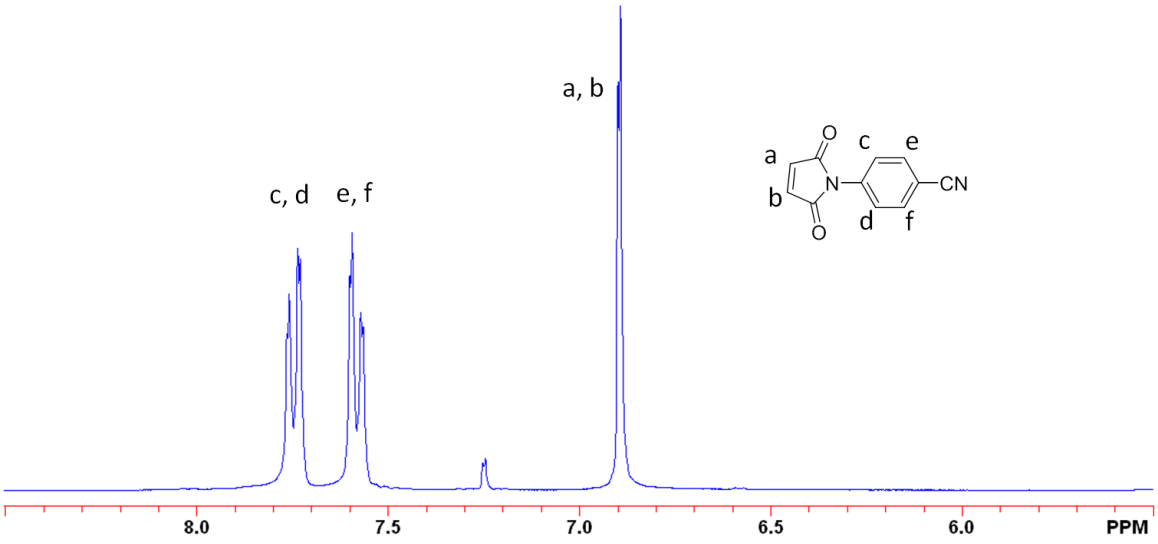

^{1}H NMR spectrum of 4-(2,5-dioxo-2,5-dihydro-1H-pyrrol-1-yl)benzonitrile (cyanophenyl maleimide).

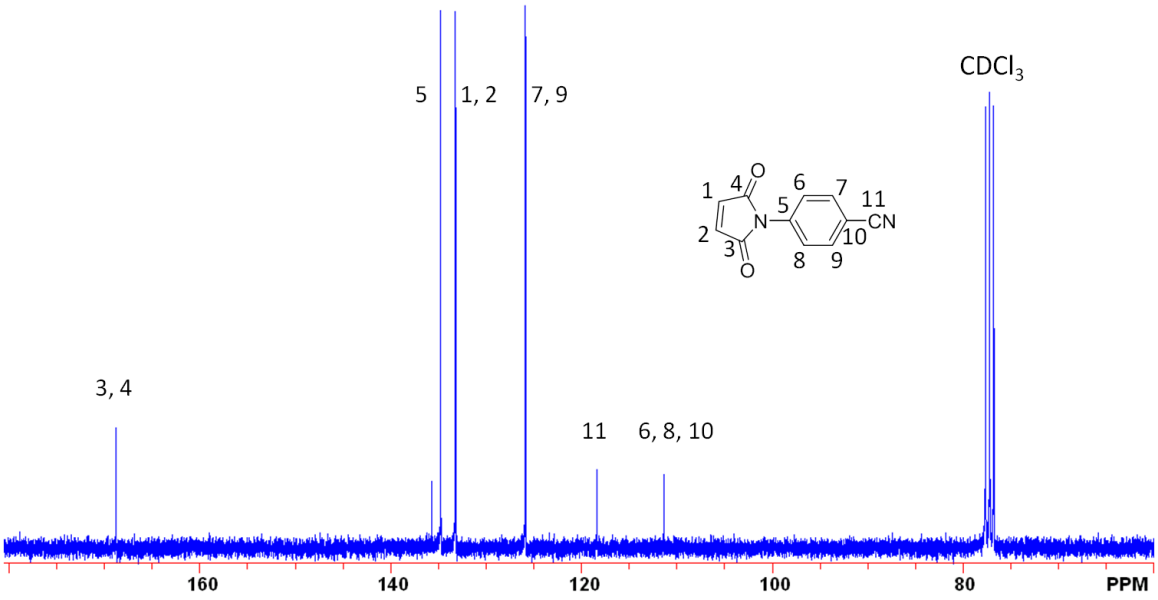

^{13}C NMR spectrum of 4-(2,5-dioxo-2,5-dihydro-1H-pyrrol-1-yl)benzonitrile (cyanophenyl maleimide).

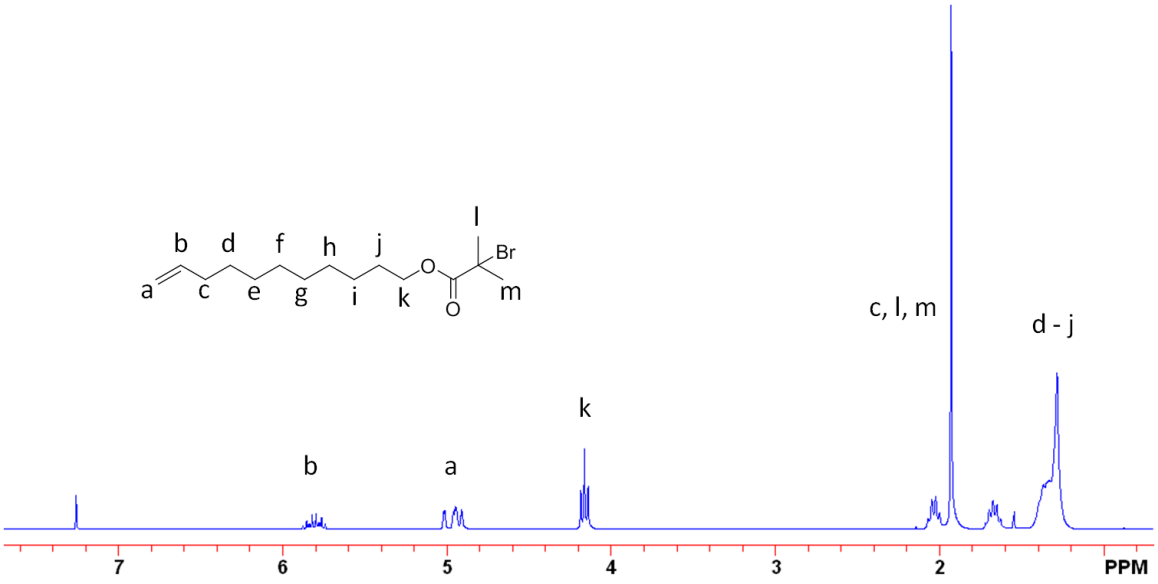

^{1}H NMR spectrum of 10-undecen-1-yl 2-bromo-2-methylpropionate (ATRP initiator precursor).

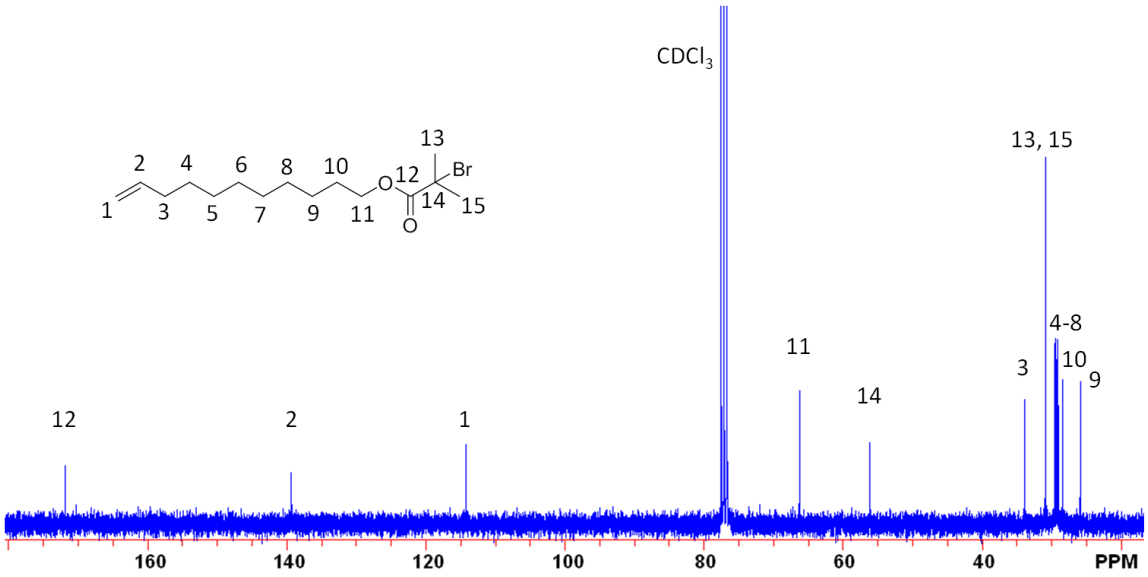

^{13}C NMR spectrum of 10-undecen-1-yl 2-bromo-2-methylpropionate (ATRP initiator precursor).

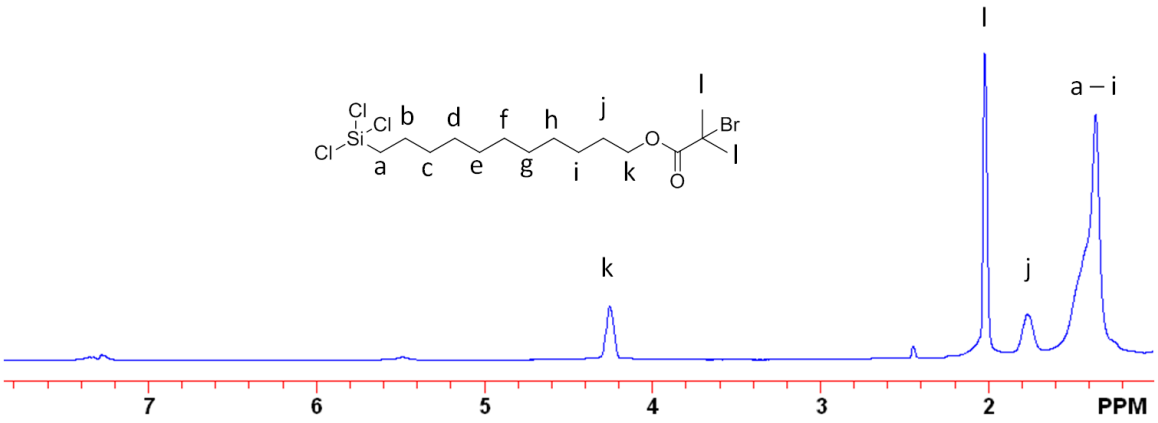

^{1}H NMR spectrum of 11-(2-bromo-2-methyl)propionyloxy)undecyl trichlorosilane (ATRP initiator-tricholorsilane).

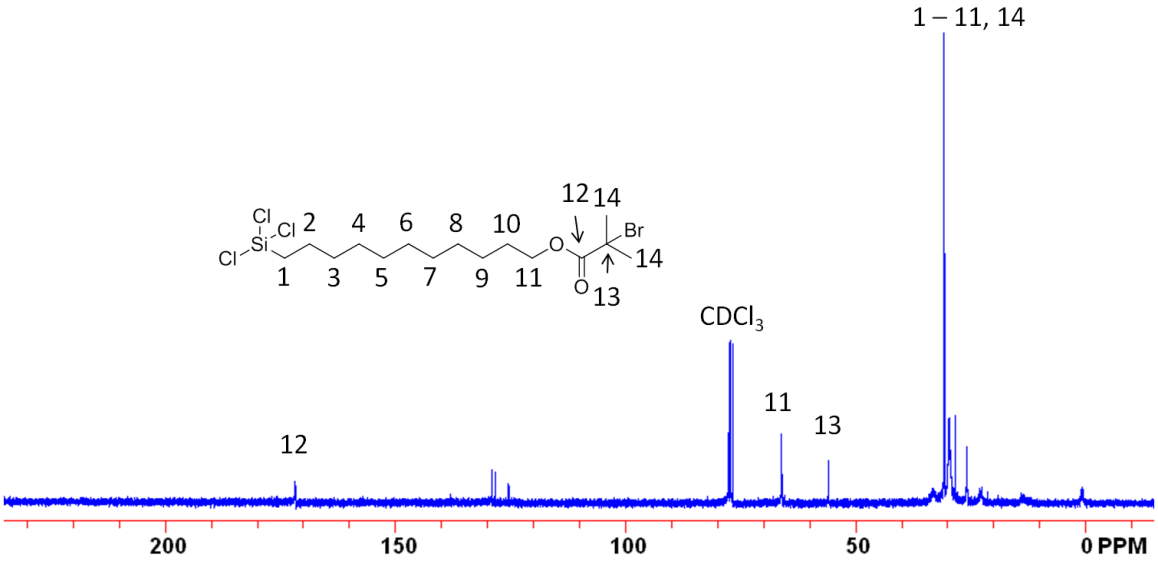

^{13}C NMR spectrum of 11-(2-bromo-2-methyl)propionyloxy)undecyl trichlorosilane (ATRP initiator-tricholorsilane).

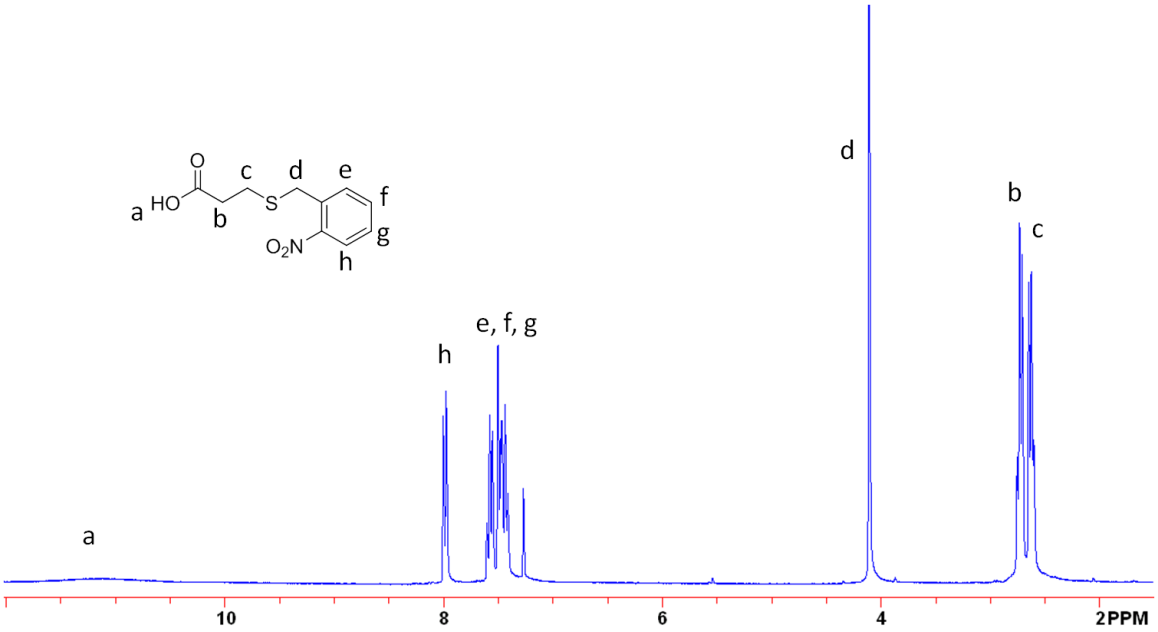

^{1}H NMR spectrum of 3-(2-nitrobenzylthio)propanoic acid.

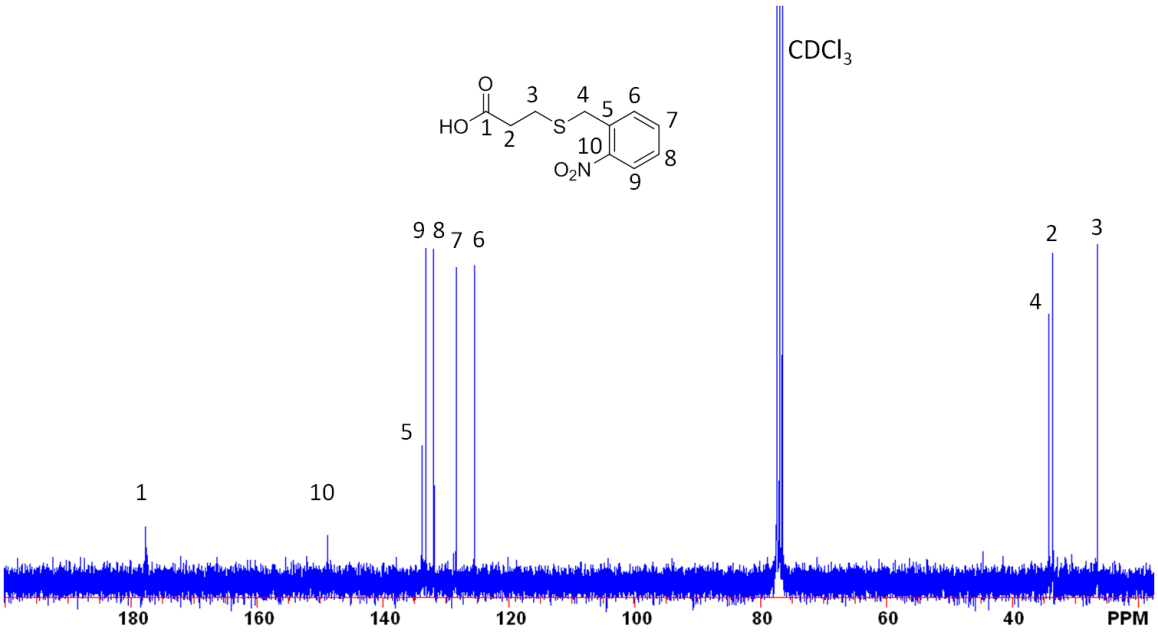

^{13}C NMR spectrum of 3-(2-nitrobenzylthio)propanoic acid.

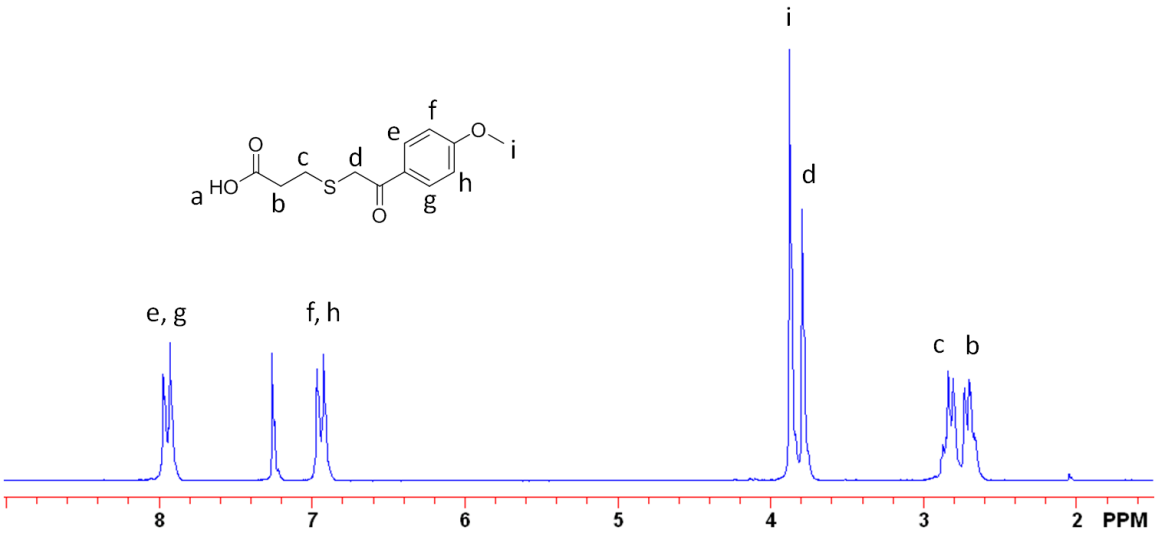

^{1}H NMR spectrum of 3-(2-(4-methoxyphenyl)-2-oxoethylthio)propanoic acid.

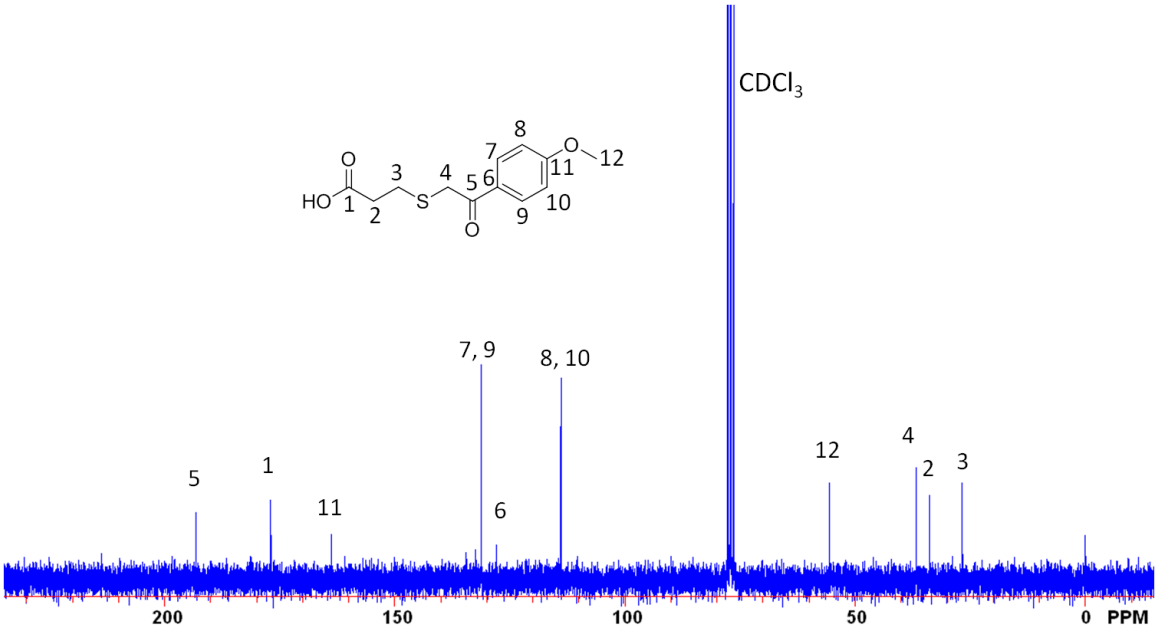

^{13}C NMR spectrum of 3-(2-(4-methoxyphenyl)-2-oxoethylthio)propanoic acid.

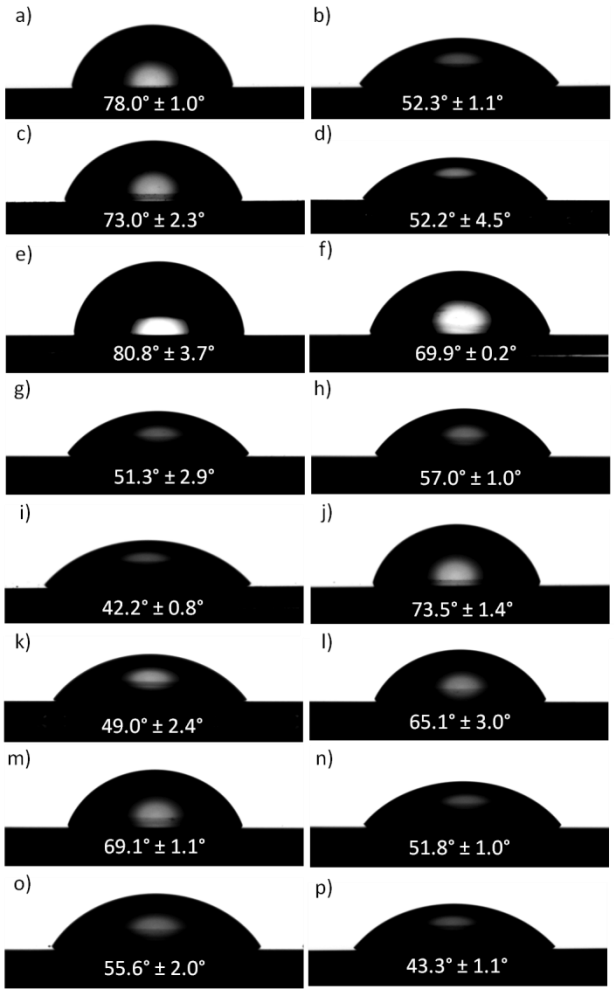

Static water contact angle measurements (WCA) for a) ATRP initiator functionalized substrate, b) HEMA polymer brush, c) photolabile *o*-NB pendent thiol modified HEMA polymer brush, d) deprotected HEMA pendent thiol polymer brush, after thiol-NCO reaction with e) 2-nitrophenyl isocyanate, f) dodecyl isocyanate, g) furfuryl isocyanate, h) admantyl isocyanate, and i) after thiol-maleimide reaction with cyanophenyl maleimide, j) photolabile *p*-MP pendent thiol modified HEMA polymer brush, k) deprotected HEMA pendent thiol polymer brush, after thiol-NCO reaction with l) 4-methoxybenzyl isocyanate, m) dodecyl isocyanate, n) furfuryl NCO, o) admantyl isocyanate, and p) after thiol-maleimide reaction with cyanophenyl maleimide.

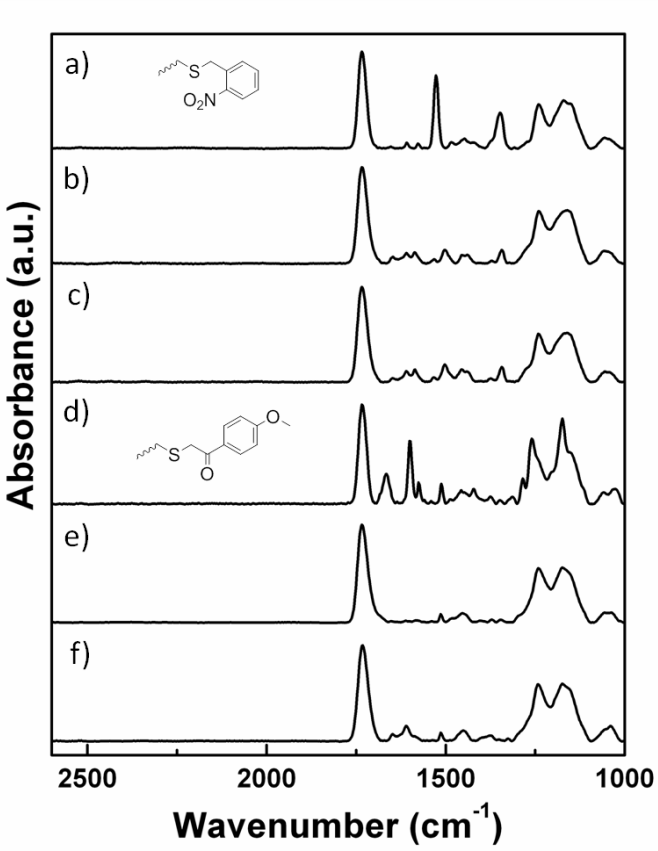

GATR-FTIR spectra of *o*-NB and *p*-MP protected pendent thiol polymer brushes followed by one-pot deprotection (UV light irradiation: 365 nm, ~70 mW/cm^2, 2 h) in anhydrous DCM and thiol-isocyanate click reactions with either 2-nitrophenyl isocyanate (**3**) or 4-methoxybenzyl isocyanate (**4**) (0.1 M) in the presence of DBU (0.3 mol% in respect to isocyanate): a) *o*-NB protected pendent thiol polymer brush, b) deprotected with DMPP and clicked with 2-nitrophenyl isocyanate, c) deprotected without DMPP and clicked with 2-nitrophenyl isocyanate, d) *p*-MP protected pendent thiol polymer brush, e) deprotected with DMPP and clicked with 4-methoxybenzyl isocyanate, and f) deprotected without DMPP and clicked with 4-methoxybenzyl isocyanate.

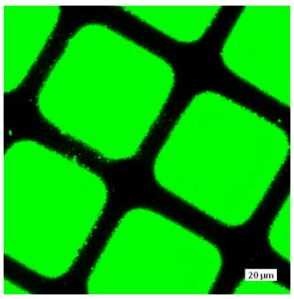

Fluorescence microscopy images of polymer brushes patterned only with fluorescein isothiocyanate (squares) at a magnification of 10x with a 433 nm laser.

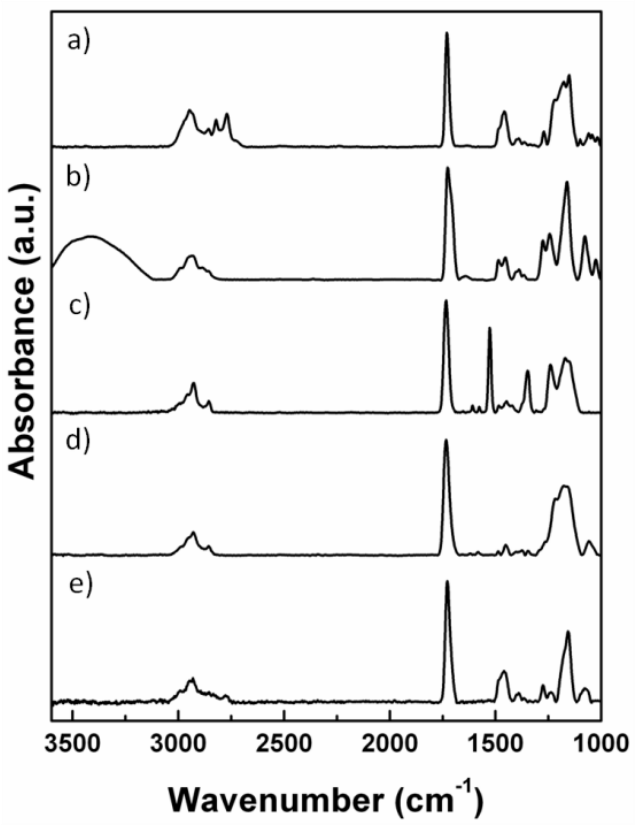

GATR-FTIR spectra for a) DMAEMA polymer brush (aliphatic amine -N-C-H- stretching vibration, 2820 cm^{-1} and 2770 cm^{-1}, C-N stretching vibration 1270 cm^{-1}), b) HEMA polymer brush (O-H stretching vibration, 3650 – 3200 cm^{-1}, primary saturated alcohols -C-C-O- 1090 – 1000 cm^{-1}), c) photolabile o-nitrobenzyl pendent thiol modified HEMA polymer brush (disappearance of O-H stretching vibration, 3650 – 3200 cm^{-1}, primary saturated alcohols -C-C-O- 1090 – 1000 cm^{-1}, appearance of NO_2 asymmetric and symmetric stretching vibrations: 1527 cm^{-1} and 1350 cm^{-1} respectively), d) HEMA pendent thiol polymer brush clicked with dodecyl isocyanate (C-H stretching vibrations 2989, 2930, 2860 cm^{-1}, $-(CH_2)_n-$ 1470 cm^{-1}), e) HEMA-b-DMAEMA polymer brush (primary saturated alcohols -C-C-O- 1090 – 1000 cm^{-1}, Aliphatic amine -N-C-H- stretching vibration, 2820 cm^{-1} and 2770 cm^{-1}, C-N stretching vibration 1270 cm^{-1}).

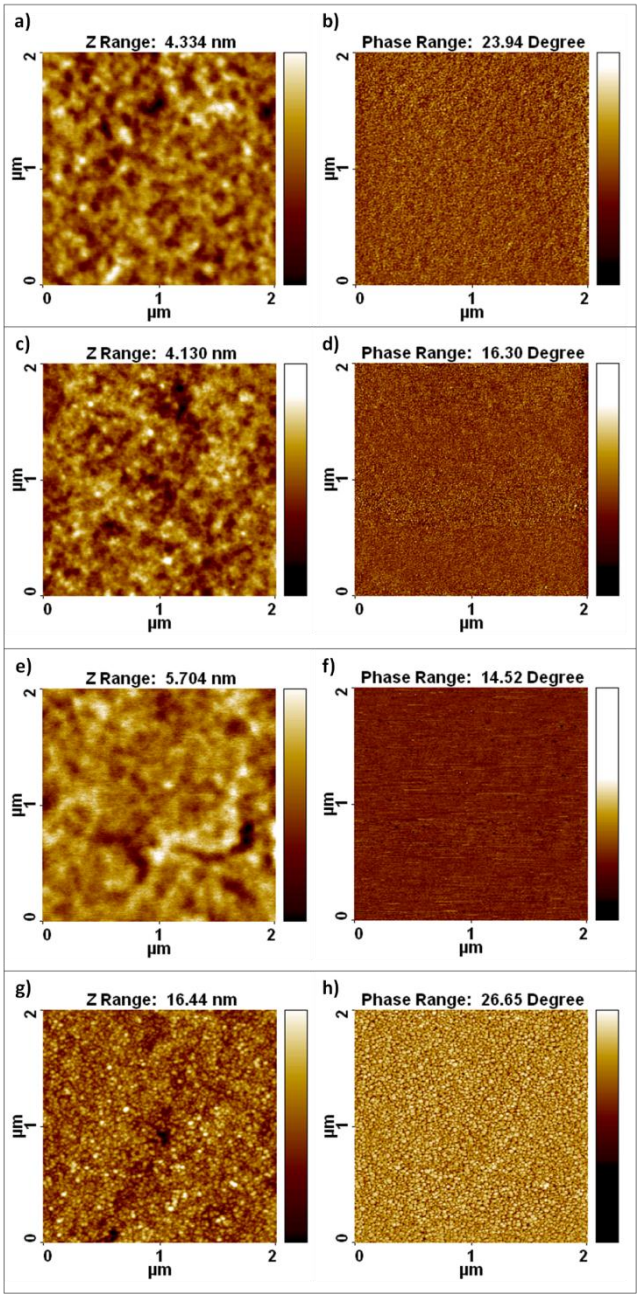

Tapping mode AFM images (height/phase) of: DMAEMA polymer brush (a-b), HEMA polymer brush (c-d), photolabile *o*-NB pendent thiol modified HEMA polymer brush (e-f), HEMA pendent thiol polymer brush clicked with dodecyl isocyanate (g-h).

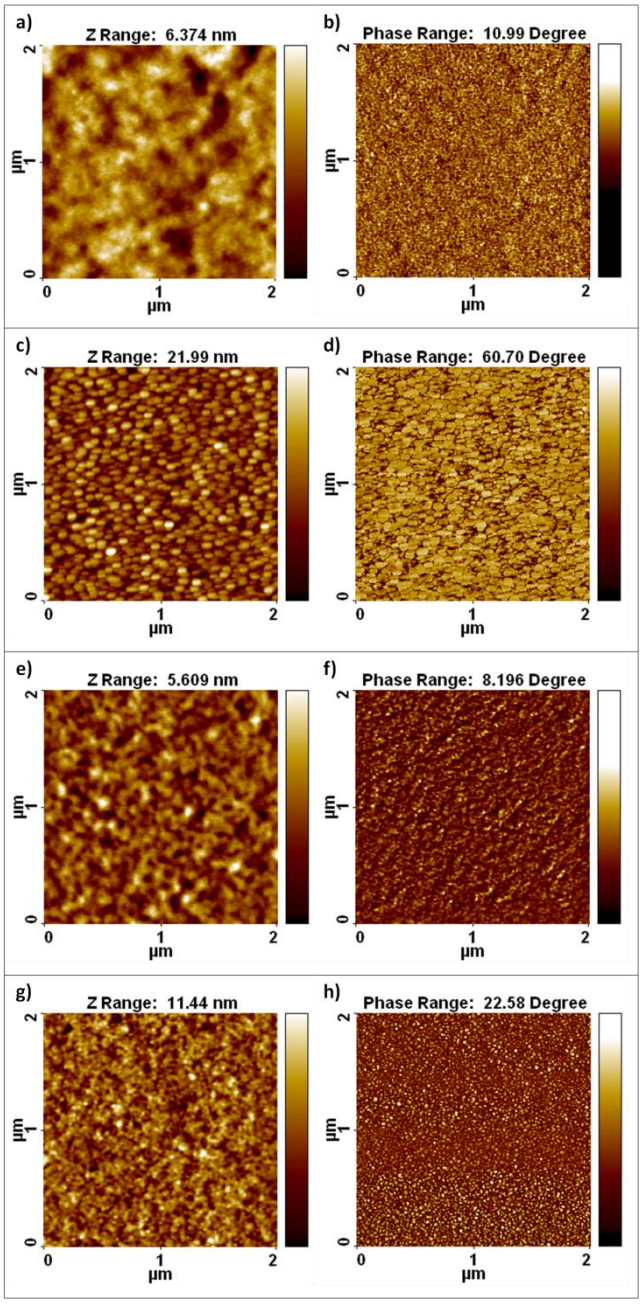

Tapping mode AFM images (height/phase) of unprotonated block copolymers: photolabile *o*-NB pendent thiol modified HEMA-b-DMAEMA polymer brush (a-b), HEMA pendent thiol-b-DMAEMA polymer brush clicked with dodecyl isocyanate (c-d), DMAEMA-b-photolabile *o*-NB pendent thiol modified HEMA polymer brush (e-f), DMAEMA-b-HEMA pendent thiol polymer brush clicked with dodecyl isocyanate (g-h).

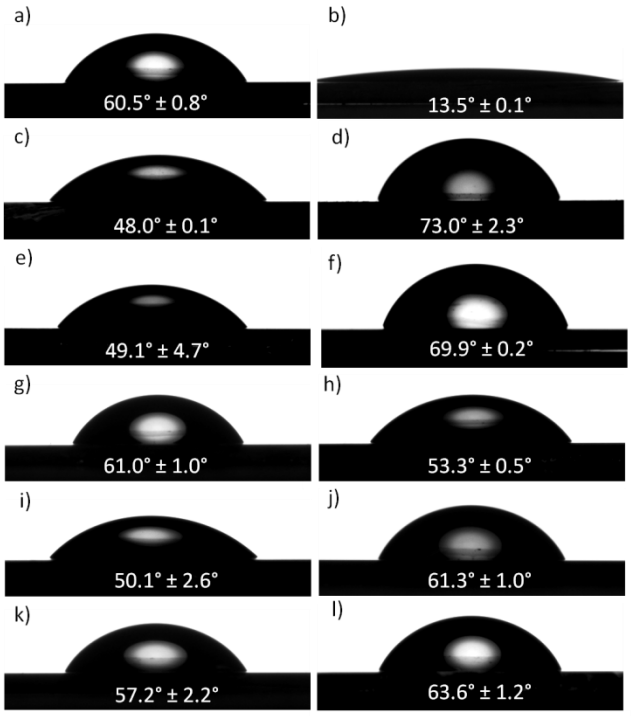

Static water contact angle measurements (WCA) for a) DMAEMA polymer brush (unprotonated), b) DMAEMA polymer brush (protonated), c) HEMA polymer brush, d) photolabile *o*-NB pendent thiol modified HEMA polymer brush, e) HEMA pendent thiol polymer brush after photolytic *o*-NB cleavage, f) HEMA pendent thiol polymer brush clicked with dodecyl isocyanate, g) HEMA-b-DMAEMA polymer brush (unprotonated), h) HEMA-b-DMAEMA polymer brush (protonated), i) photolabile *o*-NB pendent thiol modified HEMA-b-DMAEMA polymer brush (protonated), j) HEMA pendent thiol-b-DMAEMA polymer brush clicked with dodecyl isocyanate (protonated), k) DMAEMA-b-photolabile *o*-NB pendent thiol modified HEMA polymer brush (protonated), l) DMAEMA-b-HEMA pendent thiol polymer brush clicked with dodecyl isocyanate (protonated).

Polymer Brush Thickness Measurements (Units are in nanometers (nm))

	Ellipsometry Measurements (nm)		
reagents	pHEMA	protected	deprotect and thiol-click
o-NB pendent thiol polymer brush			
2-nitrophenyl isocyanate	9.1 ± 0.1	21.4 ± 0.2	24.2 ± 0.1
furfuryl isocyanate	9.2 ± 0.1	21.5 ± 0.1	20.1 ± 0.2
dodecyl isocyanate	9.7 ± 0.2	23.6 ± 0.5	24.7 ± 0.9
1-adamantyl isocyanate	9.7 ± 0.2	23.0 ± 0.3	21.5 ± 0.4
cyanophenyl maleimide	9.2 ± 0.1	21.5 ± 0.2	22.9 ± 0.5
p-MP pendent thiol polymer brush			
4-methoxybenzyl isocyanate	11.9 ± 0.1	19.1 ± 0.8	24.1 ± 0.2
furfuryl isocyanate	14.5 ± 0.1	23.4 ± 0.3	24.5 ± 0.3
dodecyl isocyanate	14.5 ± 0.3	22.8 ± 0.3	22.9 ± 0.3
1-adamantyl isocyanate	14.5 ± 0.3	22.7 ± 0.2	23.3 ± 0.5
cyanophenyl maleimide	14.5 ± 0.3	23.4 ± 0.3	25.8 ± 1.5